

Copyright is owned by the Author of the thesis. Permission is given for a copy to be downloaded by an individual for the purpose of research and private study only. The thesis may not be reproduced elsewhere without the permission of the Author.

The long-term effects of elevated CO₂ on soil organic carbon sequestration, partitioning and persistence in a grazed pasture

A thesis presented in partial fulfilment of the requirements for the degree of

Doctor in Philosophy

In

Soil Science

At Massey University, Manawatu

New Zealand

Marcela Angelica Gonzalez Moreno

2023



Abstract

The increased concentration of atmospheric carbon dioxide (CO₂) is a significant driver for climate change and also influences the cycling of soil organic carbon (OC) in ecosystems. Despite the importance of grassland soils as a sink for CO₂, the effect of long-term exposure to elevated CO₂ (eCO₂) on OC sequestration, partitioning and persistence in grazed grassland soils is poorly understood. This thesis aimed to investigate the effect of eCO₂ on soil OC stocks, the partitioning of OC in soil fractions and persistence in a grazed legume-based pasture at the New Zealand (NZ) Free Air CO₂ Enrichment (FACE) facility. The NZ-FACE, established in 1997, is the only FACE experiment worldwide that includes the influence of grazing practices on the above- and below-ground components of the OC cycle. The effect of eCO₂ on soil OC persistence and stability was assessed by measuring changes in soil OC stock, in the distribution of soil OC in the soil fractions by wet fractionation analysis and in the soil OC decomposition pathways by determining the molecular composition of soil organic matter (OM) by pyrolysis analysis followed by gas chromatography/mass spectroscopy (GC-MS) and thermally assisted hydrolysis methylation-GC-MS (THM-GC-MS) analysis to a soil depth of 250 mm.

In Chapter 3, we assessed OC storage and persistence in the soil fractions in a grazed legume-based pasture exposed to eCO₂ for 22 years on Pukepuke soil (Mollic Psammaquent) at three soil depths. **Our study revealed that after 22 years of exposure to eCO₂ there were no significant changes in the stocks of OC and N as well as the partitioning of OC within different soil fractions in the Pukepuke soil.** Interestingly, in the last 10 years at the NZ-FACE facility, there has been a sharp reduction of OC and N stocks in the Pukepuke soil, independent of the CO₂ treatment. We suggest that in the sandy Pukepuke soil under conditions of warmer temperatures and a wetter system, the deficiency that has emerged in soil nutrient

availability, the environmentally enhanced plant growth and the larger amounts of fresh OM input has caused a positive priming effect, mainly in the labile fraction. **Even though eCO₂ did not change the soil OC stocks nor OC content in the soil fractions in any soil layer, it did modify the soil nutrient status (phosphate in particular) and did increase polysaccharides and aliphatic proportions in the coarse particulate organic matter and micro-aggregates** indicating that the priming was further enhanced in eCO₂ soils with this effect being especially prominent in the 50 – 150 mm soil layer (Chapter 3).

In Chapter 4, the hypothesis that grazing animals, by returning nutrients in urine, dung, and plant litter trampled into the soil surface, would contribute to an increase in soil OC and N stocks under eCO₂ was investigated and rejected. **Despite not finding any interaction effect between eCO₂ and defoliation treatment on the soil OC stocks and partitioning in the soil fractions, the presence of an interaction effect in the soil OM molecular composition suggests that distinctly different OC decomposition pathways exist depending on pastures management under eCO₂.** Our study showed that under grazing there was an accumulation of lignin-derived OM, which reveals a higher proportion of shoot-derived rather than root-derived OC under eCO₂.

In Chapter 5, the influence of the inherent properties of a soil – which might enhance or limit the effects of eCO₂ on soil OC persistence and stability – was examined in two contrasting soils (Pukepuke and Stratford; a Entic Dystrandepet) in mesocosms installed at the NZ-FACE in May 2005 and extracted after 15 years. Our results showed that over the course of the mesocosm study, OC and N contents and stocks (to 150 mm soil depth) in the Pukepuke soil declined by 16 t ha⁻¹ under ambient CO₂ atmosphere, possibly as a result of soil disturbance during the establishment of the mesocosms. In the Stratford soil, with the ability to strongly preserve OM through mineral associations, the decline in soil OC was much smaller (5 t ha⁻¹). **Elevated CO₂ interacted with soil type and after 15 years of exposure to eCO₂, the Pukepuke soil had**

6.5 t ha⁻¹ more OC stocks, compared to the same soil under ambient CO₂ conditions, while no differences were found in the OC stocks of the Stratford soil (Chapter 4). These findings indicate that in the Pukepuke soil the eCO₂ treatment might have (i) helped overcome the impact of disturbance by favouring plant growth and generating a larger plant detritus input to the soil that enabled the partial replenishment of the OC loss at the time of mesocosm establishment, or (ii) limited the impact of disturbance, as eCO₂ often improves soil aggregation. It is crucial to consider that (i) the Stratford soil was subjected to ~50% less precipitation at the NZ-FACE compared to its original location and (ii) the mesocosm might have introduced new variables due to physical barriers. Thus, extrapolating the findings to field conditions at the NZ-FACE facility and elsewhere requires cautious interpretation.

The findings presented in this thesis contribute significantly to enhancing our understanding of the mechanistic processes underlying the influence of eCO₂ on the stabilization and mineralization of soil OM. These insights have direct implications for the development of sustainable agricultural management practices in response to a changing environment.

Acknowledgements

Throughout my PhD study, I was fortunate to have the unwavering support and guidance of my main supervisors, Prof. Marta Camps-Arbestain and Dr. Alec Mackay. Their constant supervision, constructive suggestions, and never-ending encouragement were invaluable to my success. I am deeply grateful for their dedication and commitment. Additionally, I would like to express my sincere gratitude to my co-supervisors Dr. Mark Lieffering, and Dr. Maria Minor, for their generosity in sharing their time, patience, and knowledge. Their contributions were essential to the completion of my research, and I am honoured to have had the opportunity to work with such committed and dedicated scientists.

My special thanks go to the Climate Change and Forage Innovations Team at AgResearch for (i) funding my research and studies throughout my doctoral programme and (ii) providing access to the comprehensive long-term data set that have been collected by the Team since the New Zealand (NZ) Free Air CO₂ Enrichment (FACE) facility was established in 1997.

I am also indebted to Dr. Joeri Kaal (Pyrolyscience S.L.U., Spain) for his assistance with the analysis and interpretation of the soil molecular analysis. My sincere acknowledgement is extended to Dr. Paul Newton and Dr. Alan Palmer for the guidance and extensive knowledge provided on the interpretation of the results found in this dissertation. To Dr. Roberta Gentile, for kindly sharing her data and expertise; and to Phil T. and Shona B., two amazing technicians that actively helped me throughout my field and laboratory work.

My immense gratitude to my extended family in New Zealand (Kayne Eccles, Judy and Barry Rolle and Dr. Shahista Nisa), for the endless love, and unwavering support during times of illness. Finally, to my family back home (Cecilia Moreno, Ximena Gonzalez and Ivan Gonzalez), I am eternally grateful for their unconditional love, patience and support throughout

my life; thank you for helping me grow into the person and scientist I have become. I am lucky to have you as a family.

Table of contents

Abstract.....	I
Acknowledgements.....	IV
Table of contents.....	VI
List of figures.....	XIII
List of tables.....	XVII
List of abbreviations	XVIII
Chapter 1 General Introduction	1
1.1 General background.....	2
1.1.1 Research gaps	4
1.1.2 Research objectives.....	6
1.1.3 Thesis outline.....	7
Chapter 2 Literature review	9
2.1 Anthropogenic greenhouse gas emissions and their consequences	10
2.2 Photosynthetic rate and soil organic carbon inputs under elevated CO ₂	11
2.3 Free air carbon dioxide enrichment facilities.....	12
2.3.1 Aboveground responses to elevated CO ₂ and their implications for soil carbon sequestration: insight from FACE facilities worldwide	12
2.4 Grasslands and soil organic carbon under a changing climate	13
2.4.1 Effects of elevated CO ₂ on soil organic carbon dynamics in grasslands: Insights from grassland FACE experiments.....	14

2.4.2 Interactions between climate change factors and grazing practices on soil organic carbon dynamics	15
2.4.3 The New Zealand Free Air CO ₂ Enrichment facility	17
2.5 The potential of organic carbon sequestration in soils.....	22
2.5.1 Soil organic carbon partitioning and persistence	22
2.5.2 Soil organic carbon protection	25
2.5.3 Analytical techniques for analysing soil organic carbon quantity and quality	26
2.6 Overview and research opportunities.....	29
 Chapter 3 Changes in soil aggregate size fractions and molecular composition of soil organic matter in a grazed sture after 22 years of elevated CO ₂	 33
Abstract	34
3.1 Introduction.....	35
3.2 Methods.....	40
3.2.1 Experimental setup	40
3.2.2 Above- and below-ground analyses.....	41
3.2.3 Statistical analysis.....	46
3.3 Results and discussion	47
3.3.1 Aboveground plant biomass response to elevated CO ₂ between period I and II....	47
3.3.2 Belowground response to elevated CO ₂ between period I and II.....	50
3.3.3 Organic carbon and nitrogen stocks.....	53
3.3.4 Soil organic carbon and nitrogen in the soil fractions	56
3.3.5 The effect of depth on the molecular composition of soil fractions	60
3.4 Conclusion	67
Appendix I - Extended Data for Chapter 3	68

Extended Data 3.2 Methods.....	69
Extended Data 3.2.1 Experimental setup.....	69
Extended Data 3.3.1 Aboveground plant biomass response to elevated CO ₂ between period I and II	79
Extended Data 3.3.2 Belowground response to elevated CO ₂ between period I and II ..	81
Extended Data 3.3.3 Organic carbon and nitrogen stocks.....	82
Extended Data 3.3.4 Soil organic carbon and nitrogen in the soil fractions.....	83
Extended Data 3.3.5 The effect of depth on the molecular composition of soil fractions	86
 Chapter 4 The long-term interactive effect between elevated CO ₂ and the grazing animal on soil carbon stocks and molecular composition of soil organic matter	 93
Abstract.....	94
4.1 Introduction.....	95
4.2 Methods.....	101
4.2.1 Experimental setup	101
4.2.2 Soil collection and bulk soil analysis.....	103
4.2.3 Soil wet fractionation analysis	104
4.2.4 Soil organic matter molecular composition	104
4.2.5 Statistical analysis.....	110
4.3 Results.....	111
4.3.1 Effect of elevated CO ₂ on soil organic carbon and nitrogen stocks	111
4.3.2 Effect of defoliation on soil organic carbon and nitrogen stocks	113
4.3.3 Soil organic carbon and nitrogen in the soil fractions	114
4.3.4 Soil organic matter characterization by Pyrolysis-GC-MS analysis	120

4.3.5 Soil organic matter characterization by thermally assisted hydrolysis and methylation-GC-MS analysis	124
4.3.5.1 Interaction effect between elevated CO ₂ , defoliation treatment and soil depth.	124
4.3.5.2 Influence of soil depth on soil organic matter molecular composition.....	126
4.3.5.3 Influence of defoliation on soil organic matter molecular composition	127
4.4 Discussion.....	129
4.4.1 Long-term exposure to elevated CO ₂ effect has not increase soil organic carbon and nitrogen stocks	129
4.4.2 Elevated CO ₂ did not show significant interaction effects with defoliation treatments on soil organic carbon partitioning and persistence.....	131
4.4.3 Nutrient return from grazing sustains soil organic carbon and nitrogen stocks, with implications for soil aggregates stability	133
4.4.4 Long-term CO ₂ exposure and defoliation on soil organic matter composition in a legume-based grazed pasture: insights into nutrient return, stabilization pathways, and depth-dependent variations	135
4.5 Conclusions.....	137
Appendix II - Extended Data for Chapter 4.....	139
Extended Data 4.2 Methods.....	140
Extended Data 4.2.1 Experimental set up.....	140
Extended Data 4.2.2 Soil collection and bulk analysis.....	141
Extended Data 4.2.3 Soil organic matter molecular composition	141
Extended Data 4.3 Results	147
Extended Data 4.3.1 Effect of elevated CO ₂ on organic carbon and nitrogen stocks in soils	147
Extended Data 4.3.2 Soil organic carbon and nitrogen in soil fractions	148

Extended Data 4.3.3.1 Influence of elevated CO ₂ on soil organic carbon and nitrogen pools.....	150
Extended Data 4.3.4.1 Interaction effects between elevated CO ₂ and defoliation treatment	156
Extended Data 4.3.4.2 Influence of soil depth on soil organic matter molecular composition.....	156
Extended Data 4.3.5.1 Interaction effect between elevated CO ₂ , defoliation treatment and soil depth.....	157
 Chapter 5 Influences of elevated CO ₂ on soil organic carbon quantity and quality in two contrasting soils	160
Abstract.....	161
5.1 Introduction.....	163
5.2 Methods.....	167
5.2.1 Experimental setup	167
5.2.2 Soil organic carbon and nitrogen analysis	171
5.2.3 Characterization of soil organic matter molecular composition.....	172
5.2.4 Statistical analysis.....	174
5.3 Results.....	175
5.3.1 Soil organic carbon and nitrogen stocks	175
5.3.2 Soil organic matter molecular composition	178
5.4 Discussion.....	184
5.4.1 Understanding how inherent soil properties can explain the evolution of soil organic carbon over time under ambient concentrations of atmospheric CO ₂	184
5.4.2. Understanding how inherent soil properties can explain the different responses of the two soils to elevated atmospheric CO ₂	186

5.4.3 Understanding how the inherent soil properties influence the quality of the organic matter under elevated atmospheric CO ₂	188
5.4.4 Exploring mesocosm effects on soil organic carbon dynamics	190
5.5 Conclusion	192
Appendix II – Extended Data for Chapter 5	195
Extended Data 5.1 Introduction	195
Extended Data 5.2 Methods	197
Extended Data 5.2.1 Experimental set up	198
Extended Data 5.2.3 Soil organic matter molecular composition	199
Extended Data 5.3 Results	208
Extended Data 5.3.1 Soil organic carbon and nitrogen stocks	208
Extended Data 5.4 Discussion	217
Extended Data 5.4.1 Inherent differences in soil organic carbon and nitrogen stocks in the two soils	217
Extended Data 5.4.2 Changes in soil nutrient status, aboveground biomass and botanical composition	219
Chapter 6: Overall summary and recommendation for future research	224
6.1 Overall Summary	225
6.1.1 Changes in soil organic carbon partitioning and molecular composition of soil organic matter in a grazed pasture after 22 years of elevated CO ₂	225
6.1.2 The long-term interactive effect between elevated CO ₂ and the grazing animal on soil carbon stocks and molecular composition of soil organic matter	227
6.1.3 Influences of elevated CO ₂ on soil organic carbon quantity and quality in two contrasting soils	229
6.2 Highlights of the thesis	230

6.3 Further research	232
References.....	235

List of figures

- Figure 2. 1:** Diagram showing six experimental rings on block design at the New Zealand Free Air CO₂ Enrichment facility. Yellow circles indicate elevated CO₂ rings (eCO₂) and blue circles represent ambient CO₂ rings (aCO₂)..... 19
- Figure 2. 2:** An experimental ring on the NZ Free Air CO₂ Enrichment facility (diagram adapted from Dr Mark Lieffering). Each ring under elevated CO₂ treatments is delimited by 24 standpipes connected underground by a pipe carrying CO₂. A monitor in the centre of the ring measures continuously CO₂ level, wind speed and direction to ensure the target CO₂ concentration is reached. Depending on the monitor measurements certain pipes will emit CO₂ while others remain partially or completely closed. 19
- Figure 2. 3:** Schematic diagram of microbial metabolic processes involved in the soil carbon cycling in terrestrial ecosystems (Liang et al., 2017). 24
- Figure 2. 4:** Reconciliation of current conceptual models for the fate of organic debris into a consolidated view of a soil continuum model of organic matter cycles and ecosystem controls in soil (Lehmann and Keblner, 2015). 26
- Figure 2. 5:** Fractionation scheme to isolate soil organic matter fractions developed by Six et al. (2002). 28
- Figure 3. 1:** Average aboveground plant response to time and elevated CO₂ at the NZ Free Air CO₂ Enrichment facility between period I (2005 – 2009) and period II (2015 – 2019). Error bars represent SD (n = 3). a) Net Herbage accumulation (NHA) over the period. b) Yearly average herbage production and the average proportion of C₃ grasses, C₄ grasses, legumes, and other species proportion over each period (5 years) under both CO₂ treatments. 49
- Figure 3. 2:** Belowground response of soil variables to time and elevated CO₂ at the NZ-FACE facility between period I (2005 – 2009) and period II (2015 – 2019). Bars represent the period average under ambient and elevated CO₂ treatments of soil pH, moisture and nutrient status. Error bars represent SD (n = 3). a) soil pH, b) soluble calcium, c) soil moisture, d) soluble magnesium, e) Phosphate (Olsen P), f) soluble potassium, g), sulphate-S, and h) soluble sodium..... 51

Figure 3. 3: Results of soils fractions from the NZ-FACE facility showing soil fractions sizes, carbon (C) and nitrogen (N) concentration and their C:N ratio by the end of period I (2009) and II (2019), in three soil depths, independent of CO₂ treatments: a) fraction size of coarse particulate organic matter (cPOM), b) C concentration in cPOM, c) N concentration in cPOM, d) C/N ratio of cPOM, e) fraction size of micro-aggregates, f) C concentration in micro-aggregates, g) N concentration in micro-aggregates, h) C/N ratio of micro-aggregates, i) fraction size of mineral associated organic matter (MAOM), j) C concentration in MAOM, k) N concentration in MAOM and, l) C/N ratio of MAOM. Error bars represent SD (n = 6). Three soil layers were analysed except for the MAOM fraction where only the layers 50 – 150 and 150 – 250 mm were studied. See Extended Data Table 3.6 for C recovery and N recovery. .58

Figure 3. 4: Scatter plot of a) short-chain fatty acid methyl ester (FAMES) products vs long chain fatty diacid esters (IDAMEs) products across soil fractions under elevated and ambient CO₂ and b) IDAMEs products vs long-chain fatty acid methyl esters (IFAMES) + ω-methoxy fatty acid methyl ester (oFAME) + mid-sub FAMES products across soil fractions at the NZ Free Air CO₂ Enrichment facility, data from 2019.....62

Figure 3. 5: Proportions of pyrolyzate groups in three main soil organic matter fractions: (a) coarse particulate organic matter (coarse-POM), (b) micro-aggregates and (c) mineral associated organic matter (MAOM), at ambient and elevated CO₂ at the NZ-FACE facility, data from 2019. Data is shown across the soil profile (0 – 250 mm). Error bars represent SD (n=3). Abbreviations of pyrolytic products: MCC = aliphatic, CARB = carbohydrates, NCOMP = N-containing, PHEN = phenols, MAH/PAH = mono-/polycyclic-aromatic hydrocarbons, OTHER = unidentified, LIG = the sum of lignin G, H and S (guaiacol, and syringyl) and XCOMP = halogen-containing.64

Figure 4. 1: Effect of ambient and elevated CO₂ and three defoliation treatments on soil attributes throughout the soil profile (0 – 250 mm) after 22 years of eCO₂ exposure at the NZ-FACE facility. Grazed + NT: grazed + nutrient return + treading in plant litter, a condition where animal grazing defoliates shoots, nutrients are returned to the soil through dung and urine depositions, and treading incorporates plant litter into the soil; Grazed – NT: a condition where animals grazing removes shoots yet the soil receives no dung and urine return and no treading pressure; Cut – NT: area under a 0.5 m² exclusion cage where pasture was hand-cut, where grazing, nutrient return and treading are prevented. Error bars indicate SD (n=3). ... 112

Figure 4. 2: Effect of elevated CO₂ on soil fractions after 22 years of exposure at the NZ-FACE facility, averaged across the three defoliation treatments. a) N proportion in the coarse particulate organic matter (cPOM) out of the total N pool, b) fraction size of the mineral-associated organic matter (MAOM), c) C proportion in MAOM out of the total C pool and d) N proportion in MAOM out of the total N pool. Error bars indicate SD (n = 3). 116

Figure 4. 3: Soil aggregate fraction sizes in different grazing treatments, averaged for the two CO₂ conditions, (a) coarse particulate organic matter (cPOM), b) micro-aggregates, c) mineral-associated organic matter (MAOM). Error bars indicate SD (n = 3)..... 117

Figure 4. 4: Defoliation treatment effect on organic carbon (OC) and nitrogen (N) contents in soil fractions averaged for the two CO₂ treatments, a) organic carbon content (C%) in the coarse particulate organic matter (cPOM) at three soil depths, b) nitrogen content (N%) in the cPOM at three soil depths, c) organic carbon content (C%) in micro-aggregates at three soil depths, d) nitrogen content (N%) in micro-aggregates at three soil depths, e) organic carbon content (C%) in the mineral-associated organic matter (MAOM) as proportion of the total OC pool throughout the soil profile (0 – 250 mm) and d) nitrogen content (N%) in MAOM as proportion of the total N pool throughout the soil profile (0 – 250 mm). 119

Figure 4. 5: Effect of elevated CO₂ and defoliation treatment on the major pyrolytic groups across all three soil depths. a) Sum of carbohydrate products, b) Sum of methylene chain compounds (aliphatic products), c) Sum of N-containing products, and d) Sum of lignin products. Error bars represent SD (n = 3). 121

Figure 4. 6: Pyrolysis-GC-MS results (as the percentage of total quantified peak area) for three defoliation treatments and three soil depths, averaged for the two CO₂ levels. Results are shown based on pyrolytic groups. Error bars indicate SD (n = 3). Abbreviation of products: CARB = carbohydrate, MCC = aliphatic, NCOMP = nitrogen-containing, LIG = lignin products, PHEN = phenols, OTHER = unidentified and MAH = monocyclic aromatic hydrocarbons. 123

Figure 4. 7: Effect of elevated CO₂ on selected thermally assisted hydrolysis and methylation (THM-GC-MS) products in soil of the three defoliation treatments across the entire soil profile at the NZ-FACE facility, a) long-chain fatty acid methyl ester (long-chain FAMES; microbial-derived), b) long-chain fatty acid dimethyl esters (long-chain DAME; suberin-derived), c) dimethoxybenzenes (from guayacil) and d) tri-methoxybenzenes (from syringyl). Error bars indicate SD (n = 3)..... 126

Figure 4. 8: Results of thermally assisted hydrolysis and methylation (THM-GC-MS) analysis (as the percentage of total quantified peak area) for defoliation treatments and soil depths, across both CO₂ treatments. Results are shown based on THM groups. Error bars indicate SD (n = 3). Abbreviation of products: MCC = aliphatic, MB = methoxybenzenes, CARB = carbohydrate, NCOMP = nitrogen-containing, Other = unidentified, BCA = methylated benzene carboxylic acids. 128

Figure 5. 1: New Zealand Drought Index (NZDI) chart between 2007 and 2020 in the Manawatu district (extracted from NIWA, New Zealand Drought Monitor, 2021)..... 171

Figure 5. 2: Interactive effect of elevated CO₂ and soil type on a) soil organic carbon (OC) content, b) soil nitrogen (N) content, c) soil organic carbon (OC) stock and d) soil nitrogen (N) stock in the 0 – 150 mm depth in the two soils in the mesocosms sited at the NZ Free Air CO₂ Enrichment facility after 15 years of exposure to elevated CO₂. Error bars indicate SD (n = 3, letters indicate differences to p < 0.05)..... 177

Figure 5. 3: Principal Component Analysis biplots, independent of CO₂ treatment, of the pyrolytic groups clustered by a) soil type and b) soil depth. in Pukepuke and Stratford soil from mesocosms at NZ-FACE facility Abbreviations of products: MCC = aliphatic, NCOMP = N-containing, PHEN = phenols, MAH/PAH = mono-/polycyclic-aromatic hydrocarbons, OTHER = unidentified, LIG = the sum of lignin G, H and S (guaiacol, and syringyl), Unspecific Poly = unspecific polysaccharides, PLANT_POLY = plant polysaccharides and XCOMP = halogen-containing..... 179

Figure 5. 4: Effect of elevated CO₂ on the pyrolytic products found in the Pukepuke soil samples from the NZ Free Air CO₂ Enrichment facility after 15 years of elevated CO₂ enrichment on a) total lignin and b) guaiacol lignin (Lignin G). Error bars indicate SD (n = 3, letters indicate differences to p < 0.05)..... 181

Figure 5. 5: Examples of interactive effects of elevated CO₂ and soil depth on the soil organic matter pyrolytic products (independent of soil type) from the mesocosm study sited at the NZ Free Air CO₂ Enrichment facility legume-based grazed pasture after 15 years of exposure elevated CO₂. Error bars indicate SD (n = 3, letters indicate differences to p < 0.05)..... 183

List of tables

Table 3. 1: Soil measurements from 2009 and 2019 in the three soil layers (0 – 50, 50 – 150, and 150 – 250 mm) across CO ₂ treatments at the NZ-FACE facility. Values are mean ± SD (n = 3).....	54
Table 4. 1: Soil organic matter pyrolytic products (Py-GC-MS) clustered by chemical similarity, and their predominant source of origin.....	106
Table 4. 2: Soil organic matter products clustered by chemical similarity and the predominant source of origin by thermally assisted hydrolysis and methylation followed by gas chromatography and mass spectrometer (THM-GC-MS) analysis.	107
Table 4. 3: Soil bulk density (BD), organic carbon (OC) and nitrogen (N) content and stocks in the three soil layers under the three defoliation treatments, averaged for the two CO ₂ treatments, at the NZ Free Air CO ₂ Enrichment facility. Results are means with SD (n = 3).	113
Table 5. 1: General description of original location and physico-chemical properties of the Pukepuke and Stratford soils.	169
Table 5. 2: Soil organic carbon (OC) and nitrogen (N) stocks in the Pukepuke (from rings) and Stratford (mesocosm) soils in the 0 – 50 and 50 – 150 mm soil depth, in 2009 (after 12 and 4 years of exposure to elevated CO ₂ , respectively) from the NZ-FACE legume-based grazed pasture facility (unpublished data).....	170
Table 5. 3: Soil organic carbon (OC) and nitrogen (N) stocks on soil samples collected in 2009 and 2020 from the NZ-FACE facility under ambient CO ₂ . Values are given based on ESM calculation.	175

List of abbreviations

aCO ₂	Ambient carbon dioxide
Al	Aluminium
C	Carbon
Ca	Calcium
CO ₂	Carbon dioxide
cPOM	Coarse particulate organic matter
DAME	Fatty diacid ester
DOC	Dissolved organic carbon
eCO ₂	Elevated carbon dioxide
FAME	Fatty acid methyl ester
Fe	Iron
GC	Gas chromatographer
HCl	Chlorohydric acid
HF	Hydrofluoric acid
K	Potassium
MAP	Mean annual precipitation
MAT	Mean annual temperature
MS	Mass spectrometer
MAOM	Mineral associated organic matter
N	Nitrogen
Na	Sodium
NHA	Net herbage accumulation
NH ₄	Ammonium

NT	Nutrient return + treading
NZ-FACE	New Zealand Free Air Carbon Dioxide Enrichment
OC	Organic carbon
OM	Organic matter
PCA	Principal component analysis
P	Phosphorus
PO ₄	Phosphate
Py	Pyrolysis
S	Sulphur
SO ₄	Sulphate
THM	Thermally assisted hydrolysis and methylation
TQPA	Total quantified peak area

Chapter 1 General Introduction

1.1 General background

The impact of elevated atmospheric carbon dioxide (eCO₂) is not limited to its influence on climate but also on biological systems. These effects are largely due to the increased photosynthetic rates that result in higher plant growth and production if there are no other limiting resources (Ainsworth and Long, 2020). This, in turn, leads to an increase in the amount of organic carbon (OC) that is transferred to the soil through plant litter, roots and root residues that ultimately alters soil OC dynamics (Terrer et al., 2020). Such changes in OC inputs can affect the interactions within the soil-plant system and the functioning of soil organic matter (OM; Terrer et al., 2018; Kuzyakov et al., 2019). As a result, eCO₂ concentrations in the atmosphere have the potential to increase soil OC stocks (Jastrow et al., 2005; Hungate et al., 2009; Van Groenigen et al., 2006; Terrer et al., 2020) but also to decrease them if priming occurs (Xie et al., 2005; Xu et al., 2019).

Soil OC has gained increasing attention in recent years due to its vital role in ensuring both food security and mitigating climate change (Lal, 2018). Even minor changes in CO₂ fluxes between the soil and the atmosphere can have significant impacts on global atmospheric CO₂ levels and, consequently, global climate (Liang et al., 2017; Whitehead et al., 2018; Sitters et al., 2020). Therefore, understanding the dynamics of soil OC is critical in developing effective strategies for managing carbon (C) stocks and mitigating climate change.

The capacity of the soil to sequester OC depends on the balance between photosynthetic rate, biota respiration, and the inherent capacity of the biogeochemical system to process and preserve OC (Six et al., 2002; von Lutzow et al., 2008; Wiesmeier et al., 2019). Soil OC can only increase if (i) the OC supply to the soil is in excess of soil OC losses, and (ii) its long-term persistence – which is conditioned by functional complexity (Lehmann et al., 2020) – is favoured. Soil OC persistence depends not only on the physical protection and the chemical properties of soil OC, but also on the complex level of interactions among soil-plant-microbe

systems and on abiotic conditions (Liang and Balsler, 2012; Cotrufo et al., 2015; Liang et al., 2017; Sokol and Bradford, 2019; Lehmann et al., 2020). One particular soil-plant-microbe interaction is priming. Priming refers to the phenomenon where the sudden addition of large amounts of labile OC inputs, such as root exudates or fresh plant materials, stimulates the microbial decomposition of soil OM (Chen et al., 2019). This process can either enhance or diminish the long-term stability of soil OC, particularly depending on the soil's inherent properties (Mitchell et al., 2020).

Grasslands comprise 70% of global agricultural land (Conant et al., 2011; FAO, 2019) and contain approximately 20% of the world's soil OC stocks (Whitehead et al., 2018). These soils can be a significant source or sink of CO₂ under certain management practices (Lal et al., 2018). The consequences of grasslands growing under eCO₂ on herbage accumulation and its subsequent effects on soil OC and nitrogen (N) dynamics has been assessed in experiments throughout the world using the Free Air CO₂ Enrichment (FACE) technology. From this it has been concluded that plants growing under eCO₂ often have increased nutrient uptake, which can lead to a depletion of nutrients in the soil, especially N (Kuzyakov et al., 2019). This can result in a shift in the types of microorganisms present in the soil and the activities they perform, as the nutrients required for their growth and metabolism may become limiting. As a result, there is still debate on the magnitude of plant response to eCO₂ and whether a boost in plant growth under eCO₂ will contribute to a sustained increase in soil OC stocks in the long-term.

Soil OM responds differently to eCO₂ depending on land uses and their respective management, plant species, soil resources and atmospheric conditions (Terrer et al., 2020), making it essential to consider all these factors when conducting FACE experiments. However, for practical reasons in most instances FACE studies are generally limited to one type of land use and soil type. Furthermore, FACE experiments conducted in grasslands have been largely limited to monocultures of grass and explored the influence of defoliation by cutting,

overlooking the influence the grazing animal might pose on the pasture and soil OC and N dynamics.

The NZ-FACE facility, established in 1997, is the only FACE facility worldwide investigating the effects of eCO₂ on soil OC and N dynamics of a legume-based pasture grazed by animals. It is situated near Bulls, Manawatu-Whanganui, New Zealand (40°14' S, 175°16'E), and has been operated to study the impact of rising atmospheric CO₂ concentrations on pasture biomass production, botanical composition, nutrient cycling, and soil OC dynamics of a legume-based pasture grazed by sheep. During the first 10 years of eCO₂ exposure at the NZ-FACE facility there was small increases in pasture biomass some years (Ross et al., 2013), the legume species component of pasture was boosted (Newton et al., 2014) and more assimilates were allocated to roots (Allard et al., 2005). As a result, the soil under eCO₂ received more OC inputs. This, in turn, increased the microbial C and N pools and soil respiration rates (Ross et al., 2013). This has led to a progressive N limitation (Newton et al., 2010) that coupled with low soil P concentration has limited the boost in plant growth under eCO₂ over time (Gentile et al., 2012). An earlier study of change in soil OC and N dynamics under eCO₂ (Ross et al. 2013) did not detect a change in OC and N stocks or C:N ratio of the organic fraction.

1.1.1 Research gaps

There is a need for a deeper understanding of the long-term effects of eCO₂ on the quantity and quality of OC and N in legume based grazed pastoral soils.

How the grazing animal – which selectively defoliates plants, tramples the surface (incorporating litter into the soil) and returns nutrients in dung and urine – interacts with eCO₂ to influence the quantity and quality of soil OC and N is poorly understood. Grazing strongly influences the nutrient cycle by selective defoliation and nutrient return through urine and

dung, which can enhance or limit the effects of eCO₂. With sufficient nutrient supply to support enhanced root growth under eCO₂, there might be a relative increase in stable OC over the long term (Sokol and Bradford et al., 2019). Elevated CO₂ can thus have an impact on soil microbial biomass, N mineralization rate and nitrification rate – however, despite observed increasing trends at the NZ-FACE, Deng et al. (2016) did not detect changes in mineral N. This suggests that an increased supply of nutrients is needed to support the enhanced growth rate under eCO₂. It has not been defined whether the grazer's urine and dung would facilitate the extra nutrient required to support the boost in pasture growth under eCO₂.

Studies have observed that while eCO₂ can enhance plant biomass and promote soil microbial and root respiration (Kuzyakov et al., 2019), the effectiveness of these processes in increasing soil OC stocks is strongly influenced by soil physiochemical properties, such as texture and clay mineralogy (Butterly et al., 2016), in addition to climate conditions, land use and management practices. The pathways for OC persistence in different soil types and how the response to eCO₂ is dependent on key soil properties that contribute to the storage and protection of OC are not well-understood. Soil types with higher aggregation and superficial surface area with highly reactive minerals (e.g., Fe/Al oxy-hydroxides and allophane) have not only a higher soil OC content but a higher potential to adsorb and stabilise OC in the long term, especially microbial-derived OC (McNally et al., 2017). Therefore, a comparison of a sandy soil with few reactive surfaces and a soil derived from tephra containing allophane, rich in reactive surfaces would provide valuable insights.

A comprehensive approach is needed to fully understand the ecosystem response to long-term exposure to eCO₂. Merely measuring OC and N content at the end of an experiment is not sufficient. It is important to consider the above- and below-ground growth response over time, as well as the influence of abiotic factors on the stability of the labile OC pool and the potential

destabilization of the stable OC pool to fully grasp the partitioning and persistence of soil OC in a changing climate.

This thesis aimed to fill these research gaps by testing the following hypotheses:

- A boost in pasture growth of a legume-based grassland 22 years of exposure to eCO₂, will lead to an increase in soil OC and N stocks, characterised by lower proportions of labile OC and a higher proportion of more preserved forms of OC (microbial-derived OC). This would only occur if there were enough nutrient availability to support a boost in plant growth, otherwise, the soil would be at risk of priming.
- Nutrient return from grazing animals in a legume-based grassland under long-term exposure to eCO₂ will support the increase in soil OC and N.
- Long-term exposure to eCO₂ of a legume-based grassland under grazing management increases soil OC and N, though the quantity and quality will be dependent on soil properties that are key to OC preservation (e.g., texture, mineralogy).

1.1.2 Research objectives

The main objective of this thesis was to investigate the effect of eCO₂ on soil OC and N stocks and molecular composition to assess the partitioning and persistence of soil OC in three soil layers at the NZ-FACE, which is the only grazed legume-based pasture FACE facility worldwide. Special attention has been paid to the belowground response (soil OC and N in the soil fractions, its molecular characterisation, and nutrient dynamics).

Three research aims were chosen to expand the knowledge on the effects of eCO₂ on soil OC and N in a grazed legume-based pasture, including:

- The cascade of effects (interaction effect between CO₂ x time x soil depth treatments) on the pasture response and subsequent effects on soil OC and N content, stocks and molecular composition in the soil fractions.
- The interaction effect between CO₂ x grazing animal x soil depth treatments on soil OC and N content, stocks, and molecular composition of the soil OM.
- The interaction effect between eCO₂ x soil type x soil depth treatments on soil OC and N content, stocks, and molecular composition of the soil OM.

1.1.3 Thesis outline

This thesis is composed of six chapters.

Chapter 1 provides a general introduction to the research background, hypotheses, objectives, and outline of this dissertation.

Chapter 2 presents the literature review on (i) the consequences of eCO₂ at an ecosystem level, (ii) insights from FACE facilities worldwide on the aboveground responses to eCO₂ and their implications for soil C sequestration, (iii) the response of grasslands soils to eCO₂, (iv) the potential of C sequestration in soils and (v) overview and research opportunities.

Chapter 3 covers a longitudinal evaluation of the effects of 22 years of exposure to eCO₂ on soil aggregate size fractions and molecular composition of soil OM in a legume-based grazed pasture at the NZ-FACE facility. The study provides evidence of a cascade of effects generated by eCO₂ leading to different soil OC stabilization processes over time.

Chapter 4 reports the results of an investigation of the interaction between eCO₂ and the grazing animal and subsequent effects on soil OC and N stocks, their distribution in the soil fractions and the molecular composition of soil OM. Three treatments are included to explore

the influence of the grazing animal, including (i) grazed + nutrient return + treading, (ii) grazed – nutrient return – treading and (iii) cut – nutrient return – treading) at three soil layers.

The results of our study will provide novel insight into the combined influence of eCO₂ and the grazing animal on the soil OM molecular composition and thus the preservation pathways of soil OC in different pasture management under eCO₂.

Chapter 5 covers a mesocosm study located within the NZ-FACE facility exploring the effect of eCO₂ on pasture growth and soil OC and N quality and quantity in two soils that vary in texture, mineralogy and physiochemical properties that influence OC sequestration and storage. The mesocosm study provides valuable insight in the response of two soils with markedly different parent materials, to eCO₂,

Chapter 6 includes a general summary of the experimental chapters in this dissertation and suggests some potential topics for future research.

Chapter 2 Literature review

2.1 Anthropogenic greenhouse gas emissions and their consequences

Globally, anthropogenic greenhouse gas (GHG) emissions, especially carbon dioxide (CO₂) emissions, have been increasing since the start of the industrial era, despite the international efforts made during recent years to reduce them (IPCC, 2014). Industry and transportation sectors account for 50% of the global GHG emissions, mainly through the burning of fossil fuels (EPA, 2020). Another important source of GHG emissions derives from the agricultural sector, which accounts for 10% of global emissions (EPA, 2020). Particularly, in New Zealand, the agricultural sector is responsible for almost half of the GHG emissions of the country (NZAGRC, 2012), and this has increased its CO₂ emissions by 41% between 1990 and 2015 (MFE, 2017).

Anthropogenic emissions of GHGs have been widely acknowledged as a significant driver of changes in global climate (IPCC, 2014); with important consequences observed worldwide, including in New Zealand (Karl et al., 2009; MFE, 2018). Among the consequences of a changing climate are warmer temperatures, changes in rainfall and drought patterns, rises in sea level, changes in ocean pH, and other impacts (Conant et al., 2011; Zhou et al., 2019). In New Zealand, rainfall and temperatures are expected to increase in the western and southern regions. Drought episodes are expected to double in the eastern and northern regions (NZAGRC, 2012).

The impact of increased atmospheric CO₂ extends beyond just climate, as it has been frequently observed and reported to exert a profound influence on biological systems. This is largely a result of its effects on photosynthesis (Ainsworth and Long, 2020), which can ultimately lead to alterations in carbon (C) inputs to soils. This can have downstream effects on soil C dynamics (Terrer et al., 2020), as the amount and quality of organic carbon (OC) inputs to soils

are altered, leading to changes in the overall interaction of the soil-plant system and functioning of soil organic matter (OM; Terrer et al., 2018; Kuzyakov et al., 2019).

2.2 Photosynthetic rate and soil organic carbon inputs under elevated CO₂

A direct consequence of elevated atmospheric CO₂ (eCO₂) is an enhanced photosynthetic rate (Norby and Zak, 2011; Jiang et al., 2020), which generally leads to an increase in plant biomass if other resources are available (Ainsworth and Long, 2004). These changes result in a cascade of effects influencing plant growth, water use efficiency and soil C sequestration (IPCC, 2014). It has also been reported that eCO₂ can shift the C allocation from shoot to roots boosting belowground inputs (Madhu and Hatfield, 2013). As a result, depending on climatic conditions (rainfall and temperature; Liang and Balsler, 2012), soil properties, plant species (Pendall et al., 2011) and nutrient supply (Jiang et al., 2020), eCO₂ can either increase, maintain, or decrease plant biomass (Ainsworth and Long, 2004; Kuzyakov et al., 2019; Jiang et al., 2020) and thus accordingly impacting the input of OC into the soil.

Increasing the C input rate to soils under eCO₂ (Jiang et al., 2020) can increase (Jastrow et al., 2005) or result in no change in soil OM as decomposition processes are also often stimulated (Sillen et al., 2012). The capacity of the soil to sequester OC is influenced by the balance between enhanced photosynthetic and plant growth rate, biota respiration, and the capacity of the soil to preserve OC. To better understand how these elements interact and impact on OC sequestration and persistence under eCO₂, environmental conditions, soil properties (including mineralogy), plant species, and microbial dynamics should be considered.

2.3 Free air carbon dioxide enrichment facilities

Greenhouse tunnels, open chambers, and Free Air CO₂ Enrichment (FACE) facilities are methods used to study the effects of eCO₂ on herbage production, gas emissions, and soil nutrient dynamics. The FACE facilities offer the best approach to studying the effects of eCO₂ in forests, grasslands, and crops at an ecosystem level (Ainsworth and Long, 2004), including the turnover of the soil OC (Theis et al., 2017) and its implications to the C cycle in a changing environment (Sitters et al., 2020).

2.3.1 Aboveground responses to elevated CO₂ and their implications for soil carbon sequestration: insight from FACE facilities worldwide

At FACE facilities worldwide, research on the influence of eCO₂ has mainly focused on aboveground responses, under different land uses, plant species and their respective management practices (Jones et al., 2014). From these studies, research has confirmed that eCO₂ increases photosynthetic rate, which can boost shoot biomass, (on average by 13 to 21%, but with a reported increase of up to 200% in some instances), especially during the first years of eCO₂ treatment (Ainsworth and Long, 2005; Newton et al., 2006; Deng et al., 2016; Kuzyakov et al., 2019).

Under eCO₂, C allocation from shoots to roots can be increased due to the higher nutrient requirements to support enhanced growth and thus the need to increase soil exploration by plant roots (Allard et al., 2005; Sillen and Dieleman, 2012; Madhu and Hatfield, 2013). A boost in plant biomass under eCO₂ leads to an increase in root exudation by living root and tissue turnover of decaying roots thus increasing OC input rate into the soil, which can then trigger an increase in both microbial and root respiration (Jiang et al., 2020). As the fraction of OC increases so does the amount of nitrogen (N) captured in the organic fraction. Over time a

progressive limitation of N availability may occur if no additional N is made available (Luo et al., 2004).

Additional co-limitation with phosphorus (P) availability has been reported under long-term exposure to eCO₂ (Gentile et al., 2012; Touhami et al., 2020). A limited supply of P has implications for the ongoing ability of the legume component of the pasture to continue to compete, grow, and fix N₂ biologically. Thus, only with sufficient nutrients (i.e., N and P) and water supply will the higher photosynthetic rate under eCO₂ translate into a boost in shoot growth and flow of extra fixed OC belowground with the potential to add to the OC pool in some soils (Reich et al., 2006; Hungate et al., 2009; Sillen and Dieleman, 2012; Sokol and Bradford, 2019). Findings of several meta-analyses from early short-term FACE experiments have shown that an increase in herbage accumulation under eCO₂ leads to an increase in soil OC content across a range of land uses (Jastrow et al., 2005; van Groenigen et al., 2006).

2.4 Grasslands and soil organic carbon under a changing climate

Soils are the largest OC reservoir in terrestrial ecosystems and have historically and continue to be a source of CO₂ emissions under some agricultural practices (Lal et al., 2018). Grasslands, most of which are grazed (McSherry and Ritchie, 2013; Zhou et al., 2019) account for 70% of the agricultural land worldwide (Conant et al., 2011; FAO, 2019) and contain about 20% of global soil OC stocks (Whitehead et al., 2018). These large amounts of OC stored in grassland soils should be well-managed as even a small change in CO₂ fluxes between the atmosphere and the soil can have a profound effect on the global atmospheric CO₂ pool and, therefore, the global climate (Liang et al., 2017; Whitehead et al., 2018; Sitters et al., 2020).

Soil OM underpins a wide range of ecosystem services, including the provisioning of nutrients, contributing to nutrient retention, regulating water infiltration and water holding capacity,

promoting soil biodiversity, aggregate building, and stability of soil structure (Chenu et al., 2019). Compared with forests and major crop species, most species in humid-temperate pastoral systems (e.g., those in New Zealand) have a greater proportion of root biomass in the topsoil. As a consequence, soil OM is especially concentrated in the topsoil of pastoral soils (Sokol and Bradford, 2019). Soil OC fluxes (and to a larger degree in topsoils) can be influenced by a range of factors including soil type, climate change, land use and its practices (e.g., frequency and severity of defoliation during grazing episodes), as these control the flow of OC to the belowground through litter and root death and decay which is a major factor regulating soil OM in permanent grasslands systems.

2.4.1 Effects of elevated CO₂ on soil organic carbon dynamics in grasslands:

Insights from grassland FACE experiments

A boost in above- and belowground production in grasslands under eCO₂ can subsequently increase soil OC stocks. This finding is supported by the work from longer-term (< 10 years) grasslands FACE facilities worldwide; at the Denmark-FACE facility, an increase of 12 – 22% in OC content in the top 0 – 100 mm was reported after 8 years of exposure to eCO₂. This translated to a 19% increase in OC stocks in the 300 mm topsoil (Dietzen et al., 2019). Nevertheless, some of their work has also suggested that the turnover of soil OM under eCO₂ is higher, leading to a potential loss of OC over time (Thaysen et al., 2017). In the Tasmania-FACE (Pendall et al., 2011), the boost in herbage production under eCO₂ was constrained to the grass functional type; thus, the increase in soil OC storage under eCO₂ was reported with C₄ vegetation, but not with C₃ vegetation. Similarly, an increase in herbage accumulation under eCO₂ at the BioCon facility in Minnesota led to an increase in soil OC storage. Research at the Jasper Ridge Global Change Experiment in California also suggested, based on the proportion

of amino sugars to soil OC, that under eCO₂ soil OC increases only under N fertilization (Liang et al., 2015).

In contrast to the conclusion reached by a majority of the FACE experiments under 10 years of exposure, all of the cut or mown grassland FACE studies with ≥ 10 years of exposure to eCO₂ – the Swiss-FACE (Six et al., 2001; van Groenigen et al., 2002; de Graaff et al., 2004; Xie et al., 2005; van Kessel et al., 2006 and Theis et al., 2007), the Giessen-FACE (Keidel et al., 2018) and the USDA-ARS High Plains Grasslands Research Station (Carrillo et al., 2018) – have reported no change in soil OC stocks in a pasture soil under eCO₂.

2.4.2 Interactions between climate change factors and grazing practices on soil organic carbon dynamics

Several meta-analyses have addressed the interaction between some climate change factors (changing precipitation and temperatures), but not eCO₂ on the above- and below-ground OC dynamics of grazed grasslands (Piñeiro et al., 2010; McSherry and Ritchie, 2013; Wang et al., 2016; Zhou et al., 2016, 2017; Abdalla et al., 2018; Sitters et al., 2020). The C allocation within the plant and its above- and below-ground turnover is affected by the grazing animal through its effects on defoliation (which includes selective defoliation), trampling, and nutrient return in urine and faeces (Fontaine et al., 2003; Zhou et al., 2017; Sitters et al., 2020) with subsequent effects on soil OC dynamics.

Defoliation frequency and severity are key factors in these dynamics. Intensive grazing practices reduces the amount of plant litter (shoot and root) but increases the amount of dung and urine entering the soil OC pool, while less intensive grazing leaves more plant litter available for soil OC sequestration, by increasing belowground fluxes, including soil

respiration, soil net N mineralization and soil N nitrification (Zhou et al., 2017). Sitter et al. (2020) found a strong correlation between herbage production and soil OC under both, grazing and cutting systems. This study showed that when herbage production and/or microbial activity increases, soil OC also increased independent of the defoliation regime. Piñeiro et al. (2010) also found that an increase in soil N fertility boosted herbage production and increased soil OC inputs, while also decreasing C losses by diminishing soil respiration.

According to Zhou et al. (2019), warming led to a decrease in soil respiration when grazing was involved. However, when there was an addition of N and an increase in rainfall, both autotrophic and microbial respiration were intensified. This research highlights the direct relationship between rainfall and temperature on herbage production, which in turn affects the dynamics of soil OC. When rainfall and temperature promote herbage biomass under light grazing it also results in more root exudate and biomass (McSherry and Ritchie, 2013). Root biomass also changes in response to water availability, with root biomass generally increasing under dry conditions in the search for water, as long as enough assimilates are produced. Under wet conditions, the root grows in response to the search for oxygen and nutrients (Piñeiro et al., 2010).

When analysing the interaction effects of defoliation practices and climatic parameters, Zhou et al. (2019) found no significant interactions. However, they did find that (i) grazing + warming counteracted the effect of grazing alone, by boosting plant growth and microbial activity, (ii) grazing + rainfall co-acted to increase soil respiration, and so did (iii) grazing + N addition. Sitter et al. (2020) found the influence of grazing on soil OC, soil N, and microbial activity is delimited by nutrient availability and temperature. Even though an increase in microbial activity leads to a larger OC loss by respiration (Conant et al., 2011), it also promotes

the formation of a larger OC pool (i.e., microbial necromass) that can become more easily preserved in soil over the long-term (Sokol and Bradford et al., 2019).

2.4.3 The New Zealand Free Air CO₂ Enrichment facility

Since 1997, the NZ-FACE facility, is the only FACE facility worldwide examining the influence of eCO₂ on OC and N dynamics of a grazed legume-based pasture. Since then, the NZ-FACE facility has been used to investigate the effects of increasing atmospheric concentration of CO₂ on pasture biomass production, botanical composition, nutrient cycling, and soil OC and N dynamics under sheep grazing (Dodd, 2013). The NZ-FACE is located on a site that is in permanent pasture near Bulls, Manawatu-Whanganui, New Zealand (40°14' S, 175°16'E). In this temperate climate the mean annual rainfall at the site is 875 mm with an average air temperature ranging from 8.0 °C in July to 17.4 °C in February (Allard et al., 2003). The site is characterized by periods of summer drought that result in low-herbage accumulation rate and 3 – 5% bare ground (Edwards et al., 2001). The pasture had been under permanent grazing by sheep, cattle, or goats since at least 1940 (Allard et al., 2003).

The NZ-FACE facility is divided into three blocks with two circular plots within each block (12 m diameter “ring”; Figure 2.1). The rings were chosen based on their initial botanical composition (Newton et al., 2006). In each block, one ring is exposed to the current atmospheric CO₂ concentration (aCO₂) and the other ring is treated with eCO₂ on daily basis throughout the photoperiod. It is worth mentioning that the global atmospheric CO₂ concentration has increased from ~350 to 415 ppm between 1997 and 2021. The eCO₂ rings were initially treated with 475 ppm of eCO₂, but to maintain the difference in CO₂ concentration between treatments, the eCO₂ concentration was increased to 500 ppm in 2001, a concentration likely to be reached during this century (Reich et al., 2006; IPCC, 2014). It is worth noticing that the CO₂ enrichment was suspended between 2011 and 2013. At the centre

of the treated rings, there are sensors continuously measuring the CO₂ concentration, wind speed and wind direction (Figure 2.2). These measurements are taken to ensure the targeted CO₂ concentration is continuously achieved in the treated rings.

All the rings are delimited by an electric fence to hold the stock during grazing events. Several times during each year three to five sheep are placed inside each ring allowing them to graze for three to four days (Newton et al., 2006). During grazing events, animals tread the surface and through dung and urine, OC and N are returned to the soil.

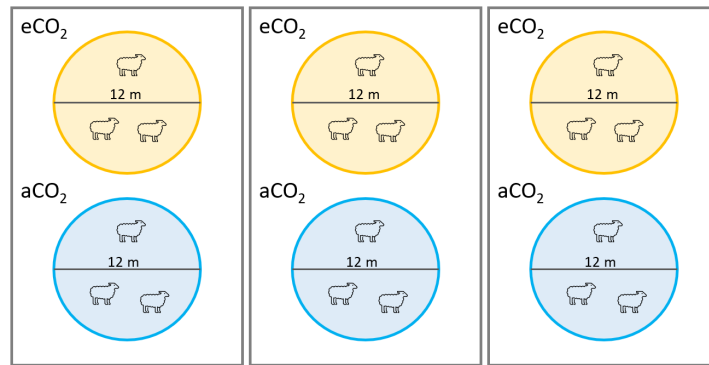


Figure 2. 1: Diagram showing six experimental rings on block design at the New Zealand Free Air CO₂ Enrichment facility. Yellow circles indicate elevated CO₂ rings (eCO₂) and blue circles represent ambient CO₂ rings (aCO₂).

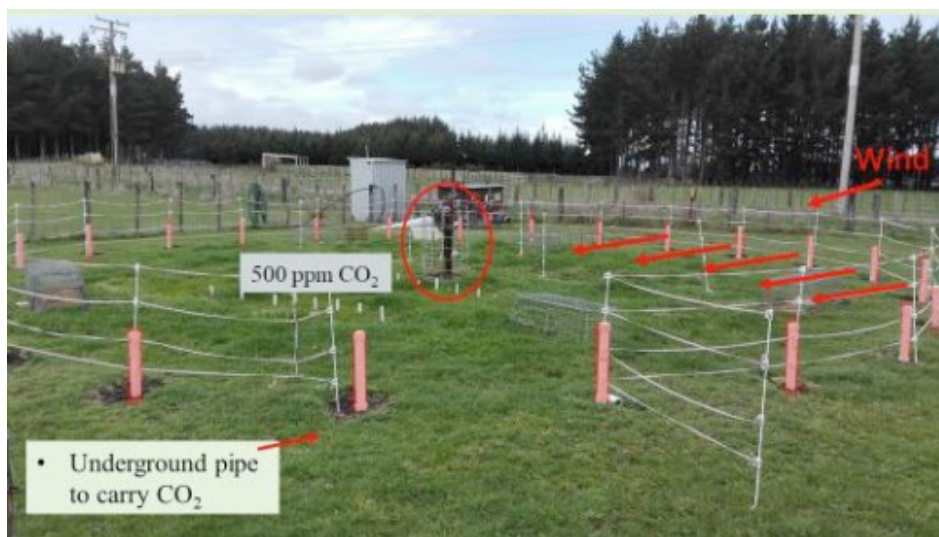


Figure 2. 2: An experimental ring on the NZ Free Air CO₂ Enrichment facility (diagram adapted from Dr Mark Lieffering). Each ring under elevated CO₂ treatments is delimited by 24 standpipes connected underground by a pipe carrying CO₂. A monitor in the centre of the ring measures continuously CO₂ level, wind speed and direction to ensure the target CO₂ concentration is reached. Depending on the monitor measurements certain pipes will emit CO₂ while others remain partially or completely closed.

The botanical composition at the site comprises a mix of 25 vascular plant species with C₃ and C₄ grasses, legumes, and forbs (Edwards et al., 2001). The rings are annually fertilised; average

application rates over the last 5 years were 38, 86, 96 and 100 kg ha⁻¹ of elemental phosphorus (P), potassium (K), sulphur (S) and calcium (Ca) respectively. Note that the only *de novo* additions of N are through biological N₂ fixation and atmospheric depositions.

The soil at the NZ-FACE facility is a Pukepuke black sand (Mollic Psammaquents) with a 0.25 m black loamy, fine sand top horizon (Cowie and Hall, 1965). In November 2005, Pukepuke soil collected from outside the rings, along with the Stratford soil (a Entic Dystrandept) were placed in mesocosm cores (250 mm diameter to a depth of 300 mm) and incorporated into each ring. In New Zealand, Andisols (which includes the Stratford soil) are found in several regions and are commonly used for pastoral farming and horticultural production, due to their physical properties and resilience.

The Stratford soil is fertile, well-drained soil that is formed from volcanic ash containing allophane. It is typically a light-coloured, fine-textured soil that is high in OM and nutrient content. It is well-suited for a wide range of crops, including pasture, forage, and horticultural crops, due to its fertility. The Stratford soil is typically rich in short-range ordered silicates, such as allophane. These minerals have been identified as important components on soil OC persistence due to their ability to strongly bond with OC, thus stabilizing and protecting it from degradation and mineralization (Shen et al., 2018).

Including the Stratford soil, a Vitric Orthic Allophanic soil in the experiment along with the Pukepuke a Peaty Sandy Gley soil allows for exploring the influence of the soil mineralogy and associated physiochemical properties of a soil on the sequestration, partitioning and persistence of soil OC under eCO₂.

2.4.3.1 Above- and below-ground response to elevated CO₂ at the NZ-FACE facility

Edwards et al. (2001) found a positive growth response of *L. perenne* and a negative response for *A. capillaris* to eCO₂ at the NZ-FACE facility, suggesting that the effect of eCO₂ is species-dependent. Similar results have been reported by Deng et al. (2016). Gentile et al. (2011) suggested that nutrient availability (N and P) is a limiting factor in sustaining enhanced growth rate under eCO₂ at the NZ-FACE facility.

An increased rate of belowground OC inputs (Allard et al., 2005) due to a faster root turnover rate has been reported under eCO₂ (Allard et al., 2004). Allard et al. (2005) also reported that an increase in microbial activity increased the loss of OC through respiration.

Increased soil respiration under eCO₂ can be associated with an increase in soil OM priming, as found in low-nutrient soils (Jiang et al., 2020). The Pukepuke soil at the NZ-FACE facility has shown reduced hydrophobicity under eCO₂ (Newton et al., 2004), which can modify soil water dynamics by increasing the infiltration capacity. Despite the non-significant short-term response (< 10 years) of OC stock in soils (0 - 50 mm) under eCO₂, a significant increase in soil respiration rate, microbial biomass C and labile OC fractions have been observed after further exposure to eCO₂ (> 10 years; Ross et al. 2013).

Overall, the grazed legume-based pasture under eCO₂ at the NZ-FACE on the Pukepuke soil has undergone changes in the botanical composition of the pasture (Newton et al., 2014), soil nutrient dynamics (Gentile et al., 2012) and hydrophobicity (Newton et al., 2004), root biomass and turnover (Allard et al., 2005), belowground OC inputs, and N dynamics (Allard et al., 2003). These changes have yet to translate into a significant detectable change in OC and N stocks or a widening in the C:N ratio of the organic fraction.

2.5 The potential of organic carbon sequestration in soils

The capacity of soil to sequester OC depends on the balance between photosynthetic rate, biota respiration, and the inherent capacity of the biogeochemical system to process, store, and preserve OC. Soil OC can only increase if the OC supply to soil is in excess of soil OC losses, and its long-term persistence – which is conditioned by functional complexity (Lehmann et al., 2020) – favours soil OC stability. Soil OC persistence depends not only on the physical protection of the soil OC and the chemical properties of soil OC, but also on the complex level of interaction among soil-plant-microbe systems and on abiotic conditions (Liang and Balser, 2012; Cotrufo et al., 2015; Liang et al., 2017; Sokol and Bradford, 2019; Lehmann et al., 2020). Proving the persistence of newly added OC, in addition to existing soil OC over the long term is difficult due to the challenges of detecting a small increase against a large background soil OC pool, in addition to often large spatial and temporal variability (Ross et al., 2004; Polley et al., 2011).

2.5.1 Soil organic carbon partitioning and persistence

Soil OC includes a range of organic structures derived from the ongoing decomposition and processing of plant OC-derived inputs (i.e., senescent shoots and roots, and root exudates) and OC-derived from macro and microfauna (Cotrufo et al., 2015). Increasing soil OC, can improve soil properties, functions and services in addition to offsetting anthropogenic CO₂ emissions (Whitehead et al., 2018), and this effect persists as long as the soil OC is stabilized and protected from further decomposition.

Recent studies have emphasised the key role of the microbial community in OC stabilization (Liang et al., 2017; Sokol and Bradford, 2019;). Liang et al. (2017) define two pathways to explain the processes leading to OC stabilization through *in vivo* turnover (an anabolic process

and *ex vivo* modification (a catabolic process; Figure 2.3). The *in vivo* turnover refers to soil OC that derives from decaying microbial-derived OC (Conant et al., 2011) whereas the *ex vivo* modification refers to the decomposition of plant-derived OC into smaller molecules through microbial degradative exo-enzymes without becoming part of microbial cells (Liang et al., 2017). In other words, the soil OC pool is a combination of the OC that has been assimilated by microbes and subsequently stored after their death (*in vivo* turnover) and residual OC components of un-ingested litter (*ex vivo* modification), along with fresh plant detritus. Both dominant pathways can lead to a continuum of soil OC fractions, from labile to stable OC, still the majority of stable soil OC pool derives from the *in vivo* turnover pathway (Cotrufo et al., 2015; Lehmann and Kleber, 2015; Liang et al., 2017).

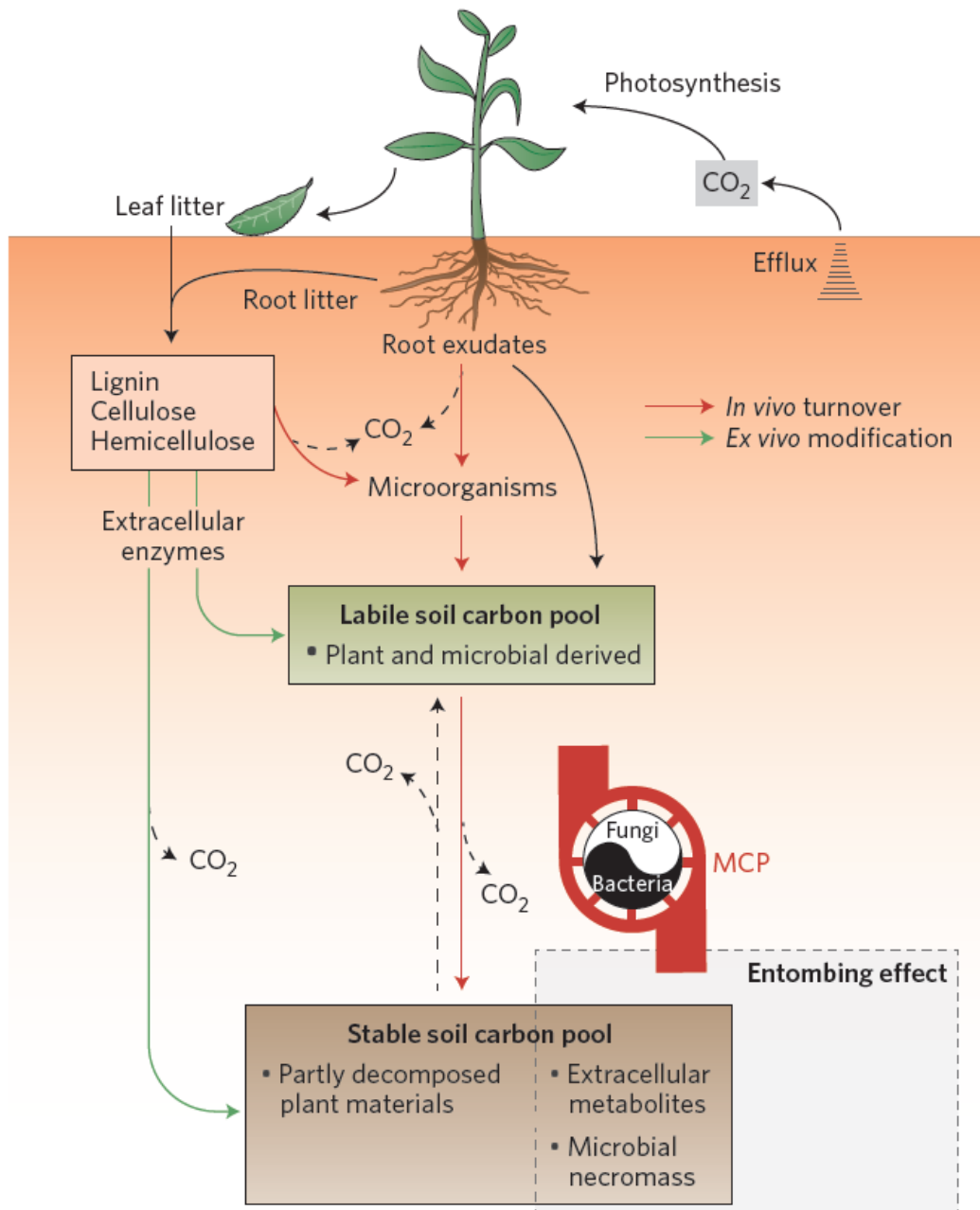


Figure 2. 3: Schematic diagram of microbial metabolic processes involved in the soil carbon cycling in terrestrial ecosystems (Liang et al., 2017).

It has been more and more accepted that soil OM is a continuum of organic material at different stages of decomposition (Horwath et al., 2015) which differ in its susceptibility to decomposition (Lehmann and Kleber, 2015). While the labile OC pool has a key role in the support of the microbial community (and to indirectly support plant growth through the

mineralisation of nutrients), the stable OC pool contributed to the delivery of other OM services, including the C sequestered to contribute to mitigating the consequences of climate change (Chenu et al., 2019). Despite the importance of soil OC dynamics in the functioning of agroecosystems, soil OC turnover and soil OM preservation are still not well understood (Shen et al., 2018; Lehmann et al., 2020; Kebler et al., 2021).

2.5.2 Soil organic carbon protection

There are multiple conceptual models on how soil OM is protected, all aimed to help explain soil OC stabilization processes, soil aggregation and soil OM turnover (Figure 2.4; Lehmann and Kebler, 2015). Soil aggregates are a combination of inorganic soil particles (i.e., sand, silt, and clay), OM and Fe/Al oxyhydroxides, with the latter two acting as binding agents keeping soil particles together (Baumhardt and Schwartz, 2005). Many authors agree on three main mechanisms of soil OC stabilization (Six et al., 2000; Kögel-Knabner et al., 2008; von Lutzow et al., 2008; Horwath et al., 2015). First, recalcitrance by inherent molecular physicochemical stability, which only applies to carbonised materials with condensed aromatic C in their structures, as is the case of pyrogenic C (von Lutzow et al., 2008). Second, protection from decomposers due to spatial inaccessibility and reduced oxygen diffusion within soil aggregates (Six et al., 2001; Six et al., 2002). Third, a chemical association of organic ligands with clay minerals and short-range order iron/aluminium (Fe/Al) oxy-hydroxides forming mineral-associated organic matter (MAOM; Kögel-Knabner et al., 2008). Thus, soils with higher surface areas and highly reactive minerals (e.g., Fe/Al oxy-hydroxides and allophane) have not

only a higher soil OC content but a higher potential to sequester, store and stabilise larger OC content in the long term.

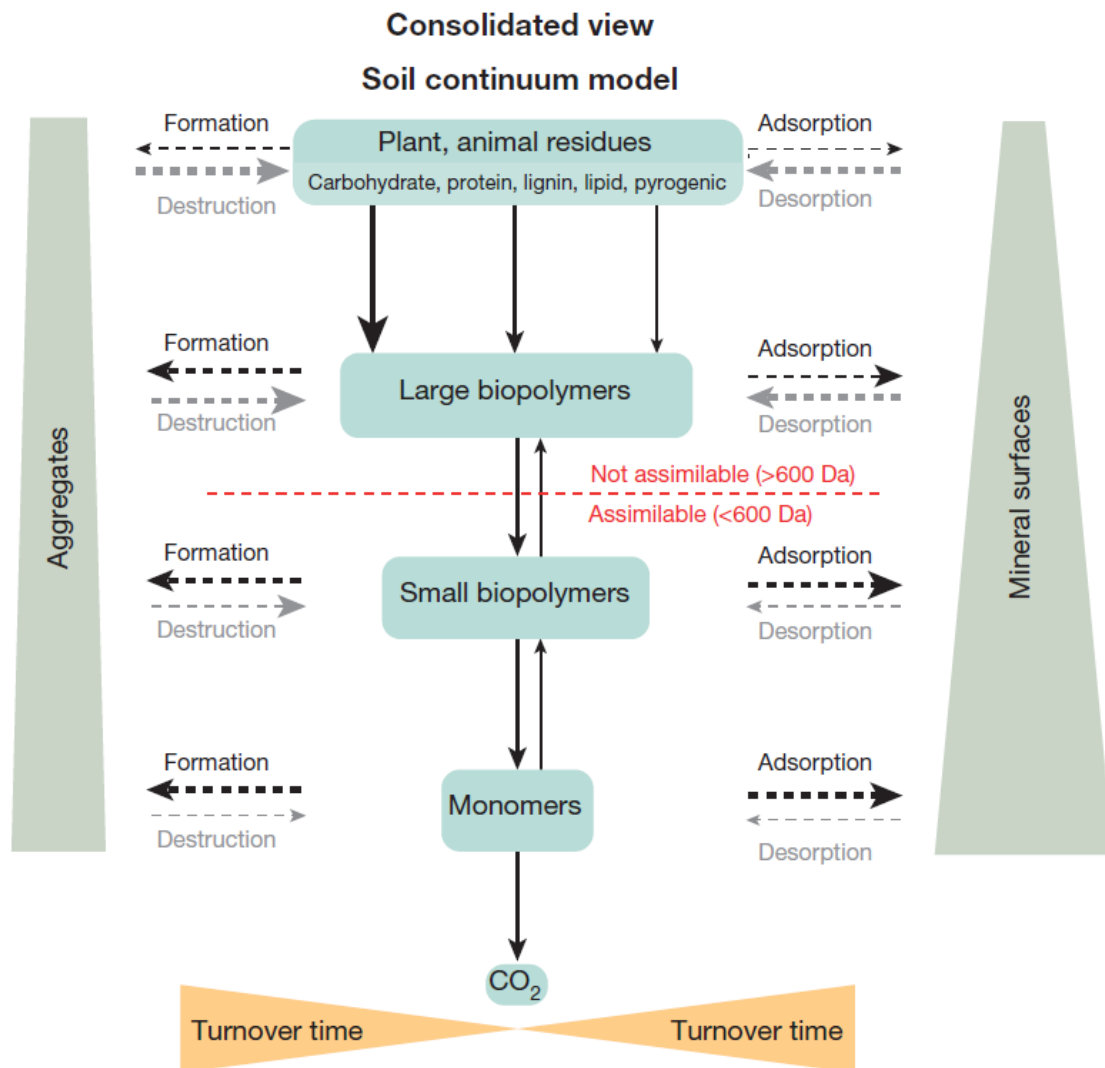


Figure 2. 4: Reconciliation of current conceptual models for the fate of organic debris into a consolidated view of a soil continuum model of organic matter cycles and ecosystem controls in soil (Lehmann and Keblner, 2015).

2.5.3 Analytical techniques for analysing soil organic carbon quantity and quality

There are several analytical techniques available for analysing soil OC quantity and quality (chemical composition). Analytical techniques, such as wet fractionation, pyrolysis (Py)

followed by gas chromatography-mass spectrometry (GC-MS) and thermally assisted hydrolysis and methylation (THM) GC-MS provide valuable information on the quantity and quality of the soil OC pool. By combining these techniques with soil OC content and C/N ratio, the origin and chemical structure of different soil OM components can be examined (Derenne and Quenea, 2015).

Wet fractionation has proven to be an efficient methodology to separate soil aggregates in different soil fractions (Figure 2.5; Six et al., 2002) with distinct stabilization mechanisms and turnover rates (von Lutzow et al., 2008). Studying soil OC and its fractions gives a qualitative analysis of soil aggregation and a quantitative assessment of labile and stable OC pools and turnover rates. Through wet fractionation, the particulate organic matter (POM) fraction (a labile fraction) and MAOM fraction (a stable fraction) can be isolated from and within soil aggregates (Jones and Donatelly, 2004; von Lutzow et al., 2007). Fraction distribution and aggregate stability depend on a variety of biotic and abiotic factors, such as climate, soil type, and land use among others (Dorji et al., 2019). In grazed grasslands, the fraction distribution is dominated by macroaggregates with high aggregate stability, while micro-aggregates are predominant on cultivated land with low aggregate stability (Okolo et al., 2020).

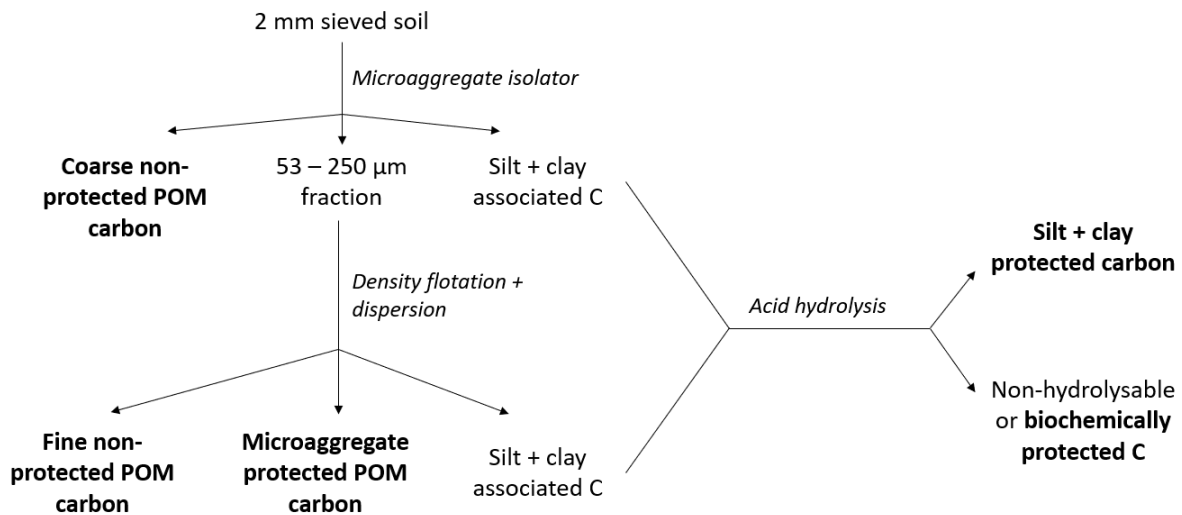


Figure 2. 5: Fractionation scheme to isolate soil organic matter fractions developed by Six et al. (2002).

The coarse POM (cPOM) fraction ($> 250 \mu\text{m}$) consists of a non-physically protected OC and is, therefore, the most labile form and available to decomposers. The micro-aggregates fraction ($250 - 53 \mu\text{m}$) is protected from decomposers through the occlusion in macro-aggregates of partially decomposed cPOM (von Lutzow et al., 2007). The labile pool, which encompasses the cPOM fraction and to some extent the micro-aggregates is strongly susceptible to biotic and abiotic stressors (Six et al., 1998; Sokol and Bradford, 2019) and consists of relatively large quantities of molecules with low chemical diversity (e.g., cellulose, hemicellulose; Lehmann et al., 2020), which can be easily used by microbial decomposers (Weismeyer et al., 2019). The MAOM fraction ($< 50 \mu\text{m}$) is protected by physicochemical interactions among clay minerals, Fe/Al oxy-hydroxides and soil OM present in micro- and macro-aggregates (Horwath et al., 2015) and is characterised by a high chemical diversity and a slow turnover rate and can stabilize OC over centuries and millennia (Sokol and Bradford, 2019). Even though the MAOM fractions have a slow turnover rate, if destabilized, MAOM can also become a source of available nutrients (Conant et al., 2011).

Pyrolysis-GC-MS and THM-GC-MS are two powerful analytical techniques that can be used to analyse the molecular composition of soil OM (Kögel-Knabner, 2000). Pyrolysis-GC-MS involves heating soil samples at high temperatures in the absence of oxygen, which breaks down complex organic compounds into simpler compounds that are then determined and quantified by GC-MS. Similarly, THM-GC-MS involves the thermal hydrolysis of soil samples, followed by GC-MS analysis.

These techniques provide semi-quantitative information on the composition and stability of soil OM, which is critical to understanding the role of the microbial community in OM decomposition and C sequestration (Buurman et al., 2007; Liang et al., 2017; Sokol and Bradford, 2019). By combining these techniques with soil OC content and its C/N ratio, insight into the origin and chemical structure of different soil OM components can be gained (Derenne and Quenea, 2015). By analysing the molecular composition of soil OM under eCO₂, it will be possible to (i) identify which organic compounds are more resistant to decomposition, (ii) assess the contribution of different sources of OM to the soil C and N pools and (iii) assess the potential for C sequestration. This information can help to develop better strategies and management practices to enhance soil C sequestration and for developing better soil OM models in a changing environment.

2.6 Overview and research opportunities

The ability of soil to sequester OC is determined by the interplay of photosynthetic rate, biota respiration, and the inherent capacity of the biogeochemical system to process and preserve OC. The increase in soil OC can occur only if (i) there is a surplus supply of OC that exceeds soil OC losses and (ii) there are mechanism for long-term stabilisation, which is affected by the functional complexity of the system. The stability and persistence of soil OC is influenced

by physical protection, chemical properties, interactions among soil-plant-microbe systems, and abiotic conditions. Demonstrating the long-term persistence of newly added OC in conjunction with existing soil OC is challenging due to the difficulty of detecting small changes in the presence of a large background pool of soil OC and the substantial spatial and temporal variability involved.

Due to differences in the scale, dimensions of the studies, land use, climate and soil type, the influence of eCO₂ on soil OC dynamics is still poorly understood (Ainsworth and Long, 2004; Madhu and Hatfield, 2013). The study of the interaction between eCO₂ and the grazing animal on soil OC stabilization is scarce (Zhou et al., 2016). There is in fact a lack of knowledge on how litter inputs and turnover and their subsequent effect on soil OC dynamics are influenced by eCO₂ (enhancing the photosynthetic rate) under grazing (e.g., defoliation, treading and nutrient return as it influences the shoot to root ratio and their turnover). Due to the complex array of interactions between plant growth, OC turnover rate and nutrient cycling, in a grazed system with a change in CO₂, it is still uncertain at a global scale if the eCO₂ stimulation effect on the C cycle can be sustained (Norby and Zak, 2011; Pendall et al., 2011; IPCC, 2013), especially in grazed grasslands in the long-term. This has profound consequences for developing accurate climate models and for informing policy in a changing environment.

The long-term NZ-FACE facility exploring the impact of eCO₂ on the labile and stable soil OC and N pool of grazed pastures and the subsequent consequences to the global C cycle provide a unique opportunity to advance our understanding of the consequences of eCO₂ as part of future climates in our system. To decipher the partitioning of OC inputs into labile OC and more recalcitrant soil OC with increasing atmospheric CO₂ concentrations, in a changing climate, emphasis needs to be paid to the following:

- (i) Understanding the persistence of soil OC and N stocks in response to long-term exposure to eCO₂ requires a comprehensive approach that goes beyond just

measuring OC and N content at the end of an experiment. To fully grasp the partitioning and persistence of soil OC with increasing atmospheric CO₂, in a changing climate it is important to consider data on above- and below-ground growth over time, as well as the influence of abiotic factors on the stability of the labile pool and the potential destabilization of the stable OC pool due to increased root exudation and respiration (Keiluweit et al., 2015), which is an expected outcome under eCO₂.

- (ii) More needs to be understood on the impact of long-term exposure to eCO₂ on soil OC and N content, stocks, and molecular composition, as well as the interplay and influence of soil type. Some studies have found that the ability of eCO₂ to increase plant biomass and stimulate soil microbial and root respiration is dependent on the soil type, but there is limited knowledge about how differences in soil physiochemical properties such as texture and mineralogy affect the pathways for OC storage and persistence in soils; especially between soils like the Pukepuke soil, a sandy soil derived from sedimentary material, with low OC and few active surfaces with the Stratford soil which is derived from volcanic ash that contains allophane, contributing to its high anion and cation exchange capacity, and the creation of stable organo-metal complexes, that results in the storage of large amount of OC.
- (iii) The interactive effect between long-term exposure to eCO₂ and the grazing animal, especially the influence of defoliation, treading of plant litter and nutrient return in dung and urine on the soil OC and N content and its molecular composition. With sufficient nutrient supply to support enhanced plant growth, and particularly root growth under eCO₂, there might be, in the long-term, a relative increase in microbial necromass and thus, stable OC (Sokol and Bradford et al., 2019). Nevertheless,

Deng et al. (2016) found increases in soil microbial biomass, N mineralization rate and nitrification rate, but no change in mineral N, indicating an increased demand for nutrients to support the enhanced growth rate under eCO₂. Grazing imposes a strong influence on the nutrient cycle which might easily enhance or dilute the effects of eCO₂. As part of the study, we explored the interactive effect between eCO₂ and the grazing animal by including two additional treatments; even though sheep at the NZ-FACE facility graze the rings year-round, little dung or urine is deposited, creating an edge effect within the rings (within 0.5 m from the fence) because of the behaviour of the animals within the ring (as the animals avoid putting their posterior near the electric fence). This has created an area over 20 years where the pasture has been defoliated by the sheep, yet dung, urine and treading are avoided creating an area of lower nutrient status within each ring. With this in mind, three areas were selected within each ring to simulate different treatments of defoliation and nutrient return by sheep (i) the centre of the ring where the sheep graze, tread, defecate and urinate; (ii) the edge of the ring where the sheep graze, but do not tread, defecate or urinate; and (iii) an area of the ring protected from the sheep by metallic cages with the pastures hand cut at the same time the rings are grazed (two cages of 1 m² each approximately inside of each ring).

Chapter 3 Changes in soil aggregate size fractions and molecular composition of soil organic matter in a grazed pasture after 22 years of elevated CO₂

Abstract

In addition to driving climate change, the rising concentration of atmospheric carbon dioxide (CO₂) has been frequently observed to exert a profound influence on biological systems. The Free Air Carbon Dioxide Enrichment (FACE) facilities have shown that elevated CO₂ (eCO₂) increases herbage accumulation and the amount of organic carbon (OC) produced and added to the soil. Higher OC inputs can result in an increase in soil OC content if this is subsequently protected from decomposition. However, the magnitude of this effect is strongly debated due to the lack of significant results worldwide. This study assessed the prolonged impact of eCO₂ on shoot biomass, soil OC, and nitrogen (N) stocks. We further explored changes in soil fractions, nutrient status, and organic matter composition, providing insights into the debated magnitude of eCO₂ effects on soil OC stabilisation pathways. We found that in the past 10 years independent of the CO₂ treatment, there has been a reduction of OC and N stocks despite a boost in shoot biomass. Furthermore, after 22 years of eCO₂ exposure, we found no increase in shoot-biomass, and no increase in soil OC or N stocks or changes in the soil fraction at three soil depths (0 – 50, 50 – 150, 150 – 250 mm). Nevertheless, eCO₂ modified the soil nutrient status (phosphate (PO₄), in particular) and increased polysaccharides and aliphatic proportions in the labile pool. The persistent reduction in OC and N stocks over the past decade, irrespective of CO₂ treatment, highlights complex interactions influenced by the concurrent context of climate change affecting the experiment (e.g., changes in drought and re-wetting cycles, in parallel with a reduced PO₄ and sulphate availability). Our results indicate that priming of the labile and newly added OC has been occurring for at least 10 years under both, ambient and elevated CO₂ treatments.

Keywords: elevated CO₂, FACE facility, grazing, soil organic carbon, carbon sequestration

3.1 Introduction

Anthropogenic greenhouse gas (GHG) emissions, especially carbon dioxide (CO₂), have increased since the start of the industrial era, and despite international efforts to limit emissions, future increases are expected (IPCC, 2014). The increased concentration of atmospheric CO₂ has been widely acknowledged as a significant driver of changes in global climate (IPCC, 2014). However, its impact extends beyond just climate, as it has been frequently observed to exert a profound influence on biological systems. This is largely a result of its effects on photosynthesis (Ainsworth and Long, 2020), which ultimately leads to alterations in organic carbon (OC) inputs to soils. This can have downstream effects on soil carbon dynamics (Terrer et al., 2020), influencing both the amount and quality of soil organic matter (OM) and OC inputs to soils and leading to changes in the functioning of ecosystems (Terrer et al., 2018; Kuzyakov et al., 2019).

Grasslands account for 70% of the agricultural land worldwide (Conant et al., 2011; FAO, 2019) and contain about 20% of global soil OC stocks (Whitehead et al., 2018). Therefore, only small changes in grasslands soil OC stocks would significantly impact the global atmospheric CO₂ pool (Liang et al., 2017; Chenu et al., 2019; Sitters et al., 2020).

The capacity of soil to sequester OC depends on the balance between photosynthetic rate, biota respiration, and the inherent capacity of the biogeochemical system to preserve OC. Soil OC can only increase if (i) the OC supply to soil is in excess of soil OC losses, and (ii) it persists in the long-term – which is conditioned by functional complexity (Lehmann et al., 2020) – favouring soil OC stability. Soil OC persistence depends not only on the physical protection of the soil OC and the chemical properties of soil OC, but also on the complex level of interaction within the soil-plant-microbes system and on abiotic conditions (Liang and Balser, 2012; Cotrufo et al., 2015; Liang et al., 2017; Sokol and Bradford, 2019; Lehmann et al., 2020).

Proving the persistence of newly added OC, in addition to soil OC existing over the long term, is difficult due to the challenges associated with detecting small changes in OC against a large background soil OC pool and large spatial and temporal variability (Ross et al., 2004; Polley et al., 2011). This adds to the difficulty of developing accurate climate models and for informing policy in a changing environment.

There are different conceptual models on how soil OM is protected, all aimed to explain soil OC stabilization processes within soil aggregates (Kebler et al., 2007; Lehmann and Kebler, 2015). Soil aggregates can be differentiated based on their fraction size, stability and turnover rates (Six et al., 2002). The soil aggregates are isolated as particulate organic matter (POM) fraction, which is a labile fraction consisting of coarse POM (cPOM) and micro-aggregates, while the mineral-associated organic matter fraction (MAOM) is a stable fraction (Six et al., 2002; Jones and Donatelly, 2004; von Lutzow et al., 2007). Recent studies have emphasised the key role of the microbial community in OC stabilization within soil aggregates (Cotrufo et al., 2015; Liang et al., 2017; Sokol and Bradford, 2019), identifying two pathways for soil OC partitioning. First, the OC that has been assimilated by microbes and subsequently stored after their death (through an anabolic process from decaying microbial-derived OC; Cotrufo et al., 2015). Secondly, the residual OC components of un-ingested litter (through a catabolic process by which extracellular enzymes break down plant-derived molecules; Liang et al., 2017). Both pathways can lead to a continuum of soil OC fractions, from labile (cPOM and micro-aggregates) to stable OC (MAOM), yet the majority of OC in the stable soil OC pool derives from the anabolic pathway (Liang et al., 2017). Many authors agree in that there are three main mechanisms of soil OC protection within soil aggregates (Six et al., 2000; von Lutzow et al., 2008; Kögel-Knabner et al., 2008). The cPOM fraction ($> 250 \mu\text{m}$) consists of unprotected OC within aggregates and is, therefore, the most labile form and available to decomposers. The micro-aggregates fraction ($250 - 53 \mu\text{m}$) is protected from decomposers through occlusion

within macro-aggregates of partially decomposed cPOM (von Lutzow et al., 2007). The labile pool, which encompasses the cPOM fraction and to some extent the micro-aggregates is strongly susceptible to biotic and abiotic stressors (Six et al., 1998; Sokol and Bradford, 2019) and consists of relatively large quantities of molecules with low chemical diversity (e.g., cellulose, hemicellulose; Lehmann et al., 2020), which can be easily used by microbial decomposers (Weismeyer et al., 2019). The MAOM fraction ($< 53 \mu\text{m}$) is protected by physico-chemical interactions among clay minerals, oxy-hydroxides and soil OM present in micro- and macro-aggregates (Horwath et al., 2015) and is characterised by a high chemical diversity and a slow turnover rate, and can stabilize OC over centuries and millennia (Sokol and Bradford, 2019). However, it can be destabilised in specific circumstances (Keiluweit et al., 2015), for example with a change in pH or under nutrient-deficient conditions.

Pyrolysis followed by gas chromatography and mass spectrometry (GC-MS) and thermally assisted hydrolysis (THM) GC-MS are powerful analytical techniques to semi-quantitatively identify the molecular composition of soil OM in the soil fractions (Kögel-Knabner, 2000; Derenne and Quenea, 2015). Combined with soil C content and its C/N ratio, these techniques can help assess the key role of the microbial community in OC stabilization and residual OC components processed by extracellular enzymes (un-ingested litter; Buurman et al., 2007a; Liang et al., 2017; Sokol and Bradford, 2019).

The global network of Free Air Carbon Dioxide Enrichment (FACE) facilities has been set up with the main objective of studying the effects of elevated CO_2 concentrations ($e\text{CO}_2$) on the response of plants in diverse ecosystems and under a range of practices. While most efforts have been concentrated on the aboveground rather than the belowground plant responses (Jones et al., 2014), the results generated to date on both the above- and below-ground plant responses has been widely variable.

From the early grassland FACE experiments (< 5 years of exposure), it was strongly suggested that the expected increase in net herbage accumulation (NHA) under eCO₂ could lead to an increase in soil OC in some situations (Jastrow et al., 2005). That said, three out of the eight FACE studies on grasslands with ≥ 5 of exposure – the Swiss-FACE (Six et al., 2001; van Groenigen et al., 2002; de Graaff et al., 2004; Xie et al., 2005; van Kessel et al., 2006 and Theis et al., 2007), the Giessen-FACE (Keidel et al., 2018) and the USDA-ARS High Plains Grasslands Research Station FACE (Carrillo et al., 2018) – have reported no change in soil OC stock under eCO₂. The Jasper Ridge Global Change Experiment (JRGCE) in California concluded that soil OC content increases only under nitrogen (N) fertilisation (Liang et al., 2015). Similarly, the BioCon facility in Minnesota (Dijkstra et al., 2004) found an increase in soil OC only when N fertilisation increased NHA. The Tasmania-FACE (Pendall et al., 2011) has reported that soil OC content increases only under a C₄ sward and not under C₃ plants. The CLIMAITE facility in Denmark reported an increase in soil OC content and stocks in the short-term (Vestergard et al., 2016; Dietzen et al., 2019), but Thaysen et al. (2017) suggested that soil OC turnover has also been stimulated, leading to a potential loss of soil OC stock over time.

Within the first years of eCO₂ exposure at the NZ-FACE facility (< 10 years), the only grassland FACE experiment grazed by livestock, the aboveground herbage production has somewhat increased under eCO₂ (Newton et al., 2014), the botanical composition has been altered (Edwards et al., 2001), and root biomass and turnover rate have increased (Allard et al., 2005), all leading to an increase in the belowground OC inputs. The eCO₂ exposure has reduced the soil hydrophobicity (Newton et al., 2004), depleted the soil of phosphate (PO₄; Gentile et al., 2012), and boosted N mineralization rates (Ross et al., 2004), but these changes did not translated into a significant detectable increase in either OC and N stocks or a widening in the

C/N ratio of the organic fraction in the first 12 years (1997 – 2009) of the study (Gentile, unpublished data).

Here, we report on the above- and below-ground response at the NZ-FACE (a sheep-grazed mixed pasture experiment) after prolonged (22 years) exposure to eCO₂, and compare that with the findings reported after the first 12 years. In addition to an investigation into the effect of long-term exposure to eCO₂ on pasture composition and herbage accumulation, we investigated the impact of the soil OC inputs (shoot-, root- or microbial-derived OC) have on the labile pool (cPOM and micro-aggregates) and/or stable (MAOM) pool. Furthermore, we explore if the anticipated increase in OC inputs from above- and below-ground plant response under eCO₂ has caused a priming effect and accelerated OC mineralization, generating more labile inputs and more microbially derived storage of soil OC, and how any changes influence the molecular composition and associated functions of the soil OC stabilization pathways.

To explore the effects of long-term exposure to eCO₂ on the above- and below-ground response at the NZ-FACE and to determine whether C storage and soil OC persistence have been favoured or limited over 12 and 22 years of eCO₂ exposure, we evaluated two periods of five years each (period I: 2005 – 2009 and period II: 2015 – 2019). Over both periods, we assessed net herbage accumulation (NHA) and botanical composition in addition to assessing the soil pH and nutrient status (except in years 2015 and 2018; see Methods section). We also determined soil OC stocks, along with the partitioning of OC within the soil fractions at the end of both periods (2009 and 2019) to three soil depths (0 – 50, 50 – 150 and 150 – 250 mm). Furthermore, to provide insight into the long-term effect of eCO₂ on the stabilization pathways we assessed the molecular composition of the soil fractions at the end of period II (performed only at 50 – 150 and 150 – 250 mm depth).

3.2 Methods

3.2.1 Experimental setup

The NZ-FACE facility is in a temperate grazed legume-based pasture located near Bulls, Manawatu-Whanganui, New Zealand (40°14' S, 175°16'E). Since 1997, the NZ-FACE facility has been used to investigate the effects of increasing atmospheric concentration of CO₂ on pasture biomass production, botanical composition, nutrient cycling and soil OC dynamics under sheep grazing (Dodd, 2013). The NZ-FACE facility is the only FACE facility worldwide examining the influence of eCO₂ on the above- and below-ground response of a pasture under grazing management, including changes in soil OC and N stocks.

The facility is divided into three blocks with two circular plots within each block (12 m diameter “ring”; Extended Data Figure 3.1a). The rings were chosen in 1997 based on their initial botanical composition (Newton et al., 2006). In each block, one ring is exposed to the ambient atmospheric CO₂ concentration (aCO₂) and the other ring is treated with eCO₂ on a daily basis throughout the photoperiod. Over the course of the study dating back to 1997 the CO₂ treatment has not been continuous, between 2011 and 2013 the NZ-FACE facility was refurbished and there was no difference in the atmospheric CO₂ concentration. Additionally, as aCO₂ has increased (from 363 ppm in 1997 to 412 ppm in 2019), the original difference in CO₂ concentration between ambient and elevated treatment has decreased (IPCC, 2021). To maintain the difference in CO₂ concentration between treatments, the CO₂ enrichment was increased to 500 ppm in the eCO₂ rings in 2011 - a concentration likely to be reached during this century (IPCC, 2014).

Edwards et al. (2001), Ross et al. (2004) and Newton et al. (2014) provide a detailed history of the study site, including soil and pasture characteristics, the installation process, and the scheduling of grazing practices inside the rings. In brief, the soil at the site is Pukepuke black

sand (a Mollic Psammaquent; Soil Taxonomy, 2006) with a 0.25 m black loamy, fine sand top horizon (Cowie and Hall, 1965), a medium-fertility sandy soil. When the aboveground biomass is around 1800–2000 kg dry matter (DM) ha⁻¹, three to four sheep are introduced to the rings and left to graze (Extended Data Figure 3.1b) until there is 800 kg dry DM ha⁻¹ of aboveground biomass (Newton et al., 2014). There are 7 – 15 grazing episodes per year depending on the herbage growth. The rings are annually fertilised to support herbage growth; the average application rates over the last 5 years were 38, 86, 96 and 100 kg ha⁻¹ of elemental phosphorus (P), potassium (K), sulphur (S) and calcium (Ca) respectively. Note that the only *de novo* additions of N are through biological N₂ fixation.

3.2.2 Above- and below-ground analyses

During 2005 – 2009 and 2015 – 2019 (periods I and II, respectively), abiotic and botanical data were collected at the site. At the end of each period, soil samples were collected to evaluate soil OC storage, partitioning and persistence.

3.2.2.1 Abiotic factors

Mean annual precipitation (MAP) and mean annual temperature (MAT) were calculated from meteorological data. The site is characterized by heavy precipitation events during winter and by summer droughts that result in low-standing biomass and a high proportion of bare ground (3–5% of the ground area; Edwards et al., 2001). It is worth noting that between 1997 and 2019, the MAT at the site has increased by 0.8 °C (Extended Data Figure 3.2a), while MAP had a slight increase of 70 mm between 1997 and 2019 (Extended Data Figure 3.2b). The average MAP and MAT in period I was 978 mm and 14.1°C, while in period II it was 968 mm and 14.8°C, respectively.

Soil moisture and nutrient status measurements were taken with 20 sub-replicates per ring stratified randomly with five measurements per quadrant within each ring. Soil moisture in the top 0 – 120 mm was measured weekly and before and after each grazing episode using a soil moisture meter (Fieldscout TDR 300 Soil Moisture Meter). Soil nutrient levels were determined yearly to evaluate fertilizer needs, and these were applied when required following standard protocols for sheep farming production (Cornforth et al., 1984). For soil nutrient analysis, 20 soil samples (0 – 75 mm depth) were collected from each ring. The samples were combined for each ring and sent to a commercial laboratory (Hills Laboratories, Hamilton, NZ) for soil pH, phosphate (PO₄), sulphate-S (SO₄), soluble Ca, sodium (Na), potassium (K) and magnesium (Mg) analyses. The soil nutrient status was not determined in 2015 and 2018.

3.2.2.2 Grazing practices

During period I there were 35 grazing episodes (7, 5, 8, 7 and 8 in each year between 2005 and 2009). During period II, pasture production allowed more than 50 grazing episodes (ranging between 9 and 14 episodes in each year between 2015 and 2019).

3.2.2.3 Herbage accumulation and botanical composition

As the NZ-FACE facility is under grazing practices, net herbage accumulation (NHA) is calculated considering each grazing episodes and estimated based on the “difference method” (Walters and Evans, 1979). Thus, over time, NHA is calculated by the difference between the herbage biomass standing prior to a grazing event minus the residual from the previous event (e.g., standing biomass pre-graze minus standing biomass the previous post-graze). To determine NHA, herbage biomass was cut (1 m x 0.073 m) at 25 mm aboveground before and after each grazing episode with eight sub-replicates per ring (two measurements per quadrant

within each ring). After each collection, the sub-replicates were combined and stored in a fridge at 2 °C.

As selective grazing has been identified to occur in the field (Newton et al., 2014), only pre-grazing samples were considered to determine the botanical composition prior to every grazing episode. For this, a subsample of the pre-graze above-standing sample was used to determine the botanical composition of each ring. Briefly, fresh herbage samples were separated by species, prior to oven drying (60 °C) to a constant weight; the weight of each species was determined. Pasture species were combined according to plant functional type (C₃ and C₄ grasses, legumes, and other species) for analysis here.

3.2.2.4 Soil organic carbon and nitrogen analysis

Soil cores were collected from the NZ-FACE facility during the southern hemisphere spring in October 2009 and November 2019 and followed an identical method of extraction. Sixteen soil cores (25 mm diameter x 250 mm depth) were collected from each ring (ambient and eCO₂). The cores were divided into three depths (0 – 50, 50 – 150, and 150 – 250 mm).

3.2.2.5 Organic carbon and nitrogen stocks

In both years, eight out of the 16 soil cores per depth were individually oven-dried for 24 hours at 105 °C prior to weighing for bulk density analysis. The remaining eight soil cores from each ring were air-dried, sieved (< 2 mm) and then combined for each ring and depth to generate 18 composite samples. The 2009 bulk soil samples were stored in sealed plastic containers in a dark room for 10 years (until 2019). All bulk samples (2009 and 2019) were analysed in 2019 for total OC and N by dry combustion in an Elementar analyser (Vario Max Cube; Analysensysteme GmbH, Germany). Soil OC and N stocks down to a specific depth were

determined using the equivalent soil mass (ESM) procedure proposed by Wendt and Hauser (2013) to overcome potential masking effects associated with changes in soil bulk density.

3.2.2.6 Organic carbon and nitrogen in soil aggregates

A subsample of the bulk soil composite sample was used for soil fractionation by wet-sieving analysis, following the soil fractionation procedure proposed by Six et al. (2002). Aggregates were physically separated into three aggregate sizes (i.e., diameter, ϕ): cPOM of 250 to 2000 $\mu\text{m } \phi$, micro-aggregates of 53 to 250 $\mu\text{m } \phi$, and silt and clay (MAOM) of $<53 \mu\text{m } \phi$. The isolator unit was composed of two sieves on a horizontal shaker and attached to a source of running RO water. Individually, the samples were soaked in RO water for 5 min and shaken in a plastic cylinder for 15 min at 150 rpm, this allowed the cPOM to be collected on a 250 μm sieve, while micro-aggregates were subsequently retained in a 53 μm sieve. After the wet sieving, the three aggregate sizes (cPOM, micro-aggregates and MAOM) were collected in aluminium pans, and oven dried at 60 °C until a constant weight, in order to determine the size of each fraction in the soil sample. As with the bulk soil samples, soil fraction samples collected in 2009 were stored until 2019; all samples were analysed by dry combustion in an Elementar analyser to determine the OC and N concentration of each fraction (Vario Max Cube; Analysensysteme GmbH, Germany). The proportion of OC and N out of the total soil OC and N pool was calculated based on the fraction size and their OC and N concentration.

3.2.2.7 Soil fractions molecular composition analytical procedure

Based on thermal degradation, macro-molecules in the soil fractions are broken down depending on their stability against high temperatures and can be identified through gas chromatography (GC) and quantified through mass spectroscopy (MS; Derenne and Quenea,

2015). Analytical Pyrolysis-GC-MS and thermally assisted hydrolysis methylation (THM) GC-MS, which allow determination of the composition of soil OM after thermal degradation of macro-molecules and subsequent separation (through GC) and identification/quantification (through MS) of their fragments (Derenne and Quenea, 2015), were used to investigate if the potential long-term impact of eCO₂ could be reflected in changes in the molecular composition of soil OM. This approach, combined with soil OC and N content, can be used to assess the role microbial community plays in the OC stabilization, alongside the residual OC components of un-ingested litter (Liang et al., 2017; Sokol and Bradford, 2019).

Soil fractions samples from 2019 were analysed through Py-GC-MS and THM-GC-MS to identify 134 and 72 chemical compounds, respectively (Extended Data Tables 3.1 and 3.2 respectively) which were classified based on their chemical structure (Buurman et al., 2007; Extended Data Tables 3.3 and 3.4, respectively). We quantified the relative proportions of the pyrolysis and THM products. A mild acid pre-treatment was performed on finely ground samples to remove reactive mineral phases such as iron (oxy)(hydro)oxides and avoid the interference of the mineral phase with the determination of the pyrolytic products (Zegouagh et al., 2004). Briefly, 0.2 g of sample was weighed into a centrifuge tube, to which an aliquot of 10% HCl was added to dissolve carbonates, and then 2% aqueous HF solution to reach the 40 mL volume. After 24 hrs of shaking, the suspensions were centrifuged (2500 rpm for 10 min) and the supernatant was discarded. The obtained residue was then rinsed three times in distilled water to wash away salts and remaining acid (with centrifugation/decantation cycles in between). The final residues were dried at 50°C and homogenized before pyrolysis and THM analysis.

Conventional Py-GC-MS was performed with a Pyroprobe (CDS Analytical) coupled to an 8860 GC and 5977 MS detector (Agilent Technologies). The samples (1 mg of ground and HF-treated material) were embedded in glass wool-containing fire-polished quartz tubes and

pyrolyzed at 650°C for 20 seconds (heating rate 10°C ms⁻¹). The pyrolysis-GC interface, GC inlet and GC-MS interface were set at 325°C. The GC was equipped with a non-polar HP-5MS 5% phenyl, 95% dimethylpolysiloxane column (length 300 mm; internal diameter 0.25 mm; film thickness 0.25 µm). Helium was used as the carrier gas (constant gas flow, 1 ml min⁻¹). The GC oven was heated from 60 to 325°C at 20°C min⁻¹. The ion source of the MS operated in electron impact mode (70 eV) at 230°C and the quadrupole detector was held at 150°C, measuring products based on the mass to charge number of ions ratio (m/z) in the 50 – 500 range.

The instrumentation and most parameters for Py-GC-MS, were also used for THM-GC-MS. Before inserting the sample-containing quartz tubes, an aliquot of 25% tetramethylammonium hydroxide (aqueous TMAH from Sigma-Aldrich) was added and the mixture was allowed to stand for one hour. Analytical parameters that differ from the ones for Py-GC-MS are the use of a five-minute solvent delay (to allow the reactant and solvent to elute before activation of the MS), and a GC oven temperature program from 70 to 325 at 20 °C min⁻¹ with a five-minute initial and three-minute final isothermal hold periods. Relative proportions of the pyrolysis and THM products were calculated as the percentage of the total quantified peak area (TQPA), using the m/z ratio of each product.

3.2.3 Statistical analysis

Linear mixed effect models (lme) for nested block design followed by an analysis of variance for simple effects (if needed), pairwise tests and permutations were applied to abiotic, NHA, botanical composition, and soil C and N data. The differences between soil depth and CO₂ treatments and their interaction effect over the last 22 years of exposure (yearly and by period)

were explored. R Studio was used to run all the statistical analysis through “lme” and “predictmeans” packages (RStudio version 1.2.5033).

The pyrolysis and THM results were evaluated using principal components analysis (PCA) to identify mechanisms with major influence on product distributions in the whole dataset. The relative proportions of individual products (% TQPA), sums of types of products (% TQPA) and the principal components obtained by PCA were used to compare results from Py-GC-MS and THM-GC-MS (individual compounds % as input) and to compare these results to OC content and C/N ratio. The qualitative analysis was followed by a lme analysis on the sum of the type of products and each individual product to identify the effects of CO₂ treatment, depth, and soil fractions on the soil OM molecular composition.

3.3 Results and discussion

3.3.1 Aboveground plant biomass response to elevated CO₂ between period I and II

The cumulative NHA under eCO₂ was higher than under aCO₂ during both periods (period I by +12.0%; period II by +6.1%), but the differences were not significant ($p = 0.4713$; Figure 3.1a). Across the CO₂ treatment, period II had 34% more cumulative NHA compared to period I ($p = 0.0007$; Figure 3.1a). In both periods, NHA shows high variability between years ($p < 0.0001$) ranging on average from 72.8 to 136.4 g m⁻² after each grazing episode, leading to between 796.5 to 1,421.9 g m⁻² of herbage accumulated each year (Extended Data Figure 3.3a).

For pasture composition, no CO₂ effect was observed in either the average proportion of C₃ or C₄ grasses, or the proportion of other species within each period (Figure 3.1b). Yet, some inconsistent effect was found on the proportion of legumes (CO₂ x time interaction, $p =$

0.0254). For example, in years 2009 and 2017, pastures under eCO₂ had a larger legume proportion than pastures under aCO₂ conditions, but in year 2015 the opposite was found (Extended Data Figure 3.3d). High variability in the average proportion of C₃ and C₄ grasses, legumes and other species (all $p < 0.0001$) between years in both CO₂ treatments was also found (Extended Data Figure 3.3b, c, d and e, respectively). Overall, the average proportion of C₃ grasses did not change between the two periods, while C₄ grasses and legumes increased from 1.8 and 3.3% (respectively) in period I to 4.2% and 7.7% in period II, respectively ($p = 0.0003$ and $p < 0.0008$, respectively; Figure 3.1b). These increases were accompanied by a decrease in the average proportions of other species (e.g., *Plantago lanceolata* L., *Cerastium glomeratum* Thuill, *Hypochaeris radicata* L.) from 11.9% in period I to 4.9% in period II ($p < 0.0001$).

Most studies have reported a boosting of NHA during the first years of eCO₂ application (Ainsworth and Long, 2005; Edwards et al., 2001; Deng et al., 2015). However, climatic conditions (rainfall and temperature; Liang and Balser, 2012), plant species (Pendall et al., 2011) and nutrient availability (Gentile et al., 2012) are likely to influence the response to eCO₂ resulting in either an increase (Ainsworth and Long, 2005), a decrease (Jiang et al., 2020), or no effect in NHA. High NHA variability over time and under different CO₂ environments in our study indicates that herbage production of the system was dependent on other and stronger factors. With no N fertiliser applied to the pastures at the NZ-FACE, the rhizobia in a symbiotic relationship with the legumes is the only source of N through N₂ fixation.

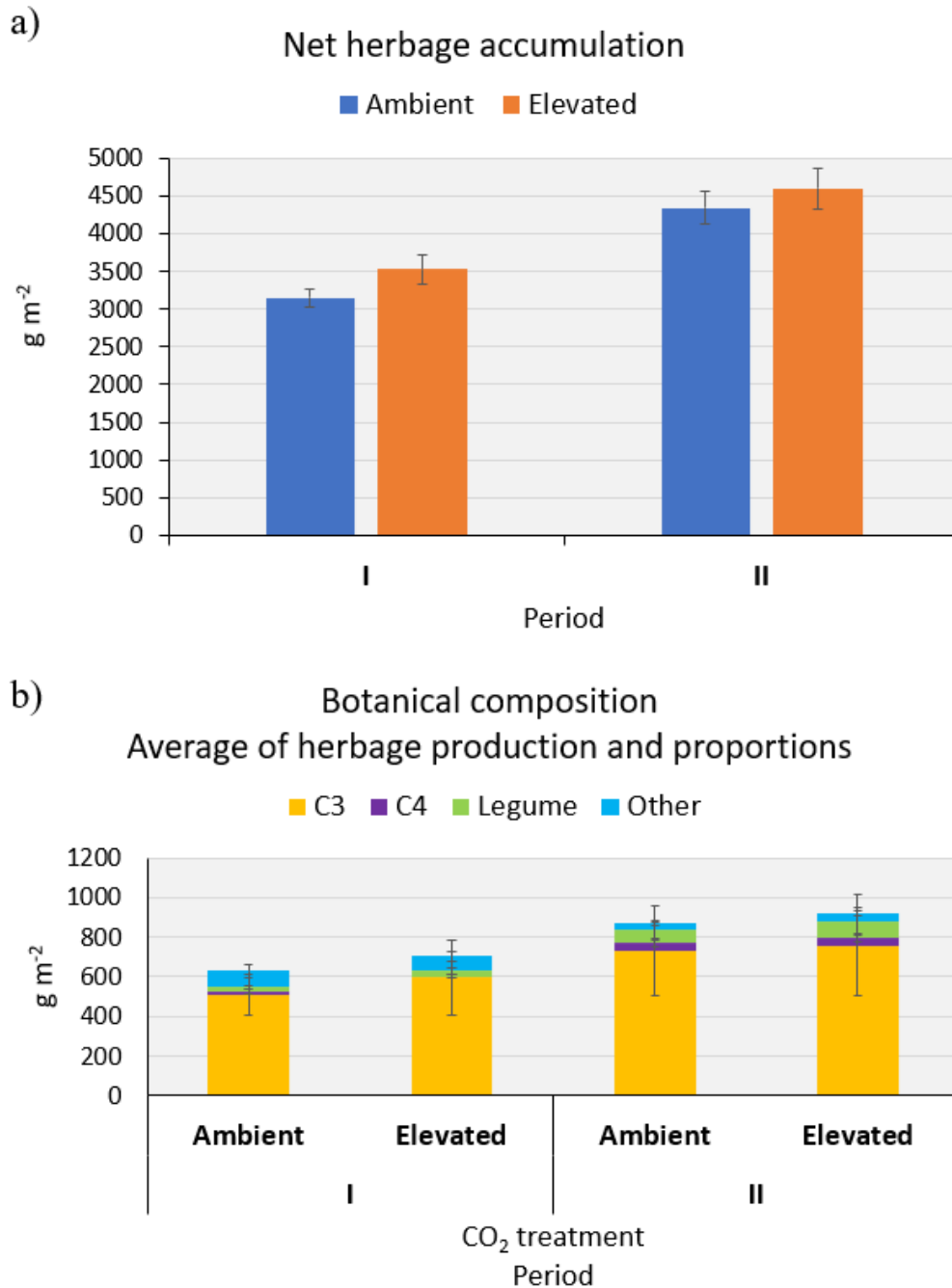


Figure 3. 1: Average aboveground plant response to time and elevated CO₂ at the NZ Free Air CO₂ Enrichment facility between period I (2005 – 2009) and period II (2015 – 2019). Error bars represent SD (n = 3). a) Net Herbage accumulation (NHA) over the period. b) Yearly average herbage production and the average proportion of C₃ grasses, C₄ grasses, legumes, and other species proportion over each period (5 years) under both CO₂ treatments.

Previous studies at this site (Edwards et al., 2001; Newton et al., 2010; Deng et al., 2016) and other FACE sites (Pendall et al., 2011) have shown strong relationship between the effect of eCO₂ and plant species, specially a consistent boost in legume content under eCO₂ within the first years of treatment (< 6 years; Newton et al., 2014). In fact, it has been shown that down-regulation of the photosynthetic capacity after long-term exposure to eCO₂ is attenuated in species with N₂-fixing abilities, such as legumes (Hebeisen et al., 1997). Despite the increase in legume proportion across CO₂ treatments, with an average increase of 3% (during the first period) and of 8% (during the second period), the legume contents of both ambient and eCO₂ pastures were low compared with common pasture mixtures in New Zealand (Charlton and Stuart, 1999), being on average <5% during the first period and <10% during the second period. Therefore, low levels of N₂ fixation by legumes are anticipated at the site in both, ambient and eCO₂ swards and even more so under eCO₂.

3.3.2 Belowground response to elevated CO₂ between period I and II

Elevated CO₂ had no direct or interaction effect over time on soil pH (Figure 3.2a), calcium (Ca; (Figure 3.2b), soil moisture (Figure 3.2c), potassium (K; Figure 3.2f) and sulphate-S (SO₄; Figure 3.2g). In period I, soil magnesium (Mg; Figure 3.2d) showed an interaction effect of CO₂ x time, with a larger concentration in eCO₂ soils in 2009 ($p = 0.0169$), yet no effect of eCO₂ during period II was found (Extended Data Figure 3.4d). The effect of eCO₂ was significant for PO₄ (Figure 3.2e) with a drop that was distinguishable in both periods ($p \leq 0.05$) and consistent over the years (Extended Data Figure 3.4e). Sulphate-S concentration in soil water extracts followed a similar trend to that of PO₄, but differences were not significant at $p < 0.05$ (Extended Data Figure 3.4g). Interestingly, we found some unexpected CO₂ x time interaction effects: soil soluble sodium (Figure 3.2h) was lower under eCO₂ soil during period II ($p = 0.0044$), yet this effect was variable between years (Extended Data Figure 3.4h).

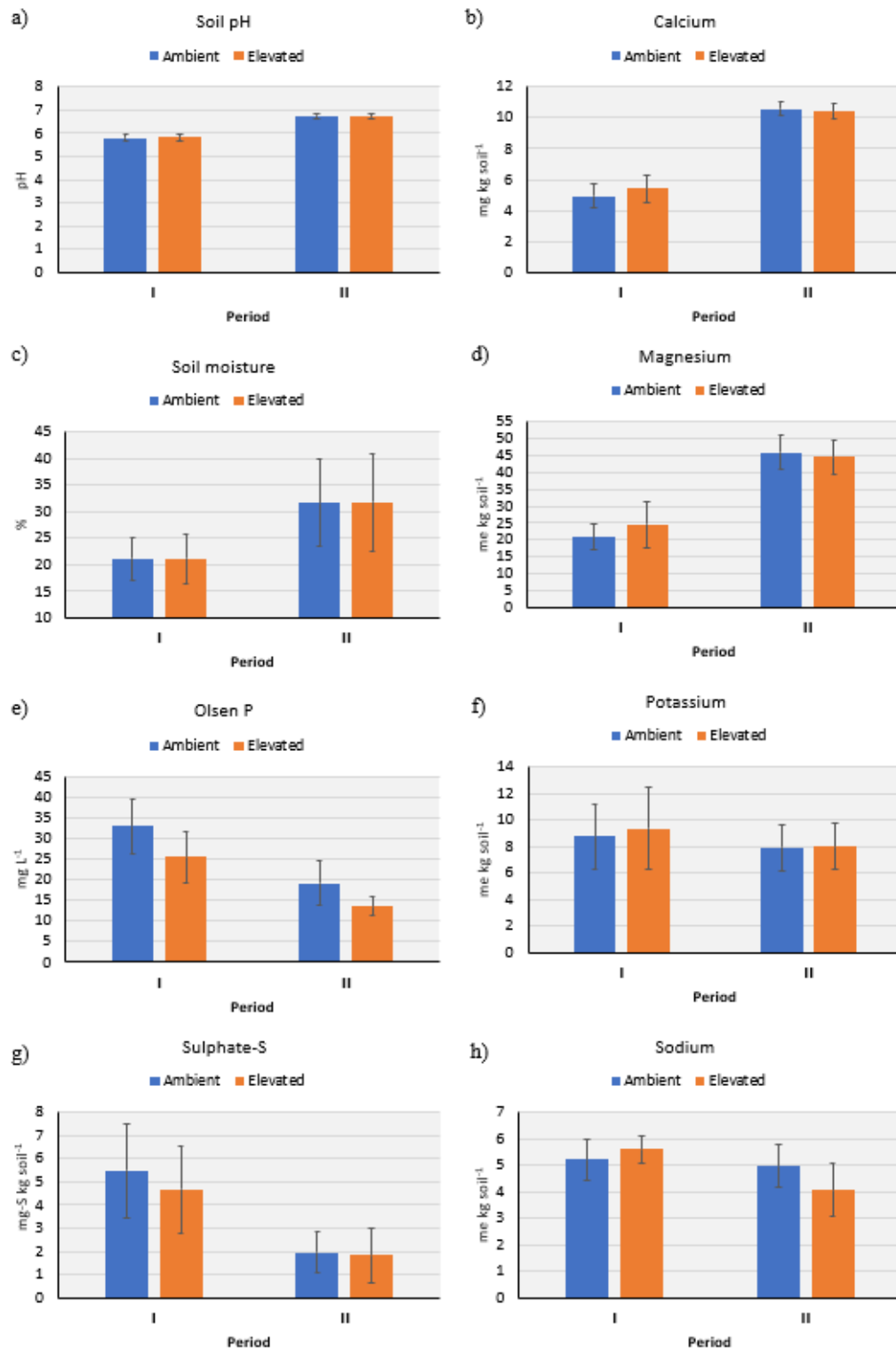


Figure 3. 2: Belowground response of soil variables to time and elevated CO₂ at the NZ-FACE facility between period I (2005 – 2009) and period II (2015 – 2019). Bars represent the period average under ambient and elevated CO₂ treatments of soil pH, moisture and nutrient status. Error bars represent SD (n = 3). a) soil pH, b) soluble calcium, c) soil moisture, d) soluble

magnesium, e) Phosphate (Olsen P), f) soluble potassium, g), sulphate-S, and h) soluble sodium.

Over time and independently of the CO₂ treatment, soil pH has increased ($p < 0.0001$), shifting from mildly acidic (5.8 ± 0.1) in period I to neutral soil pH in period II (6.7 ± 0.1). This has been paralleled by an increase in the bioavailability of soil Ca and Mg (both significant at $p < 0.0001$), and a drop in available Na during period II ($p = 0.0001$; Extended Data Figure 3.4b, d and h, respectively). The soil moisture was highly variable over the years ($p < 0.0001$; Extended Data Figure 3.4c) and higher in period II vs. period I (31.7 ± 8.5 vs $21.1 \pm 4.3\%$; $p < 0.0001$) despite an increase in the mean annual temperature between periods at the site (by 0.7 °C in period II) and the unchanged average rainfall (see methods section). This result suggests that during period II the soil had a higher aggregation level compared to period I.

Potassium also varied over the years ($p = 0.0478$), yet values have remained within the recommended level to support plant growth (Extended Data Figure 3.4f). For PO₄ and SO₄ anionic forms, there was a drop in their concentrations over time, significant at $p < 0.0001$, which in the case of PO₄ values fell from levels recommended to support plant growth (between 20 and 30 mg L⁻¹) to below-recommended values (19.2 ± 5.5 and 13.5 ± 2.3 mg L⁻¹ for ambient and eCO₂ soils, respectively) despite adequate PO₄ fertiliser applications. Sulphate-S values have been consistently lower than recommended (between 10 and 12 mg L⁻¹) levels, with even lower concentration during period II ($p < 0.0001$) reaching levels below 2 mg L⁻¹, constraining plant growth across CO₂ treatments.

A lower SO₄ and PO₄ content in the soil during period II could be explained by the increase in NHA over time causing their mining (Richardson et al., 2011), regardless of CO₂ treatment, as more key nutrients were being taken up to support the enhanced plant growth during this period. There was a residual increase in basic cations (Ca, Mg) and an associated alkalisation of the soil (Tandy et al., 2021). The further decline in soil PO₄ caused by the relative increase

in NHA under eCO₂ during both periods has led to a plant PO₄ deficiency, suggesting that PO₄ could be a limiting nutrient in sustaining the CO₂ fertilization effect at the NZ-FACE facility, as seen by many others (Gentile et al., 2012; Deng et al., 2015; Jin et al., 2015; Kuzyakov et al., 2019). The drop in PO₄ under eCO₂ is consistent with the reported CO₂-induced down-regulation of this nutrient, causing a lower N:P ratio of herbage and root biomass (Deng et al., 2015).

3.3.3 Organic carbon and nitrogen stocks

The cascade of effects generated by eCO₂ has affected the soil-plant system at different scales and rates, making it difficult to define the true effect of eCO₂ on soil OC stabilization and turnover in the long term. When comparing samples taken in 2009 (12 years of CO₂ fertilization) and in 2019 (22 years of CO₂ fertilization), we have found no significant changes due to eCO₂ in soil bulk density ($p = 0.5808$), OC and N content ($p = 0.6816$ and $p = 0.4706$, respectively), OC and N stocks ($p = 0.4409$ and $p = 0.4078$, respectively), or C:N ratio values ($p = 0.9094$; Extended Data Table 3.5).

Independently of CO₂ treatment, we have detected some important changes over time in all soil measurements (Table 3.1). Soil bulk density varied over the years depending on soil depth ($p < 0.0001$). In the topsoil (0 – 50 mm) bulk density increased over time, while in the 50 – 150 mm and 150 – 250 mm soil layers it decreased. Across all soil depths, the soil bulk density had decreased by the end of period II ($p = 0.0484$). As expected, the soil bulk density increased with soil depth ($p < 0.0001$). Given that over time and across CO₂ treatment, the topsoil has been significantly compacted over time and de-compacted in the deeper horizons, we applied a cubic spline to compare N and OC stocks based on soil weight rather than volume (Wendt et al., 2013).

Table 3. 1: Soil measurements from 2009 and 2019 in the three soil layers (0 – 50, 50 – 150, and 150 – 250 mm) and soil profile (0 – 250 mm) means across CO₂ treatments at the NZ-FACE facility. Values are mean ± SD (n = 3).

Depth	Year	Bulk density (g soil cm ⁻³)	OC (g C kg soil ⁻¹)	N (mg N kg soil ⁻¹)	C:N ratio	OC stock (t ha ⁻¹)	N stock (t ha ⁻¹)
0 - 50 mm							
	2009	0.93 ± 0.06 (f)	48.97 ± 3.63 (a)	4.40 ± 0.36 (a)	11.1 ± 0.16 (a)	24.31 ± 1.72 (d)	2.19 ± 0.17 (d)
	2019	0.99 ± 0.03 (e)	46.92 ± 3.67 (a)	4.25 ± 0.24 (a)	11.0 ± 0.27 (a)	23.40 ± 1.75 (d)	2.12 ± 0.12 (d)
50 - 150 mm							
	2009	1.19 ± 0.06 (c)	32.63 ± 3.99 (b)	3.17 ± 0.32 (b)	10.3 ± 0.35 (b)	33.46 ± 3.77 (a)	3.24 ± 0.32 (a)
	2019	1.09 ± 0.04 (d)	29.25 ± 2.47 (b)	2.90 ± 0.21 (b)	10.1 ± 0.29 (b)	29.84 ± 2.56 (b)	2.95 ± 0.21 (b)
150 - 250 mm							
	2009	1.39 ± 0.08 (a)	19.27 ± 2.52 (c)	1.92 ± 0.21 (c)	10.0 ± 0.37 (b)	21.08 ± 2.01 (c)	2.12 ± 0.13 (c)
	2019	1.25 ± 0.04 (b)	15.23 ± 2.58 (d)	1.58 ± 0.21 (d)	9.6 ± 0.39 (c)	16.37 ± 2.41 (d)	1.70 ± 0.19 (d)
0 - 250 mm							
	2009	1.17 ± 0.06 (a)	33.62 ± 2.83 (a)	3.16 ± 0.25 (a)	10.49 ± 0.22 (a)	78.85 ± 6.65 (a)	7.54 ± 0.55 (a)
	2019	1.11 ± 0.03 (b)	30.47 ± 1.26 (a)	2.91 ± 0.11 (a)	10.23 ± 0.17 (a)	69.61 ± 3.50 (b)	6.78 ± 0.30 (b)

In period II, and across the soil profile, OC stocks were 11.7% lower ($p = 0.0107$) than in period I. Organic C stocks have decreased in every soil layer (-3.7%, -10.8% and -22.4% respectively), with significant reductions in the deeper layer (150 – 250 mm) and losing its significance in the topsoil, leading to an interaction effect between time and soil depth ($p = 0.0265$). Similarly, across the whole soil profile (0 – 250 mm), N stocks were 10.1% lower in period II ($p = 0.0095$) than in period I. Nitrogen stocks decreased in every soil layer (-3%, -8.8% and -19.5%, respectively), yet the decline was only significant at 150 – 250 mm depth (-19.5%, $p = 0.0160$),. Soil OC content across the 0 – 250 mm soil depths has decreased by 9.4% over time ($p = 0.0275$) and soil N content decreased by 3.5% ($p = 0.0312$). Changes in the soil OC and N content have led to a slight decrease in the C/N ratio over time ($p = 0.0554$). As expected with increased soil depth, OC ($p < 0.0001$) and N ($p < 0.0001$) content in the soil decreased as so did the C/N ratio ($p < 0.0001$). These observations indicate that the relative decrease in OC

content over time was larger than that of N content, reflecting the conservation of N in the system through microbial OM processing (more supporting data is provided below), and explaining the decrease in soil C/N value over time.

Increasing NHA leads to an increase in OC input to the soil and, most importantly, under eCO₂ more OC is reported to be allocated to the belowground through root biomass and exudates, which might lead to a priming effect, increasing the turnover rate of soil OM (Madhu and Hatfield, 2013). As with many other studies (Kuzyakov et al., 2019), the NZ-FACE facility has reported a faster root turnover rate (Allard et al., 2004) attributed to an increase in the root-derived OC inputs under eCO₂ (Allard et al. 2005). An increase in microbial activity and growth (and thus microbial respiration) in response to the boost in NHA leads to an increase in the turnover rate of microbial necromass (Allard et al., 2005), which could either become preserved through interactions of this microbial-processed OM with mineral surfaces, if available, or cause positive priming if nutrients are needed to fulfil plant needs, as observed in low-nutrient soils under eCO₂ (Jiang et al., 2020).

Despite the observed 34% increase in accumulated NHA between period I and II (mean across CO₂ treatments), the lower soil OC and N stocks detected by the end of period II (2019) can be attributed to several contributing factors: a) an increase in soil moisture and temperature over time might have favoured a high NHA-associated detritus input to the soil, and thus an enhanced microbial growth (also favoured by the increase in soil moisture and temperature), which under the existing low PO₄ and SO₄ fertility conditions might have led to positive priming (due to high quantity of low-quality OC input; Lavalley et al., 2020); b) this positive priming might have caused a residual concentration of alkalinity in the system (e.g., residual concentration of Ca and Mg), causing an increased soil pH; c) this alkalinisation of the system weakens inner-sphere bonds and H-bonds involving organic molecules, and thus the strength through which these molecules are protected (Kleber, 2010).

The increase in NHA in period II might have modified the soil OC distribution, partitioning and persistence of soil aggregates despite the lack of effect on soil OC content and stocks. Also, it could be the case that the observed decrease in OC and N stocks over time is masking a weaker eCO₂ effect. Therefore, the stability and protection of soil aggregates deserve a more detailed analysis.

3.3.4 Soil organic carbon and nitrogen in the soil fractions

In this study we used wet fractionation analysis to separate soil aggregates to (i) study the effect of eCO₂ on aggregates OC and N content, stability, and persistence, and (ii) determine if the decline in soil OC stocks over time (11.7% less OC stock by the end of period II) was caused by a preferential reduction of specific OC pools. Physical recovery was on average 99.3%, the chemical OC recovery was 105.2%, and that of N was 103.6% (Extended Data Table 3.6). The results indicate that exposure to eCO₂ has not caused any change in the soil fractions considered here (neither the fraction size, soil OC and N content and proportion, nor the C:N ratio), except for the N proportion in cPOM, where across years, cPOM in eCO₂ soils has shown an increase in N proportion out of the total soil N pool ($p = 0.0361$; Extended Data Table 3.7).

We have found some interactions between soil fraction size and time for OC and N content, OC and N proportion of the total OC and N pool, and C/N ratio (Figure 3.3), especially in the cPOM fraction. By 2019, the size of cPOM fraction in the total soil mass has decreased significantly (by ~17% considering the whole depth; $p < 0.0001$; Figure 3.3a) as did the soil OC ($p = 0.0119$) and N ($p = 0.0098$) content (Figure 3.3b and 3.3c, respectively). Thus, the OC ($p = 0.0002$) and N ($p = 0.0002$) proportion in cPOM out of the total soil OC and N has significantly decreased (Extended Data Figure 3.5a and b, respectively). The strong decrease in N concentration of the cPOM fraction found in 2019 has resulted in a significant increase in

the C:N ratio of the topsoil, with no change in the 50 – 150 mm layer, and narrowing in the 150 – 250 mm layer ($p = 0.0006$; Figure 3.3d). The decrease in the fraction size of cPOM in 2019 came along with a significant increase in the fraction size of micro-aggregates ($p < 0.0001$; Figure 3.3e). Despite the lack of change in OC and N content in the micro-aggregates fraction (Figure 3.3f and 3.3g), their proportional contribution to the total soil OC and N pool increased ($p = 0.0018$ and $p = 0.0011$, respectively; Extended Data Figure 3.5c and d, respectively), especially in deeper layers ($p = 0.0001$). The C:N ratio of micro-aggregates was significantly lower by 2019 ($p = 0.0288$), although the decrease was small in absolute terms (Figure 3.3h). The MAOM fraction size (Figure 3.3i) and its N and OC content (Figure 3.3j and 3.3k, respectively) have remained stable over time, and so has the C:N ratio. In period II, the MAOM OC and N proportion out of the total soil OC and N pool, respectively increased in the 150 – 250 mm horizon (Extended Data Figure 3.5e and f, respectively), with no changes in the topsoil. We attribute the differences in MAOM-associated OC and N proportions to the slight increase in the fraction size of MAOM (Figure 3.3i). Interestingly, the C:N ratio of MAOM increased with soil depth ($p = 0.0007$; Figure 3.3l) and was higher than the cPOM and micro-aggregates C:N ratio.

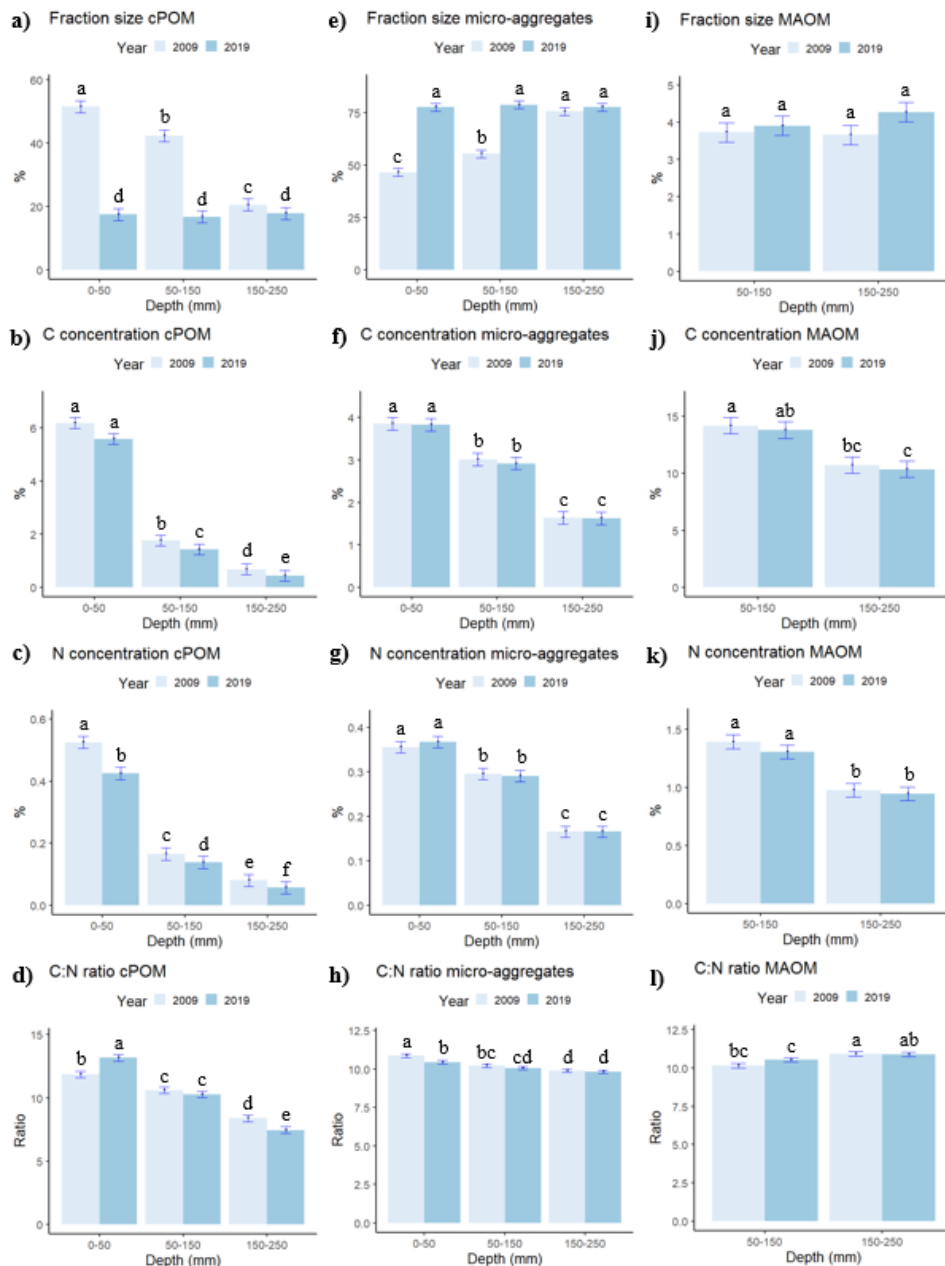


Figure 3.3: Results of soils fractions from the NZ-FACE facility showing soil fractions sizes, carbon (C) and nitrogen (N) concentration and their C:N ratio by the end of period I (2009) and II (2019), in three soil depths, independent of CO₂ treatments: a) fraction size of coarse particulate organic matter (cPOM), b) C concentration in cPOM, c) N concentration in cPOM, d) C/N ratio of cPOM, e) fraction size of micro-aggregates, f) C concentration in micro-aggregates, g) N concentration in micro-aggregates, h) C/N ratio of micro-aggregates, i) fraction size of mineral associated organic matter (MAOM), j) C concentration in MAOM, k) N concentration in MAOM and, l) C/N ratio of MAOM. Error bars represent SD (n = 6). Three

soil layers were analysed except for the MAOM fraction where only the layers 50 – 150 and 150 – 250 mm were studied. See Extended Data Table 3.6 for C recovery and N recovery.

Regardless of CO₂ treatment, a reduced OC and N contribution from cPOM to bulk soil despite a larger NHA, and a proportion of micro-aggregates fraction, suggest the occurrence of a faster mineralization process of the labile OM pool during period II. This is especially supported by the fact that under grazed grasslands, the OM is expected to be dominated by cPOM fraction (Okolo et al., 2020), as was observed in period I – but not in period II, when micro-aggregates were the predominant fraction across soil depths. As no differences in N and OC concentration in micro-aggregates (Figure 3.3f and g, respectively) and in MAOM were observed over time (Figure 3.3j and k, respectively), we attribute the decrease in soil OC and N stocks to a reduction in the size and OC content in the cPOM fraction. This could be to some extent attributed to the increase in temperature and soil moisture (Lavalle et al., 2020) and the priming for nutrients in the fresh labile pool.

The level of protection of micro-aggregates and cPOM fractions can be strongly influenced by changes in rainfall patterns (Sokol and Bradford, 2019) and management practices (Six et al., 1998). Most importantly, we can demonstrate that the MAOM fraction, the most stable pool, has not changed under eCO₂ nor over time, therefore priming of old or new C in the stable pool can be disregarded. The increase in temperatures has apparently not affected this fraction, although the enhanced microbial activity with temperature has been seen by others (Lavalle et al., 2020). However, a saturation of the specific contact area of MAOM cannot be ignored (Six et al., 2002), considering the low silt and clay content of this soil.

3.3.5 The effect of depth on the molecular composition of soil fractions

The pyrolytic products in the two soil depths (50 – 150 and 150 – 250 mm) showed the molecular composition of OM changes with the soil physical fraction and soil depth (Extended Data Figure 3.6a, b and c, respectively). With a change in soil depth from 50 – 150 to 150 – 250 mm, the proportion of aboveground plant-derived OM (lignocellulose, i.e. lignin and holocellulose) decreased ($p < 0.0001$) and the proportion of aliphatic (MCC) compounds increased ($p = 0.0238$). The proportion of polysaccharide (carbohydrates) fingerprints were not significantly affected by soil depth, but the carbohydrate index (Kien and Kogel-Knabner, 2003), defined as the sum of anhydrosugars and pyrans divided by the total carbohydrate pool, decreased with soil depth ($p < 0.0006$; Extended Data Table 3.8) suggesting a shift from plant-derived carbohydrates to microbial-derived compounds with higher persistence with increasing soil depth.

As with pyrolysis, THM results showed that soil depth and the fraction size have an impact on soil OM composition (Extended Data Figure 3.7a, b and c, respectively). The proportions of fingerprints from aboveground plant-derived OM (lignocellulose, i.e., holocellulose and lignin) decreased with increasing depth ($p = 0.0002$), while the proportions of those from aliphatic compounds increased ($p = 0.0012$), especially of cutin and suberin-derived fatty acids (mostly due to short-chain fatty acid methyl esters (sFAMES; $p = 0.0181$)). The proportion of microbial N-containing moieties also increased with depth ($p = 0.0338$), especially degraded microbial OM (“fresher” N-rich remains of microbial chitin, and microbial and perhaps vegetal protein), are concentrated in the 150 – 250 mm soil layer. The cPOM was enriched in short-chain FAMES ($p = 0.0193$) and lignin-derived mono-methoxybenzenes ($p = 0.0875$; Extended Data Figure 3.7a).

3.3.5.1 Differences in molecular composition between organic matter in the soil fractions

Overall and across the two CO₂ treatments, the cPOM had more degraded aliphatic OM and perhaps microbial (not suberin) aliphatic OM. Micro-aggregates had a larger proportion of aliphatic compounds (long-chain FAMES, DAMES, and mid-chain methoxy-FAMES). While the storage of suberin in the MAOM fraction is the main OC preservation mechanism detected by THM-GC-MS in these samples (thus, not mineral stabilization), Py-GC-MS also indicated higher lignin proportions (Extended Data Figure 3.6c). Mineral-associated OM also had relatively high proportions of plant-derived lignin and polysaccharides, implying that the MAOM may contain some mineral-stabilized lignocellulose remains which are generally associated with plant-derived products (Stewart et al., 2011) that are depleted in the cPOM and micro-aggregates fractions (Extended Data Figure 3.6 and 3.7, respectively) due to lack of reactive mineral phase. The MAOM had the largest proportions of long-chain fatty acid methyl esters (IFAMES; $p = 0.008$) and fatty diacids methyl esters (DAMES; short-chain DAMES $p = 0.0174$ and long-chain DAMES $p = 0.0127$; Extended Data Figure 3.7b), clearly showing that the aliphatic enrichment in MAOM is related to suberin, and thus probably root-derived OM (Kögel-Knaber, 2002), as corroborated by alkanes and alkenes enrichment after Py-GC-MS analysis. Moreover, the MAOM fraction was not enriched in N-rich microbial residues (Extended Data Figure 3.7c). The short-chain FAME products (largely microbial-derived; Buurman and Roscoe, 2011) were negatively correlated with long-chain DAMES products (suberin-derived; Figure 3.4a), indicating that there is indeed mineral-stabilised plant material of both root and shoot biomass (Figure 3.4b). The plant-derived compounds were concentrated in the theoretically more processed fractions, pointing towards selective preservation of more recalcitrant forms of soil OM (read: root-derived suberin) in micro-aggregates and MAOM.

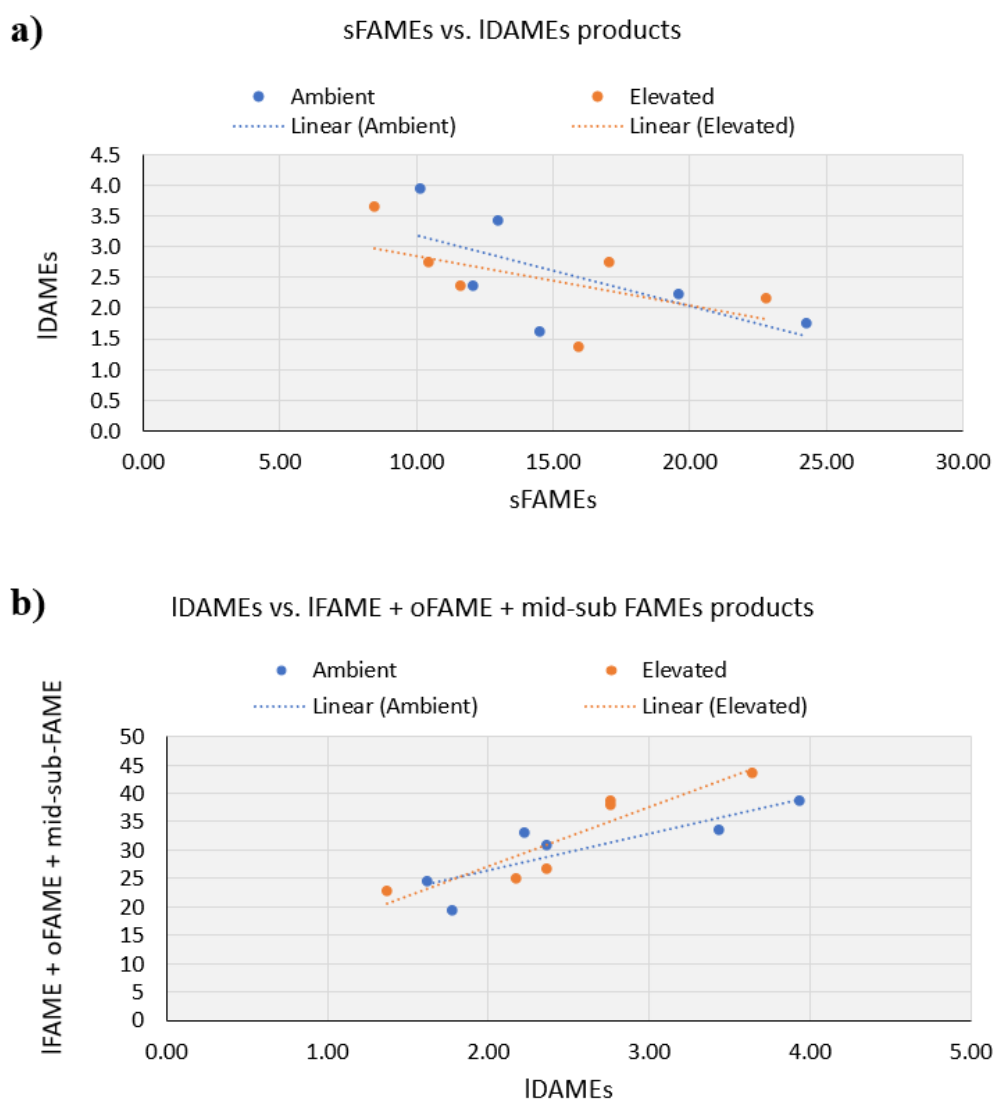


Figure 3. 4: Scatter plot of a) short-chain fatty acid methyl ester (FAMES) products vs long chain fatty diacid esters (IDAMEs) products across soil fractions under elevated and ambient CO₂ and b) IDAMEs products vs long-chain fatty acid methyl esters (IFAMES) + ω -methoxy fatty acid methyl ester (oFAME) + mid-sub FAMES products across soil fractions at the NZ Free Air CO₂ Enrichment facility, data from 2019.

3.3.5.2 Products of pyrolytic and thermally assisted hydrolysis methylation under elevated CO₂

Despite the decrease in the cPOM fraction between 2009 and 2019, there was an increase in the carbohydrates (polysaccharides) under eCO₂ ($16.7 \pm 2.4\%$ vs. $32.3 \pm 4.5\%$; $p = 0.0256$; Figure 3.5a). Although many carbohydrate product proportions were higher under eCO₂, especially in the 50 – 150 mm depth layer ($p = 0.0248$), only 5-methyl-2-furaldehyde (an unspecific polysaccharide) showed a significant increase at that depth ($p = 0.0470$; Extended Data Figure 3.8a). Furthermore, plant polysaccharides have not been affected by eCO₂, yet the proportion of unspecific polysaccharides (probably microbial-derived) has almost doubled (16.5 ± 2.3 vs. $31.4 \pm 4.9\%$) under eCO₂ in the 50 – 150 mm soil layer ($p = 0.0355$; Extended Data Figure 3.8b). Increased unspecific polysaccharides under eCO₂ indicate a higher soil aggregation as microbial polysaccharides act as binding agents (Kien and Kogel-knaber, 2003). The opposite effect was found in the mono-aromatic hydrocarbons (MAH) group (Figure 3.5a), which was depleted in the cPOM under eCO₂, ($p = 0.0316$), especially in the 50 – 150 mm layer ($p = 0.0401$). Toluene was also depleted in cPOM under eCO₂ (Extended Data Figure 3.8c); however, mono-aromatic hydrocarbons (MAH) and phenols may arise from different sources (Dignac et al., 2005). When analysing the individual aliphatic products, many alkanes and alkenes were depleted in the cPOM under eCO₂ ($p < 0.05$), especially again in the 150 – 250 mm soil layer (Extended Data Figure 3.8d to i, respectively). Even though not significant at $p < 0.05$, cPOM from eCO₂ soils had an increased proportion of lignin-derived products (methoxy-phenols) and a lower proportion of other phenols, poly-aromatic hydrocarbons and aliphatic compounds, especially short-chain alkanes and alkenes (C₁₃-C₂₃; Extended Data Figure 3.8d to i, respectively), indicating higher proportions of fresh plant debris (Buurman et al., 2009) in the cPOM from eCO₂ soil.

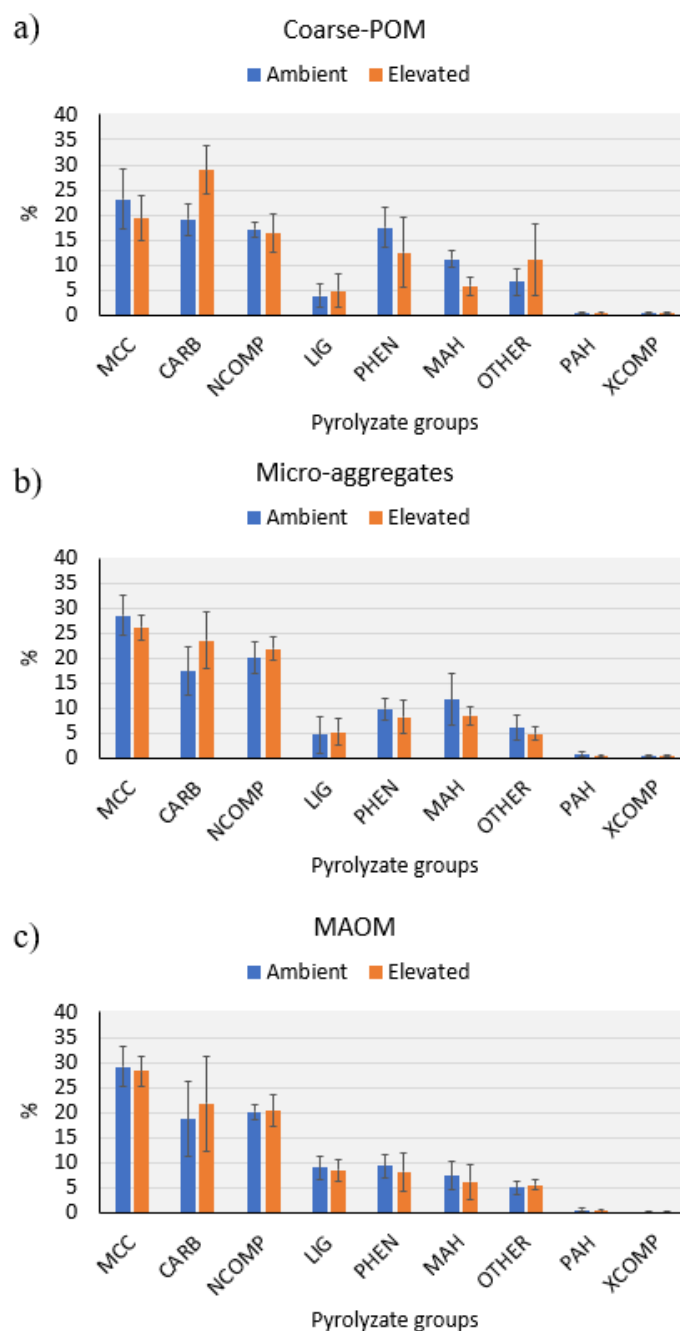


Figure 3. 5: Proportions of pyrolyzate groups in three main soil organic matter fractions: (a) coarse particulate organic matter (coarse-POM), (b) micro-aggregates and (c) mineral associated organic matter (MAOM), at ambient and elevated CO₂ at the NZ-FACE facility, data from 2019. Data is shown across the soil profile (0 – 250 mm). Error bars represent SD (n=3). Abbreviations of pyrolytic products: MCC = aliphatic, CARB = carbohydrates, NCOMP = N-containing, PHEN = phenols, MAH/PAH = mono-/polycyclic-aromatic hydrocarbons,

OTHER = unidentified, LIG = the sum of lignin G, H and S (guaiacol, and syringyl) and XCOMP = halogen-containing.

We found a CO₂ x soil depth interaction in the phenols group in micro-aggregates ($p = 0.0350$), where eCO₂ micro-aggregates had a lower proportion of phenol products compared to aCO₂ in the 150 – 250 mm soil layer ($p = 0.0052$; Extended Data Figure 3.9a and b, respectively). A decrease in phenol products in bulk soil (coupled with other markers) under eCO₂ has been associated with a priming effect in forest soils (Phillips et al., 2012), while phenol products enrichment in a paddy field has been associated with an increase in root litter and exudates inputs or an increase in fungal decomposition (Xiong et al., 2019, 2021).

Under eCO₂, and interacting with soil depth, the aliphatic OM in micro-aggregates (Figure 3.5b) was depleted in short-chain alkanes and alkenes (fatty acid C_{18:1}, alkyl-amide C₂₂ ($p = 0.0405$), fatty acid C₂₀ especially in the 50 – 150 layer ($p = 0.0416$), alkane C₂₂ in the 150 – 250 mm layer ($p = 0.0074$), alkene C₁₉ at both depths ($p = 0.0189$) and alkene C₁₉; Extended Data Figure 3.9c to h, respectively) and enriched in long-chain ones (methyl-ketone C₂₅, C₂₇ and C₂₉ in the 150 – 250 mm layer ($p = 0.0059$, 0.0250 and 0.0442, respectively), in alkane C₃₀ especially in 150 – 250 mm layer ($p = 0.0138$), and alkene C₂₄ and C₂₅ in 150 – 250 mm layer ($p = 0.0173$ and 0.0094, respectively; Extended Data Figure 3.10a to i, respectively).

These results indicate a shift in the balance between plant- and microbial-derived aliphatic products towards the former (Buurman et al., 2009). Even though not significant to $p < 0.05$, eCO₂ micro-aggregates also have a higher proportion of carbohydrates while ambient micro-aggregates had a higher proportion of aliphatic pyrolytic products (Extended Data Figure 3.10b), suggesting that under eCO₂ the system favours the incorporation of plant polysaccharides rather than plant lignin in micro-aggregates.

Exposure to eCO₂ had little effect on the molecular composition of MAOM fraction (Figure 3.5c) although some trends were found. This analysis was limited to only 2/3 of the samples, thus lacking statistical power. The MAOM fraction showed some strong trends (Extended Data Figure 3.10c) in the 50 – 150 mm soil layer, with a lower proportion of aliphatic and polyaromatic hydrocarbons and high contributions of lignin and plant-derived polysaccharides under eCO₂ indicating that (recent) plant root inputs may also be concentrated in the MAOM fraction.

In summary, recent plant-derived OM was detected by Py-GC-MS in the more labile OC pool (cPOM and micro-aggregates) and in the stable pool (MAOM; which could be linked to the increase of NHA found in period II). Furthermore, the soil at the NZ-FACE (undergoing priming of fresh inputs) shows a strong eCO₂ influence on the molecular composition of the relatively labile pools (cPOM and micro-aggregates), while the overall more stable pool remained statistically unchanged despite the important trends observed. Elevated CO₂ appears to cause the enrichment of polysaccharides (19.1 ± 3.1 vs $29.0 \pm 4.8\%$; mainly unspecific ones, not plant-derived) and depletion of aliphatic compounds (23.2 ± 6.0 vs $19.4 \pm 4.3\%$) in cPOM. In micro-aggregates, eCO₂ appears to cause a depletion of short alkanes and increases the long-chain alkane and alkene, perhaps due to stronger input fluxes rather than an in-soil decomposition effect, suggesting that even when there is higher OC sequestration (more OC fluxes into the soil), the mineralization rate is larger (especially in the cPOM) than stabilisation processes in the soil.

Regardless of changing the molecular composition of soil fractions, the relative increase in NHA (not significant even though there was a 12% CO₂ fertilization effect on NHA in period I) did not lead to an eCO₂ effect on soil OC stocks, soil OC content, nor had affected the persistence in the soil fractions after 12 and 23 years of CO₂ exposure. Furthermore, based on these observations, we confirm that bulk soil and its fractions have the same susceptibility to


losing soil OC and N under eCO₂ and ambient soil when subjected to other drivers for soil OC stabilization (such as increased average temperatures, increased soil moisture, enhanced NHA, increased soil pH, the release of cations, and reduced PO₄ and SO₄ availability).

3.4 Conclusion

In conclusion, we found that in period II (2015 – 2019) the NZ-FACE facility was **(i)** showing an increasing deficiency of soil nutrient status, despite **(ii)** receiving larger amounts of fresh plant inputs and higher soil moisture. This was associated with **(iii)** a reduction of the cPOM fraction and OC content of this fraction, an increase in the micro-aggregates fraction which maintained its OC content, and no change in the MAOM fraction, which led to **(iv)** an overall 12% and 10% reduction of soil OC and N stocks, respectively. Furthermore, **(v)** the Py-GC/MS analysis suggests that partitioning between the labile and stable OC pool occurs, and **(vi)** under eCO₂, the labile pool is enriched in polysaccharides and aliphatic products. Based on these findings, we suggest that in the sandy soil at the NZ-FACE facility, the deficiency in soil PO₄ (especially found in eCO₂ soil), the environmentally-enhanced plant growth (larger CO₂ concentration and warmer and wetter system), the larger amounts of fresh OM input cause a positive priming effect, mainly in the labile fraction (cPOM and micro-aggregates), which is further enhanced in eCO₂ soils; this effect is especially prominent in the second soil horizon (50 – 150 mm). We have defined the mechanisms of the biochemical partitioning of soil OC and how the priming – especially within the labile pool – is occurring at this site under the interaction between warming, eCO₂ and depth, however, we suggest that using labelled C (¹⁴C) in more developed soils with higher replicate numbers is required to better understand the effects of eCO₂ on soil OC persistence in a changing climate.

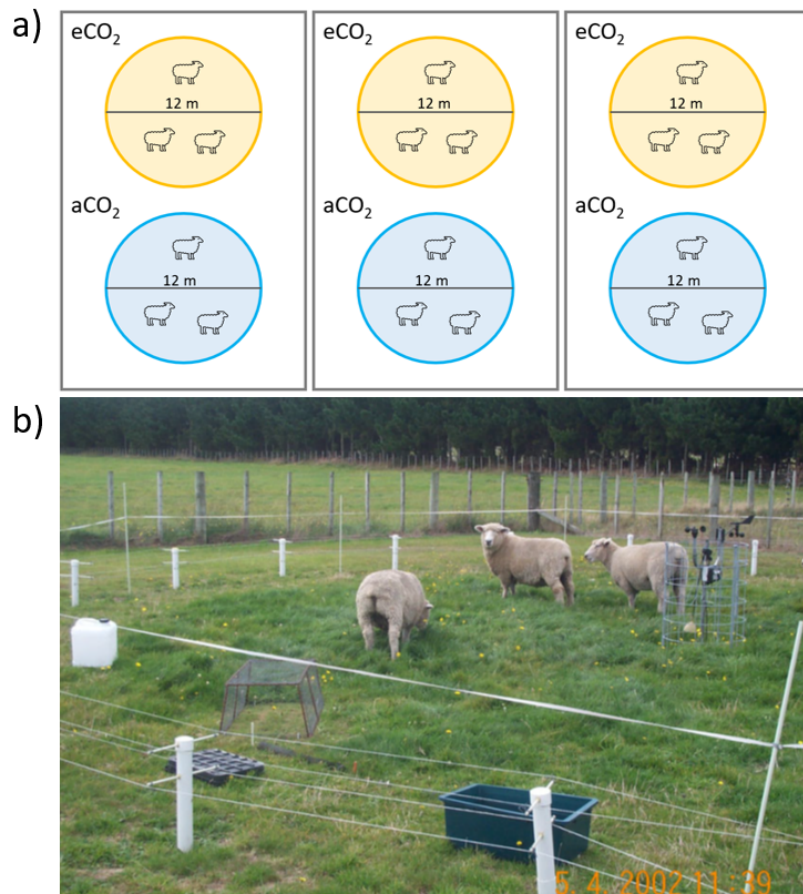
Appendix I - Extended Data for Chapter 3

STATEMENT OF CONTRIBUTION DOCTORATE WITH PUBLICATIONS/MANUSCRIPTS

We, the student and the student's main supervisor, certify that all co-authors have consented to their work being included in the thesis and they have accepted the student's contribution as indicated below in the Statement of Originality.			
Student name:			
Name and title of main supervisor:			
In which chapter is the manuscript/published work?			
What percentage of the manuscript/published work was contributed by the student?			
Describe the contribution that the student has made to the manuscript/published work:			
Please select one of the following three options:			
<input type="checkbox"/> The manuscript/published work is published or in press Please provide the full reference of the research output:			
<input type="checkbox"/> The manuscript is currently under review for publication Please provide the name of the journal:			
<input type="checkbox"/> It is intended that the manuscript will be published, but it has not yet been submitted to a journal			
Student's signature:		Main supervisor's signature:	
<i>This form should be placed at the beginning of each relevant thesis chapter.</i>			

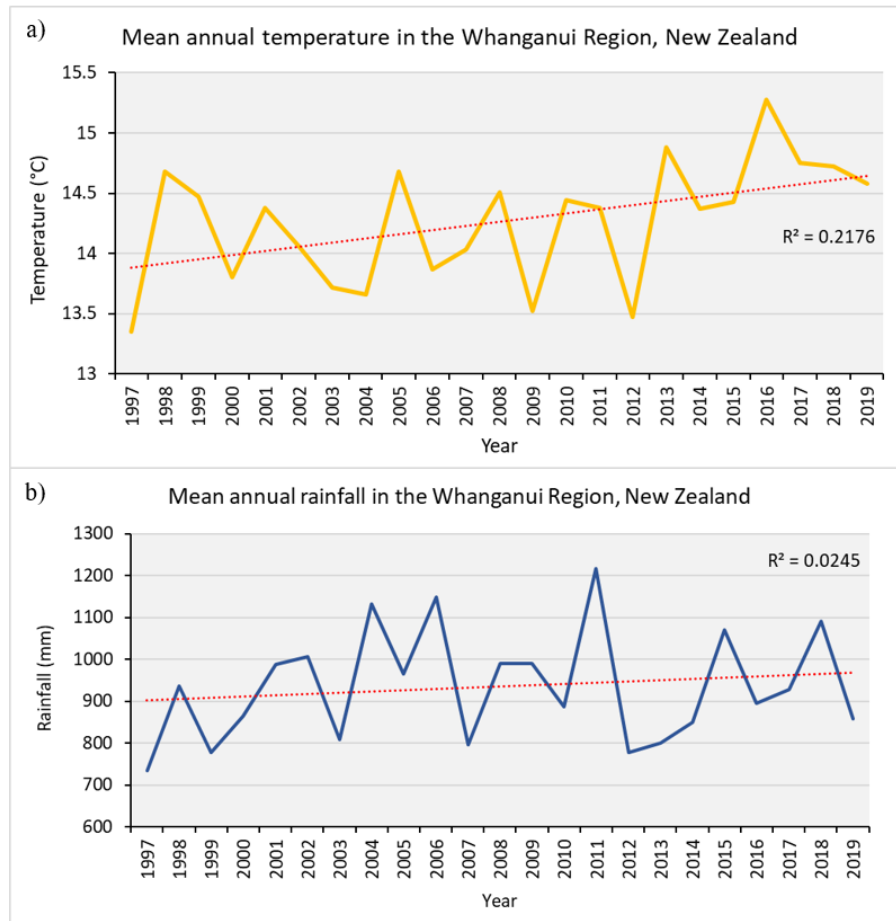
Extended Data 3.2 Methods

Extended Data 3.2.1 Experimental setup



Extended Data Figure 3.1: Representation of the New Zealand Free Air CO₂ Enrichment facility a) experimental blocks design and b) an CO₂ ring being grazed by sheep. The picture shows the standpipes carrying CO₂ being protected by an electric fence (Extracted from Newton et al., 2014).

Extended Data 3.2.2.1 Abiotic factors



Extended Data Figure 3.2: Climate data from the Whanganui Region, New Zealand between 1997 – 2019 on a) mean annual temperature and b) mean annual rainfall.

Extended Data 3.2.2.7 Soil fractions molecular composition analytical procedure

Extended Data Table 3.1: List of pyrolysis-GC/MS products found in soil fractions after 22 years of exposure to elevated CO₂ at the New Zealand Free Air CO₂ Enrichment facility.

Retention Time	m/z	Product	group
1.474	94+96	Bromomethane	XCOMP
1.494	142+127	Iodomethane	XCOMP
1.504	60	Acetic acid	CARB
1.614	78	Benzene	MAH
1.735	79	Pyridine	NCOMP
1.735	67	Pyrrole	NCOMP
1.785	91+92	Toluene	MAH
1.815	59	Acetamide	NCOMP
1.815	84+54	(2H)-furan-3-one	CARB
1.906	95+96	3/2-furaldehyde	CARB
1.966	80+81	Methylpyrrole	NCOMP
2.026	93+66	Methylpyridine	NCOMP
2.298	110+109	5-methyl-2-furaldehyde	CARB
2.328	94+66	Phenol	PHEN
2.418	103	Benzonitrile	NCOMP
2.438	114+58	4-hydroxy-5,6-dihydro-(2H)-pyran-2-one	CARB
2.569	112	2-hydroxy-3-methyl-2-cyclopenten-1-one	CARB
2.609	113+128	Dianhydrorhamnose	CARB
2.739	107+108	4-methylphenol	PHEN
2.800	128	Methyl-4-hydroxy-5,6-dihydro-(2H)-pyran-2-one	CARB
2.830	109+124	Guaiacol	LIG G
2.930	98+68	Levoglucosenone	CARB
2.970	95	4-pyridone (T)	NCOMP
3.021	99	2,5-pyrrolidinedione (succinamide)	NCOMP
3.051	117+89	Benzene acetonitrile	NCOMP
3.061	107+122	Dimethylphenol	PHEN
3.141	107+122	4-ethylphenol	PHEN
3.292	57+69	5-hydroxymethyl-2-tetrahydrofuraldehyde-3-one	CARB
3.382	69+57	1,4:3,6-dianhydro-alpha-D-glucopyranose	CARB
3.312	128	Naphthalene	PAH
3.282	123+138	4-methylguaiacol	LIG G
3.392	120+91	4-vinylphenol	LIG H
3.412	133+134	Ethylbenzaldehyde (T)	OTHER
3.483	83+125	Unidentified compound	OTHER
3.643	79	Picolinamide (T)	NCOMP
3.663	137+152	4-ethylguaiacol	LIG G

3.774	134+119	Unidentified compound	OTHER
3.784	117+89	Indole	NCOMP
3.804	142+115	Methylnaphthalene	PAH
3.884	142+115	Methylnaphthalene	PAH
3.834	150+135	4-vinylguaiacol	LIG G
3.985	154+139	Syringol	LIG S
4.164	154	Biphenyl	PAH
4.206	130+131	Methylindole	NCOMP
4.256	151+152	Vanillin	LIG G
4.206	60+73	Levogalactosan	CARB
4.487	60+73	Levomannosan	CARB
4.768	60+73	Levoglucosan	CARB
4.396	168+153	4-methylsyringol	LIG S
4.416	164+149	4-(2-propenyl)guaiacol (trans)	LIG G
4.457	116	4-methylbenzoic acid ?	OTHER
4.517	100	Unidentified compound	OTHER
4.929	100	Unidentified compound	OTHER
4.607	94	Unidentified compound	OTHER
4.627	151+166	4-acetylguaiacol	LIG G
4.698	125+167	Trihydro-2-acetamido-2-deoxyglucose (Stankiewicz)	NCOMP
4.718	167+182	4-ethylsyringol	LIG S
4.788	137	4-(propan-2-one)guaiacol	LIG G
4.889	180	4-vinylsyringol	LIG S
5.059	166	Fluorene	PAH
5.099	121+138	Vanillic acid (T)	LIG G
5.310	182+181	Syringaldehyde	LIG S
5.421	194+179	4-(2-propenyl)guaiacol (trans)	LIG S
5.451	55+56	Prist-1-ene	MCC
5.561	186+93	Diketodipyrrole	NCOMP
5.571	181+196	4-acetylsyringol	LIG S
5.702	167+210	4-(propan-2-one) syringol	LIG S
5.863	178	Phenanthrene/anthracene (DP)	PAH
5.943	70+154	Diketopiperazine	NCOMP
6.048	70+154	Diketopiperazine	NCOMP
6.084	81+82	Phytadiene 2	MCC
6.144	74+87	Fame C ₁₆	MCC
6.375	70+194	Diketopiperazine (Cyclo(Pro-Pro))	NCOMP
6.797	74+87	Fame C ₁₈	MCC
6.877	55+69	Fatty acid C _{18:1}	MCC
6.998	97	Alkyl nitrile C ₁₈	MCC
7.470	83+280	Unidentified compound	OTHER
7.610	175+272	Unidentified compound	OTHER
9.579	151+416	Gamma-tocopherol	OTHER
9.880	165+430	Alpha-tocopherol	OTHER
7.018	59+72	Alkylamide C ₁₆	MCC
7.610	59+72	Alkylamide C ₁₈	MCC

8.665	59+72	Alkylamide C ₂₂	MCC
8.434	58+59	Methylketone C ₂₅	MCC
9.017	58+59	Methylketone C ₂₇	MCC
9.686	58+59	Methylketone C ₂₉	MCC
10.553	58+59	Methylketone C ₃₁	MCC
5.582	60+73	Fatty acid C ₁₄	MCC
5.823	60+73	Fatty acid i/a C ₁₅	MCC
5.933	60+73	Fatty acid C ₁₅	MCC
6.285	60+73	Fatty acid C ₁₆	MCC
6.917	60+73	Fatty acid C ₁₈	MCC
7.510	60+73	Fatty acid C ₂₀	MCC
8.072	60+73	Fatty acid C ₂₂	MCC
3.674	57+71	Alkane C ₁₃	MCC
4.115	57+71	Alkane C ₁₄	MCC
4.537	57+71	Alkane C ₁₅	MCC
4.939	57+71	Alkane C ₁₆	MCC
5.321	57+71	Alkane C ₁₇	MCC
5.692	57+71	Alkane C ₁₈	MCC
6.044	57+71	Alkane C ₁₉	MCC
6.375	57+71	Alkane C ₂₀	MCC
6.696	57+71	Alkane C ₂₁	MCC
7.008	57+71	Alkane C ₂₂	MCC
7.299	57+71	Alkane C ₂₃	MCC
7.580	57+71	Alkane C ₂₄	MCC
7.851	57+71	Alkane C ₂₅	MCC
8.113	57+71	Alkane C ₂₆	MCC
8.374	57+71	Alkane C ₂₇	MCC
8.635	57+71	Alkane C ₂₈	MCC
8.929	57+71	Alkane C ₂₉	MCC
9.227	57+71	Alkane C ₃₀	MCC
9.569	57+71	Alkane C ₃₁	MCC
9.940	57+71	Alkane C ₃₂	MCC
10.372	57+71	Alkane C ₃₃	MCC
3.643	55+69	Alkene C ₁₃	MCC
4.085	55+69	Alkene C ₁₄	MCC
4.507	55+69	Alkene C ₁₅	MCC
4.909	55+69	Alkene C ₁₆	MCC
5.300	55+69	Alkene C ₁₇	MCC
5.672	55+69	Alkene C ₁₈	MCC
6.024	55+69	Alkene C ₁₉	MCC
6.355	55+69	Alkene C ₂₀	MCC
6.676	55+69	Alkene C ₂₁	MCC
6.988	55+69	Alkene C ₂₂	MCC
7.289	55+69	Alkene C ₂₃	MCC
7.570	55+69	Alkene C ₂₄	MCC
7.851	55+69	Alkene C ₂₅	MCC

8.103	55+69	Alkene C ₂₆	MCC
8.384	55+69	Alkene C ₂₇	MCC
8.675	55+69	Alkene C ₂₈	MCC
8.959	55+69	Alkene C ₂₉	MCC
9.217	55+69	Alkene C ₃₀	MCC
9.589	55+69	Alkene C ₃₁	MCC

Extended Data Table 3.2: List of thermally assisted hydrolysis and methylation GC/MS products found in soil fractions after 22 years of exposure to eCO₂ at the New Zealand Free Air CO₂ Enrichment facility.

RT	m/z	THM product	group
6.955	74+87	C ₁₄ FAME	sFAME
7.146	74+87	iso/anteiso C ₁₅ FAME	sFAME
7.226	74+87	C ₁₅ FAME	sFAME
7.506	74+87	C ₁₆ FAME	sFAME
8.020	74+87	C ₁₈ FAME	sFAME
8.484	74+87	C ₂₀ FAME	IFAME
8.924	74+87	C ₂₂ FAME	IFAME
9.376	74+87	C ₂₄ FAME	IFAME
9.898	74+87	C ₂₆ FAME	IFAME
10.571	74+87	C ₂₈ FAME	IFAME
11.374	74+87	C ₃₀ FAME	IFAME
8.090	55+74	Omega-methoxy C ₁₆ FAME	oFAME
9.456	55+74	Omega-methoxy C ₂₂ FAME	oFAME
9.998	55+74	Omega-methoxy C ₂₄ FAME	oFAME
10.671	55+74	Omega-methoxy C ₂₆ FAME	oFAME
11.545	55+74	Omega-methoxy C ₂₈ FAME	oFAME
5.609	98	Unidentified proline product	NCOMP
6.724	98	Unidentified proline product	NCOMP
7.076	98	Unidentified proline product	NCOMP
8.331	98	C ₁₆ DAME (tr)	IDAME
9.245	98	C ₂₀ DAME (tr)	IDAME
9.747	98	C ₂₂ DAME	IDAME
10.350	98	C ₂₄ DAME	IDAME
11.123	98	C ₂₆ DAME	IDAME
5.268	129	C ₆ metasaccharinic acid ME	CARB
5.368	129	C ₆ metasaccharinic acid ME	CARB
6.021	129	C ₆ metasaccharinic acid ME	CARB
6.152	129	C ₆ metasaccharinic acid ME	CARB
6.242	129	C ₆ metasaccharinic acid ME	CARB
5.188	135+136	4-methoxybenzaldehyde (P4)	1MB
5.770	135+166	4-methoxybenzoic acid ME (P6)	1MB

5.760	144+145	Dimethy-lindole	NCOMP
5.720	153+168	1,2,3-trimethoxybenzene (S1)	3MB
5.810	101+127	Unidentified carbohydrate	CARB
5.861	88	Trimethyl-levoglucosan	CARB
5.820	171 (58, 114)	1,3,5-trimethyl-2,4,6-trione-1,3,5-triazine (TMAH)	OTHER
5.911	168+139	1,3,5-trimethoxybenzene	MB 135
6.011	121	4-methoxybenzeneacetic acid ME (P24)	1MB
6.021	55+69	Unidentified MCC	non-FAME MCC
6.102	118+161	Unidentified N compound	NCOMP
6.111	163	Benzene dicarboxylic acid ME	BCA
6.321	163	Benzene dicarboxylic acid ME	BCA
6.182	115+175	C ₅ metasaccharinic acid ME	CARB
6.212	166+165	3,4-dimethoxybenzaldehyde (G4)	2MB
6.403	55+59	Azelaic acid ME (C ₉ DAME)	sDAME
6.453	158+159	Trimethyl-indole	NCOMP
6.523	165+180	3,4-dimethoxyacetophenone (G5)	2MB
6.383	151+182	Vanillic acid ME	2MB
6.594	196+165	3,4-dimethoxybenzoic acid ME (G6)	2MB
6.704	151+210	3,4-dimethoxybenzeneacetic acid ME (G24)	2MB
6.754	194+179	2-(3,4-dimethoxyphenyl)-1-methoxyethylene (G7,G8) (DP)	2MB
6.835	69+111	Unidentified product	OTHER
6.895	161+192	Trans 1-propenoic acid-4-methoxybenzene ME (P18)	MB cinn
6.895	195+210	3,4,5-trimethoxyacetophenone (S5)	3MB
6.995	226+211	3,4,5-trimethoxybenzoic acid ME (S6)	3MB
7.076	148+186	Unidentified product	OTHER
7.166	209+224	1-(3,4,5-trimethoxyphenyl)-2-methoxyethylene (S7,S8)	3MB
7.216	181	1-(3,4-dimethoxyphenyl)-1,2,3-trimethoxypropane (G14,G15)	2MB
7.468	222+191	Trans-3-(3,4-dimethoxyphenyl)-3-propenoate (G18)	MB cinn
7.538	211	1-(3,4,5-trimethoxyphenyl)-1,2,3- trimethoxypropane (S14,S15)	3MB
7.980	241+256	Unidentified product	OTHER
8.401	71+95	10,16-dimethoxy C ₁₆ FAME	midsub FAME
8.562	169+201	Unidentified mid-chain substituted FAME	midsub FAME
8.622	187+201	8,16-dimethoxy C ₁₆ FAME	midsub FAME
8.813	87+155	Unidentified mid-chain substituted FAME	midsub FAME
9.035	71+81	9,10,18-trimethoxy C ₁₈ FAME	midsub FAME
9.245	71+81	Unidentified mid-chain substituted FAME	midsub FAME
9.637	83+97	Methoxyalkane	non-FAME MCC
10.942	83+97	Methoxyalkane	non-FAME MCC
9.697	73+86	N-methyl-Cxx-alkylamide	non-FAME MCC
9.772	87+100	N,N-dimethyl-Cxx-alkylamide	non-FAME MCC
10.440	179+444	Alpha-tocopherol (methylated)	OTHER

Extended Data Table 3.3: Soil organic matter pyrolytic products (Py-GC-MS) found at the New Zealand Free Air CO₂ Enrichment facility clustered by chemical similarity, and their predominant source of origin.

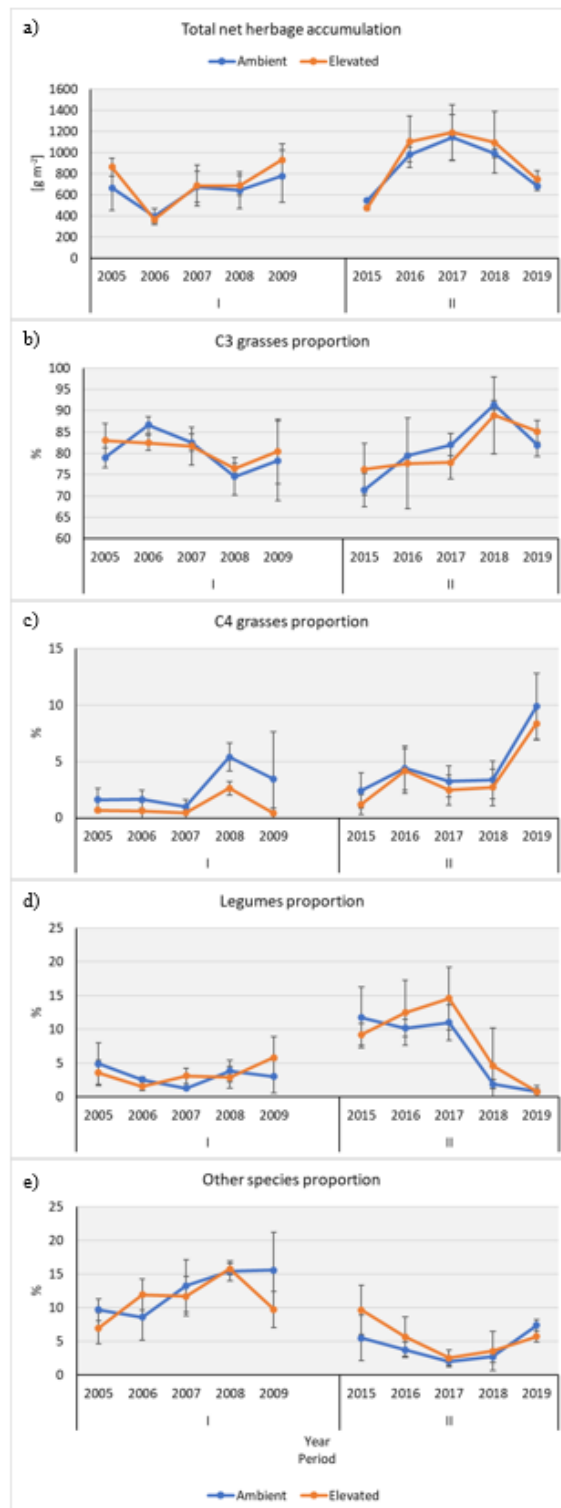
Product	The potential source of origin
Methylene chain compounds (MCC)	Compounds with a long-chain chain aliphatic backbone (alkanes, alkenes, fatty acids, etc.). Derived from microbial and plant-derived molecules (cutin, suberin, epicuticular waxes, etc.).
Carbohydrate products	A chemically diverse group, including acetic acid, furans, furaldehydes, cyclopentenones, pyrans and anhydrosugars. Largely derived from structural polysaccharides in plants (e.g., cellulose, hemicellulose, starch) and microbial polysaccharides (chitin, peptidoglycan).
N-containing products	Compounds with at least one atom of N, including pyrroles, pyridines, acetamidogugars, cyanobenzenes, indoles and diketopiperazines. Derived mainly from macromolecules of protein (of plant and microbial origin), chitin (from fungi and arthropods) and peptidoglycan (bacterial OM). Acetamide, succinimide, acetamidogugars are used as markers of chitin.
Lignin	The products of lignin (4-vinylphenol, guaiacols, syringols) indicate vascular plant-derived OM. These products are useful as markers of plant-derived OM and their balance can provide indications of lignin source (e.g., herbaceous vs. woody).
Other phenols	Other phenols are products of microbial OM, lignin and other sources, and therefore of little diagnostic value.
Halogen-containing	Two compounds containing halogens, i.e., bromomethane and iodomethane, were included in the analysis due to quite large peaks in some samples. We associate this with the small distance from the FACE to the coastline.
Monocyclic-aromatic hydrocarbons (MAH)	Compounds such as benzene, toluene and xylenes are not indicative of a specific source. Given that toluene prevails in most samples suggests most of the MAH signal corresponds to microbial OM.
Polycyclic aromatic hydrocarbons (PAH)	The PAHs can be pyrogenic, but at low levels (< 1 %, which is the case here), the presence of such OM cannot be ascertained because secondary reactions of uncharred OM and resinous moieties can also yield PAHs.
Others	Benzaldehydes, tocopherols and unidentified products.

Extended Data Table 3.4: Soil organic matter thermally assisted hydrolysis and methylation GC/MS products found at the New Zealand Free Air CO₂ Enrichment facility clustered by chemical similarity and the predominant source of origin.

Products	The potential source of origin
Short-chain FAME (sFAME)	Aliphatic, short chain (< C ₂₀) length fatty acid methyl ester (sFAME) are probably mostly bacterial in origin, possible products of any OM precursor. They include a branched C ₁₅ FAME (iso/anteiso configuration) which is probably mostly bacterial, whereas the other short FAMEs are possible products of any OM precursor.
Long-chain FAME (IFAME)	Aliphatic, long chain (≥ C ₂₀) fatty acid methyl esters (IFAME), mostly from plant-derived aliphatic macromolecules (cutin and suberin) and epicuticular waxes.
ω-methoxy-FAME	ω-methoxy-FAMEs (oFAMEs), usually ascribed to cutin and suberin.
Short-chain DAME (sDAME)	Mainly azelaic acid (dimethyl ester), from fragmented unsaturated C ₁₈ fatty acids (e.g., oleic acid).
Long-chain DAME (IDAME)	Long-chain (> C ₂₀) methylated fatty diacids are key products of suberin and are thus associated with bark and root-derived materials.
Other MCC	Other methylene chain compounds include <i>N</i> -methyl-alkylamides and <i>N,N</i> -dimethylalkylamides, two methoxyalkanes and an unidentified compound (alkene or unsaturated FAMEs).
N-containing	Include proline derivatives, alkylindoles and a phthalimide. Mostly of microbial origin. As the TMAH reagent contains N and hydrolysis of microbial OM under THM conditions is poor, these compounds are to be interpreted with caution.
Carbohydrate products	The carbohydrate products, e.g., C ₅ and C ₆ methylated metasaccharinic acids and trimethyllevoglucosan. Underestimation of polysaccharides due to poor hydrolysis.
1MB	Monomethoxy benzenes are, in this case, mainly lignin-derived (compounds P4, P6 and P24 in lignin nomenclature).
2MB	1,2-dimethoxybenzenes are probably mostly derived from guaiacyl structures in lignin (plant-derived).
3MB	1,2,3-trimethoxybenzenes may originate from syringyl moieties in lignin and pyrogallol moieties in tannin (plant-derived).

MB135	1,3,5-trimethoxybenzenes. May originate from cutan and condensed tannin (plant-derived).
MBcinn	“Cinnamyl type” methoxybenzenes (THM products of <i>p</i> -coumaric, ferulic and caffeic acid) are often associated with lignin and lignin-like phenolics in herbaceous litter but suberin (aliphatic macromolecule) also contains a phenolic domain that can yield these THM products
BCA	Methylated benzene carboxylic acids are not diagnostic of any specific source. They are likely THM products of lignin or degraded lignin, but other sources may contribute.
Mid-chain methoxy-FAME	C ₁₆ and C ₁₈ FAMEs with methoxy substitution at the C ₉ and/or C ₁₀ , and terminal (C ₁₆ /C ₁₈) positions. Key products of cutin and suberin. The proportions of mid-chain methoxy-FAMEs and long DAMEs provide information on the balance between cutin from plant cuticles and suberin from barks and roots.
Other	Other compounds include α -tocopherol and two unidentified products.

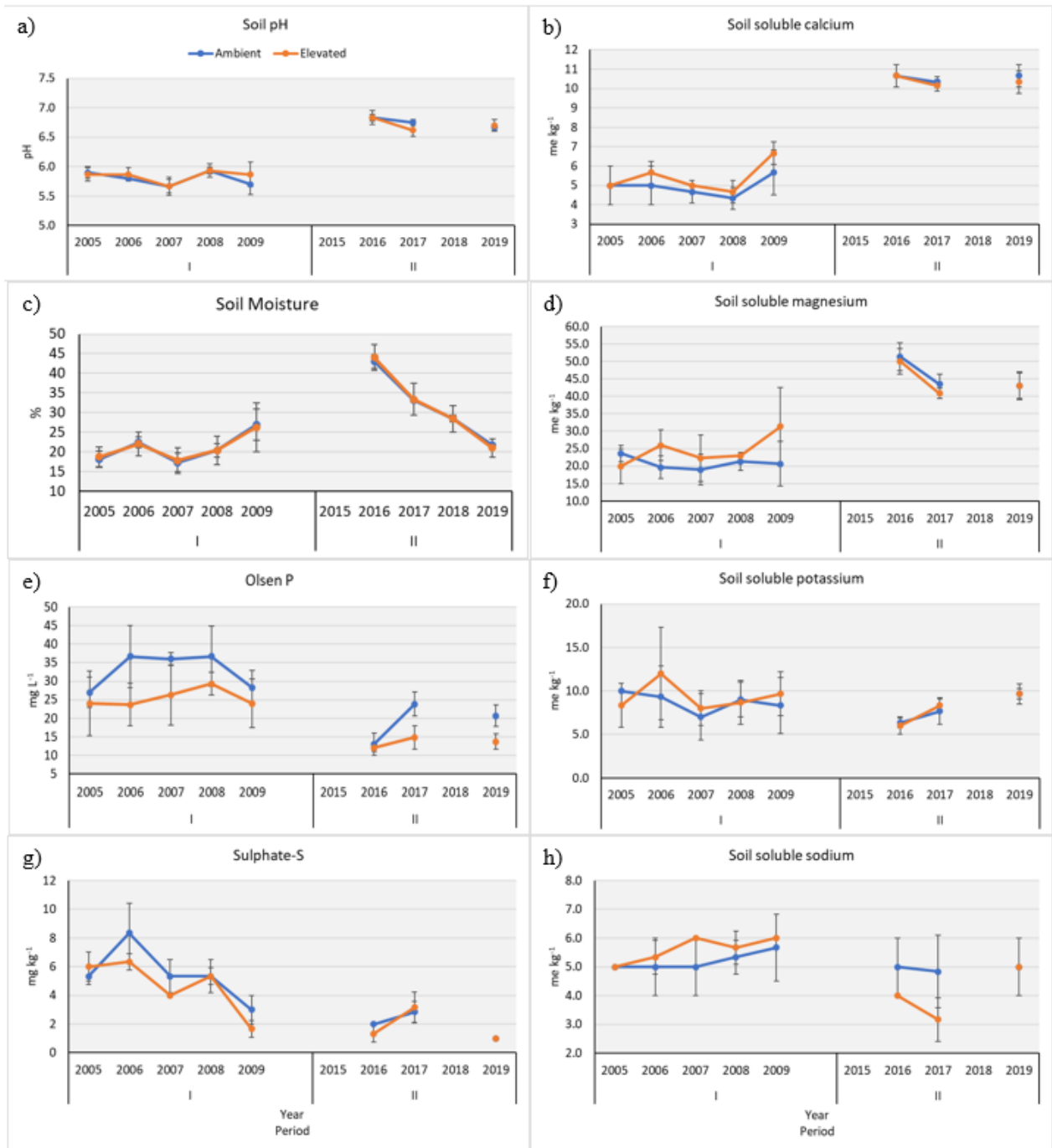
Extended Data 3.3.1 Aboveground plant biomass response to elevated CO₂ between period I and II



Extended Data Figure 3.3: Above plant biomass and botanical composition at the New Zealand Free Air CO₂ Enrichment facility between period I (2005 – 2009) and period II (2015 – 2019) on a) total net herbage accumulation (NHA), b) proportion of C₃ grasses, c) proportion

of C₄ grasses, d) proportion of legumes and e) proportion of other species proportions. Each data represents the average proportion measured before each grazing episode. Error bars represent the standard deviation (n = number of grazing episodes in one year).

Extended Data 3.3.2 Belowground response to elevated CO₂ between period I and II



Extended Data Figure 3.4: Belowground response to elevated CO₂ of a) Soil pH, b) soil soluble calcium, c) soil moisture, d) soil soluble magnesium, e) Olsen P, f) soil soluble potassium, g) sulphate-S, h) soil soluble sodium at the New Zealand Free Air CO₂ Enrichment

facility between period I (2005 – 2009) and period II (2015 – 2019). Each data point represents the average of elevated and ambient CO₂ rings. Error represents the SD (n = 3).

Extended Data 3.3.3 Organic carbon and nitrogen stocks

Extended Data Table 3.5: Soil bulk density, organic carbon (OC) and nitrogen (N) content, stocks, and its C:N ratio under elevated and ambient CO₂ after 12- and 22-years exposure to elevated CO₂ (2009 and 2019 respectively) on three soil horizons at the New Zealand Free Air CO₂ Enrichment facility. Results are the average of elevated CO₂ and ambient CO₂ rings given with SD (n = 3).

Depth (mm)	Year	CO ₂	Bulk density (g cm ⁻³)	Soil OC content (g C kg soil ⁻¹)	Soil N content (mg N kg soil ⁻¹)	C/N ratio	OC stock (tonne ha ⁻¹)	N stock (tonne ha ⁻¹)
0 - 50	2009	Ambient	0.96 ± 0.06	47.60 ± 4.81	4.23 ± 0.45	11.25 ± 0.14	23.72 ± 2.27	2.11 ± 0.22
		Elevated	0.90 ± 0.07	50.33 ± 2.05	4.57 ± 0.21	11.02 ± 0.06	24.91 ± 1.11	2.26 ± 0.11
	2019	Ambient	1.01 ± 0.01	44.87 ± 2.41	4.13 ± 0.21	10.85 ± 0.09	22.45 ± 1.20	2.07 ± 0.10
		Elevated	0.96 ± 0.02	48.97 ± 3.90	4.37 ± 0.25	11.20 ± 0.29	24.35 ± 1.87	2.17 ± 0.12
50 - 150	2009	Ambient	1.22 ± 0.05	32.00 ± 5.64	3.10 ± 0.44	10.28 ± 0.42	33.29 ± 5.01	3.21 ± 0.39
		Elevated	1.15 ± 0.07	33.27 ± 2.61	3.23 ± 0.23	10.29 ± 0.35	33.63 ± 3.23	3.27 ± 0.32
	2019	Ambient	1.11 ± 0.02	30.00 ± 2.69	2.93 ± 0.29	10.23 ± 0.11	31.00 ± 2.68	3.02 ± 0.29
		Elevated	1.07 ± 0.04	28.50 ± 2.52	2.87 ± 0.15	9.93 ± 0.36	28.68 ± 2.28	2.88 ± 0.13
150 - 250	2009	Ambient	1.43 ± 0.07	18.40 ± 2.46	1.83 ± 0.25	10.04 ± 0.15	20.46 ± 2.22	2.06 ± 0.17
		Elevated	1.35 ± 0.09	20.13 ± 2.75	2.00 ± 0.17	10.04 ± 0.57	21.69 ± 2.00	2.17 ± 0.08
	2019	Ambient	1.27 ± 0.02	14.90 ± 2.55	1.53 ± 0.21	9.68 ± 0.39	16.59 ± 2.28	1.70 ± 0.19
		Elevated	1.23 ± 0.05	15.57 ± 3.13	1.63 ± 0.25	9.49 ± 0.44	16.15 ± 3.04	1.71 ± 0.23

Extended Data 3.3.4 Soil organic carbon and nitrogen in the soil fractions

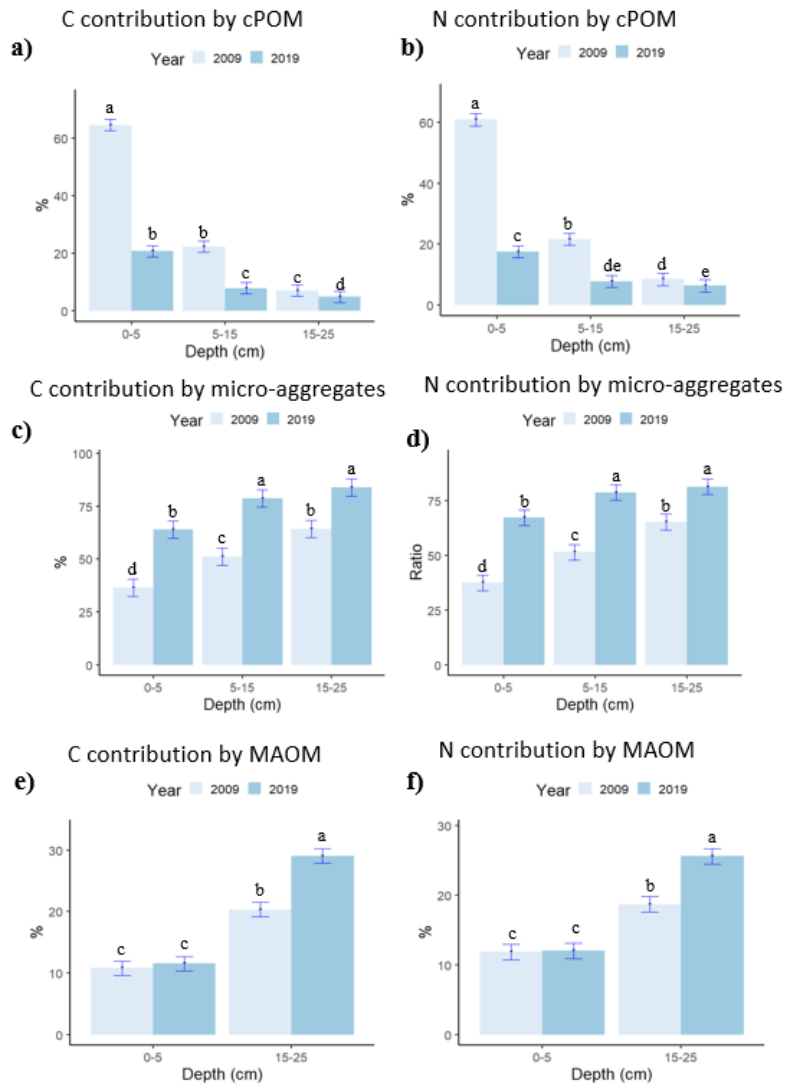
Extended Data Table 3.6: Physical recovery (mass recovery after wet fractionation analysis) and chemical recovery (sum of fraction size) on soil samples from the New Zealand Free Air CO₂ Enrichment facility after 22 years of exposure to elevated CO₂.

CO ₂	Block	Ring	Depth (mm)	Physical Recovery		Chemical Recovery			
				%	Δ%	N	ΔN%	C	ΔC%
Elevated	1	1	0 - 50	98.7	-1.3	101.6	1.6	104.5	4.5
			50 - 150	99.4	-0.6	110.9	10.9	110.4	10.4
			150 -250	99.5	-0.5	120.6	20.6	127.4	27.4
	2	2	0 - 50	99.2	-0.8	99.6	-0.4	95.5	-4.5
			50 - 150	99.4	-0.6	112.5	12.5	115.9	15.9
			150 -250	99.8	-0.3	96.1	-3.9	100.3	0.3
	3	3	0 - 50	99.0	-1.0	87.0	-13.0	83.8	-16.2
			50 - 150	99.4	-0.6	95.4	-4.6	96.8	-3.2
			150 -250	99.5	-0.5	116.5	16.5	120.6	20.6
Ambient	1	4	0 - 50	99.3	-0.7	106.0	6.0	107.3	7.3
			50 - 150	99.2	-0.8	92.7	-7.3	90.4	-9.6
			150 -250	99.6	-0.4	92.1	-7.9	90.7	-9.3
	2	5	0 - 50	98.8	-1.2	89.2	-10.8	89.8	-10.2
			50 - 150	99.0	-1.0	97.9	-2.1	99.7	-0.3
			150 -250	99.7	-0.3	135.2	35.2	145.2	45.2
	3	6	0 - 50	98.8	-1.2	97.6	-2.4	96.5	-3.5
			50 - 150	99.4	-0.6	95.0	-5.0	95.6	-4.4
			150 -250	99.7	-0.3	119.2	19.2	122.4	22.4
			Max	99.8	-0.3	135.2	35.2	145.2	45.2
			Min	98.7	-1.3	87.0	-13.0	83.8	-16.2
			Average	99.3	-0.7	103.6	3.6	105.2	5.2

Extended Data Table 3.7: Soil coarse particulate organic matter (coarse POM), micro-aggregates and mineral associated organic matter (MAOM) distribution, organic carbon (OC) and nitrogen (N) concentration and contribution (%) under elevated and ambient CO₂ after 12- and 22-years exposure to elevated CO₂ (2009 and 2019 respectively) at the New Zealand Free Air CO₂ Enrichment facility (SD n = 3).

Coarse POM								
Depth (mm)	Year	CO ₂	Distribution	OC %	N %	C/N ratio	OC contribution	N contribution
0 - 50	2009	Ambient	54.02 ± 7.57	5.67 ± 0.76	0.47 ± 0.07	12.09 ± 0.30	64.44 ± 11.32	60.06 ± 11.26
		Elevated	49.02 ± 5.62	6.70 ± 0.92	0.58 ± 0.01	11.61 ± 0.47	64.94 ± 8.41	61.83 ± 9.69
	2019	Ambient	17.71 ± 3.98	4.90 ± 0.69	0.37 ± 0.06	13.27 ± 0.29	19.73 ± 6.67	16.20 ± 5.80
		Elevated	17.17 ± 2.66	6.27 ± 0.39	0.48 ± 0.04	13.08 ± 0.67	21.82 ± 0.39	18.74 ± 1.42
50 - 150	2009	Ambient	43.01 ± 5.08	1.51 ± 0.29	0.15 ± 0.03	10.34 ± 0.34	20.41 ± 3.33	20.23 ± 2.59
		Elevated	41.68 ± 6.65	2.00 ± 0.64	0.18 ± 0.05	10.85 ± 0.42	24.36 ± 4.16	23.07 ± 3.67
	2019	Ambient	18.04 ± 1.86	1.10 ± 0.20	0.11 ± 0.02	10.24 ± 0.42	6.57 ± 1.02	6.55 ± 0.87
		Elevated	15.44 ± 1.7	1.75 ± 0.54	0.17 ± 0.05	10.28 ± 0.20	9.25 ± 2.05	8.95 ± 2.09
150 - 250	2009	Ambient	22.68 ± 1.61	0.66 ± 0.16	0.08 ± 0.02	8.51 ± 0.44	7.99 ± 1.01	9.41 ± 0.73
		Elevated	18.41 ± 3.78	0.70 ± 0.21	0.08 ± 0.02	8.25 ± 0.91	6.16 ± 0.46	7.53 ± 0.79
	2019	Ambient	19.02 ± 1.48	0.39 ± 0.11	0.05 ± 0.01	7.22 ± 1.29	5.01 ± 1.28	6.69 ± 1.17
		Elevated	16.52 ± 1.64	0.47 ± 0.18	0.06 ± 0.02	7.70 ± 0.85	4.82 ± 0.39	5.95 ± 0.43
Micro-aggregates								
Depth (mm)	Year	CO ₂	Distribution	OC %	N %	C/N ratio	OC contribution	N contribution
0 - 50	2009	Ambient	44.12 ± 7.70	3.82 ± 0.40	0.35 ± 0.03	10.92 ± 0.14	35.44 ± 6.22	36.59 ± 6.99
		Elevated	48.99 ± 5.68	3.89 ± 0.35	0.36 ± 0.03	10.79 ± 0.06	37.61 ± 1.63	38.43 ± 2.01
	2019	Ambient	77.15 ± 3.08	3.74 ± 0.34	0.36 ± 0.03	10.37 ± 0.19	64.66 ± 10.11	67.57 ± 9.57
		Elevated	78.12 ± 2.67	3.93 ± 0.22	0.37 ± 0.02	10.51 ± 0.24	63.15 ± 9.20	67.07 ± 7.21
50 - 150	2009	Ambient	54.75 ± 5.19	3.07 ± 0.47	0.30 ± 0.04	10.33 ± 0.24	52.73 ± 5.72	52.47 ± 5.69
		Elevated	55.97 ± 6.74	2.96 ± 0.34	0.29 ± 0.03	10.09 ± 0.24	49.62 ± 4.94	50.62 ± 5.42
	2019	Ambient	77.00 ± 0.93	2.80 ± 0.40	0.28 ± 0.04	10.12 ± 0.15	71.77 ± 4.95	72.52 ± 3.36
		Elevated	80.49 ± 2.23	3.04 ± 0.49	0.30 ± 0.04	9.98 ± 0.42	85.49 ± 8.93	85.06 ± 8.48
150 - 250	2009	Ambient	73.87 ± 0.88	1.61 ± 0.29	0.16 ± 0.03	10.02 ± 0.27	64.43 ± 6.87	64.50 ± 6.06
		Elevated	77.33 ± 3.28	1.66 ± 0.20	0.17 ± 0.02	9.75 ± 0.33	64.33 ± 10.26	66.09 ± 9.72
	2019	Ambient	76.31 ± 1.07	1.58 ± 0.29	0.16 ± 0.03	9.83 ± 0.19	82.71 ± 22.67	80.69 ± 17.81
		Elevated	78.84 ± .16	1.68 ± 0.43	0.17 ± 0.04	9.81 ± 0.49	84.91 ± 12.34	82.10 ± 11.65
MAOM								
Depth (mm)	Year	CO ₂	Distribution	OC %	N %	C/N ratio	OC contribution	N contribution
50 - 150	2009	Ambient	3.66 ± 0.28	14.66 ± 0.79	1.42 ± 0.07	10.30 ± 0.26	11.35 ± 1.60	12.39 ± 1.67
		Elevated	3.80 ± 0.31	13.69 ± 1.39	1.37 ± 0.13	10.01 ± 0.09	10.29 ± 0.06	11.33 ± 0.05
	2019	Ambient	4.15 ± 1.07	14.79 ± 2.07	1.40 ± 0.20	10.58 ± 0.14	13.49 ± 2.58	13.83 ± 2.53
		Elevated	3.67 ± 0.15	12.81 ± 1.62	1.22 ± 0.12	10.52 ± 0.31	9.65 ± 1.62	10.23 ± 1.22

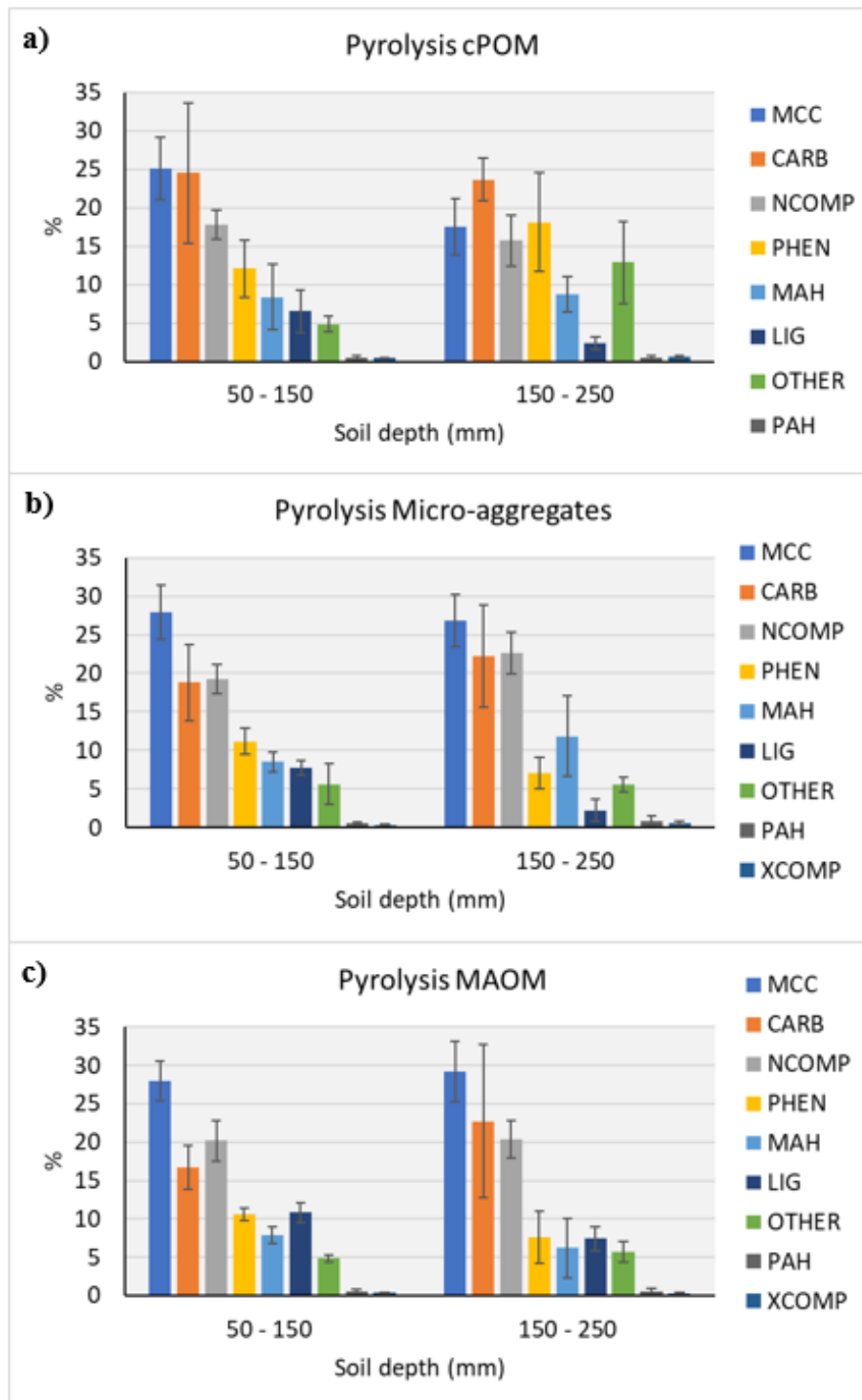
150 - 250	2009	Ambient	3.31 ± 0.68	10.88 ± 0.54	0.99 ± 0.06	11.02 ± 0.17	19.62 ± 3.24	17.94 ± 3.42
		Elevated	4.01 ± 0.39	10.55 ± 1.69	0.97 ± 0.11	10.86 ± 0.56	21.01 ± 2.96	19.46 ± 3.12
	2019	Ambient	4.33 ± 1.01	10.91 ± 0.24	1.00 ± 0.04	10.93 ± 0.22	31.72 ± 4.87	28.10 ± 4.38
		Elevated	4.23 ± 0.46	9.77 ± 2.35	0.89 ± 0.16	10.86 ± 0.68	26.38 ± 3.29	23.03 ± 2.50



Extended Data Figure 3.5: Interactive effect between soil depth and time, after 12- and 22-years exposure to elevated CO₂ at the New Zealand Free Air CO₂ Enrichment facility on a) carbon (C) contribution by the coarse particulate organic matter (cPOM), b) nitrogen (N) contribution by cPOM, c) C contribution by micro-aggregates, d) N contribution by micro-aggregates, e) C contribution by mineral associated organic matter (MAOM), f) N contribution

by MAOM. Error bars indicate SD (n = 3). Contribution indicates the % of C that is allocated by each fraction in the soil sample.

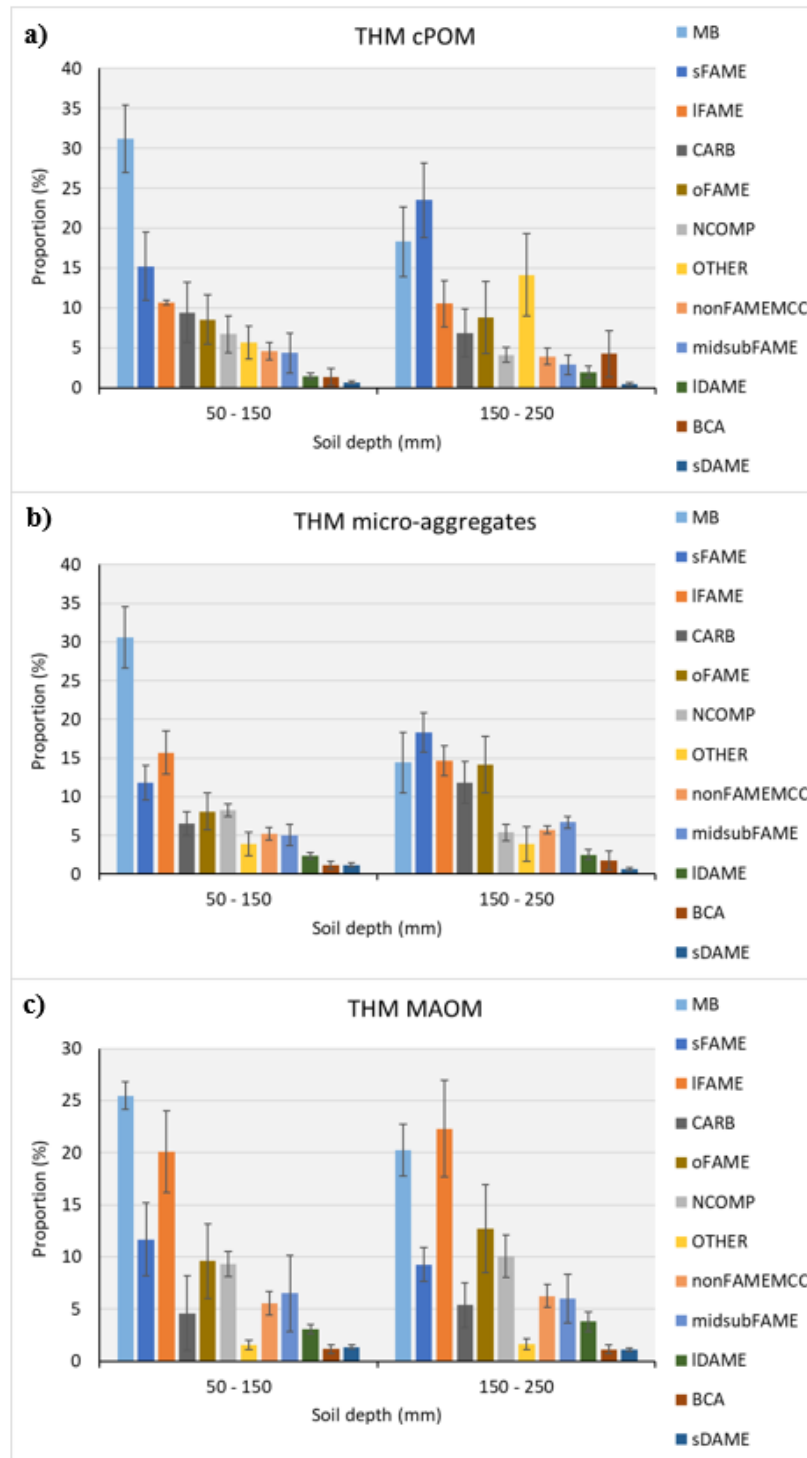
Extended Data 3.3.5 The effect of depth on the molecular composition of soil fractions



Extended Data Figure 3.6: Pyrolysis-GC-MS results by groups of pyrolytic products in each soil fraction from the New Zealand Free Air CO₂ Enrichment facility at two soil depths (50 – 150 and 150 – 250 mm) across CO₂ treatment in a) coarse particulate organic matter (cPOM), b) micro-aggregates and c) mineral associated organic matter (MAOM).

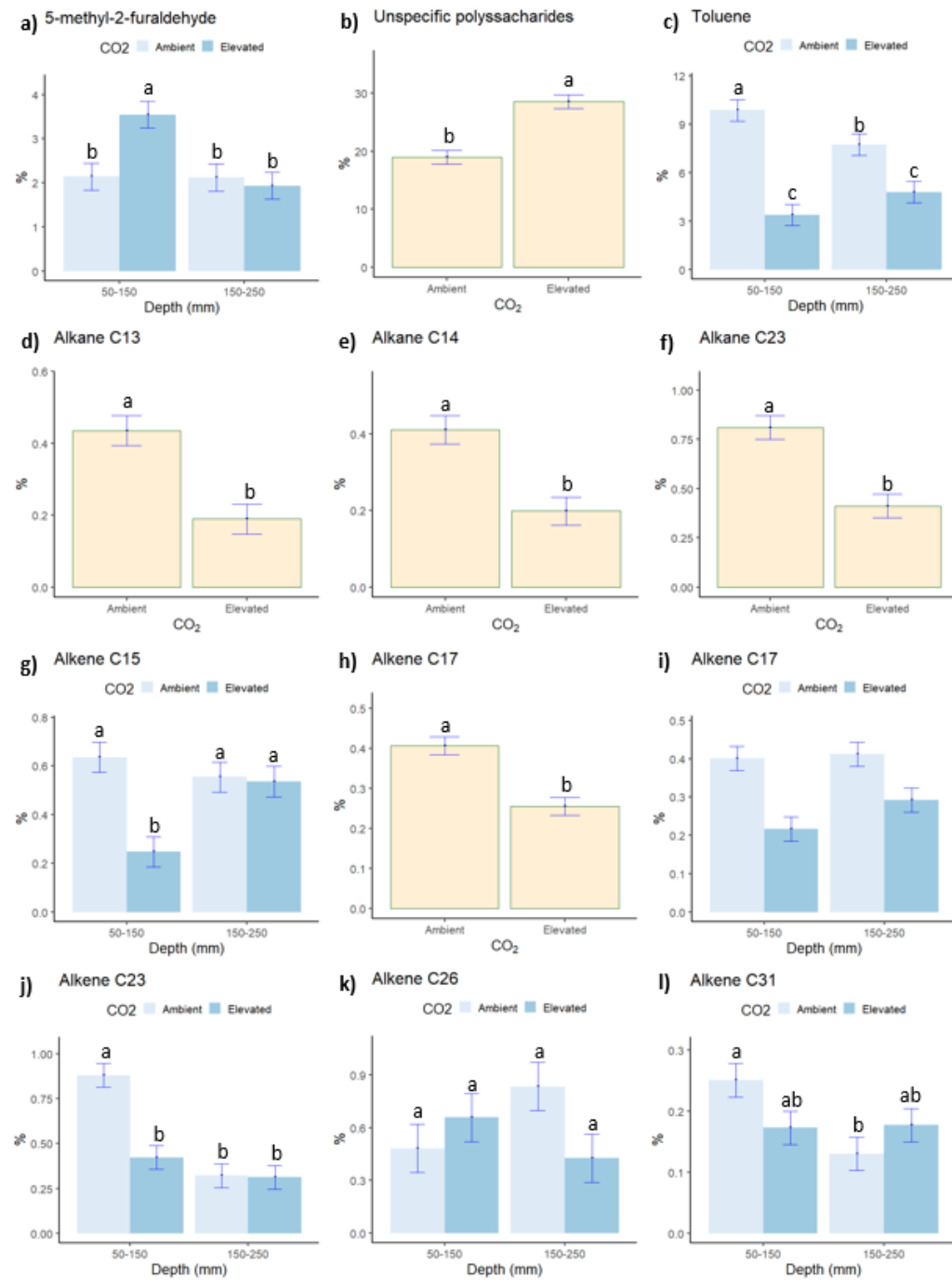
Extended Data Table 3.8: Carbohydrate index of coarse particulate organic matter (cPOM), micro-aggregates and mineral-associated organic matter (MAOM) fractions found on soil fractions after 22 years of exposure to elevated CO₂ at the New Zealand Free Air CO₂ Enrichment facility.

Fraction	Depth (mm)	Ambient CO ₂	Elevated CO ₂
cPOM	50 – 150	0.08 ± 0.01	0.12 ± 0.07
Micro-aggregates	50 – 150	0.25 ± 0.06	0.24 ± 0.03
MAOM	50 – 150	0.53 ± 0.00	0.49 ± 0.01
cPOM	150 – 250	0.01 ± 0.00	0.02 ± 0.01
Micro-aggregates	150 – 250	0.03 ± 0.03	0.1 ± 0.05
MAOM	150 – 250	0.41 ± 0.03	0.45 ± 0.13



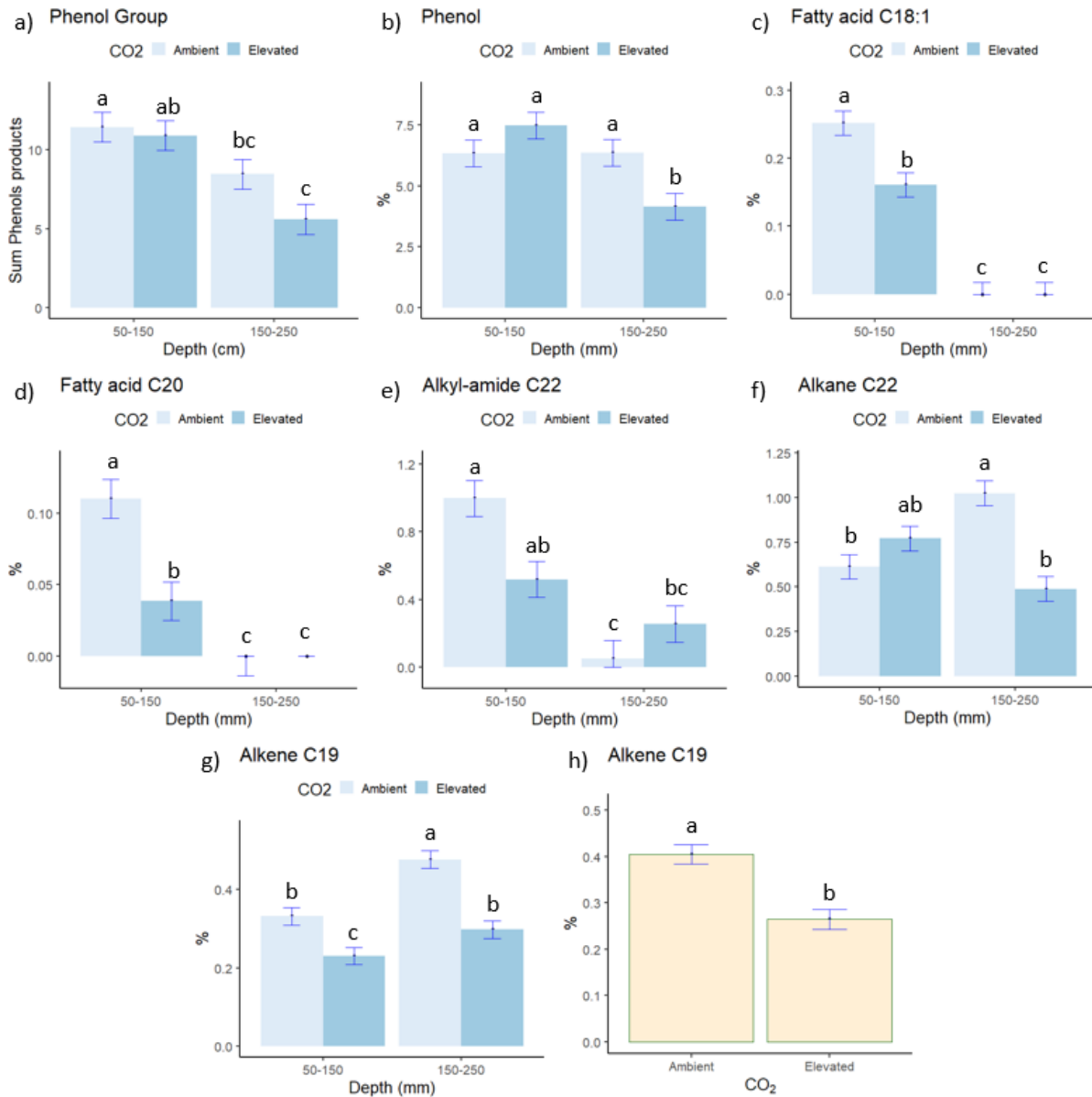
Extended Data Figure 3.7: Thermally assisted hydrolysis and methylation GC/MS results by groups of products in each soil fraction from the New Zealand Free Air CO₂ Enrichment facility at two soil depths (50 – 150 and 150 – 250 mm) across CO₂ treatment in a) coarse particulate

organic matter (cPOM), b) micro-aggregates and c) mineral associated organic matter (MAOM).

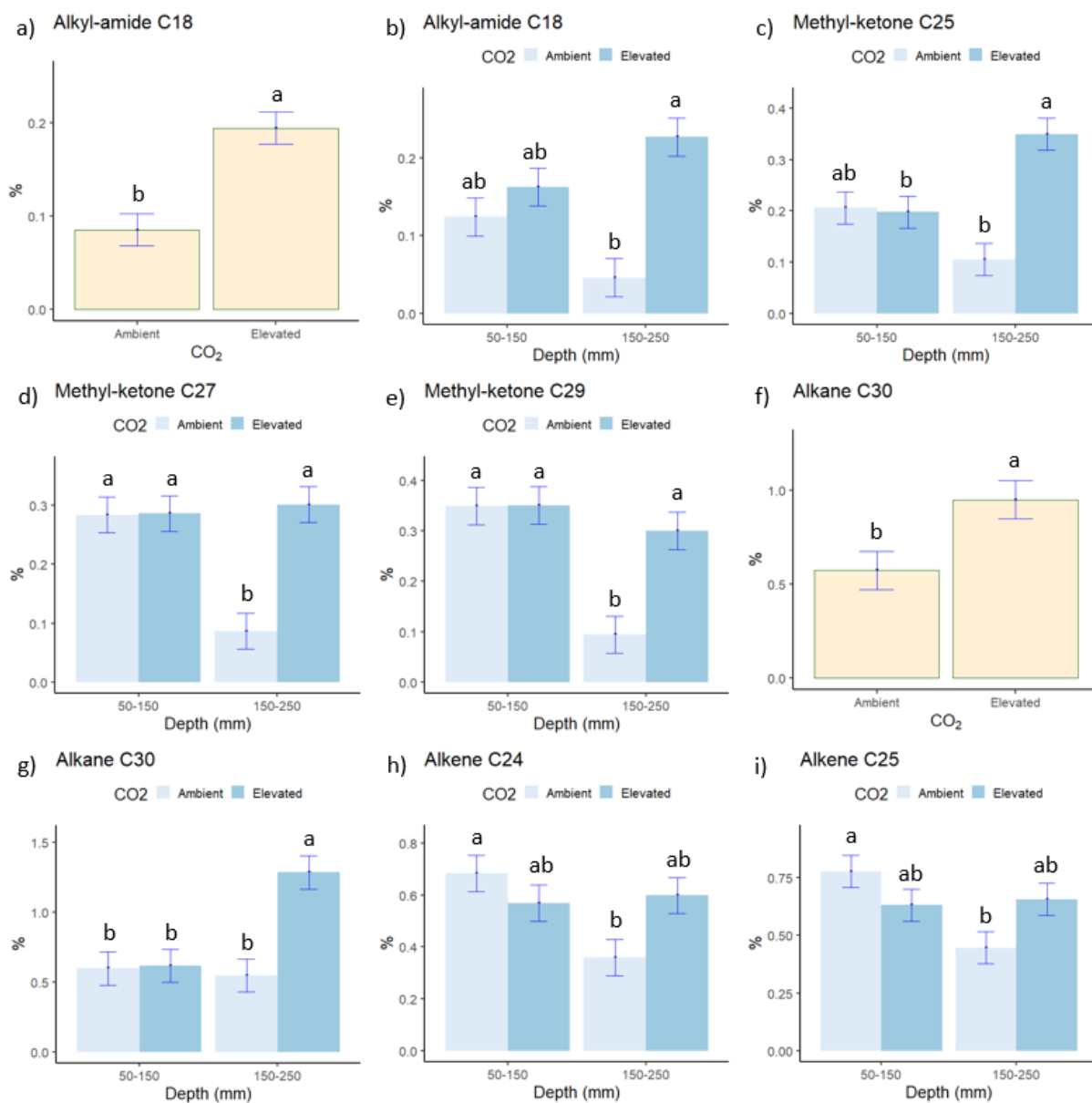


Extended Data Figure 3.8: Interactive effect between CO₂ treatment and soil depth on pyrolytic products of coarse particulate organic matter from the New Zealand Free Air CO₂ Enrichment facility on a) 5-methyl-2-furaldehyde, b) unspecific polysaccharides, c) toluene, d) alkane C₁₃, e) alkane C₁₄, f) alkane C₂₃, g) alkene C₁₅, h) alkene C₁₇, i) alkene C₁₇, j) alkene

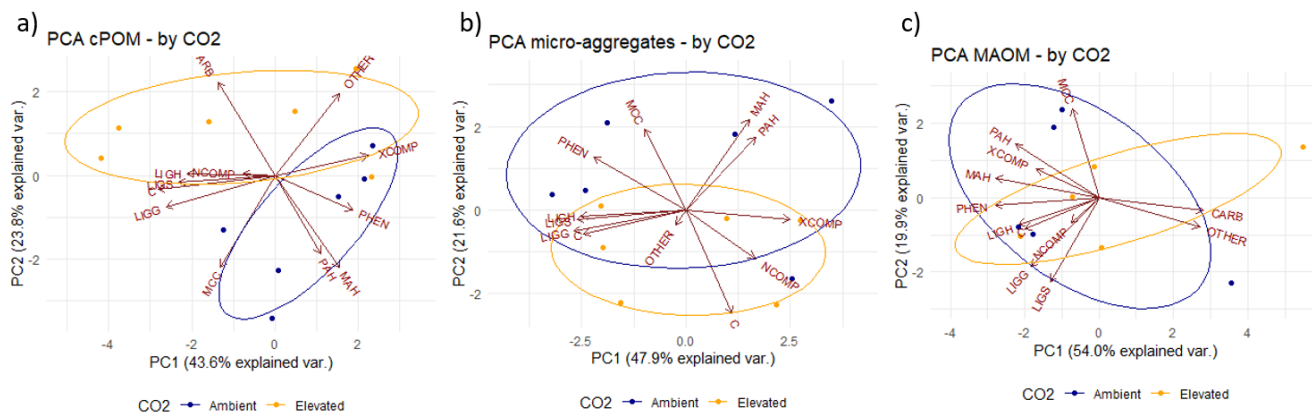
C₂₃, k) alkene C₂₆ and l) alkene C₃₁. Error bars represent SD (n = 3, letters indicate significance to p < 0.05).



Extended Data Figure 3.9: Interactive effect between CO₂ treatment and soil depth on pyrolytic products of micro aggregates from the New Zealand Free Air CO₂ Enrichment in a) phenol group, b) phenol products, c) fatty acid C_{18:1}, d) fatty acid C₂₀, e) alkyl-amide C₂₂, f) alkane C₂₂, g) alkene C₁₉ and h) alkene C₁₉.



Extended Data Figure 3.10: Interactive effect between CO₂ treatment and soil depth on pyrolytic products of micro aggregates at the New Zealand Free Air CO₂ Enrichment in a) alkyl-amide C₁₈, b) alkyl-amide C₁₈, c) methyl-ketone C₂₅, d) methyl-ketone C₂₇, e) methyl-ketone C₂₉, f) alkane C₃₀, g) alkane C₃₀, h) alkene C₂₄ and i) alkene C₂₄.



Extended Data Figure 3.11: Differences of molecular composition between soil fractions at the New Zealand Free Air CO₂ Enrichment shown by PCA of Pyrolysis GC/MS products on a) coarse particulate organic matter (cPOM) fraction, b) micro-aggregates fraction and, c) mineral associated organic matter (MAOM) fraction. Ellipses indicate CO₂ treatment (yellow = elevated CO₂ and blue = ambient CO₂).

Chapter 4 The long-term interactive effect between elevated CO₂ and the grazing animal on soil carbon stocks and molecular composition of soil organic matter

Abstract

Several studies have examined the influence of grazing and climate change factors such as temperature and precipitation, on the above- and the below-ground response of organic carbon (OC) dynamics in grasslands. However, an important climate change factor that has not been investigated is elevated carbon dioxide (eCO₂). With the use of Free Air CO₂ Enrichment (FACE) facilities, research has confirmed that eCO₂ has the potential to boost pasture growth, contributing to an increase OC input to the soil. Nevertheless, the persistence of the extra added OC in the soil is still being debated. Here we show quantitative and qualitative results for soil organic matter (OM) at three soil depths (0 – 50, 50 – 150 and 150 – 250 mm) from the only FACE facility worldwide that explores the influence of eCO₂ on soil OC and nitrogen (N) changes in a grazed legume-based pasture. We explored the interactive effects between eCO₂ and the grazing animals on soil OC and N stocks, the partitioning of OC and N into soil fractions (through wet fractionation analysis) and the soil OM molecular composition (by pyrolysis- and thermally assisted hydrolysis and methylation- gas chromatography and mass spectrometry). The hypothesis that the grazing animals would contribute to a larger OC and N in the soil under eCO₂ was rejected. Nevertheless, our study did find that in the grazed pasture soils under eCO₂ there was an accumulation of lignin-derived OC indicating an accumulation of plant-derived OC. In the hand-cut pasture soils under eCO₂, where the grazing animals were excluded, there was an accumulation of long-chain methylated fatty diacids (DAMEs) products indicating the accumulation of root-derived OC, especially in deeper soil layers. This suggests that the OC stabilization pathways do differ with a change in pasture management under eCO₂. Further research is required to understand why these pathways have changed.

Key words: elevated CO₂, grazing, pasture management, soil organic carbon, soil carbon sequestration

4.1 Introduction

Anthropogenic greenhouse gas emissions are driving changes in climate (IPCC, 2014), with a sharp increase in atmospheric carbon dioxide (CO₂) in recent decades that reached 415 ppm in 2022. In addition to the effects on global climate, the elevated concentration of atmospheric CO₂ (eCO₂) is frequently found to be a major driver of changes in biological systems (Kuzyakov et al., 2019), mostly through its impact on photosynthesis and associated carbon (C) inputs to soils (Jones and Donnelly, 2004). Soils are the largest organic C (OC) reservoir in terrestrial ecosystems (Kuzyakov et al., 2019) and have historically and continue to be a source of CO₂ emissions under some agricultural practices (Lal et al., 2018). Grasslands, most of which are grazed (McSherry and Ritchie, 2013; Zhou et al., 2019), account for 70% of the agricultural land worldwide (Conant et al., 2011; FAO, 2019) and contain about 20% of global soil OC stocks (Whitehead et al., 2018). Given the large amounts of OC stored in grazed grasslands, small changes in their soil OC stocks have significant consequences for the global atmospheric CO₂ pool and, therefore, the global climate (Liang et al., 2017; Sitters et al., 2020).

Through Free Air CO₂ Dioxide Enrichment (FACE) experimental facilities, research has confirmed that eCO₂ increases the photosynthetic rate, leading to a boost in plant shoot biomass ranging on average from 13 to 21%, but with a reported increase of up to 200% in some instances, especially during the first years of eCO₂ treatment (Ainsworth and Long, 2005; Newton et al., 2006; Deng et al., 2016; Kuzyakov et al., 2019). The higher nutrient requirements to support enhanced growth under eCO₂ can result in an increase in C allocation to roots (Allard et al., 2005; Sillen and Dieleman, 2012; Madhu and Hatfield, 2013). Furthermore, a boost in plant biomass can lead to a higher organic matter (OM) input rate into the soil, especially from the root, which can result in an increase in both microbial activity and root respiration under eCO₂ (Jiang et al., 2020). As the amount of OC increases, so does the amount of nitrogen (N) contained in the soil OM. Over time, and if the C:N ratio does not

decrease, a progressive limitation of N availability (PNL) may occur (Luo et al., 2004). Additional co-limitation with phosphate (PO_4) availability has been reported under long-term exposure to eCO_2 (Gentile et al., 2012; Touhami et al., 2020). In grasslands without N fertilization, legumes serve as the primary source of newly fixed N and are typically limited by PO_4 . The growth rate enhancement of legumes under eCO_2 is influenced by the availability of soil P (Edwards et al., 2005). Therefore, a reduced supply of PO_4 has implications for the legume component's ability to effectively compete, grow, and carry out biological N fixation within the pasture (Gentile et al., 2012). Thus, unless there is a sufficient nutrient (i.e., N and PO_4) supply and sufficient water, the higher photosynthetic rate possible under eCO_2 is unlikely to translate into a boost in shoot growth and an increased flow of the added C entering belowground to the roots and in plant litter to add to the soil OC pool (Reich et al., 2006; Hungate et al., 2009; Sillen and Dieleman, 2012; Sokol and Bradford, 2019).

Several meta-analyses that include FACE experiments of < 5 years in duration across a range of land uses strongly suggested that an increase in herbage accumulation under eCO_2 would lead to an increase in soil OC (Jastrow et al., 2005; Van Groeginen et al., 2006). Some longer-term grasslands FACE experiments, which ran for > 5 years but < 10 years, corroborate that finding. For example, after 8 years of exposure to eCO_2 , the Denmark-FACE reported an increase of 12 – 22% in OC content in the top 100-mm of soil depth (Vestergard et al., 2016), translating into a 19% increase in OC stocks in the 300 mm topsoil (Dietzen et al., 2019). However, some of the longer-term studies at the Denmark-FACE suggest that the turnover of soil OM under eCO_2 is stimulated to a greater extent than under ambient CO_2 (aCO_2) conditions, limiting and in some cases could lead to a potential loss, rather than a gain in OC over time (Thaysen et al., 2017). In the Tasmania-FACE (Pendall et al., 2011), an increase in soil OC stocks under eCO_2 was reported with C_4 vegetation, but not with C_3 vegetation. This was consistent with the fact that the C_4 herbage production increased under eCO_2 while

decomposition rates failed to match the boost in OC inputs to the soil. Similarly, the BioCon facility in Minnesota (Dijkstra et al., 2004) only detected an increase in soil OC under eCO₂ when N was applied, consistent with the associated increase in herbage accumulation.

Despite the generally positive effect of eCO₂ on soil OC reported in the short-to medium term studies (0 – 10 years exposure to eCO₂) none of the cut or mown grassland FACE studies with ≥ 10 years of exposure to eCO₂ – these include the Swiss-FACE (Six et al., 2001; van Groenigen et al., 2002; de Graaff et al., 2004; Xie et al., 2005; van Kessel et al., 2006 and Theis et al., 2007), the Giessen-FACE (Keidel et al., 2018) and the USDA-ARS High Plains Grasslands Research Station (Carrillo et al., 2018) – have reported any changes in soil OC under eCO₂. At the NZ-FACE grazed grasslands facility, the only study including a legume-based pasture and grazing practices by sheep, the small increases reported in aboveground biomass have also yet to translate into a significant increase in OC and N stocks or a widening in the C:N ratio of the organic fraction (Dodd, 2013; Newton et al., 2014). One of the major reasons for establishing the NZ-FACE facility was to develop a better understanding of how eCO₂ influences soil OC storage, size fractions, and cycling in a legume-based pasture grazed by animals (Ross et al., 2013).

Several meta-analyses address in depth the influence of grazing and the influence of some climate change factors (temperature and precipitation), but not eCO₂, on the above- and the below-ground response of C dynamics of grasslands (Pineiro et al., 2010; McSherry and Ritchie, 2013; Wang et al., 2016; Zhou et al., 2016, 2017; Abdalla et al., 2018; Sitters et al., 2020). The C allocation within the plant and its turnover above- and below-ground are affected by the grazing animal in a number of ways, including major factors in nutrient return (urine and faeces), selective defoliation and trampling (Fontaine et al., 2003; Zhou et al., 2017; Sitters et al., 2020), with subsequent effects on OC inputs and dynamics belowground. Grazing intensity is a key factor in these dynamics. Overall, intensive grazing will increase the amount

of OC entering the soil OC pool via dung and urine and reduce the amount of OC entering the pool through plant litter (shoot and root). Low-intensity grazing, on the other hand, will see more plant litter entering the soil as OC and less dung and urine. The change in the sources of OC will influence OC sequestration and belowground fluxes, including soil respiration, soil net N mineralization and soil N nitrification (Zhou et al., 2017). Sitters et al. (2020) found a strong correlation between herbage production and soil OC under both grazed and cutting treatments; they found that when herbage production and/or microbial activity increases, then soil OC increases, independently of the defoliation treatment. A similar correlation was found by Pineiro et al. (2010), where an increase in soil N fertility boosted herbage production, increasing OC inputs and OC stocks in the soil, while also decreasing C losses by diminishing soil respiration. Zhou et al. (2019) found that low intensity grazing under warming conditions caused a decline in soil respiration, but no change in OC stocks in the soil, while N addition and increased precipitation, regardless of warming, intensified respiration rates (both autotrophic and microbial respiration), significantly increasing the soil OC stocks by 0.8%. Though, the size effect of grazing on soil OC is also dependent on precipitation and temperature, indicating that the impact of grazers on soil OC varies greatly depending on the biotic and abiotic context (McSherry and Ritchie, 2013). When analysing the interaction effects of grazing intensity and climatic parameters, Zhou et al. (2019) found no significant interactions; however, they found that grazing + warming counteracted the effect of grazing alone, by boosting plant growth and microbial activity, grazing + precipitation co-acted to increase soil respiration and so did grazing + N addition. Sitters et al. (2020) found the influence of grazing on soil OC, soil N, and microbial activity is delimited by nutrient availability and temperature. Even though an increase in microbial activity leads to a higher C loss by respiration (Conant et al., 2011), it also increases litter decomposition rates and

promotes the formation of an OC pool (i.e., microbial necromass) that can become preserved in soil over the long-term (Sokol and Bradford et al., 2019).

In general, as a legume-based pasture ages, the soil C:N ratio is expected to decrease under grazing conditions, due to a progressive but slow increase in soil N with either no change or an increase in C losses (Lambert et al., 2000, Zhou et al., 2017; Sitters et al., 2020). This will continue until the C:N ratio approaches 10 (He et al., 2019), at which point the mineralogy of the soil will determine the total amount of OC that can be stored as minerals have a finite surface contact area. Under eCO₂ conditions, the C:N ratio in new OM entering the soil OC fraction could be expected to be higher due to (i) a boost in the photosynthetic rate (Wang et al., 2021), and (ii) a reduced nutrient pool (N and P) to sustain the enhanced growth rate expected under eCO₂ (Ross et al., 2013). If the soil nutrient status declines due to higher plant demand, two processes are expected to occur: (i) a slowing and ultimately a decline in the amount of fresh OC inputs, and (ii) an increase in the decomposition of existing soil OM, with a subsequent impact on the C:N ratio of the remaining OM (Xu et al., 2019). This has the potential to change the persistence and stability of the remaining OM. Globally, the extent to which the potential increase in photosynthetic rate under eCO₂ translates into an actual increase in pasture growth is still uncertain, due to other limiting factors, such as water and nutrients, constraining plant growth. Additionally, it remains unclear whether the observed increase in plant growth reported in the literature translates in sustained increases in OC in the soil over time (Norby and Zak, 2011; Pendall et al., 2011; IPCC, 2013), especially in grazed systems.

At the NZ-FACE grazed legume-based grasslands facility under eCO₂, there has been an increase in aboveground biomass in some years (Newton et al., 2014) and an increase in the OC allocation to roots (Allard et al., 2005). To sustain a higher growth rate under eCO₂ an adequate supply of nutrients is required (Kuzyakov et al., 2019). Both N and P have been

identified as primary co-limiting factors limiting the pasture response to eCO₂ (Newton et al., 2010; Gentile et al., 2012). The increased rate of OC inputs to the soil under eCO₂ observed at the NZ-FACE facility has been positively correlated with the soil microbial activity (Allard et al., 2004). This potentially limits the overall potential gain in OC stocks in the soil under eCO₂ (Allard et al., 2005). The absence of any increase in OC stocks in the soil at the NZ-FACE site even after 13 years of exposure to eCO₂ and despite the boost in pasture growth in some years (Ross et al., 2013), might reflect the fact the soil already has a high OM content, with a C:N ratio approaching 10:1, and consequently with little capacity to preserve the additional necromass-derived OC (Terrer et al., 2018), given the soil sandy texture and associated mineralogy. It is worth noting that the study of Ross et al. (2013) was limited to an examination of the changes in OC in the upper 50 mm of the soil.

As part of our analysis, we explored the interactive effects between eCO₂ and grazing by including three defoliation treatments, (i) areas subjected to selective defoliation, trampling, and receiving nutrient return through dung and urine by the grazing animal, (ii) limiting the influence of grazing animal to selective defoliation, but preventing the animal from treading, defecating, or urinating on the pasture and (iii) excluding the animal using cages, with pasture being hand-cut. The hypothesis was that we would observe an interaction effect between CO₂ and defoliation treatment where under eCO₂ there would be an increase in the soil OC content and stocks supported by the grazing animal, as the nutrient return through grazer's deposition would sustain the nutrient supply required to support increased plant growth and the flow of the extra OC to the soil. The OC inputs in dung and in plant litter trampled in by the grazing animal would be expected to contribute to a greater supply of OC for increasing soil OC stocks, compared to the OC inputs from the other two defoliation treatments. The N input in urine from the grazing animal has the potential to act as a primer to increase microbial activity and the mineralisation of both fresh and old OC, as well as increase soil respiration rates, especially

under eCO₂. If the priming effect of the N in the urine on the microbial community is primarily affecting the recent and fresh labile OC fractions, this will limit the amount of OC available for storage, the associated aggregate building capacity, and the potential to increase soil OC stocks. If the priming occurs on old recalcitrant soil OC, resulting in N mining, then a reduction of OC and N content of the stable fraction is expected, along with some changes in aggregate size distribution and stability. Any changes under eCO₂ in the stability pathways of soil OC in these fractions should be reflected in the soil OM molecular composition, where priming of the labile fraction from recent C inputs would result in a lower proportion of lignin-derived C and higher proportions of microbial-derived C (aliphatic and N-containing products) compared to soils under a cut pasture. The opposite trend would be found if the priming effect is primarily impacting the stable fraction. The objective of our study was to extend the analysis of the effect of exposure to eCO₂ of a legume-based grazed pasture at the NZ-FACE facility from 12 out to 22 years, focusing on the soil OC and N pools and its partitioning (quantitative) and molecular composition (qualitative) of the soil OM.

4.2 Methods

4.2.1 Experimental setup

The NZ-FACE facility is the only FACE facility worldwide examining the influence of eCO₂ on the dynamics of a grazed legume-based pasture, which includes changes in soil OC and N stocks. The facility is divided into three blocks with two circular plots within each block (12 m diameter “rings”; Extended Data Figure 4.1a). Edwards et al. (2001), Ross et al. (2004) and Newton et al. (2014) provide a detailed description of the study site, including the installation process and the logistic of grazing practices inside the rings. The rings were chosen in 1997 based on their initial botanical composition (Newton et al., 2006). In each block, one ring is

exposed to the current atmospheric CO₂ concentration (aCO₂) and the other ring is enriched with eCO₂ daily throughout the photoperiod. As the atmospheric CO₂ concentration kept increasing (363 ppm in 1997 to 412 ppm in 2019), the original difference in CO₂ concentration between ambient and eCO₂ treatment decreased. Over the course of the study dating back to 1997 the CO₂ treatment has not been continuous, between 2011 and 2013 the NZ-FACE facility was refurbished and there was no difference in the atmospheric CO₂ concentration. Furthermore, to maintain the difference in CO₂ concentration between treatments, the CO₂ enrichment was increased to 500 ppm CO₂ in the elevated rings in 2013 - a concentration likely to be reached during this century (IPCC, 2014).

The soil at the site is the Pukepuke black sand (a Mollic Psammaquent) with a 0.25 m black loamy, fine sand top horizon (Cowie, 1965), OM content of < 7% with a C:N ratio < 10:1. Sheep at the NZ-FACE facility graze the permanent legume-based pasture growing in the rings year-round (Extended Data Figure 4.1b). In brief, when the aboveground biomass is around 1800–2000 kg dry wt ha⁻¹, three to five sheep are introduced to the rings and contained by electric fences surrounding each ring. The sheep are left to graze until there is 800 kg dry wt ha⁻¹ of aboveground biomass (Edwards et al., 2001). This usually results in a grazing event of three – four days (Newton et al., 2010). There are 4 – 14 grazing episodes per year depending on the biotic and abiotic conditions and therefore herbage growth.

The behaviour of the animals within the ring is avoiding putting their posterior near the electric fence installed around the perimeter of each ring which means that while the animals graze to the edge of the ring, there is no treading and little or no dung or urine deposited within 0.5 m from the fence. This creates an area where pasture is defoliated (shoot removal) by the sheep, but there is no dung or urine nutrient return and no stock treading pressure. This has created over 20 years an area of lower aboveground biomass and nutrient status within each ring. With this in mind, within each ring, three sampling areas were selected to simulate the following: **a)**

the centre of the ring (grazed + nutrient return and treading in plant litter (NT)), a condition where the animal defoliates shoots, nutrients are returned to the soil through dung and urine depositions, and treading incorporates plant litter into the soil (Extended Data Figure 4.1c); **b**) edge of the ring (grazed – NT treatment), where animals defoliates shoots yet the soil receives minimal dung and urine return and no treading pressure (Extended Data Figure 4.1d); **c**) an area under a 0.5 m² exclusion cages where pasture was hand-cut (cut – NT treatment), and grazing, nutrient return and treading are prevented. The two exclusion cages in each ring were lifted to study pasture growth (Extended Data Figure 4.1e), is but was put back in the same location after each pasture cut over the last 22 years. The pasture in the cages was hand-cut on every grazing episode.

4.2.2 Soil collection and bulk soil analysis

Soil cores were collected from the during the southern hemisphere spring in November 2019. Sixteen soil cores (25 x 250 mm) were collected from each of the three areas within each ring (aCO₂ and eCO₂). The soil cores were divided *in-situ* into three depths (0 – 50, 50 – 150, and 150 – 250 mm). Eight of the 16 soil cores per depth were individually oven-dried for 24 h at 105 °C prior to weighing for bulk density analysis. The remaining eight soil cores were air dried, sieved (< 2 mm) and then combined giving one sample for each of the three defoliation treatments and three depths for each ring (6 rings) to generate 54 composite samples across all CO₂ treatments. The samples were analysed for total C and N by dry combustion in an Elementar analyser (Vario Max Cube; Analysensysteme GmbH, Germany) located at the Grasslands campus, AgResearch, New Zealand. No acid pre-treatment to remove inorganic C was performed as the soil pH was close to neutral and not significantly different between CO₂ treatments (Extended Data Table 4.1), thus insignificant amount of inorganic C was expected

to be found. Soil OC and N stocks down to a specific depth were determined from the equivalent soil mass (ESM) procedure proposed by Wendt and Hauser (2013) to overcome potential masking effects associated with changes in soil bulk density.

4.2.3 Soil wet fractionation analysis

A subsample of the bulk soil composite sample was used for soil fractionation by wet-sieving analysis, following the soil fractionation procedure proposed by Six et al. (2002). Aggregates were physically separated into three aggregate sizes (i.e., diameter): coarse particulate organic matter (cPOM) of 250 to 2000 μm \varnothing , micro-aggregates of 53 to 250 μm \varnothing , and mineral associated OM, (MAOM) in silt and clay of < 53 μm \varnothing . The isolator unit was composed of two sieves on a horizontal shaker and attached to a source of running RO water. Individually, the samples were soaked in RO water for 5 min and shaken in a plastic cylinder (for 15 min at 150 rpm), which allowed the cPOM to be collected on a 250 μm sieve, while micro-aggregates were subsequently retained in a 53 μm sieve. After the wet sieving, the three aggregate sizes (cPOM, micro-aggregates and MAOM) were collected in aluminium pans, oven-dried at 60 °C until constant weight, and weighted to determine the distribution of aggregates size fractions in the soil sample. The soil fractions were analysed for total C and N by dry combustion in an Elementar analyser (Vario Max Cube; Analysensysteme GmbH, Germany).

4.2.4 Soil organic matter molecular composition

A sub-sample of bulk soils composite sample was analysed through pyrolysis (Py-) gas chromatographer/mass spectrometry (GC-MS) and thermally assisted hydrolysis and methylation (THM-) GC-MS identifying 134 and 72 compounds, respectively (Extended Data Tables 4.2 and 4.3 respectively). We quantified the relative proportions of the pyrolysis (sum

100%) and THM products (sum 100%) and we assessed the source of the soil OC (Tables 4.1 and 4.2, respectively) under aCO₂ and eCO₂ conditions in each defoliation treatment on three soil depths. These were statistically analysed for interaction effects between CO₂, defoliation and soil depth treatments on individual Py- and THM-GC-MS products followed by cluster analysis based on the source of OC.

Table 4. 1: Soil organic matter pyrolytic products (Py-GC-MS) found at the NZ Free Air CO₂ Enrichment facility, clustered by chemical similarity, and their predominant source of origin.

Product	The potential source of origin
Methylene chain compounds (MCC)	Compounds with a long-chain chain aliphatic backbone (alkanes, alkenes, fatty acids, etc.). Derived from microbial and plant-derived molecules (cutin, suberin, epicuticular waxes, etc.).
Carbohydrate products	A chemically diverse group, including acetic acid, furans, furaldehydes, cyclopentenones, pyrans and anhydrosugars. Largely derived from structural polysaccharides in plants (e.g., cellulose, hemicellulose, starch) and microbial polysaccharides (chitin, peptidoglycan).
N-containing products	Compounds with at least one atom of N, including pyrroles, pyridines, acetamidoglycans, cyanobenzenes, indoles and diketopiperazines. Derived mainly from macromolecules of protein (of plant and microbial origin), chitin (from fungi and arthropods) and peptidoglycan (bacterial OM). Acetamide, succinimide, acetamidoglycans are used as markers of chitin.
Lignin	The products of lignin (4-vinylphenol, guaiacols, syringols) indicate vascular plant-derived OM. These products are useful as markers of plant-derived OM and their balance can provide indications of lignin source (e.g., herbaceous vs. woody).
Other phenols	Other phenols are products of microbial OM, lignin and other sources, and therefore of little diagnostic value.
Halogen-containing	Two compounds containing halogens, i.e., bromomethane and iodomethane, were included in the analysis due to quite large peaks in some samples. We associate this with the small distance from the FACE to the coastline.
Monocyclicaromatic hydrocarbons (MAH)	Compounds such as benzene, toluene and xylenes are not indicative of a specific source. Given that toluene prevails in most samples suggests most of the MAH signal corresponds to microbial OM.
Polycyclic aromatic hydrocarbons (PAH)	The PAHs can be pyrogenic, but at low levels (< 1 %, which is the case here), the presence of such OM cannot be ascertained because secondary reactions of uncharred OM and resinous moieties can also yield PAHs.
Others	Benzaldehydes, tocopherols and unidentified products.

Table 4. 2: Soil organic matter products found at the NZ Free Air CO₂ Enrichment facility, clustered by chemical similarity and the predominant source of origin by thermally assisted hydrolysis and methylation followed by gas chromatography and mass spectrometer (THM-GC-MS) analysis.

Products	The potential source of origin
Short-chain FAME (sFAME)	Aliphatic, short chain (< C ₂₀) length fatty acid methyl ester (sFAME) are probably mostly bacterial in origin, possible products of any OM precursor. They include a branched C ₁₅ FAME (iso/anteiso configuration) which is probably mostly bacterial, whereas the other short FAMEs are possible products of any OM precursor.
Long-chain FAME (IFAME)	Aliphatic, long chain (≥ C ₂₀) fatty acid methyl esters (IFAME), mostly from plant-derived aliphatic macromolecules (cutin and suberin) and epicuticular waxes.
ω-methoxy-FAME	ω-methoxy-FAMEs (oFAMEs), usually ascribed to cutin and suberin.
Short-chain DAME (sDAME)	Mainly azelaic acid (dimethyl ester), from fragmented unsaturated C ₁₈ fatty acids (e.g., oleic acid).
Long-chain DAME (IDAME)	Long-chain (> C ₂₀) methylated fatty diacids are key products of suberin and are thus associated with bark and root-derived materials.
Other MCC	Other methylene chain compounds include <i>N</i> -methyl-alkylamides and <i>N,N</i> -dimethylalkylamides, two methoxyalkanes and an unidentified compound (alkene or unsaturated FAMEs).
N-containing	Include proline derivatives, alkylindoles and a phthalimide. Mostly of microbial origin. As the TMAH reagent contains N and hydrolysis of microbial OM under THM conditions is poor, these compounds are to be interpreted with caution.
Carbohydrate products	The carbohydrate products, e.g., C ₅ and C ₆ methylated metasaccharinic acids and trimethyllevoglucosan. Underestimation of polysaccharides due to poor hydrolysis.
1MB	Monomethoxy benzenes are, in this case, mainly lignin-derived (compounds P4, P6 and P24 in lignin nomenclature).
2MB	1,2-dimethoxybenzenes are probably mostly derived from guaiacyl structures in lignin (plant-derived).

3MB	1,2,3-trimethoxybenzenes may originate from syringyl moieties in lignin and pyrogallol moieties in tannin (plant-derived).
MB135	1,3,5-trimethoxybenzenes. May originate from cutan and condensed tannin (plant-derived).
MBcinn	“Cinnamyl type” methoxybenzenes (THM products of <i>p</i> -coumaric, ferulic and caffeic acid) are often associated with lignin and lignin-like phenolics in herbaceous litter but suberin (aliphatic macromolecule) also contains a phenolic domain that can yield these THM products
BCA	Methylated benzene carboxylic acids are not diagnostic of any specific source. They are likely THM products of lignin or degraded lignin, but other sources may contribute.
Mid-chain methoxy-FAME	C ₁₆ and C ₁₈ FAMEs with methoxy substitution at the C ₉ and/or C ₁₀ , and terminal (C ₁₆ /C ₁₈) positions. Key products of cutin and suberin. The proportions of mid-chain methoxy-FAMEs and long DAMEs provide information on the balance between cutin from plant cuticles and suberin from barks and roots.
Other	Other compounds include α -tocopherol and two unidentified products.

4.2.4.1 Analytical procedure for pyrolysis- and thermally assisted hydrolysis and methylation- GC-MS analysis

A mild acid pre-treatment was performed on fine ground samples to remove reactive mineral phases such as iron (oxy)(hydro)oxides, i.e., 2% hydrofluoric acid (HF) solution treatment. Briefly, 0.2 g of sample was weighed into 50 mL polyethylene centrifuge tubes, to which an aliquot of 10% HCl was added to dissolve carbonates, and then 2% aqueous HF solution added until the 40 mL mark (i.e., 39 – 40 mL of HF solution). After 24 h of shaking, the suspensions were centrifuged (2500 rpm for 10 min) and the supernatant was discarded. This HF treatment was not repeated as the extracts' colours were not indicative of a major release of oxides, and limiting the rounds of treatment is expected to limit the loss of low-molecular-weight mineral-bound OM. The obtained residue was then rinsed three times in distilled water to wash away salts and remaining acid (with centrifugation/decantation cycles in between). The final residues were dried at 50 °C and homogenized before analysis.

Conventional Py-GC-MS was performed with a Pyroprobe (CDS Analytical) coupled to an 8860 GC and 5977 MSD (Agilent Technologies). The samples (1 mg of ground and HF-treated material) were embedded in glass wool containing fire-polished quartz tubes and pyrolyzed at 650 °C (set-point temperature) for 20 seconds (heating rate 10 °C ms⁻¹). The pyrolysis-GC interface, GC inlet, and GC-MS interface were set at 325 °C. The GC was equipped with a (non-polar) HP-5MS 5% phenyl, 95% dimethylpolysiloxane column (length 30 m; internal diameter 0.25 mm; film thickness 0.25 µm). Helium was used as the carrier gas (constant gas flow, 1 ml min⁻¹). The GC oven was heated from 60 to 325 °C at 20 °C min⁻¹. The ion source of the MS operated in electron impact mode (70 eV) at 230 °C and the quadrupole detector was held at 150 °C, measuring fragments in the m/z 50–500 range. Relative proportions of the pyrolysis products were calculated as the percentage of the total quantified peak area (TQPA), using the main fragment ions (m/z) of each product.

The instrumentation and most parameters for Py-GC-MS were also used for THM-GC-MS. Before inserting the sample-containing quartz tubes, an aliquot of 25 % tetramethylammonium hydroxide (aqueous TMAH from Sigma-Aldrich) was added and the mixture was allowed to stand for at least 1 h. Analytical parameters that differ from the ones for Py-GC-MS were the use of a 5 min solvent delay (to allow the reactant and solvent to elute before activation of the MS), and a GC oven temperature program from 70 to 325 at 20 °C min⁻¹ with a 5 min initial and 3 min final isothermal hold periods. The THM-GC-MS products were semi-quantified using their main *m/z* ratio to % of TQPA.

4.2.5 Statistical analysis

The differences between CO₂, defoliation and soil depth treatments and their interaction effects were explored. Linear mixed effect models (lme) for the nested block design followed by pairwise tests and permutations were applied to aboveground biomass, soil nutrient status and soil OC and N data. The Py- and THM-GC-MS results were evaluated using principal components analysis (PCA) by correlation to identify factors with major influence on product distributions in the whole dataset. The relative proportions of individual products (% TQPA), sums of types of products (% TQPA) and the principal components obtained by PCA were used to compare results from Py- and THM-GC-MS (individual compounds % as input) to soil OC content and C/N ratio. The qualitative analysis was followed by a lme analysis on the sum of the type of products and each individual product to identify the effects of CO₂ treatment, soil type and depth on the soil OM molecular composition. R Studio was used to run all the statistical analysis through “lme” and “predictmeans” packages (RStudio version 1.2.5033).

4.3 Results

4.3.1 Effect of elevated CO₂ on soil organic carbon and nitrogen stocks

Twenty-two years of exposure of a grazed legume-based pasture to eCO₂ had no effect on soil bulk density (Figure 4.1a), OC and N contents (Figure 4.1c and d, respectively), OC and N stocks (Figure 4.1e and f, respectively), or the C:N ratio (Figure 4.1b) in any of the three soil depths (0 – 50, 50 – 150 and 150 – 250 mm). The grazing animal, in returning nutrients in urine and dung and in trampled plant litter (grazed + NT treatment) did not contribute to an increase in soil OC and N contents under eCO₂ (Figure 4.1c and d, respectively). The C:N ratio values in the grazed + NT treatment did not significantly differ between ambient and eCO₂ (10.3 ± 0.2 vs 10.2 ± 0.2 , respectively; Figure 4.1b). Limiting the influence of the grazing animal to just selective defoliation of the pasture (grazed – NT) or excluding the grazing animal by cutting the pasture (cut – NT), did not change the soil OC and N contents under eCO₂ (Figure 4.1c and d, respectively) nor their stocks (Figure 4.1e and f, respectively). Thus, no interaction effects were found between eCO₂ and defoliation treatment on soil OC and N contents and stocks. Furthermore, no interaction effect was found between eCO₂ and soil depth on soil OC and N contents (Extended Data Table 4.4).

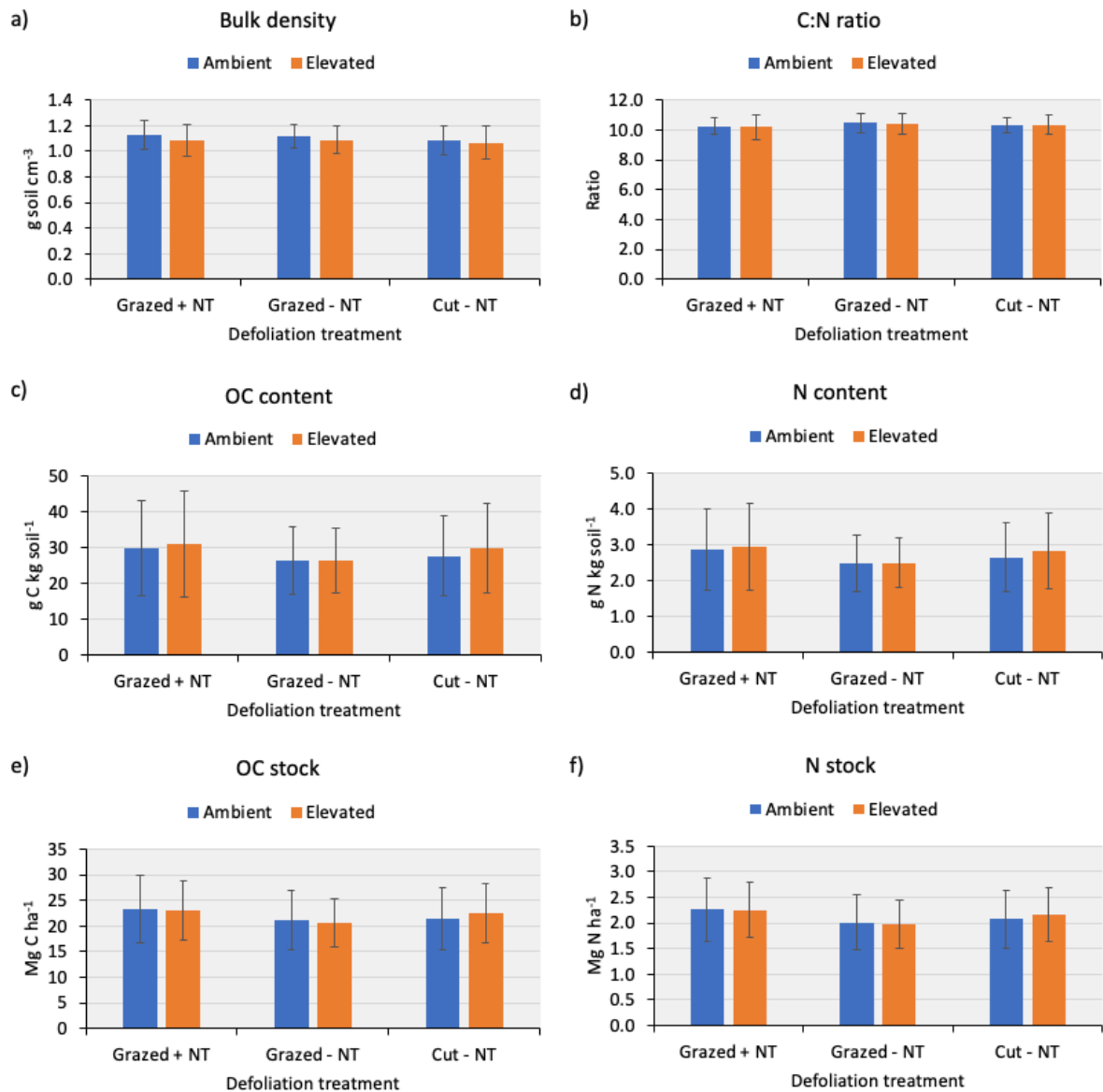


Figure 4. 1: Effect of ambient and elevated CO₂ and three defoliation treatments on soil attributes throughout the soil profile (0 – 250 mm) after 22 years of eCO₂ exposure at the NZ-FACE facility. Grazed + NT: grazed + nutrient return + treading in plant litter, a condition where animal grazing defoliates shoots, nutrients are returned to the soil through dung and urine depositions, and treading incorporates plant litter into the soil; Grazed – NT: a condition where animals grazing removes shoots yet the soil receives no dung and urine return and no treading pressure; Cut – NT: area under a 0.5 m² exclusion cage where pasture was hand-cut, where grazing, nutrient return and treading are prevented. Error bars indicate SD (n=3).

4.3.2 Effect of defoliation on soil organic carbon and nitrogen stocks

A consistent interaction effect was found between defoliation treatments and soil depth (averaged across the two CO₂ treatments) for soil bulk density ($p = 0.0462$), soil OC and N contents ($p = 0.0005$ and 0.0002 , respectively) and stocks ($p = 0.033$ and 0.0213 , respectively; Table 4.3). The interactive effect between defoliation and soil depth was more strongly observed in the topsoil (0 – 50 mm), than in the second depth (50 – 150 mm). There were no differences in the 150 – 250 mm depth (Table 4.3).

Table 4. 3: Soil bulk density (BD), organic carbon (OC) and nitrogen (N) content, C:N ratio and stocks in the three soil layers under the three defoliation treatments, averaged for the two CO₂ treatments, at the NZ Free Air CO₂ Enrichment facility. Results are means with SD (n = 3).

Depth (mm)	Defoliation treatment	BD (g cm ⁻³)	N content mg N g soil ⁻¹	OC content g C kg soil ⁻¹	C/N ratio	N stock (Mg N ha ⁻¹)	OC stock (Mg C ha ⁻¹)
0 - 50	Grazed + NT	0.99 ± 0.03 (de)	4.25 ± 0.24 (a)	46.92 ± 3.67 (a)	11.03 ± 0.27 (a)	2.12 ± 0.12 (c)	23.40 ± 1.75 (b)
	Grazed – NT	1.02 ± 0.05 (cd)	3.27 ± 0.16 (c)	36.65 ± 1.75 (c)	11.22 ± 0.15 (a)	1.63 ± 0.08 (e)	18.34 ± 0.89 (cd)
	Cut – NT	0.96 ± 0.07 (e)	3.82 ± 0.44 (b)	41.85 ± 5.21 (b)	10.96 ± 0.20 (a)	1.90 ± 0.21 (cd)	20.83 ± 2.49 (bc)
50 - 150	Grazed + NT	1.09 ± 0.04 (b)	2.90 ± 0.21 (d)	29.25 ± 2.47 (d)	10.08 ± 0.29 (bc)	2.95 ± 0.21 (a)	29.84 ± 2.56 (a)
	Grazed – NT	1.06 ± 0.02 (bc)	2.60 ± 0.20 (e)	26.87 ± 2.39 (d)	10.33 ± 0.19 (b)	2.64 ± 0.22 (b)	27.39 ± 2.67 (a)
	Cut – NT	1.05 ± 0.04 (bc)	2.78 ± 0.25 (de)	28.52 ± 3.16 (d)	10.23 ± 0.27 (b)	2.78 ± 0.22 (ab)	28.49 ± 2.82 (a)
150 - 250	Grazed + NT	1.25 ± 0.04 (a)	1.58 ± 0.21 (f)	15.23 ± 2.58 (e)	9.58 ± 0.39 (d)	1.70 ± 0.19 (de)	16.37 ± 2.41 (d)
	Grazed – NT	1.23 ± 0.05 (a)	1.62 ± 0.19 (f)	15.82 ± 1.92 (e)	9.78 ± 0.25 (cd)	1.72 ± 0.15 (de)	16.84 ± 1.46 (d)
	Cut – NT	1.22 ± 0.03 (a)	1.62 ± 0.29 (f)	15.98 ± 3.43 (e)	9.83 ± 0.46 (cd)	1.69 ± 0.28 (de)	16.68 ± 3.33 (d)

Soil bulk density in the topsoil (0 – 50 mm) of grazed + NT and cut – NT treatments was similar (0.99 ± 0.03 vs 0.96 ± 0.07 g soil cm⁻³); in the grazed – NT soils the bulk density was slightly higher (1.02 ± 0.05 g soil cm⁻³). No significant differences in bulk density in the deeper soil layers were observed, and as expected, the soil bulk density increased with soil depth ($p < 0.0001$; Table 4.1).

Differences in OC and N contents in the 0 – 50 mm soil depth between the three defoliation treatments were significant, with the grazed + NT soils having larger OC and N contents compared to grazed – NT and to a lesser degree the cut – NT treatments. The grazed – NT soils had the smaller OC and N contents. At 50 – 150 mm soil depth, there were no differences in soil OC content between the three defoliation treatments, yet N content was significantly higher in the grazed + NT soils compared to grazed – NT soils (2.9 ± 0.2 vs 2.6 ± 0.2 mg N g soil⁻¹) and cut – NT soils (2.9 ± 0.2 vs 2.8 ± 0.4 mg N g soil⁻¹). Organic C and N content decreased with soil depth as expected ($p < 0.0001$), as did the C:N ratio values ($p < 0.0001$). The C:N ratio showed little change despite differences in OC and N content between the three defoliation treatments and no interactions with soil depth.

With the small interaction effect found between the three defoliation treatments and soil depth on soil bulk density, a cubic spline was used to compare OC and N stocks on a soil weight rather than on a volume basis (Wendt and Hauser, 2013). The grazed pasture receiving nutrient inputs in dung and urine (grazed + NT) had significantly larger OC and N stocks than the system just defoliated by sheep (grazed – NT) and slightly larger than cut pasture treatment in the 0 – 50 mm soil depth. In the following soil layer (50 – 150 mm) only N stocks in the grazed + NT treatment were significantly larger than those in grazed – NT (2.95 ± 0.21 vs. 2.64 ± 0.22 Mg N ha⁻¹).

4.3.3 Soil organic carbon and nitrogen in the soil fractions

On average, there was a 99.3% physical recovery (mass recovery after wet fractionation analysis) and 107% chemical recovery (sum of fraction size) in soil samples from the three soil depths of the three defoliation treatments after 22 years of exposure to eCO₂ (Extended Data Table 4.5).

4.3.3.1 Influence of elevated CO₂ on soil organic carbon and nitrogen pools

Elevated CO₂ did not influence the cPOM fraction size, OC and N contents, C:N ratio or this fraction's OC and N proportion out of the total soil OC and N pools in any soil layer (Extended Data Figure 4.2a, b, c, d, e and f respectively). Nevertheless, there were some CO₂ x depth interaction effects independent of the defoliation treatment, where at 50 – 150 mm depth, the N proportion in the cPOM fraction out of the total soil N was higher under eCO₂ compared to aCO₂ soils ($p = 0.0217$; Figure 4.2a). Similar results have been found at the NZ-FACE facility (Gonzalez-Moreno et al., unpublished). When the interactive effect of eCO₂ and grazing were evaluated, some trends were observed in the cPOM, with larger OC and N contents under eCO₂ especially under grazed + NT and cut – NT treatments (Extended Data Figure 4.2c and d).

Soil micro-aggregates were not influenced by eCO₂. Further, there were no interaction effects between eCO₂ and defoliation treatment or soil depth on this fraction, its OC and N contents and proportions out of the total OC and N pools, or C:N ratio (Extended Data Figure 4.3a, b, c, d, e and f). Across the defoliation treatments, micro-aggregate fraction size in soils under eCO₂ was consistently larger (Extended Data Figure 4.3a) but had similar OC and N content compared to micro-aggregates from the soil under aCO₂ (Extended Data Figure 4.3c and d, respectively). Furthermore, in micro-aggregates from soils under eCO₂, the OC and N proportions out of the total soil OC and N were constantly smaller in the topsoil (0 – 50 mm) and consistently larger in the deeper soil layers (Extended Data Figure 4.3e and f, respectively).

The MAOM aggregate size fraction showed a CO₂ x depth interaction effect, where MAOM from the second soil layer (50 – 150 mm) under eCO₂ has a slightly smaller fraction size compared to fraction size under aCO₂ conditions ($p = 0.0099$; Figure 4.2b). The OC and N content in MAOM were consistently smaller under eCO₂ across defoliation treatments and soil depths (Extended Data Figure 4.4c and d). Across defoliation treatments, the proportion of OC and N in MAOM out of the total soil OC and N content was significantly smaller under eCO₂

($p = 0.042$ and $p = 0.048$, respectively; Figure 4.2c and d, respectively). Despite the consistent trend of reduced OC and N content and C:N ratio in MAOM under eCO_2 compared with aCO_2 , these differences were not significant at $p < 0.05$.

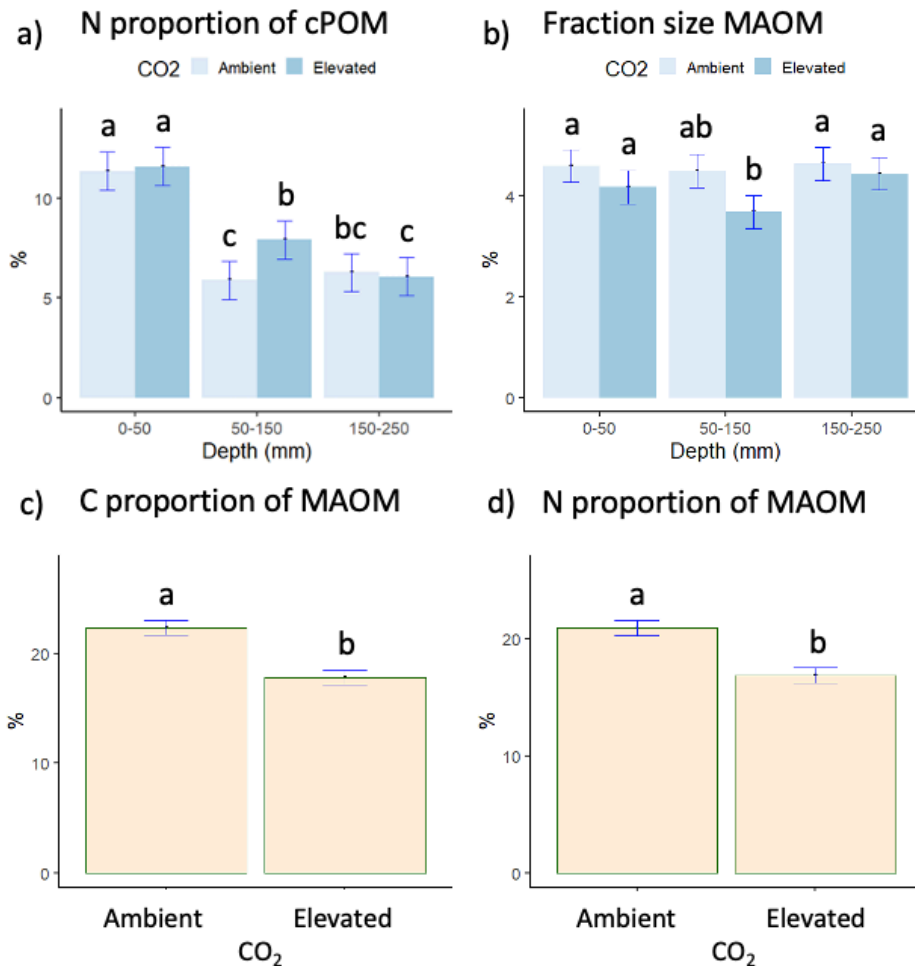


Figure 4. 2: Effect of elevated CO₂ on soil fractions after 22 years of exposure at the NZ-FACE facility, averaged across the three defoliation treatments. a) N proportion in the coarse particulate organic matter (cPOM) out of the total N pool, b) fraction size of the mineral-associated organic matter (MAOM), c) C proportion in MAOM out of the total C pool and d) N proportion in MAOM out of the total N pool. Error bars indicate SD (n = 3).

4.3.3.2 Influence of defoliation effect on soil organic carbon and nitrogen pools

Averaged across the two CO₂ treatments, we found a consistent defoliation treatment x soil depth interaction effect on the cPOM ($p = 0.0425$), micro-aggregates ($p = 0.0217$) and MAOM fraction size ($p = 0.0145$). The cPOM fraction size in the topsoil (0 – 50 mm) was significantly larger in the grazed + NT ($17.4 \pm 3.0\%$) compared to grazed – NT ($14.9 \pm 3.3\%$) and cut – NT ($15.0 \pm 3.1\%$) treatments. This effect dissipated in deeper soil layers ($p = 0.0425$; Figure 4.3a). The grazed + NT soil tended to have a slightly smaller micro-aggregates fraction size ($77.6 \pm 2.6\%$) in the topsoil, compared to the grazed – NT ($79.4 \pm 3.4\%$) and cut – NT ($78.9 \pm 2.9\%$) treatments (Figure 4.3b). Again, the effect dissipated with increasing soil depth. Interestingly, the MAOM fraction size fluctuated more throughout the soil profile, with grazed + NT having the smallest fraction size of MAOM especially compared to grazed – NT in the top and second soil layers (Figure 4.3c).

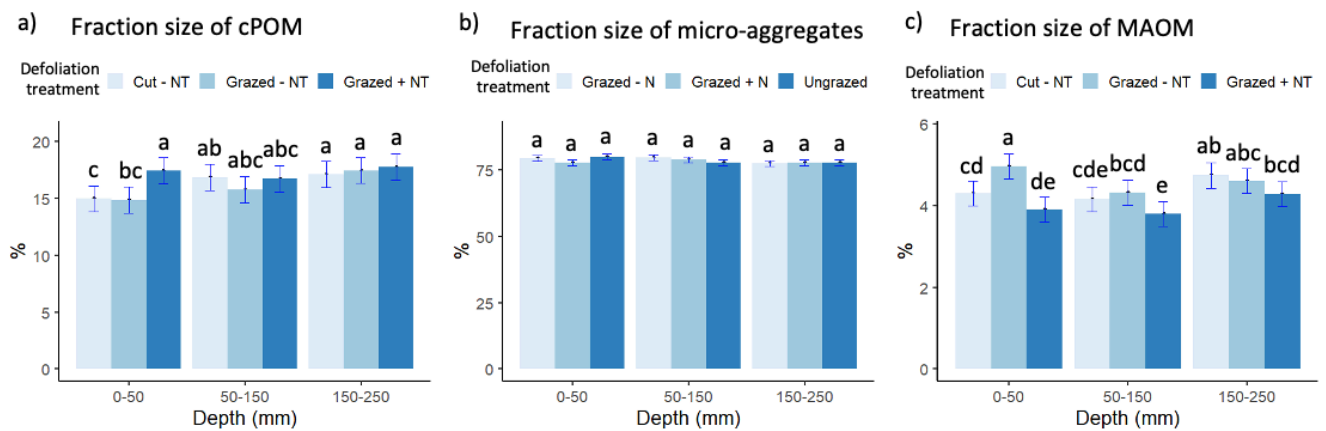


Figure 4. 3: Soil aggregate fraction sizes in different grazing treatments, averaged for the two CO₂ conditions, (a) coarse particulate organic matter (cPOM), b) micro-aggregates, c) mineral-associated organic matter (MAOM). Error bars indicate SD (n = 3).

A strong interaction effect was found between defoliation treatment and soil depth for OC and N contents ($p = 0.003$ and $p < 0.0001$, respectively) of the cPOM fraction. The cPOM fraction from grazed + NT had the largest OC content in the topsoil compared to grazed – NT and cut

– NT treatments. In the second soil depth (50 – 150 mm) a similar but less pronounced trend was found (Figure 4.4a). Similarly, N content in the cPOM in the topsoil was larger in grazed + NT soils compared to the other two defoliation treatments (Figure 4.4b). The grazed – NT treatment had significantly smaller N content in the cPOM than the grazed + NT and cut – NT treatments at 0 – 50 and 50 – 150 mm depths. Because of the changes in the cPOM aggregate size distribution and its OC and N contents, we found a strong defoliation treatment x depth interaction effect on OC and N proportion in cPOM out of the total soil OC and N pool ($p = 0.0073$ and $p < 0.0001$, respectively) matching the same trends found in OC and N contents of the cPOM throughout the soil profile (Extended Data Figure 4.5a , b, c and d).

As with the cPOM fraction, there was an interaction effect between defoliation treatment and soil depth in micro-aggregates. This was strongly observed in the OC and N contents in the micro-aggregates fraction in the topsoil (Figure 4.4c and d, respectively). The grazed + NT and cut – NT had similar OC and N contents, but OC and N were larger where the shoots were defoliated by the grazing animals, but no nutrients were returned (grazed – NT). Despite the strong defoliation treatment x soil depth interaction effect on OC and N concentrations in micro-aggregates, the only significant main effects were associated with soil depth ($p < 0.0001$ for both) and not the defoliation treatment ($p = 0.2837$ and $p = 0.2091$, respectively).

The MAOM fraction in the topsoil was also influenced by defoliation treatment (Extended Data Figure 4.7a, b, c and d). Throughout the soil profile (0 – 250 mm) in grazed + NT soils the MAOM fraction size was smaller, and despite having slightly larger OC and N (not significant), the proportions of OC and N in MAOM (out of the total soil OC and N pool) were significantly smaller in grazed + NT ($p < 0.0001$ for both) than in the other two defoliation treatments. Interestingly, the grazed – NT soil showed a larger proportion of the MAOM-associated stable OC and N out of the total pools ($p < 0.0001$ for both; Figure 4.4e and f respectively).

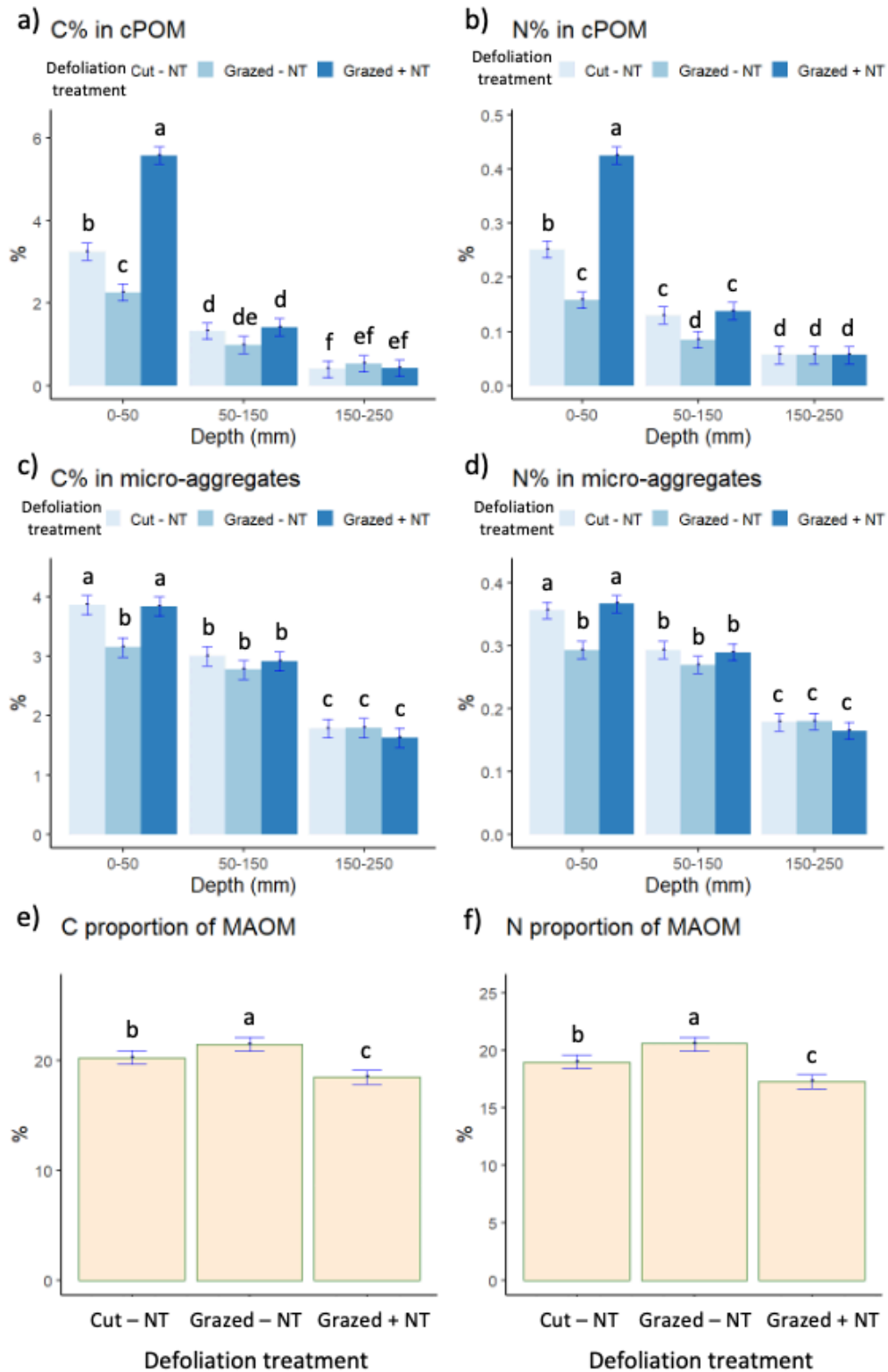


Figure 4. 4: Defoliation treatment effect on organic carbon (OC) and nitrogen (N) contents in soil fractions averaged for the two CO₂ treatments, a) organic carbon content (C%) in the coarse particulate organic matter (cPOM) at three soil depths, b) nitrogen content (N%) in the cPOM at three soil depths, c) organic carbon content (C%) in micro-aggregates at three soil depths, d)

nitrogen content (N%) in micro-aggregates at three soil depths, e) organic carbon content (C%) in the mineral-associated organic matter (MAOM) as proportion of the total OC pool throughout the soil profile (0 – 250 mm) and d) nitrogen content (N%) in MAOM as proportion of the total N pool throughout the soil profile (0 – 250 mm).

4.3.4 Soil organic matter characterization by Pyrolysis-GC-MS analysis

4.3.4.1 Interaction effects between elevated CO₂ and defoliation treatment

Elevated CO₂ had no effect on any of the 134 pyrolyzates or the pyrolytic groups. There was a small interaction effect between defoliation treatment and eCO₂ in that soils from grazed + NT were enriched in C₂₇ alkene (a long-chain aliphatic product, $p = 0.0199$; Extended Data Figure 4.8a). An eCO₂ x soil depth interaction ($p = 0.0423$) was found for 4-vinylphenol (from *p*-coumaric acid, associated with herbaceous litter; Extended Data Figure 4.8b), which was found in higher proportions in the 50 – 150 mm soil layer than either in the topsoil or in the 150 – 250 mm layer (Extended Data Figure 4.8b). The analysis was marked with a large amount of variation between replicates.

Although statistical significance was not detected, there were consistently lower levels of polysaccharide products (Figure 4.5a) and higher levels of aliphatic compounds (Figure 4.5b) under eCO₂ in all three defoliation treatments. With the exception of the grazed + NT treatment, levels of N-containing compounds also seem to increase as a result of eCO₂ (Figure 4.5c), while the lignin proportion did not differ between the two CO₂ treatments (Figure 4.5d). However, the error associated with these measurements was too high to make any conclusions based on this data alone.

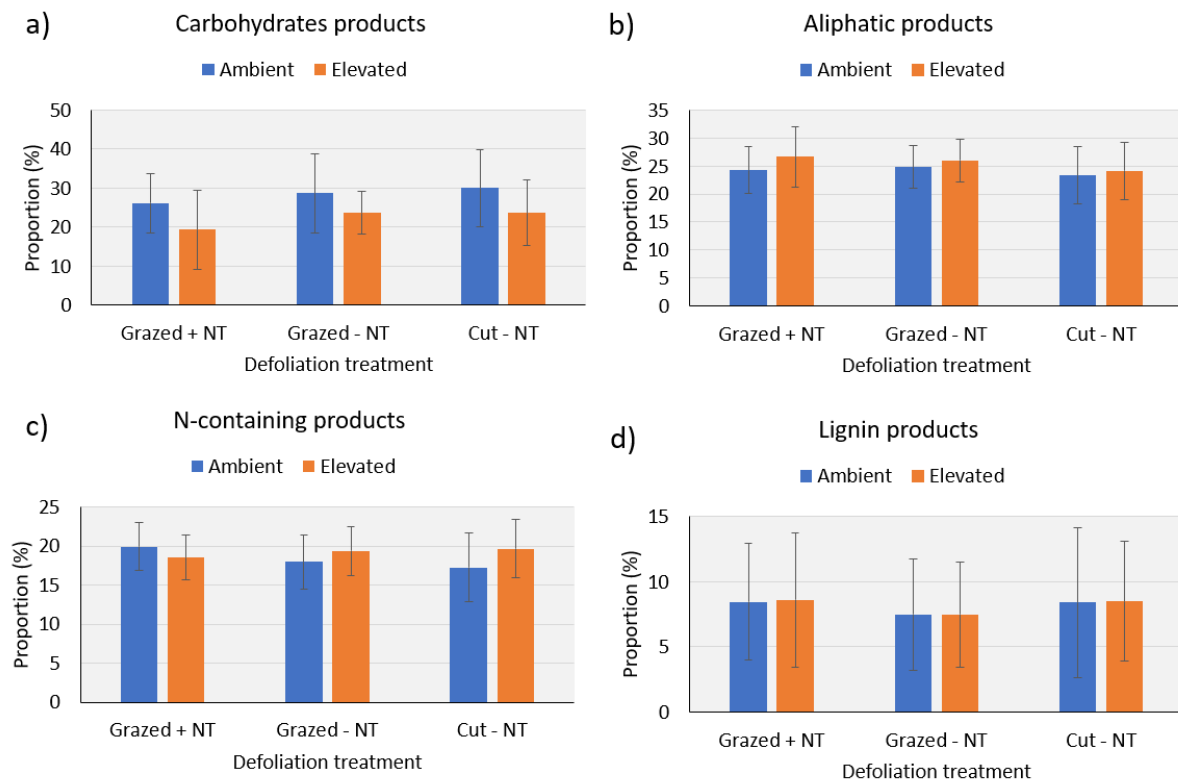


Figure 4. 5: Effect of elevated CO₂ and defoliation treatment on the major pyrolytic groups across all three soil depths. a) Sum of carbohydrate products, b) Sum of methylene chain compounds (aliphatic products), c) Sum of N-containing products, and d) Sum of lignin products. Error bars represent SD (n = 3).

4.3.4.2 Influence of soil depth on soil organic matter molecular composition

Lignin phenols ($p < 0.0001$), other phenols ($p = 0.0154$) and plant polysaccharides ($p < 0.0001$) decreased with soil depth, while MAH ($p = 0.0004$), MCC ($p < 0.0001$), and N-containing products ($p < 0.0001$) increased with soil depth (Figure 4.6), as did the lignin oxidation parameters ($p = 0.005$; Extended Data Table 4.6), independently of CO₂ and defoliation treatment.

4.3.4.3 Influence of defoliation on soil organic matter molecular composition

The effect of defoliation treatment on the pyrolytic groups and products was significant throughout the soil profile. This effect was independent of CO₂ treatment. The grazed – NT treatment was found to be depleted in lignin (syringol units specifically) compared to grazed + NT and cut – NT treatments ($p = 0.0447$), with this effect more evident in the deeper soil layers (50 – 150 and 150 – 250 mm; Figure 4.6a, b and c). There was a grazing x depth interaction effect, where many N-containing products in the grazed – NT treatment had a larger content in the topsoil and a lower content in the second soil layer, compared to the other defoliation treatments.

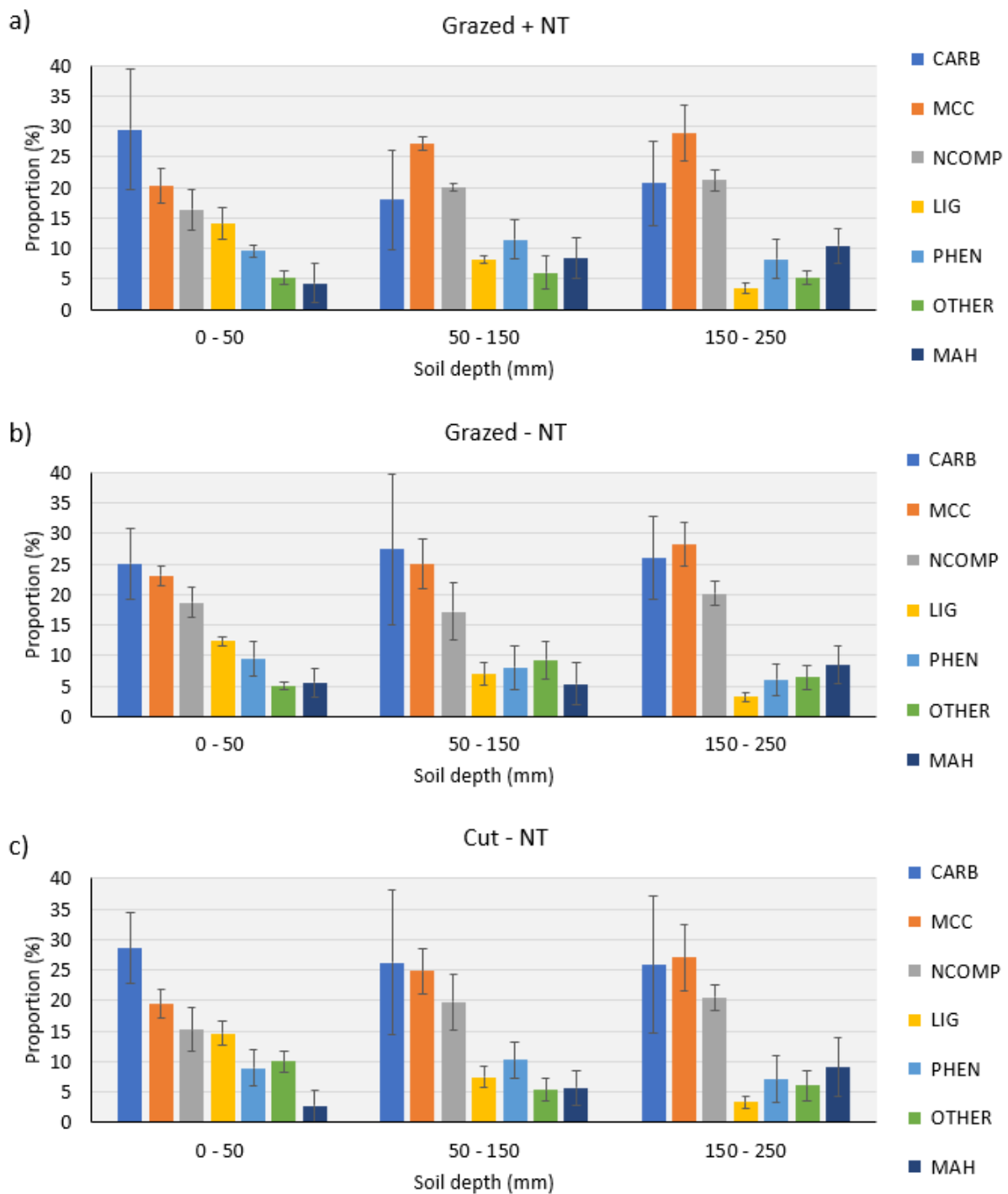


Figure 4. 6: Pyrolysis-GC-MS results (as the percentage of total quantified peak area) for three defoliation treatments and three soil depths, averaged for the two CO₂ levels. Results are shown based on pyrolytic groups. Error bars indicate SD (n = 3). Abbreviation of products: CARB =

carbohydrate, MCC = aliphatic, NCOMP = nitrogen-containing, LIG = lignin products, PHEN = phenols, OTHER = unidentified and MAH = monocyclic aromatic hydrocarbons.

4.3.5 Soil organic matter characterization by thermally assisted hydrolysis and methylation-GC-MS analysis

4.3.5.1 Interaction effect between elevated CO₂, defoliation treatment and soil depth

Elevated CO₂ had no measurable effect on any of the 78 THM individual products or groups in the soil OM. Nevertheless, a CO₂ x defoliation interaction effect ($p = 0.0289$) was found in long-chain FAMES (cutin- and suberin-derived OC) where under eCO₂ these products in the grazed – NT soil were 2.2% lower (Figure 4.7a). The opposite was found with ω -methoxy C₁₆ FAME ($p = 0.0212$) and ω -methoxy C₂₂ FAME ($p = 0.0429$), also derived from cutin, suberin and waxes, these products were slightly enriched in the grazed – NT soils under eCO₂ by 0.4 and 0.7%, respectively.

It is worth noting that there was a CO₂ x defoliation treatment interaction ($p = 0.0632$) for long-chain DAMEs products, which are mainly suberin-derived OC, where the cut – NT soils under eCO₂ were enriched in long-chain DAMEs (by 0.5%) (Figure 4.7b). We also found a CO₂ x soil depth interaction, where the third soil layer (150 – 250 mm) had higher proportions of long-chain DAMEs under eCO₂ ($p = 0.0201$) (Extended Data Figure 4.8c).

We found a single triple interaction between CO₂ x defoliation x soil depth where N-methyl-C_{xx}-alkylamide (a non-FAME MCC) was 0.8% lower under eCO₂ in the third soil layer (150 – 250 mm) of the cut – NT treatment. The opposite was found in the grazed + NT treatment,

where under eCO₂ the proportion of this non-FAME MCC was 1% higher in the same soil layer (p = 0.0044; Extended Data Table 4.7).

The lignin products of di- and tri-methoxybenzenes (guaiacyl and syringyl, respectively) showed a CO₂ x defoliation interaction effect on individual products. The cut – NT soil under eCO₂ was consistently lower in proportions of di- and tri-methoxybenzenes products (Figure 4.9c and d, respectively), which included 2-(3,4-dimethoxy-phenyl)-1-methoxyethylene (G7,G8) (p = 0.0125), 1-(3,4-dimethoxy-phenyl)-1,2,3-trimethoxypropane (G14,G15) (p = 0.0289), 3,4,5-trimethoxyacetophenone (S5) (p = 0.0544) and 1-(3,4,5-trimethoxyphenyl)-2-methoxyethylene (S7,S8) (p = 0.0021; Extended Data Figure 4.9a, b, c and d, respectively). A triple CO₂ x defoliation x soil depth interaction was found for mono-methoxybenzenes (p = 0.01), where eCO₂ soils from the cut – NT treatment had higher proportions of mono-methoxybenzenes (lignin-derived) in the topsoil (6.2 % under aCO₂ vs. 9.3% under eCO₂), the effect diminished at 50 – 150 mm (8.0 vs 9.2%), while in the third soil layer (150 – 250 mm) the opposite trend was found and eCO₂ soils were depleted in mono-methoxybenzenes compared to aCO₂ soils from the same treatment (7.2 vs. 5.15%; Extended Data Table 8).

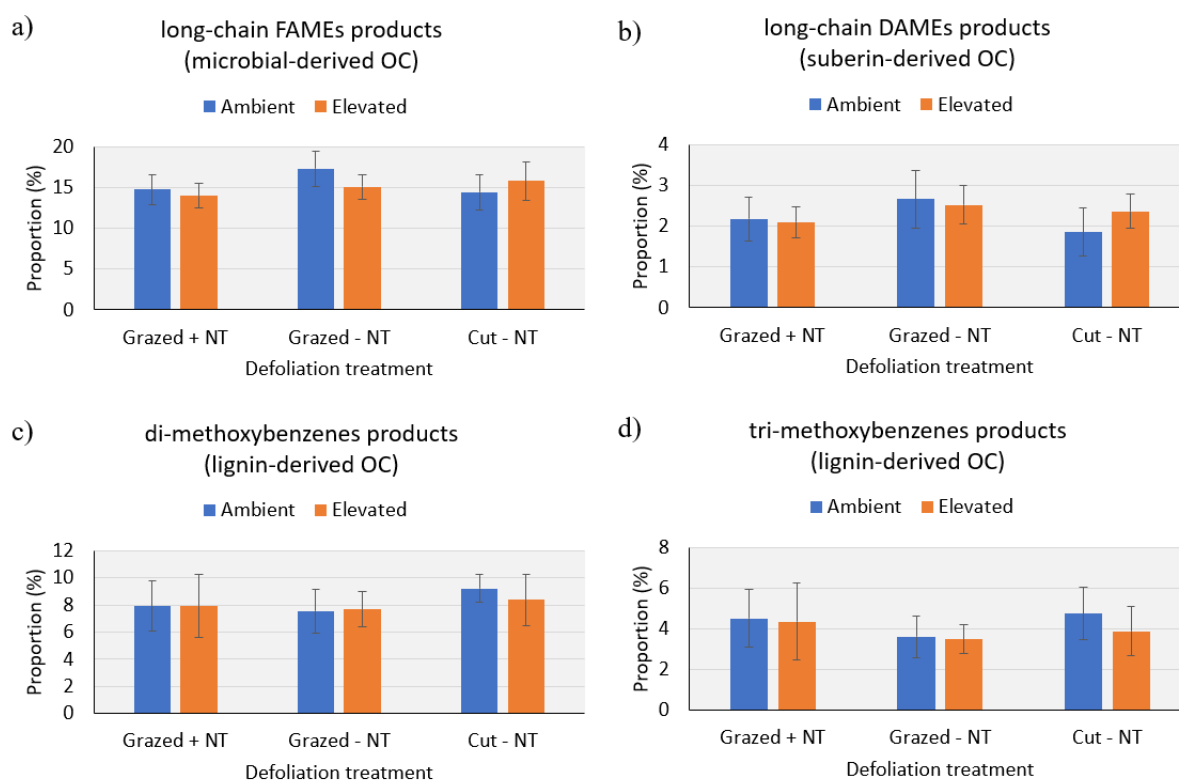


Figure 4. 7: Effect of elevated CO₂ on selected thermally assisted hydrolysis and methylation (THM-GC-MS) products in soil of the three defoliation treatments across the entire soil profile at the NZ-FACE facility, a) long-chain fatty acid methyl ester (long-chain FAMES; microbial-derived), b) long-chain fatty acid dimethyl esters (long-chain DAME; suberin-derived), c) di-methoxybenzenes (from guayacil) and d) tri-methoxybenzenes (from syringyl). Error bars indicate SD (n = 3).

4.3.5.2 Influence of soil depth on soil organic matter molecular composition

Independent of CO₂ treatment, the THM-GC-MS results show that soil depth played a major role in influencing the soil OM molecular composition (Figure 4.8a, b and c). The proportion of THM aliphatic group (methylene chain compounds) increased with soil depth ($p < 0.0001$; Figure 4.8), and this increase was driven by the higher proportions of short-chain FAME ($p < 0.0001$), and short- and long-chain dimethyl esters DAMEs ($p = 0.0049$ and 0.0014 ,

respectively) in deeper soil layers. While the proportions of all methoxybenzenes, including mono-, di- and tri-methoxybenzenes, decreased with increasing soil depth ($p < 0.0001$; Figure 4.8), products of p-coumaric, ferulic and caffeic acids (lignin- and suberin-derived; MBcinn in Table 4.2) also decreased with soil depth ($p < 0.0001$) as did the proportion of MB135 ($p < 0.0001$).

4.3.5.3 Influence of defoliation on soil organic matter molecular composition

The proportion of aliphatic products was strongly influenced by defoliation treatment ($p < 0.0001$; Figure 4.8). Soils of the pastures grazed by animals but receiving no dung or urine return (grazed – NT treatment) had higher proportions of long-chain diacids (mostly from suberin, probably largely root-derived) compared to soil of the grazed + NT and cut – NT treatments ($p = 0.0036$). Similarly, soils from the grazed – NT treatment showed the highest proportions of long-chain fatty acid methyl ester (FAMES) compared to grazed + NT and to a lesser extent to the cut – NT treatment ($p = 0.0276$). The mono-methoxybenzenes showed a strong defoliation treatment effect ($p < 0.0001$; cut – NT > grazed + NT > grazed – NT) which was corroborated by the proportions of 1,2-dimethoxybenzenes (mostly guaiacyl lignin-derived) and 1,2,3-trimethoxybenzenes (mostly syringyl lignin-derived) ($p = 0.0008$ and $p = 0.0004$, respectively). The THM products of p-coumaric, ferulic and caffeic acids (MBcinn in Table 4.2; lignin- and suberin-derived) were also influenced by the defoliation treatment ($p = 0.0281$), with cut – NT showing the highest proportions of these products compared to grazed + NT and grazed – NT treatments. The N-containing products had higher proportions ($p = 0.0124$) in the cut – NT (9.2%) soils compared to grazed – NT (7.8%) and grazed + NT (7.2%).

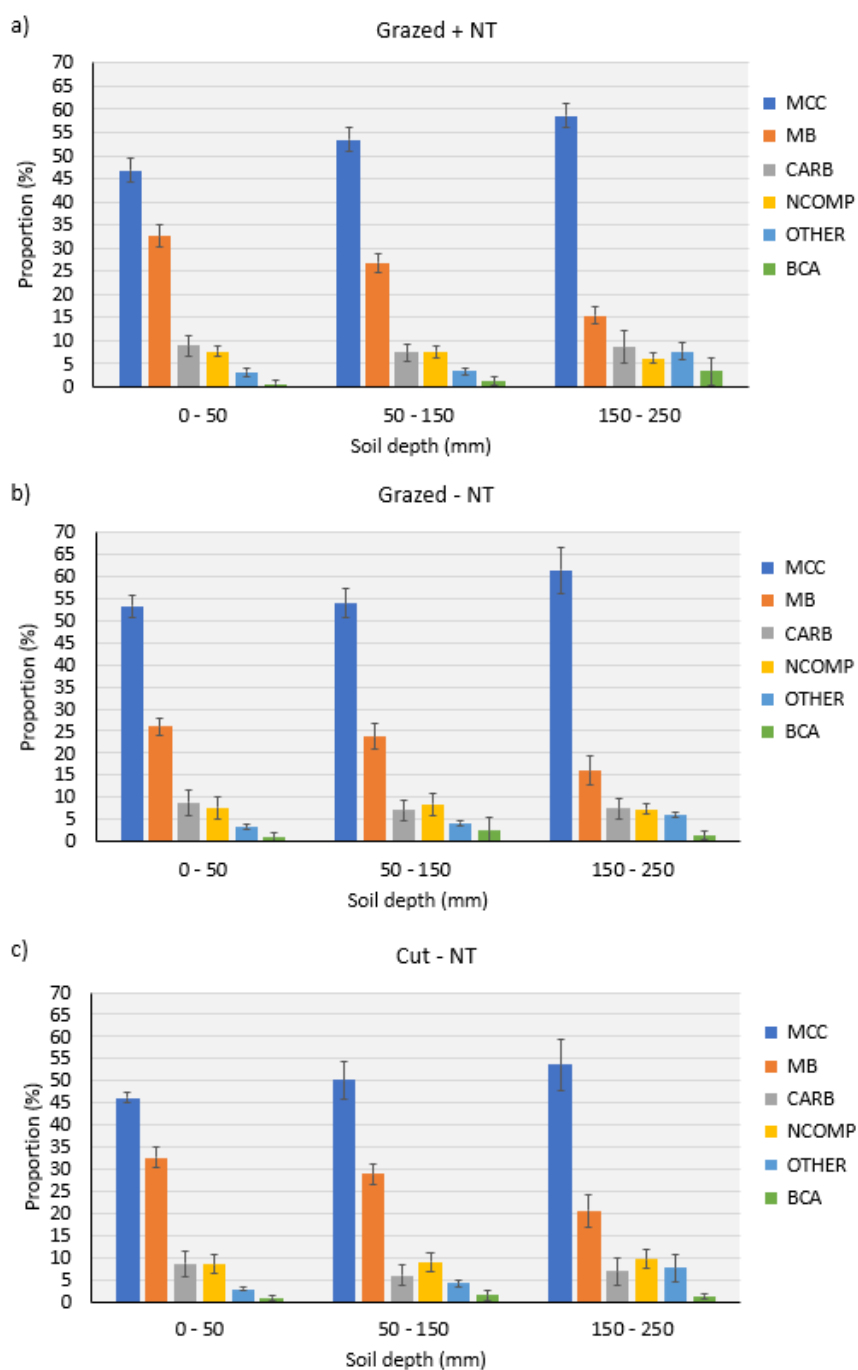


Figure 4. 8: Results of thermally assisted hydrolysis and methylation (THM-GC-MS) analysis (as the percentage of total quantified peak area) for defoliation treatments and soil depths, across both CO₂ treatments. Results are shown based on THM groups. Error bars indicate SD (n = 3). Abbreviation of products: MCC = aliphatic, MB = methoxybenzenes, CARB =

carbohydrate, NCOMP = nitrogen-containing, Other = unidentified, BCA = methylated benzene carboxylic acids.

4.4 Discussion

4.4.1 Long-term exposure to elevated CO₂ effect has not increase soil organic carbon and nitrogen stocks

Prolonged (22 years) exposure of the grazed legume-based pasture to eCO₂ at the NZ-FACE facility had no effect on the bulk density and OC and N content of the Pukepuke sandy soil. Restricting the animals to just selective defoliation and not allowing the return of nutrients in dung and urine or cutting and removing the pasture with no return of plant litter, did not change that outcome. We had hypothesised that the grazing animals returning nutrients in urine, dung and plant litter trampled into the soil surface (grazed + NT treatment) from the boost in pasture growth under eCO₂ would have contributed to an increase in soil OC and N contents under eCO₂. We had also suggested that the two defoliation-only treatments, (grazed – NT and cut – NT), with the latter eliminating any selective defoliation, would not result in an increase in soil OC and N contents, which was the case here, because the pasture response to eCO₂ would have been constrained by the limited supply of nutrients, especially N.

Overall, 22 years of exposure of the grazed legume-based pasture to eCO₂ has also not translated into an increase in soil OC and N stocks or a change in the C:N ratio in the grazed + NT treatment. This is consistent with the results found at the NZ-FACE facility after 10 years (Ross et al., 2013). The study of Ross et al. (2013) was limited to examining the effect of eCO₂ in the top 0 – 50 mm of soil. Other FACE facilities have reported increases in OC content in pasture soils under eCO₂ only with additional N inputs, beyond that of the N provided by

biological N-fixation by the legumes (Dijkstra et al., 2004; Liang et al., 2015). In the present study, the N available for plant growth within the grazed system was limited by the legume amount in the sward. Clearly, the N return in urine and dung was insufficient to replace N losses and build the N supply to boost plant growth and increase soil OC content under eCO₂. In addition to the lack of N, other factors, such as water, given the limited water holding capacity of Pukepuke sandy soil, could have also contributed to the observed results.

Similar to the findings reported by others, where defoliation of the pasture has been limited to cutting (Lenhart et al., 2016; Keidel et al., 2018), in the present study no increase in soil OC and N contents were found in defoliation either by cutting (cut – NT) or by the grazing animals (grazed – NT) under eCO₂. The cut – NT treatment in this study represents the best comparison we have with other grasslands FACEs, as the grazers' depositions of dung and urine and litter trampled were avoided and defoliation (which can be selective by the grazing animal) has been replaced by cutting, the standard pasture management practice applied in other grasslands FACE facilities. Interestingly, the grazed – NT treatment and to a lesser degree the cut – NT treatment, had lower soil OC and particularly N content than the grazed + NT treatment. The difference in soil N between the grazed – NT and cut – NT defoliation treatments might reflect the selective defoliation of the legume component of the sward by the grazing animals, something that would not occur with cutting. Over time and with no nutrient return in dung and urine that would deplete the N supply in the soil.

It is intriguing to compare the present study, which represents the only long-term investigation of the impact of eCO₂ on soil OC stocks under grazing of a permanent legume-based pasture, with other FACE experiments conducted worldwide, as they provide a unique perspective on how soil OC and N partitioning and persistence under grazing may respond to rising atmospheric CO₂ concentrations. Our results are consistent with those from other long-term

grassland FACE facilities experiments (see Introduction section), where eCO₂ has not increased soil OC. This contradicts a recent meta-analysis by Terrer et al. (2021) based on a combination of data obtained from FACE facilities and open chambers, along with the use of ecosystem models and assumptions in the absence of data. Terrer et al. (2021) concluded that eCO₂ increased herbage production in grasses on average by 9%, resulting in on average an 8% increase in soil OC stocks. The present study does not support this conclusion.

4.4.2 Elevated CO₂ did not show significant interaction effects with defoliation treatments on soil organic carbon partitioning and persistence

We found no interaction effect between eCO₂ and the three defoliation treatments as they influenced the coarse POM (> 250 µm) fraction. However, there was a higher proportion of N in cPOM out of the total soil N pool in the second soil layer (50 – 150 mm) under eCO₂. The associated increase in N content was not associated with a change in the aggregate size distribution. Although a slightly higher aggregate size distribution of a cPOM fraction with a lower C:N ratio was found at the site after 4 years of eCO₂ exposure (Allard et al., 2005), our results show that increase in cPOM abundance was not sustained after 22 years of exposure to eCO₂. At that time, the increase in cPOM was attributed to the boost in herbage production and legume proportion (Allard et al., 2005), which has also not been sustained (Newton et al., 2014).

Detailed studies analysing the effects of eCO₂ on the soil fractions are limited to the grasslands Swiss-FACE (Six et al., 2001; van Groenigen et al., 2002; Xie et al., 2005) and Gi-FACE (Keidel et al., 2018). From these, the Swiss-FACE reported after six years of exposure to eCO₂

an increase in the aggregate size distribution of macro-aggregates (> 2 mm) but no associated change in OC content (Six et al., 2001). This effect of eCO₂ on aggregate size was also reported by the same authors to be plant species-dependent. After eight years of eCO₂ exposure at the same site, van Groenigen et al. (2002) reported that eCO₂ increased the N proportion in cPOM out of the total soil N pool only under high N application. None of the analyses at the Swiss-FACE reported changes in micro-aggregates (53 – 250 µm) or in MAOM (< 53 µm). After more than 13 years of exposure to eCO₂ at the Gi-FACE, eCO₂ did not change the fraction size of cPOM or MAOM but decreased the fraction size of micro-aggregates at depths of 0 – 75 and 150 – 450 mm and its OC content at all soil depths, leading to no increase in soil OC content (Keidel et al., 2018).

The lower OC content in the MAOM fraction under eCO₂ found in this study, have been observed by others. Dorodnikov et al. (2011) found after 4 years of a FACE experiment under wheat crops a decreasing trend of OC and N contents in the MAOM fraction under eCO₂ although this difference did not reach significance. The authors suggested that in this fraction the overall losses of C under eCO₂ may occur at the expense of older soil OC.

It is worth noting that the soil pH at this study site spiked from mild acidic to neutral between 2009 and 2019 (Gonzalez-Moreno et al., unpublished). This would support the reduction of OC of the stable fraction (MAOM) as the organo-mineral complexes are weakened in alkaline environments (Six et al., 2004), if so, the reduction in soil OC and N proportion out of the total pools under eCO₂ would have been accompanied by differences in the soil pH between CO₂ treatments, which is not the case here (Gonzalez-Moreno, Chapter 3). The disruption of soil aggregates and subsequent promotion of C oxidation could also explain the decrease in the OC and N proportion of MAOM under eCO₂. However, one might argue that if so, we would see an interaction effect with the grazing treatment. Priming might also explain the reduction of

OC and N proportion in MAOM across grazing treatments as priming is independent of N availability (Allard et al., 2006).

4.4.3 Nutrient return from grazing sustains soil organic carbon and nitrogen stocks, with implications for soil aggregates stability

Across the two CO₂ treatments, the return of nutrients in dung and urine and in plant litter from the treading effect of the animals (grazed + NT) helps to sustain soil OC and N stocks compared with those in the grazed – NT treatment. Limiting the influence of the grazing animals to just selective defoliation or excluding the animals and cutting the pastures with no clippings return resulted in a decline in OC and N stocks (and contents) in the upper two soil depths. The difference in soil N between the grazed (grazed – NT) and cut (cut – NT) defoliation treatments might reflect the selective defoliation of the legume component of the sward by the grazing animals, something that does not occur with cutting. Over time and with no nutrient return in dung and urine that would deplete the N supply in the soil. Furthermore, at the NZ-FACE facility and independently of CO₂ treatments and soil depth, the size distribution of soil OM is dominated by micro-aggregates (>70%), followed by cPOM (~20%) and MAOM (~10%). In general, the aggregate size distribution of soil OM in grasslands is dominated by cPOM, followed by micro-aggregates and MAOM (van Groenigen et al., 2002; Dorji et al., 2020). This difference reflects the limited aggregate building and stability of the Pukepuke sandy soil.

Overall, across both CO₂ treatments, nutrient return from animals (grazed + NT) has shown a positive effect on soil OC and N, with significantly higher OC and N contents and stocks compared to grazed – NT. In grazed – NT the soil bulk density was slightly higher, potentially influencing water infiltration rates, but given the coarse texture nature of the soil this effect is likely to be small. The absence of any nutrient return in dung and urine in the grazed – NT

would have constrained herbage production and as a result, contributed to depletion of the soil OC pool (Pineiro et al., 2010). Nutrient return through depositions in dung and urine only influences soil OC in the 0 – 50 mm topsoil, while the effect is stronger on soil N, influencing N up to 0 – 150 mm. Differences in bulk soil between grazing treatments were mainly due to the differences in OC and N content of the labile fraction (cPOM and micro-aggregates). Interestingly, and contrary to what was found in literature, grazing + NT decreased the aggregate size distribution of MAOM, leading to a small reduction in the OC and N proportion out of the total soil OC and N pool compared to grazed – NT and cut – NT soils.

Additionally, the soil under grazed + NT treatment had a larger soil OC and N content than cut – NT soil, which is the strong evidence of the importance of nutrient return through dung and urine. However, this increase only occurred in the labile fraction in areas with nutrient inputs through animal deposition and in the topsoil only, while the proportion of OC and N in stable fraction (MAOM) out of total soil OC in those same areas was reduced. We attribute the differences of OC and N contents between grazed + NT and cut – NT to pasture plant community, as herbage production and N dynamics are constrained to plant species (Pineiro et al., 2010) and selective grazing promoting legume defoliation (Newton et al., 2004). Grazing did not change the C:N ratio in bulk soil, nor in its fractions, as a finding by Sitters et al. (2020) also reported. In comparison, Pineiro et al. (2010) found that grazing increases the C:N ratio of the soil OM, especially in the labile fraction, when N is limited without affecting the recalcitrant pool.

4.4.4 Long-term CO₂ exposure and defoliation on soil organic matter composition in a legume-based grazed pasture: insights into nutrient return, stabilization pathways, and depth-dependent variations

This is the first study that has attempted to explore the influence of a long-term eCO₂ exposure on the products of OM decomposition in the soil fractions of a legume-based grazed pasture. We found that long-term exposure (22 years) of the pasture to eCO₂ did not translate into any significant changes in the molecular composition of the OM of the Pukepuke soil under any of the three defoliation treatments. Further, despite a decrease in OC and N contents and stocks in the two defoliation-only treatments (grazed – NT and cut – NT), no significant changes in the molecular composition of soil OM were measured. There were, nevertheless, some interactions between defoliation treatments and soil depth. Only very few significant effects of eCO₂ on the Py-GC-MS groups and products were observed, which is largely due to the much larger influence of soil depth and variation between replicates. Although not significant, there was a consistently lower level of polysaccharide products in all three defoliation treatments under eCO₂ and higher levels of aliphatic compounds, which might indicate that eCO₂ accelerated the selective decomposition of polysaccharides (Kien and Kögel-Knabner, 2003) with the resultant accumulation of more recalcitrant plant and microbial aliphatic remains (Kögel-Knabner, 2002). With exception of the grazed + NT treatment, levels of N-containing compounds also seem to have increased under eCO₂, possibly indicating enhanced formation or stabilization of a N-rich microbial OM pool under eCO₂ in grazed – NT and cut – NT treatments. However, in cut – NT soil under eCO₂, the higher proportions of long-chain DAMEs were accompanied by lower proportions of bi- and tri-methoxybenzenes, indicating a

higher amount of suberin-derived OC (Kögel-Knabner, 2002) compared to aCO₂ cut – NT soil but also compared to grazed + NT soil under eCO₂.

To a less extent and independent of CO₂ treatment, defoliation influenced the soil OM molecular composition. The grazed – NT soil was depleted in lignin (syringol units specifically) compared to grazed + NT and cut – NT treatments following the same trend as the soil OC content and potentially reflecting the lack of herbage production (Buurman et al., 2009) in soils that are grazed with no return of nutrient through dung, urine or trampling (grazed – NT treatment). Nutrient return and treading (grazed + NT) seem to reduce the polysaccharides proportion and tend to increase the proportion of aromatic hydrocarbons, aliphatic and N-containing products indicating a high contribution of degraded/microbial OM (Kögel-Knabner et al., 2002), which suggests greater mineralization rates of plant materials in grazed + NT soils than in cut – NT conditions.

In summary, we found a positive interaction effect between eCO₂ and the defoliation treatments, where dung and urine (grazed + NT) promotes the accumulation of lignin-derived OM products and avoids the depletion of these products when compared with the cut – NT treatment. Yet the opposite interaction effect was found in long-chain DAMEs products, where cut – NT soils under eCO₂ have higher proportions of root derived-C. These findings suggest that under eCO₂, grazing with nutrient return (grazed + NT) promoted the accumulation of shoot-derived OC, while in cut – NT soils it promoted the accumulation of root-derived C. Even though we found no interaction effect between eCO₂ and defoliation on soil OC content, we did find an interaction effect in the soil OM molecular composition which indicates different OC stabilization pathways depending on pastures management under eCO₂. Nevertheless, more research is needed to decipher why these stabilization pathways are changing.

Independent of CO₂ and defoliation treatment, soil depth controls the variation in soil OM molecular composition as seen from pyrolysis and THM-GC-MS results. Lignin phenols, other phenols and plant polysaccharides decreased with soil depth, while mono-aromatic hydrocarbons, aliphatic, and N-containing products increased with soil depth. These changes reflect the shift from lignocellulose-based plant-derived OC in the surface soil to microbial-derived and relatively recalcitrant plant and/or microbial-derived aliphatic OC in deeper soil layers (Buurman et al., 2009). Similarly, lignin oxidation parameters increased with depth, indicating a more advanced state of decay of lignin in deeper soil layers (Stewart et al., 2011), and thus that the depth influence is not limited to the higher litter input rates at the surface.

4.5 Conclusions

This study provides a unique perspective on how soil OC and N stocks and molecular composition of soil OM under grazing may respond to rising atmospheric CO₂ concentrations. After 22-years of eCO₂ exposure of a grazed legume-based pasture, the OC and N stocks had not changed in the Pukepuke sandy soil. This is consistent with early samplings after 10 years of pasture exposure to eCO₂ at the same site, although that analysis was limited to the topsoil (0 – 50 mm). The hypothesis that the grazing animals returning nutrients in urine, dung, and plant litter trampled into the soil surface would have contributed to an increase in soil OC and N contents under eCO₂ is thus rejected. When pastures were cut (cut – NT) or the grazing animals were only able to graze without nutrient return (grazed – NT) there was a decline in OC and N contents in the soil, demonstrating the importance of nutrient return from grazing animals in sustaining existing stocks.


Our study revealed that in soils with dung and urine (grazed + NT), eCO₂ increased the accumulation of lignin-derived OM, promoting the accumulation of plant-derived OC. While

in cut – NT soils, eCO₂ increased the accumulation of long-chain DAMEs products, promoting the accumulation of root-derived OC, especially in deeper soil layers. Despite not finding any interaction effect between eCO₂ and defoliation treatment on the OC and N content in the soil or its fractions, the presence of an interaction effect in the soil OM molecular composition suggests that distinct OC stabilization pathways exist depending on pastures management under eCO₂. Further research is required to understand why these pathways are changing under eCO₂.

Appendix II - Extended Data for Chapter 4

STATEMENT OF CONTRIBUTION DOCTORATE WITH PUBLICATIONS/MANUSCRIPTS

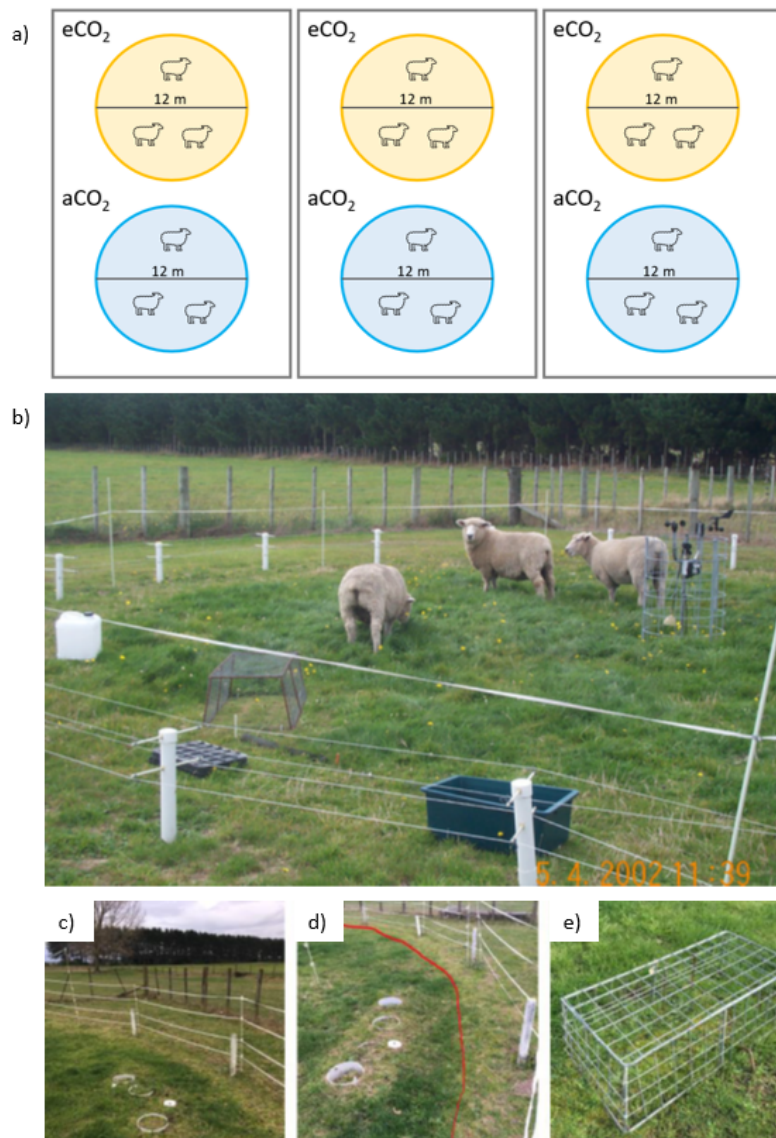
We, the student and the student's main supervisor, certify that all co-authors have consented to their work being included in the thesis and they have accepted the student's contribution as indicated below in the Statement of Originality.

Student name:			
Name and title of main supervisor:			
In which chapter is the manuscript/published work?			
What percentage of the manuscript/published work was contributed by the student?			
Describe the contribution that the student has made to the manuscript/published work:			
Please select one of the following three options:			
<input type="checkbox"/>	<p>The manuscript/published work is published or in press Please provide the full reference of the research output:</p>		
<input type="checkbox"/>	<p>The manuscript is currently under review for publication Please provide the name of the journal:</p>		
<input type="checkbox"/>	<p>It is intended that the manuscript will be published, but it has not yet been submitted to a journal</p>		
Student's signature:		Main supervisor's signature:	

This form should be placed at the beginning of each relevant thesis chapter.

Extended Data 4.2 Methods

Extended Data 4.2.1 Experimental set up



Extended Data Figure 4.1: a) experimental design of the NZ-FACE experiment divided into blocks, b) Picture showing the dimensions of the experiment with sheep grazing inside the rings. c) Picture showing the treatment where the grazer defoliates, urinates, defecates and treading is exerted (grazed + NT treatment), d) Picture showing the delimitation between the grazed + NT and grazed - NT where grazers remove shoot yet the site receives no dung and urine return and treading and c) the Cut - NT treatment where grazing, nutrient return and treading are all prevented with the use of an exclusion cage.

Extended Data 4.2.2 Soil collection and bulk analysis

Extended Data Table 4.1: Soil pH values (0 – 75 mm) on samples collected in 2020 at the NZ Free Air CO₂ Enrichment facility.

Defoliation treatment	CO ₂	pH
Cut - NT	Elevated	6.54 (a)
	Ambient	6.52 (a)
Grazed + NT	Elevated	6.51 (a)
	Ambient	6.48 (a)
Grazed - NT	Elevated	6.21 (b)
	Ambient	6.16 (b)

Extended Data 4.2.3 Soil organic matter molecular composition

Extended Data Table 4.2: List of pyrolysis-GC/MS products found in soil fractions after 22 years of exposure to elevated CO₂ at the NZ Free Air CO₂ Enrichment facility.

Retention Time	m/z	Product	group
1.474	94+96	Bromomethane	XCOMP
1.494	142+127	Iodomethane	XCOMP
1.504	60	Acetic acid	CARB
1.614	78	Benzene	MAH
1.735	79	Pyridine	NCOMP
1.735	67	Pyrrole	NCOMP
1.785	91+92	Toluene	MAH
1.815	59	Acetamide	NCOMP
1.815	84+54	(2H)-furan-3-one	CARB
1.906	95+96	3/2-furaldehyde	CARB
1.966	80+81	Methyl-pyrrole	NCOMP
2.026	93+66	Methyl-pyridine	NCOMP
2.298	110+109	5-methyl-2-furaldehyde	CARB
2.328	94+66	Phenol	PHEN
2.418	103	Benzonitrile	NCOMP
2.438	114+58	4-hydroxy-5,6-dihydro-(2H)-pyran-2-one	CARB
2.569	112	2-hydroxy-3-methyl-2-cyclopenten-1-one	CARB

2.609	113+128	Dianhydrorhamnose	CARB
2.739	107+108	4-methylphenol	PHEN
2.800	128	Methyl-4-hydroxy-5,6-dihydro-(2H)-pyran-2-one	CARB
2.830	109+124	Guaiacol	LIG G
2.930	98+68	Levogluosenone	CARB
2.970	95	4-pyridone (T)	NCOMP
3.021	99	2,5-pyrrolidinedione (succinamide)	NCOMP
3.051	117+89	Benzene acetonitrile	NCOMP
3.061	107+122	Dimethylphenol	PHEN
3.141	107+122	4-ethylphenol	PHEN
3.292	57+69	5-hydroxymethyl-2-tetrahydrofuraldehyde-3-one	CARB
3.382	69+57	1,4:3,6-dianhydro-alpha-D-glucopyranose	CARB
3.312	128	Naphthalene	PAH
3.282	123+138	4-methylguaiacol	LIG G
3.392	120+91	4-vinylphenol	LIG H
3.412	133+134	Ethylbenzaldehyde (T)	OTHER
3.483	83+125	Unidentified compound	OTHER
3.643	79	Picolinamide (T)	NCOMP
3.663	137+152	4-ethylguaiacol	LIG G
3.774	134+119	Unidentified compound	OTHER
3.784	117+89	Indole	NCOMP
3.804	142+115	Methylnaphthalene	PAH
3.884	142+115	Methylnaphthalene	PAH
3.834	150+135	4-vinylguaiacol	LIG G
3.985	154+139	Syringol	LIG S
4.164	154	Biphenyl	PAH
4.206	130+131	Methylindole	NCOMP
4.256	151+152	Vanillin	LIG G
4.206	60+73	Levogalactosan	CARB
4.487	60+73	Levomannosan	CARB
4.768	60+73	Levogluosan	CARB
4.396	168+153	4-methylsyringol	LIG S
4.416	164+149	4-(2-propenyl)guaiacol (trans)	LIG G
4.457	116	4-methylbenzoic acid ?	OTHER
4.517	100	Unidentified compound	OTHER
4.929	100	Unidentified compound	OTHER
4.607	94	Unidentified compound	OTHER
4.627	151+166	4-acetylguaiacol	LIG G
4.698	125+167	Trihydro-2-acetamido-2-deoxyglucose (Stankiewicz)	NCOMP
4.718	167+182	4-ethylsyringol	LIG S
4.788	137	4-(propan-2-one)guaiacol	LIG G
4.889	180	4-vinylsyringol	LIG S
5.059	166	Fluorene	PAH
5.099	121+138	Vanillic acid (T)	LIG G
5.310	182+181	Syringaldehyde	LIG S

5.421	194+179	4-(2-propenyl)guaiacol (trans)	LIG S
5.451	55+56	Prist-1-ene	MCC
5.561	186+93	Diketodipyrrole	NCOMP
5.571	181+196	4-acetylsyringol	LIG S
5.702	167+210	4-(propan-2-one) syringol	LIG S
5.863	178	Phenanthrene/anthracene (DP)	PAH
5.943	70+154	Diketopiperazine	NCOMP
6.048	70+154	Diketopiperazine	NCOMP
6.084	81+82	Phytadiene 2	MCC
6.144	74+87	Fame C ₁₆	MCC
6.375	70+194	Diketopiperazine (Cyclo(Pro-Pro))	NCOMP
6.797	74+87	Fame C ₁₈	MCC
6.877	55+69	Fatty acid C _{18:1}	MCC
6.998	97	Alkyl nitrile C ₁₈	MCC
7.470	83+280	Unidentified compound	OTHER
7.610	175+272	Unidentified compound	OTHER
9.579	151+416	Gamma-tocopherol	OTHER
9.880	165+430	Alpha-tocopherol	OTHER
7.018	59+72	Alkylamide C ₁₆	MCC
7.610	59+72	Alkylamide C ₁₈	MCC
8.665	59+72	Alkylamide C ₂₂	MCC
8.434	58+59	Methylketone C ₂₅	MCC
9.017	58+59	Methylketone C ₂₇	MCC
9.686	58+59	Methylketone C ₂₉	MCC
10.553	58+59	Methylketone C ₃₁	MCC
5.582	60+73	Fatty acid C ₁₄	MCC
5.823	60+73	Fatty acid i/a C ₁₅	MCC
5.933	60+73	Fatty acid C ₁₅	MCC
6.285	60+73	Fatty acid C ₁₆	MCC
6.917	60+73	Fatty acid C ₁₈	MCC
7.510	60+73	Fatty acid C ₂₀	MCC
8.072	60+73	Fatty acid C ₂₂	MCC
3.674	57+71	Alkane C ₁₃	MCC
4.115	57+71	Alkane C ₁₄	MCC
4.537	57+71	Alkane C ₁₅	MCC
4.939	57+71	Alkane C ₁₆	MCC
5.321	57+71	Alkane C ₁₇	MCC
5.692	57+71	Alkane C ₁₈	MCC
6.044	57+71	Alkane C ₁₉	MCC
6.375	57+71	Alkane C ₂₀	MCC
6.696	57+71	Alkane C ₂₁	MCC
7.008	57+71	Alkane C ₂₂	MCC
7.299	57+71	Alkane C ₂₃	MCC
7.580	57+71	Alkane C ₂₄	MCC
7.851	57+71	Alkane C ₂₅	MCC
8.113	57+71	Alkane C ₂₆	MCC

8.374	57+71	Alkane C ₂₇	MCC
8.635	57+71	Alkane C ₂₈	MCC
8.929	57+71	Alkane C ₂₉	MCC
9.227	57+71	Alkane C ₃₀	MCC
9.569	57+71	Alkane C ₃₁	MCC
9.940	57+71	Alkane C ₃₂	MCC
10.372	57+71	Alkane C ₃₃	MCC
3.643	55+69	Alkene C ₁₃	MCC
4.085	55+69	Alkene C ₁₄	MCC
4.507	55+69	Alkene C ₁₅	MCC
4.909	55+69	Alkene C ₁₆	MCC
5.300	55+69	Alkene C ₁₇	MCC
5.672	55+69	Alkene C ₁₈	MCC
6.024	55+69	Alkene C ₁₉	MCC
6.355	55+69	Alkene C ₂₀	MCC
6.676	55+69	Alkene C ₂₁	MCC
6.988	55+69	Alkene C ₂₂	MCC
7.289	55+69	Alkene C ₂₃	MCC
7.570	55+69	Alkene C ₂₄	MCC
7.851	55+69	Alkene C ₂₅	MCC
8.103	55+69	Alkene C ₂₆	MCC
8.384	55+69	Alkene C ₂₇	MCC
8.675	55+69	Alkene C ₂₈	MCC
8.959	55+69	Alkene C ₂₉	MCC
9.217	55+69	Alkene C ₃₀	MCC
9.589	55+69	Alkene C ₃₁	MCC

Extended Data Table 4.3: List of thermally assisted hydrolysis and methylation GC/MS products found in soil fractions after 22 years of exposure to elevated CO₂ at the NZ Free Air CO₂ Enrichment facility.

RT	m/z	THM product	group
6.955	74+87	C ₁₄ FAME	sFAME
7.146	74+87	iso/anteiso C ₁₅ FAME	sFAME
7.226	74+87	C ₁₅ FAME	sFAME
7.506	74+87	C ₁₆ FAME	sFAME
8.020	74+87	C ₁₈ FAME	sFAME
8.484	74+87	C ₂₀ FAME	IFAME
8.924	74+87	C ₂₂ FAME	IFAME
9.376	74+87	C ₂₄ FAME	IFAME
9.898	74+87	C ₂₆ FAME	IFAME
10.571	74+87	C ₂₈ FAME	IFAME
11.374	74+87	C ₃₀ FAME	IFAME
8.090	55+74	Omega-methoxy C ₁₆ FAME	oFAME
9.456	55+74	Omega-methoxy C ₂₂ FAME	oFAME

9.998	55+74	Omega-methoxy C ₂₄ FAME	oFAME
10.671	55+74	Omega-methoxy C ₂₆ FAME	oFAME
11.545	55+74	Omega-methoxy C ₂₈ FAME	oFAME
5.609	98	Unidentified proline product	NCOMP
6.724	98	Unidentified proline product	NCOMP
7.076	98	Unidentified proline product	NCOMP
8.331	98	C ₁₆ DAME (tr)	IDAME
9.245	98	C ₂₀ DAME (tr)	IDAME
9.747	98	C ₂₂ DAME	IDAME
10.350	98	C ₂₄ DAME	IDAME
11.123	98	C ₂₆ DAME	IDAME
5.268	129	C ₆ metasaccharinic acid ME	CARB
5.368	129	C ₆ metasaccharinic acid ME	CARB
6.021	129	C ₆ metasaccharinic acid ME	CARB
6.152	129	C ₆ metasaccharinic acid ME	CARB
6.242	129	C ₆ metasaccharinic acid ME	CARB
5.188	135+136	4-methoxybenzaldehyde (P4)	1MB
5.770	135+166	4-methoxybenzoic acid ME (P6)	1MB
5.760	144+145	Dimethyl-indole	NCOMP
5.720	153+168	1,2,3-trimethoxybenzene (S1)	3MB
5.810	101+127	Unidentified carbohydrate	CARB
5.861	88	Trimethyl-levoglucosan	CARB
5.820	171 (58, 114)	1,3,5-trimethyl-2,4,6-trione-1,3,5-triazine (TMAH)	OTHER
5.911	168+139	1,3,5-trimethoxybenzene	MB 135
6.011	121	4-methoxybenzeneacetic acid ME (P24)	1MB
6.021	55+69	Unidentified MCC	non-FAME MCC
6.102	118+161	Unidentified N compound	NCOMP
6.111	163	Benzene dicarboxylic acid ME	BCA
6.321	163	Benzene dicarboxylic acid ME	BCA
6.182	115+175	C ₅ metasaccharinic acid ME	CARB
6.212	166+165	3,4-dimethoxybenzaldehyde (G4)	2MB
6.403	55+59	Azelaic acid ME (C ₉ DAME)	sDAME
6.453	158+159	Trimethyl-indole	NCOMP
6.523	165+180	3,4-dimethoxyacetophenone (G5)	2MB
6.383	151+182	Vanillic acid ME	2MB
6.594	196+165	3,4-dimethoxybenzoic acid ME (G6)	2MB
6.704	151+210	3,4-dimethoxybenzeneacetic acid ME (G24)	2MB
6.754	194+179	2-(3,4-dimethoxyphenyl)-1-methoxyethylene (G7,G8) (DP)	2MB
6.835	69+111	Unidentified product	OTHER
6.895	161+192	Trans 1-propenoic acid-4-methoxybenzene ME (P18)	MB cinn
6.895	195+210	3,4,5-trimethoxyacetophenone (S5)	3MB
6.995	226+211	3,4,5-trimethoxybenzoic acid ME (S6)	3MB
7.076	148+186	Unidentified product	OTHER
7.166	209+224	1-(3,4,5-trimethoxyphenyl)-2-methoxyethylene (S7,S8)	3MB

7.216	181	1-(3,4-dimethoxyphenyl)-1,2,3-trimethoxypropane (G14,G15)	2MB
7.468	222+191	Trans-3-(3,4-dimethoxyphenyl)-3-propenoate (G18)	MB cinn
7.538	211	1-(3,4,5-trimethoxyphenyl)-1,2,3- trimethoxypropane (S14,S15)	3MB
7.980	241+256	Unidentified product	OTHER
8.401	71+95	10,16-dimethoxy C ₁₆ FAME	midsub FAME
8.562	169+201	Unidentified mid-chain substituted FAME	midsub FAME
8.622	187+201	8,16-dimethoxy C ₁₆ FAME	midsub FAME
8.813	87+155	Unidentified mid-chain substituted FAME	midsub FAME
9.035	71+81	9,10,18-trimethoxy C ₁₈ FAME	midsub FAME
9.245	71+81	Unidentified mid-chain substituted FAME	midsub FAME
9.637	83+97	Methoxy-alkane	non-FAME MCC
10.942	83+97	Methoxy-alkane	non-FAME MCC
9.697	73+86	N-methyl-Cxx-alkylamide	non-FAME MCC
9.772	87+100	N,N-dimethyl-Cxx-alkylamide	non-FAME MCC
10.440	179+444	Alpha-tocopherol (methylated)	OTHER

Extended Data 4.3 Results

Extended Data 4.3.1 Effect of elevated CO₂ on organic carbon and nitrogen stocks in soils

Extended Data Table 4.4: Results of bulk density analysis on soil samples from the NZ Free Air CO₂ Enrichment facility considering the effect of CO₂, defoliation treatment and soil depth.

Soil depth (mm)	Defoliation treatment	CO ₂	Bulk density (g cm ⁻³)	N content (mg N kg soil ⁻¹)	C content (g C kg soil ⁻¹)	C/N ratio	N stock (t ha ⁻¹)	C stock (t ha ⁻¹)
0 - 50								
Grazed – NT		Ambient	1.1 ± 0.02	3.3 ± 0.2	36.7 ± 2.0	11.1 ± 0.1	1.7 ± 0.1	18.4 ± 1.0
		Elevated	1.0 ± 0.04	3.2 ± 0.2	36.6 ± 2.0	11.3 ± 0.2	1.6 ± 0.1	18.3 ± 1.0
Grazed + NT		Ambient	1.0 ± 0.01	4.1 ± 0.2	44.9 ± 2.4	10.9 ± 2.4	2.1 ± 0.1	22.5 ± 1.2
		Elevated	1.0 ± 0.02	4.4 ± 0.3	49.0 ± 3.9	11.2 ± 3.9	2.2 ± 0.1	24.4 ± 1.9
Cut – NT		Ambient	1.0 ± 0.09	3.7 ± 0.2	40.0 ± 2.3	10.9 ± 2.3	1.8 ± 0.1	20.0 ± 1.1
		Elevated	0.9 ± 0.04	4.0 ± 0.6	43.7 ± 7.3	11.0 ± 7.3	2.0 ± 0.3	21.7 ± 3.5
50 - 150								
Grazed – NT		Ambient	1.1 ± 0.02	2.7 ± 0.2	27.8 ± 2.2	10.4 ± 2.2	2.7 ± 0.2	28.5 ± 2.2
		Elevated	1.1 ± 0.02	2.5 ± 0.3	26.0 ± 2.7	10.2 ± 2.7	2.6 ± 0.3	26.2 ± 3.0
Grazed + NT		Ambient	1.1 ± 0.02	2.9 ± 0.3	30.0 ± 2.7	10.2 ± 2.7	3.0 ± 0.3	31.0 ± 2.7
		Elevated	1.1 ± 0.04	2.9 ± 0.2	28.5 ± 2.5	9.9 ± 2.5	2.9 ± 0.1	28.7 ± 2.3
Cut – NT		Ambient	1.1 ± 0.03	2.8 ± 0.2	28.2 ± 1.6	10.2 ± 1.6	2.8 ± 0.2	28.5 ± 1.9
		Elevated	1.0 ± 0.04	2.8 ± 0.4	28.8 ± 4.7	10.3 ± .7	2.8 ± 0.3	28.5 ± 4.0
150 - 250								
Grazed – NT		Ambient	1.2 ± 0.04	1.5 ± 0.1	15.1 ± 0.6	9.8 ± 0.6	1.7 ± 0.1	16.4 ± 0.8
		Elevated	1.2 ± 0.06	1.7 ± 0.3	16.6 ± 2.7	9.7 ± 2.7	1.8 ± 0.2	17.2 ± 2.1
Grazed + NT		Ambient	1.3 ± 0.02	1.5 ± 0.2	14.9 ± 2.6	9.7 ± 2.6	1.7 ± 0.2	16.6 ± 2.3
		Elevated	1.2 ± 0.05	1.6 ± 0.3	15.6 ± 3.1	9.5 ± 3.1	1.7 ± 0.2	16.1 ± 3.0
Cut – NT		Ambient	1.2 ± 0.03	1.5 ± 0.3	14.9 ± 3.3	9.9 ± 3.3	1.6 ± 0.3	15.8 ± 3.6
		Elevated	1.2 ± 0.04	1.7 ± 0.3	17.1 ± 3.9	9.8 ± 3.9	1.8 ± 0.3	17.5 ± 3.6

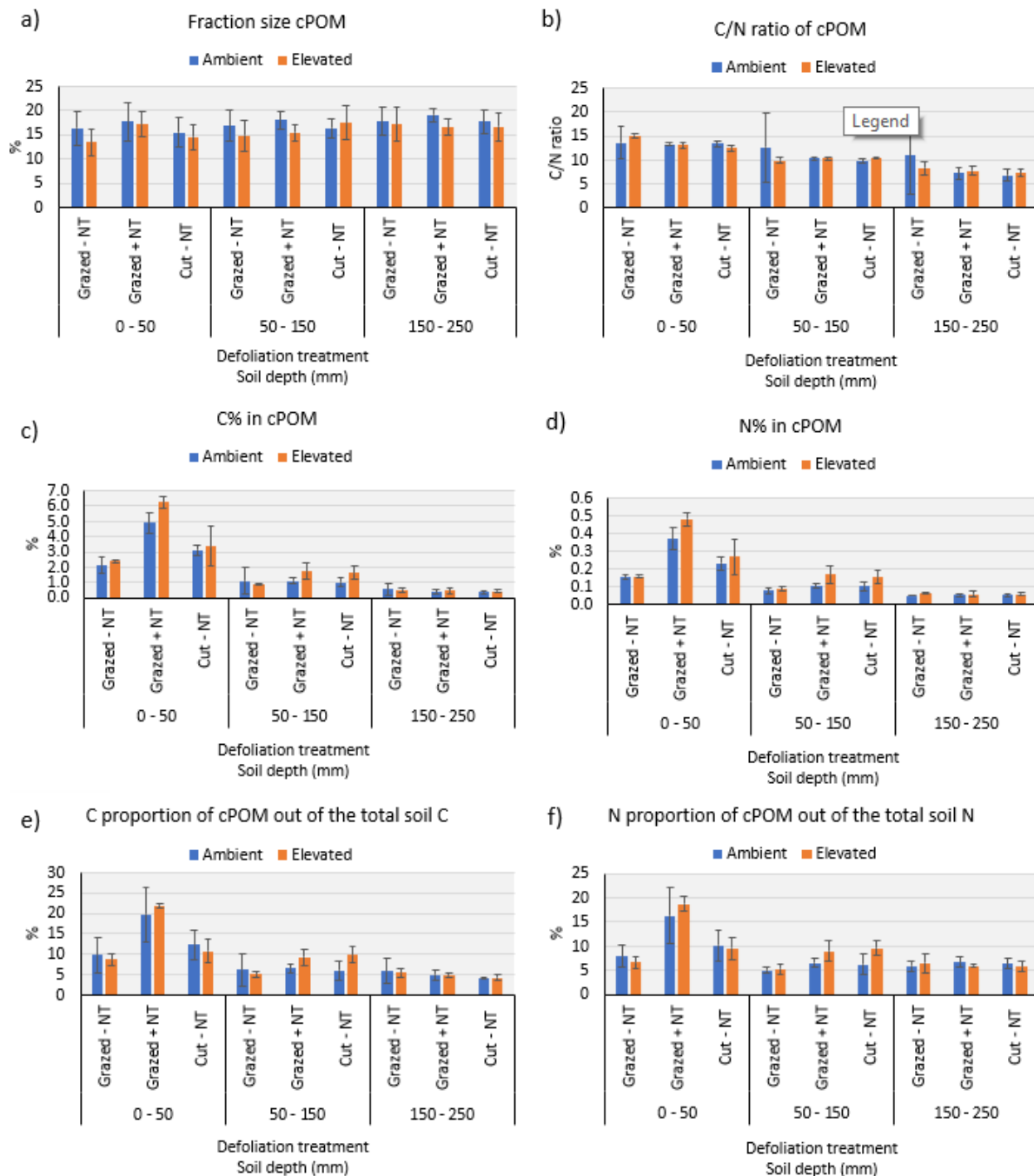
Extended Data 4.3.2 Soil organic carbon and nitrogen in soil fractions

Extended Data Table 4.5: Physical recovery (mass recovery after wet fractionation analysis) and chemical recovery (sum of fraction size) on soil samples from the NZ Free Air CO₂ Enrichment facility after 22 years of exposure to elevated CO₂ over three defoliation treatments at three soil depth.

Ring	Block	CO ₂	Defoliation	Depth (mm)	Physical recovery		Chemical recovery			
					%	Δ%	C	ΔC	N	ΔN
1	1	Elevated	Grazed + NT	0-50	98.7	1.3	104.5	4.5	101.6	1.6
1	1	Elevated	Grazed + NT	50-150	99.4	0.6	110.4	10.4	110.9	10.9
1	1	Elevated	Grazed + NT	150-250	99.5	0.5	127.4	27.4	120.6	20.6
1	1	Elevated	Grazed - NT	0-50	99.5	0.5	86.9	-13.1	90.2	-9.8
1	1	Elevated	Grazed - NT	50-150	99.6	0.4	105.5	5.5	108.4	8.4
1	1	Elevated	Grazed - NT	150-250	99.7	0.3	131.0	31.0	124.7	24.7
1	1	Elevated	Cut - NT	0-50	99.0	1.0	106.3	6.3	104.4	4.4
1	1	Elevated	Cut - NT	50-150	99.3	0.7	104.4	4.4	105.6	5.6
1	1	Elevated	Cut - NT	150-250	99.7	0.4	116.8	16.8	113.7	13.7
2	2	Elevated	Grazed + NT	0-50	99.2	0.8	95.5	-4.5	99.6	-0.4
2	2	Elevated	Grazed + NT	50-150	99.4	0.6	115.9	15.9	112.5	12.5
2	2	Elevated	Grazed + NT	150-250	99.8	0.3	100.3	0.3	96.1	-3.9
2	2	Elevated	Grazed - NT	0-50	99.2	0.8	96.2	-3.8	98.1	-1.9
2	2	Elevated	Grazed - NT	50-150	99.5	0.5	109.4	9.4	106.7	6.7
2	2	Elevated	Grazed - NT	150-250	99.7	0.3	134.3	34.3	132.6	32.6
2	2	Elevated	Cut - NT	0-50	99.8	0.2	93.3	-6.7	92.9	-7.1
2	2	Elevated	Cut - NT	50-150	99.0	1.0	100.1	0.1	102.7	2.7
2	2	Elevated	Cut - NT	150-250	99.4	0.6	129.0	29.0	126.9	26.9
3	3	Elevated	Grazed + NT	0-50	99.0	1.0	83.8	-16.2	87.0	-13.0
3	3	Elevated	Grazed + NT	50-150	99.4	0.6	96.8	-3.2	95.4	-4.6
3	3	Elevated	Grazed + NT	150-250	99.5	0.5	120.6	20.6	116.5	16.5
3	3	Elevated	Grazed - NT	0-50	98.8	1.2	79.3	-20.7	84.1	-15.9
3	3	Elevated	Grazed - NT	50-150	99.0	1.0	113.2	13.2	113.1	13.1
3	3	Elevated	Grazed - NT	150-250	99.4	0.6	110.8	10.8	109.2	9.2
3	3	Elevated	Cut - NT	0-50	98.9	1.1	86.0	-14.0	88.3	-11.7
3	3	Elevated	Cut - NT	50-150	99.1	0.9	112.6	12.6	111.1	11.1
3	3	Elevated	Cut - NT	150-250	99.6	0.5	115.3	15.3	111.7	11.7
4	1	Ambient	Grazed + NT	0-50	99.3	0.7	107.3	7.3	106.0	6.0
4	1	Ambient	Grazed + NT	50-150	99.2	0.8	90.4	-9.6	92.7	-7.3
4	1	Ambient	Grazed + NT	150-250	99.6	0.4	90.7	-9.3	92.1	-7.9
4	1	Ambient	Grazed - NT	0-50	99.0	1.0	102.3	2.3	101.7	1.7
4	1	Ambient	Grazed - NT	50-150	99.6	0.4	105.3	5.3	105.0	5.0
4	1	Ambient	Grazed - NT	150-250	98.7	1.3	111.9	11.9	107.0	7.0
4	1	Ambient	Cut - NT	0-50	98.9	1.1	103.4	3.4	101.6	1.6

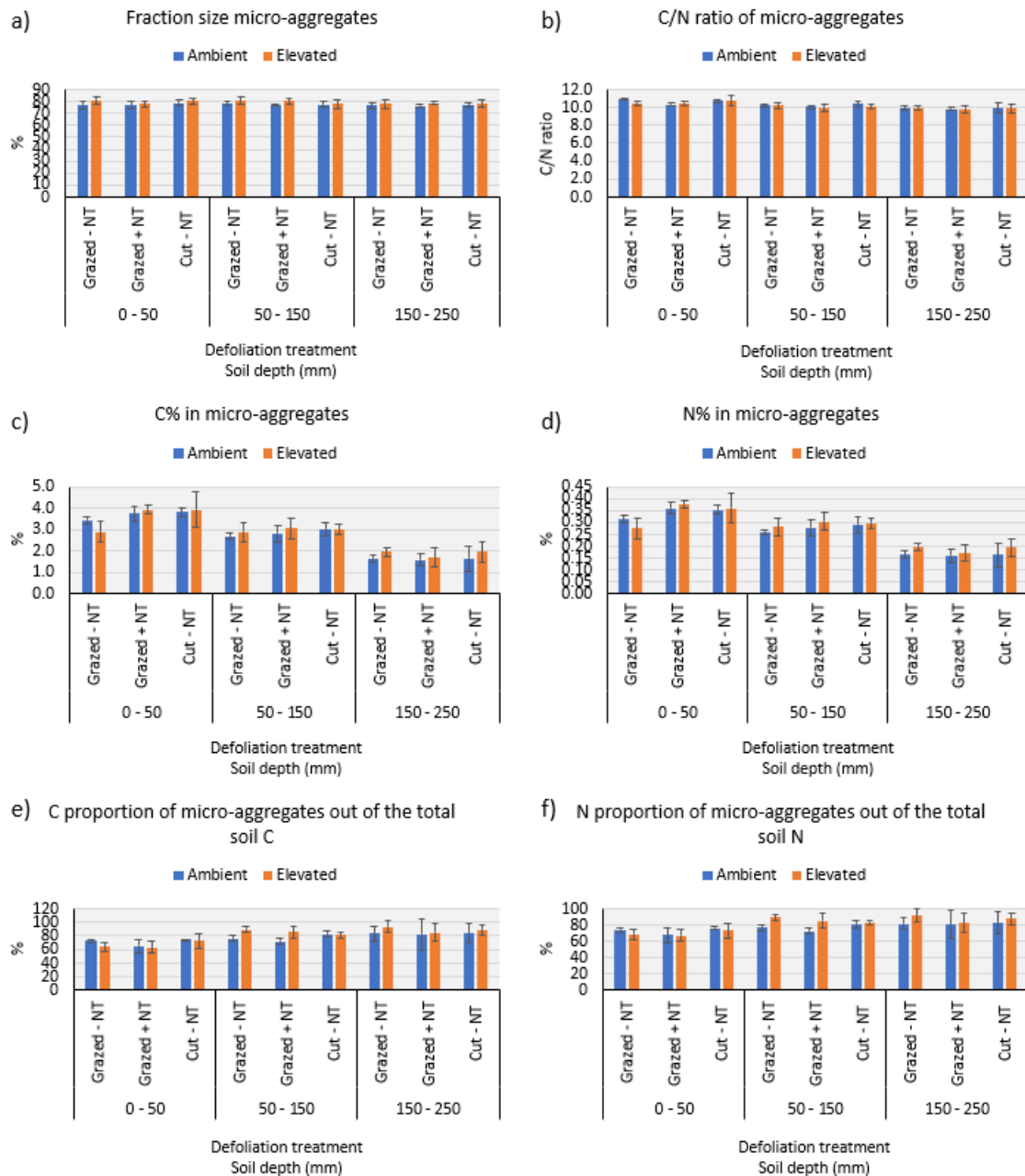
4	1	Ambient	Cut - NT	50-150	99.4	0.6	102.9	2.9	97.9	-2.1
4	1	Ambient	Cut - NT	150-250	99.8	0.2	106.1	6.1	104.7	4.7
5	2	Ambient	Grazed + NT	0-50	98.8	1.2	89.8	-10.2	89.2	-10.8
5	2	Ambient	Grazed + NT	50-150	99.0	1.0	99.7	-0.3	97.9	-2.1
5	2	Ambient	Grazed + NT	150-250	99.7	0.3	145.2	45.2	135.2	35.2
5	2	Ambient	Grazed - NT	0-50	99.6	0.4	106.3	6.3	103.6	3.6
5	2	Ambient	Grazed - NT	50-150	101.5	-1.5	100.7	0.7	101.1	1.1
5	2	Ambient	Grazed - NT	150-250	99.4	0.6	111.1	11.1	116.0	16.0
5	2	Ambient	Cut - NT	0-50	99.0	1.0	104.5	4.5	103.1	3.1
5	2	Ambient	Cut - NT	50-150	96.5	3.5	108.2	8.2	108.7	8.7
5	2	Ambient	Cut - NT	150-250	99.5	0.5	122.3	22.3	120.5	20.5
6	3	Ambient	Grazed + NT	0-50	98.8	1.2	96.5	-3.5	97.6	-2.4
6	3	Ambient	Grazed + NT	50-150	99.4	0.6	95.6	-4.4	95.0	-5.0
6	3	Ambient	Grazed + NT	150-250	99.7	0.3	122.4	22.4	119.2	19.2
6	3	Ambient	Grazed - NT	0-50	99.2	0.8	93.6	-6.4	95.7	-4.3
6	3	Ambient	Grazed - NT	50-150	98.9	1.1	100.9	0.9	97.2	-2.8
6	3	Ambient	Grazed - NT	150-250	99.5	0.5	140.0	40.0	126.9	26.9
6	3	Ambient	Cut - NT	0-50	98.9	1.1	99.3	-0.7	100.2	0.2
6	3	Ambient	Cut - NT	50-150	99.2	0.8	113.0	13.0	109.8	9.8
6	3	Ambient	Cut - NT	150-250	99.4	0.6	135.6	35.6	131.4	31.4

Extended Data 4.3.3.1 Influence of elevated CO₂ on soil organic carbon and nitrogen pools



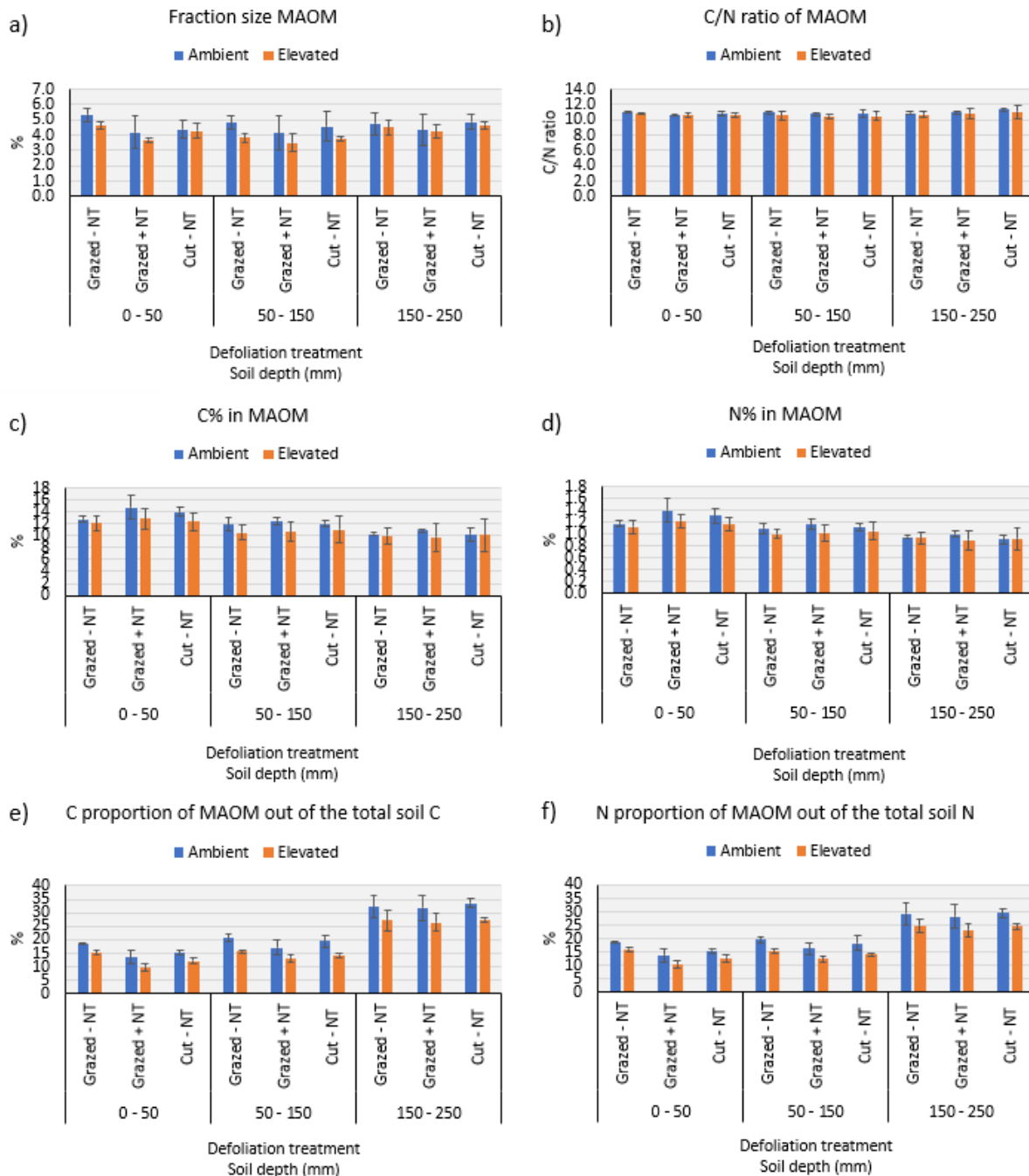
Extended Data Figure 4.2: Effect of elevated CO₂ on coarse particulate organic matter (cPOM) from the NZ Free Air CO₂ Enrichment facility under different defoliation treatments and soil depths on a) cPOM fraction size, b) cPOM C:N ratio value, c) Carbon concentration

of cPOM, d) Nitrogen concentration of cPOM, e) Carbon proportion of cPOM out of the total soil C content and f) Nitrogen proportion of cPOM out of the total soil N content



Extended Data Figure 4.3: Effect of elevated CO₂ on micro-aggregates from the NZ Free Air CO₂ Enrichment facility under different defoliation treatments and soil depths on a) micro-aggregates fraction size, b) micro-aggregates C:N ratio value, c) Carbon concentration of micro-aggregates, d) Nitrogen concentration of micro-aggregates, e) Carbon proportion of

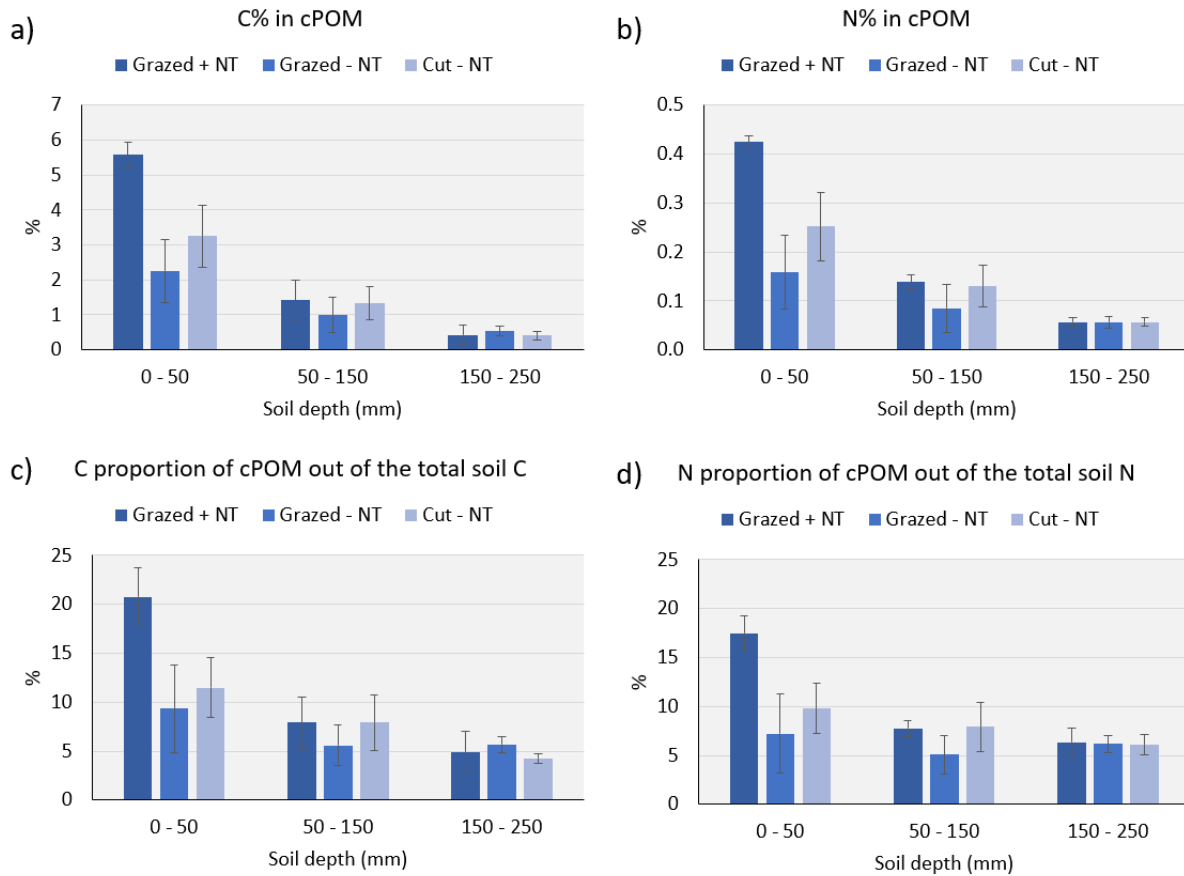
micro-aggregates out of the total soil C content and f) Nitrogen proportion of micro-aggregates out of the total soil N content



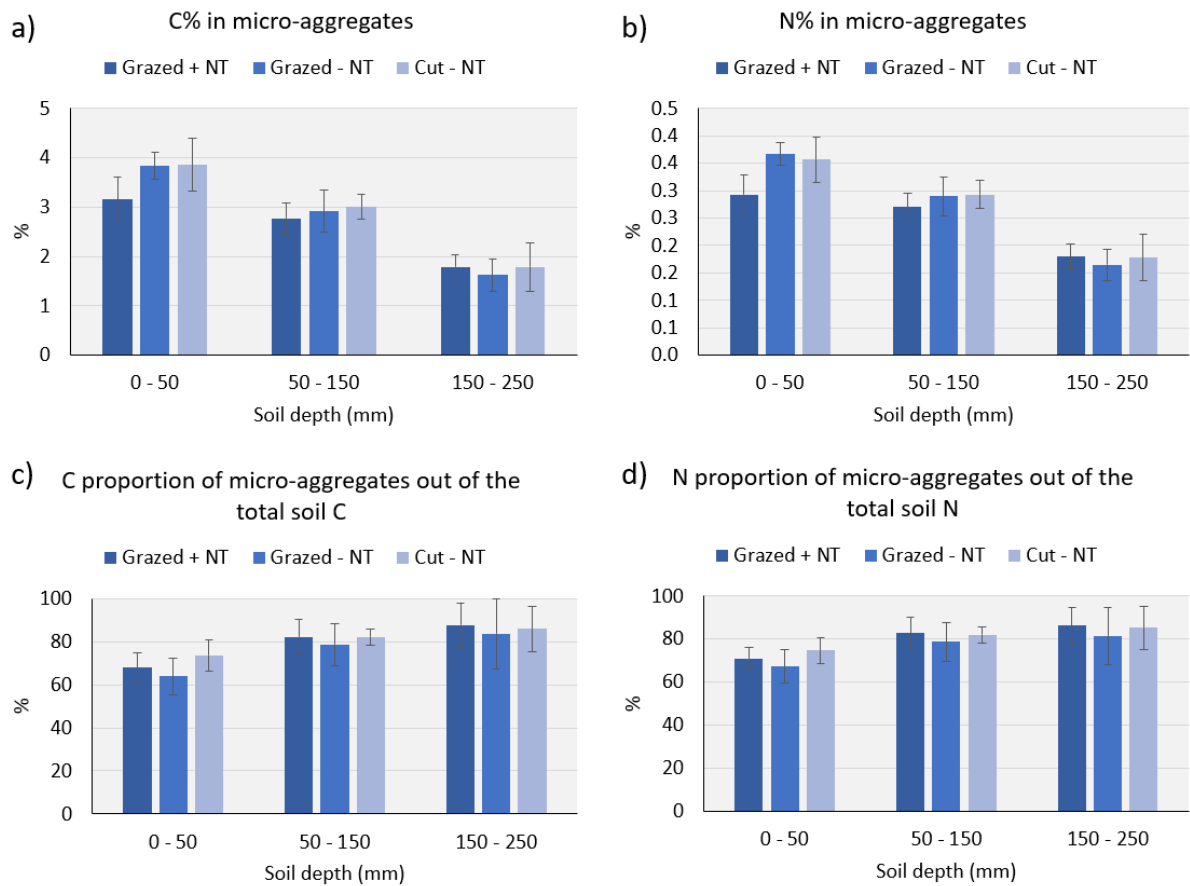
Extended Data Figure 4.4: Effect of elevated CO₂ on mineral associated organic matter (MAOM) from the NZ Free Air CO₂ Enrichment facility under different defoliation treatments and soil depths on a) MAOM fraction size, b) MAOM C:N ratio value, c) Carbon concentration

of MAOM, d) Nitrogen concentration of MAOM, e) Carbon proportion of MAOM out of the total soil C content and f) Nitrogen proportion of MAOM out of the total soil N content

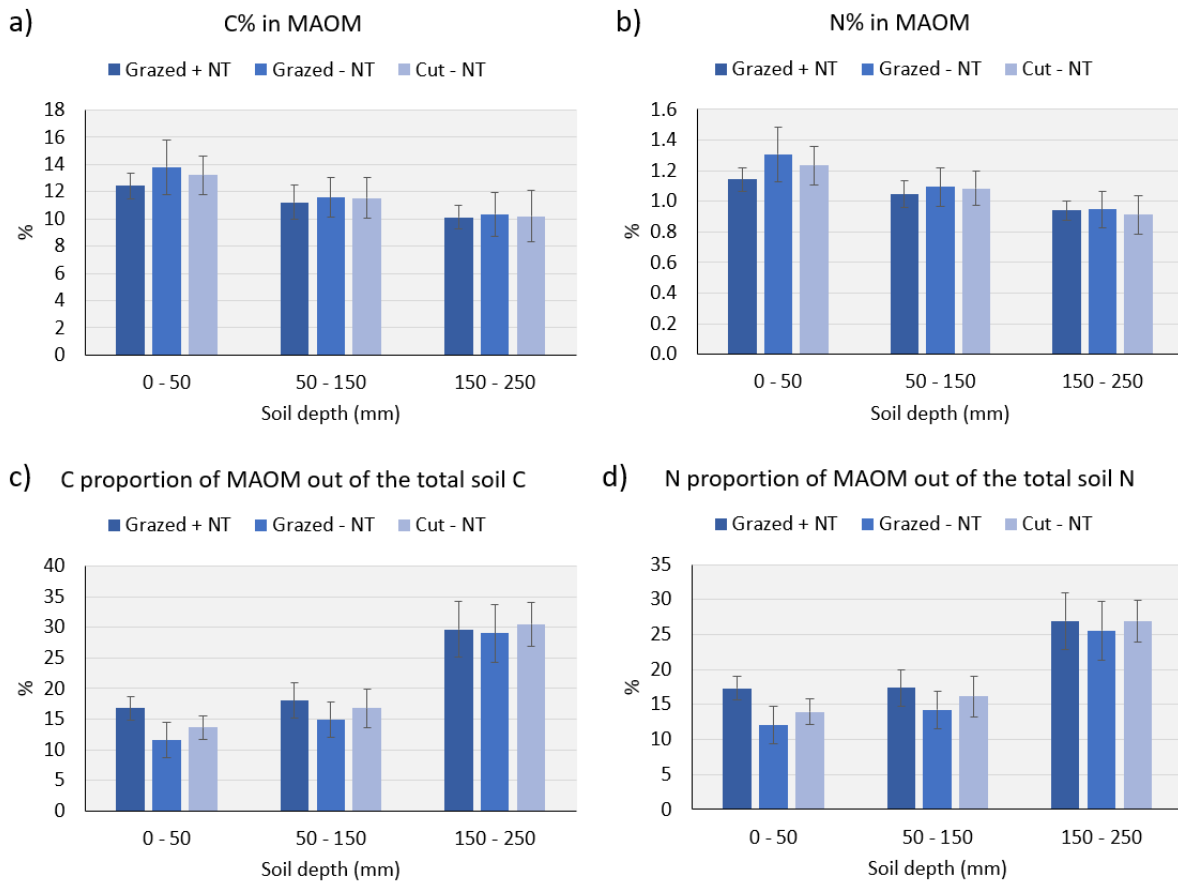
Extended Data 5.3.3.2 Influence of defoliation effect on soil organic carbon and nitrogen pools



Extended Data Figure 4.5: Carbon (C) and nitrogen (N) results on the coarse particulate organic matter (cPOM) fraction from the NZ Free Air CO₂ Enrichment facility independent of CO₂ treatment under three defoliation treatments at three soil depths. on a) Carbon concentration of cPOM, b) Nitrogen concentration of cPOM, c) Carbon proportion of cPOM out of the total soil C content and d) Nitrogen proportion of cPOM out of the total soil N content.

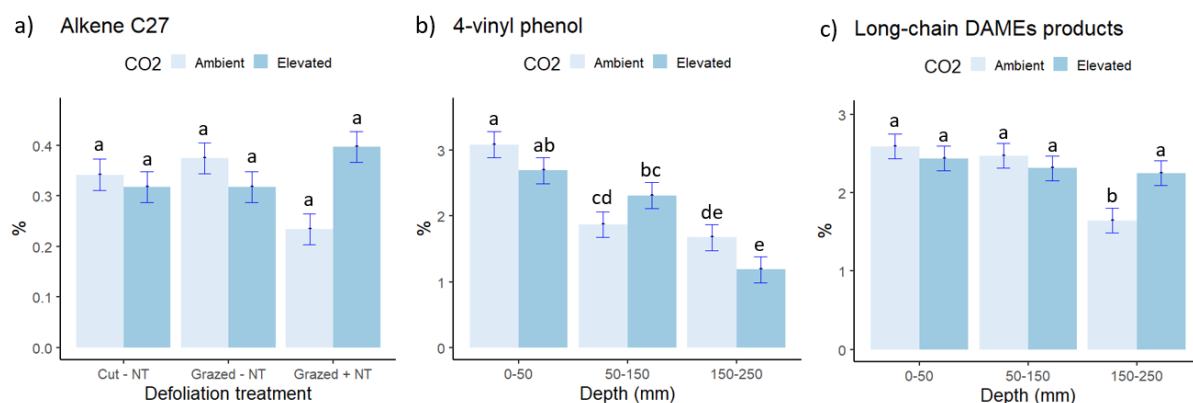


Extended Data Figure 4.6: Carbon (C) and nitrogen (N) results on the micro-aggregates fraction from the NZ Free Air CO₂ Enrichment facility independent of CO₂ treatment under three defoliation treatments at three soil depths. on a) Carbon concentration of micro-aggregates, b) Nitrogen concentration of micro-aggregates, c) Carbon proportion of micro-aggregates out of the total soil C content and d) Nitrogen proportion of micro-aggregates out of the total soil N content.



Extended Data Figure 4.7: Carbon (C) and nitrogen (N) results on the mineral associated organic matter (MAOM) fraction from the NZ Free Air CO₂ Enrichment facility independent of CO₂ treatment under three defoliation treatments at three soil depths. on a) Carbon concentration of MAOM, b) Nitrogen concentration of MAOM, c) Carbon proportion of MAOM out of the total soil C content and d) Nitrogen proportion of MAOM out of the total soil N content.

Extended Data 4.3.4.1 Interaction effects between elevated CO₂ and defoliation treatment



Extended Data Figure 4.8: Interaction effect of elevated CO₂ and defoliation treatment on pyrolytic products found in soil samples at the NZ Free Air CO₂ Enrichment facility on three soil layers on a) C₂₇ alkene, b) 4-vinylphenol and c) Long-chain (> C₂₀) methylated fatty diacids (long-chain DAMEs).

Extended Data 4.3.4.2 Influence of soil depth on soil organic matter molecular composition

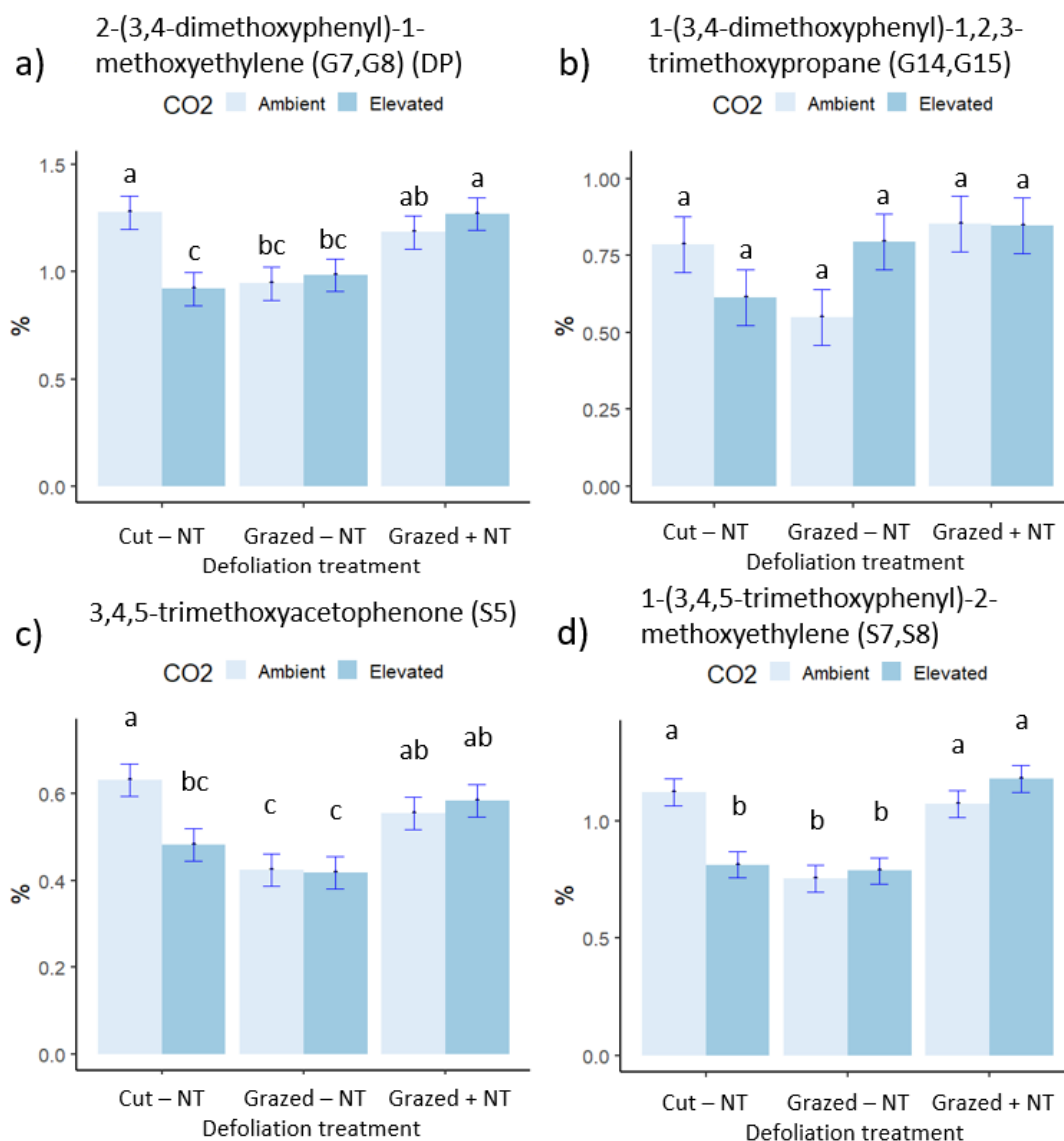
Extended Data Table 4.6: Lignin oxidation parameters on three soil layers and defoliation treatment (independent of CO₂) on soil samples from the NZ Free Air CO₂ Enrichment facility.

Depth (mm)	Grazed + NT	Grazed - NT	Cut - NT
0 – 50	14.00 ± 2.60	12.31 ± 0.66	14.62 ± 2.04
50 – 150	8.08 ± 0.61	6.98 ± 1.96	7.43 ± 1.76
150 – 250	3.51 ± 0.78	3.20 ± 0.67	3.31 ± 0.99

Extended Data 4.3.5.1 Interaction effect between elevated CO₂, defoliation treatment and soil depth

Extended Data Table 4.7: Triple interaction between CO₂ x defoliation x depth treatment on N-methyl-Cxx-alkylamide (a non-FAME MCC) from soil samples at the NZ Free Air CO₂ Enrichment facility.

Depth	Treatment (CO ₂ x Defoliation x Depth)	Mean	Group
0 – 50 mm	Ambient : Cut – NT : 0 – 50	0.375	C
	Elevated : Cut – NT : 0 – 50	0.705	BC
	Ambient : Grazed – NT : 0 – 50	0.408	C
	Elevated : Grazed – NT : 0 – 50	0.415	C
	Ambient : Grazed + NT : 0 – 50	0.415	C
	Elevated : Grazed + NT : 0 – 50	0.457	C
	50 – 150 mm	Ambient : Cut – NT : 50 – 150	0.631
Elevated : Cut – NT : 50 – 150		0.854	ABC
Ambient : Grazed – NT : 50 – 150		0.639	BC
Elevated : Grazed – NT : 50 – 150		0.545	BC
Ambient : Grazed + NT : 50 – 150		0.493	C
Elevated : Grazed + NT : 50 – 150		0.425	C
150 – 250 mm		Ambient : Cut – NT : 150 – 250	1.523
	Elevated : Cut – NT : 150 – 250	0.722	BC
	Ambient : Grazed – NT : 150 – 250	0.773	ABC
	Elevated : Grazed – NT : 150 – 250	0.513	C
	Ambient : Grazed + NT : 150 – 250	0.384	C
	Elevated : Grazed + NT : 150 – 250	1.309	AB



Extended Data Figure 4.9: Interactive effect of CO₂ and defoliation treatment on 1,2-dimethoxybenzenes (2MB) on a) 2-(3,4-dimethoxyphenyl)-1-methoxyethylene (G7,G8) (DP), b) 1-(3,4-dimethoxyphenyl)-1,2,3-trimethoxypropane (G14,G15) and 1,2,3-trimethoxybenzenes (3MB) on c) 3,4,5-trimethoxyacetophenone (S5) and d) 1-(3,4,5-trimethoxyphenyl)-2-methoxyethylene (S7,S8) products of soil samples from the NZ Free Air CO₂ Enrichment facility.

Extended Data Table 4.8: Triple interaction effect of CO₂ x defoliation and depth treatment on mono-methoxybenzenes on soil samples from the NZ Free Air CO₂ Enrichment facility.

Depth	Treatment (CO ₂ x Defoliation x Depth)	Mean	Group
0 – 50 mm	Ambient : Cut – NT : 0 – 50	6.195	BCD
	Elevated : Cut – NT : 0 – 50	9.345	A
	Ambient : Grazed – NT : 0 – 50	5.116	CDE
	Elevated : Grazed – NT : 0 – 50	4.386	DE
	Ambient : Grazed + NT : 0 – 50	8.024	AB
	Elevated : Grazed + NT : 0 – 50	7.798	AB
50 – 150 mm	Ambient : Cut – NT : 50 – 150	7.958	AB
	Elevated : Cut – NT : 50 – 150	9.155	A
	Ambient : Grazed – NT : 50 – 150	6.258	BCD
	Elevated : Grazed – NT : 50 – 150	4.987	CDE
	Ambient : Grazed + NT : 50 – 150	6.763	BC
	Elevated : Grazed + NT : 50 – 150	7.919	AB
150 – 250 mm	Ambient : Cut – NT : 150 – 250	7.225	ABC
	Elevated : Cut – NT : 150 – 250	5.149	CDE
	Ambient : Grazed – NT : 150 – 250	3.381	E
	Elevated : Grazed – NT : 150 – 250	3.898	E
	Ambient : Grazed + NT : 150 – 250	4.230	DE
	Elevated : Grazed + NT : 150 – 250	4.072	DE

Chapter 5 Influences of elevated CO₂ on soil organic carbon quantity and quality in two contrasting soils

Abstract

Despite the importance of grassland soils as a sink for carbon dioxide (CO₂), the effect of elevated CO₂ (eCO₂) on soil organic carbon (OC) partitioning and persistence in grassland soils with contrasting inherent physiochemical properties is not well understood. We conducted an experiment in mesocosms at the legume-based grazed pasture of the Free Air CO₂ Enrichment (FACE) facility in New Zealand in which two contrasting soils were exposed for 15 years (2005 – 2020) to eCO₂: (i) a mollic Psammaquent (Pukepuke) soil developed from sand, and (ii) an entic Dystrandept (Stratford) developed from volcanic ash. Our results showed that over the course of the study, OC and N contents and stocks (to 150 mm depth) of the Pukepuke soil under ambient CO₂ atmosphere (aCO₂) sharply declined (16 t ha⁻¹), while the decline in OC and N stocks in Stratford was smaller (5 t ha⁻¹). Soil disturbance during the establishment of the mesocosms cannot be ruled out as a factor contributing to the decline in OC stocks in the weakly structured Pukepuke soil, while in the more stable OC found in the Stratford would be more resistant to decomposition following disturbance. Exposure to eCO₂ for 15 years partly compensated for these losses in the Pukepuke soil resulting in soil OC stocks 6.5 t ha⁻¹ larger than with aCO₂, whereas in the Stratford soil, there was no significant change in OC stocks between the two CO₂ treatments ($p < 0.05$). Compared with aCO₂ treatments at the end of the study, the organic matter (OM) of both soils under eCO₂ was relatively enriched with intact plant-derived OC in the 0 – 50 mm of soil depth, but the opposite was observed at 50 – 150 mm soil depth. These results reveal that (i) the Stratford soil is more resilient than the Pukepuke soil to soil disturbances (when setting up the mesocosms) and weather extremes that occurred during the course of the experiment, (ii) eCO₂ was able to partially mitigate the impact of the soil disturbances (during the establishment of the study) and weather extremes on the decline of soil OC stocks through enhanced plant growth and associated plant-detritus input to soils, with this effect being more accentuated in the top 50 mm of soil, and (iii) under eCO₂ there

was priming of native OM below the 50 mm soil depth. These results emphasize the need for further research to better understand the effects of eCO₂ on soil OC and nutrient dynamics and the factors that regulate these effects.

5.1 Introduction

Anthropogenic pressure on atmospheric composition, especially the increase in atmospheric carbon dioxide (CO₂) concentration is driving changes in climate (IPCC, 2014). A direct consequence of elevated atmospheric CO₂ (eCO₂) – tested across multiple Free Air CO₂ Enrichment (FACE) facilities worldwide – is an enhanced photosynthetic rate (Norby and Zak, 2011; Jiang et al., 2020) which generally leads to an increase in plant biomass if other resources are available (Ainsworth and Long, 2004). However, depending on climatic conditions (rainfall and temperature; Liang and Balsler, 2012), soil properties (Hagedorn et al., 2001), plant species (Pendall et al., 2011), nutrient supply (Jiang et al., 2020) and duration of the study, eCO₂ can increase, maintain, or decrease plant biomass (Ainsworth and Long, 2004; Jiang et al., 2020), leading to a cascade of effects on soil organic carbon (OC).

Soils are the largest C reservoir in terrestrial ecosystems (Cheng et al., 2013) and have the potential to act as either a sink or a source of CO₂, this being dependent on changes in land use and associated management and environmental conditions. Grasslands account for 70% of the agricultural land worldwide (Conant et al., 2011; FAO, 2019) and contain about 20% of global soil OC stocks (Whitehead et al., 2018). Grasslands, most of which are permanent and grazed *in situ*, instead of cultivated, have a greater capacity to store OC than annual cropping species due to the ability to sustain higher OC input rates mostly from root-derived OC (root exudates and senescent roots) and the absence of physical disturbance (e.g., cultivation), which minimizes the breaking down of soil aggregates and thus, the exposure of soil organic matter (OM) to microbial attack. Given the areal extent of grasslands, even a small change in the OC stocks of their soils can have significant consequences for the global atmospheric CO₂ pool and, therefore, climate (Liang et al., 2017; Sitters et al., 2020).

Grasslands exposed to < 5 years of eCO₂ in FACE experiments have shown that an increase in herbage accumulation under eCO₂ can lead to an increase in soil OC (Jastrow et al., 2005). In longer-term grasslands FACE experiments, but still < 10 years (with a range of different soil types and experimental settings; Extended Data Table 5.1), consistent increases in soil OC content under eCO₂ have been reported in coarse-textured soils, compared with soils with finer textures and greater buffering capacity. Vestergard et al. (2016) found, on a nutrient-poor sandy Entisol at the Denmark-FACE, an increase of 12 – 22% in OC content in the upper 100-mm topsoil after 8 years of exposure to eCO₂, which translated into a 19% increase in soil OC stocks to 300 mm depth (Dietzen et al., 2019). Similarly, the nutrient-poor sandy soil (argic Udipsamment) of the BioCon facility, in Minnesota (Dijkstra et al., 2004, 2005), showed an increase in soil OC under eCO₂, where N fertiliser addition resulted in an increase in herbage accumulation. The clayey black Vertisol in the Tasmania-FACE (Pendall et al., 2011) showed an increase in soil OC content under eCO₂ with C₄ vegetation but not with C₃ vegetation, as only the C₄ plants were boosted under eCO₂. At the Jasper Ridge Global Change Experiment (JRGCE) in California on a loam textured Alfisol, it has been concluded that under eCO₂, soil OC only increases under N fertilisation (Liang et al., 2015).

Some longer-term studies (but ≥ 10 years) suggest that the turnover of soil OM is more stimulated under eCO₂ compared to ambient CO₂ (aCO₂) conditions, leading to a potential loss rather than to a net gain in soil OC over time (Thaysen et al., 2017), especially in sandy soils (Xu et al., 2019). In fact, none of the cut grassland FACE studies with ≥ 10 years of exposure to eCO₂ – including the Swiss-FACE on a sandy loam soil (eutric Cambisol; Six et al., 2001; van Groenigen et al., 2002; de Graaff et al., 2004; Xie et al., 2005; van Kessel et al., 2006 and Theis et al., 2007), the Giessen-FACE on a sandy clay loam over a clay layer (fluvic Gleysol; Keidel et al., 2018) and the USDA-ARS High Plains Grasslands Research Station (Carrillo et al., 2018) on a fine loamy soil (Mollisol) – have reported an increase in soil OC stocks under

eCO₂. At the NZ-FACE grazed grasslands facility on a black loamy fine sand (mollic Psammaquent), the small increases reported in aboveground biomass (~7%) is yet to translate into a significant increase in soil OC and N stocks or a widening in the C:N ratio of this black loamy fine sand soil (Dodd, 2013, Newton et al., 2014). A faster turnover of newly added OC (Van Groenigen et al., 2017) and/or priming, where the newly added OC stimulates the mineralisation of existing soil OM (Langley et al., 2009; Procter et al., 2015; Xu et al., 2019) have been identified as one of the mechanisms to explain the lack of soil OC increase following long-term exposure to eCO₂, despite increased plant growth.

The capacity of soils to store and stabilize OC in the long-term is a function of the balance between enhanced photosynthetic rate and the subsequent increase in plant growth, biota respiration, and the soil's ability to store and protect OC from decomposers (Six et al., 2001). If environmental conditions and management practices are maintained over time, a steady state is reached at a specific soil OC content for a soil with a specific OC input (Parfitt et al., 2000; Six et al., 2002). Soil OC is mostly protected from decomposers by (i) spatial inaccessibility to decomposers and associated enzymes, and reduced oxygen diffusion within soil aggregates (Six et al., 2001; Six et al., 2002) and (ii) by different physicochemical interactions, loosely binding organic ligands through van der Waals bonds and direct cations-bridging, and bonding organic ligands with clay minerals and short-range order Fe/Al oxy-hydroxides to form more stable complexes of mineral-associated OM (MAOM; Keblner et al., 2007; Kögel-Knabner et al., 2008)). Soils with fine texture and/or predominance of short-range order minerals, with the ability to form stable aggregates, have a greater potential to stabilise more OC-derived molecules in the soil surface and within soil aggregates compared to coarse-textured soils and/or poor in short-range Fe/Al hydrous oxides, with limited ability for aggregate building.

Many of the studies exploring the quantity and quality of OC in grassland systems under eCO₂ have been restricted to a single soil type per study. In fact, many of these studies appear to have

been restricted to coarse-texture soils, with limited reactive surfaces and limited ability for aggregate building. Few studies have assessed the interaction effect between soil type and eCO₂ (Procter et al., 2014, 2015). Soils differing in clay mineralogy and texture and, thus, in the abundance of reactive surfaces and aggregation may interact with eCO₂ to influence the partitioning of OC belowground, its incorporation into the soil OC pool, and the molecular composition and protection of the resulting OM.

We hypothesised that the OC stocks in soils under long-term pastoral use with limited potential to store and protect OC, due to their mineralogy, texture, and weakly developed aggregate structures (e.g., sandy soil derived from sedimentary materials) will not experience any additional OC gains under eCO₂. Instead, these soils could be at risk of priming their native soil OC in response to a boost in soil OC inputs from the additional pasture growth under eCO₂, resulting in an overall decline in the soil OM quality (low chemical diversity) and quantity (Chen et al., 2019; Xu et al., 2019). On the other hand, OC stocks in soils under long-term pastoral use derived from volcanic ash, with a mineralogy and textural class, that enables strong aggregate building and stabilisation, protecting the OC from decomposers (e.g., soil derived from volcanic ash), may have a greater capacity to assimilate the additional fresh OC inputs under eCO₂ without invoking priming. As a result, the soil will respond to eCO₂ with an increase in soil OC, although this will be tempered by the OC deficit of the soil.

The objective of this research was to determine how exposure to eCO₂ for 15 years influences the soil OC and N content, and the OM molecular composition of two soils under long-term pastoral use with marked differences in mineralogy and associated physicochemical properties (i.e., sandy soil, with an 87% sand and lack of short-range order constituents vs. a sandy loam soil, with a 40% sand and abundance of allophane), both soils having been managed under permanent pasture for an extended period and hence likely to be under steady state with regards soil OC stocks (under aCO₂).

5.2 Methods

5.2.1 Experimental setup

Since the late ninety's, the NZ-FACE facility has been used to investigate the effects of eCO₂ on pasture biomass production, botanical composition, soil nutrient cycling and soil OC dynamics under sheep grazing (Dodd, 2013). Located in a temperate grazed pasture near Bulls, Manawatu-Wanganui, New Zealand (40°14' S, 175°16'E), the NZ-FACE facility is the only FACE facility worldwide examining the influence of eCO₂ on the dynamics of grazed legume-based pastures. The facility is divided into three blocks with two circular plots within each block (12 m diameter “rings”; Extended Data Figure 5.1a). The rings were chosen in 1997 based on their initial botanical composition (Newton et al., 2006). In each block, one ring is exposed to the current atmospheric CO₂ concentration (aCO₂) and the other ring is treated with CO₂ on a daily basis throughout the photoperiod. Over the course of the study dating back to 1997 the CO₂ treatment has not been continuous, between 2011 and 2013 the NZ-FACE facility was refurbished and there was no difference in the atmospheric CO₂ concentration. Moreover, the rings were initially treated with 475 ppm of CO₂, yet in 2013 the CO₂ concentration was increased to 500 ppm of CO₂, a concentration likely to be reached during this century (IPCC, 2014).

At the site, the soil is Pukepuke, a peaty sandy gley, with a black loamy, fine sand topsoil horizon (Mollic Psammaquent; Cowie, 1965; NSDR, 2020). Edwards et al. (2001), Ross et al. (2004) and Newton et al. (2014) provide a detailed description of the study site, including the installation process and the logistic of grazing practices inside the rings. Briefly, when the aboveground biomass was around 1800 – 2000 kg dry matter (DM) ha⁻¹, three to four sheep are introduced to the rings (Extended Data Figure 5.1b) and left to graze until there is 800 kg dry DM ha⁻¹ of aboveground biomass (Newton et al., 2014). There are 7 – 15 grazing episodes

per year depending on the herbage growth. The rings are annually fertilised; the average application rates over the last five years were 38, 86, 96 and 100 kg ha⁻¹ of elemental phosphorus (P), potassium (K), sulphur (S) and calcium (Ca), respectively. Note that the only *de novo* additions of N are through biological N₂ fixation.

To extend the analysis at the NZ-FACE, four mesocosms (300 x 250 mm) were installed in each ring in 2005, two containing the Pukepuke soil and two containing the Stratford soil, a Vitric Orthic Allophanic soil (Extended Data Figure 5.1c). The Pukepuke soil was collected from the field found alongside the aCO₂ rings of the FACE facility, while the Stratford soil was taken from the Taranaki Agricultural Research Station, New Plymouth (140 km northwest of the NZ-FACE facility). These soils have markedly different physicochemical properties and have developed under different rainfall regimes (Table 5.1). The Pukepuke soil derived from sedimentary materials has a weakly developed structure, with the micro-aggregates having little strength or stability, breaking down readily to the soil constituents. The soil has a low anion and cation exchange capacity. Combined with the coarse-textured nature of the soil, there is little capacity to create stable organo-metal complexes.

The Stratford soil in contrast has a coarse sandy loam texture with a moderately well-developed soil structure, rich in allophane (11%; Robinson, 2000), with an abundance of reactive surfaces (i.e., short-range order constituents and abundance of allophane) which provides the capacity to create stable organo-mineral complexes (Parfitt, 2009).

Table 5. 1: General description of original location and physico-chemical properties of the Pukepuke and Stratford soils.

General soil description	Pukepuke soil	Stratford soil	References
Location	NZ-FACE facility, Bulls, Manawatu, New Zealand	Taranaki Agricultural Research Station, New Plymouth, Taranaki, New Zealand	Personal communication
Vegetation	Permanent pasture	Permanent pasture	*,** NSDR, 2020.
Management	Grazed	Grazed	*Ross et al., 2013 **Parfitt et al., 1985
NZ soil Class	Peaty Sandy Gley	Vitric Orthic Allophanic	*,** NSDR, 2020.
NZ Genetic Class	Yellow-brown sand	Yellow-brown loam	*,** NSDR, 2020.
USDA Soil class	Mollic Psammaquent	Entic Dystrandept	* Ross et al., 2013 **Parfitt et al., 1985
Parental Material	Sedimentary sand	Medium textured andesitic ash	*Cowie and Campbell, 1965; **Burgess, 1966
Topography	Flat	Rolling	*NSDR, 2020 **Parfitt et al., 1985
MAT (°C)	12.9	12.1	*,** https://en.climate-data.org/oceania/new-zealand-9/
MAP (mm)	1086	1935	*,** https://en.climate-data.org/oceania/new-zealand-9/
Drainage	poorly drain	Well drained	*Cowie and Campbell, 1965; **Burgess, 1966
pH (in H₂O)	5.8 to 6.7	5.7 to 6.5	*Cowie and Campbell, 1965; **Burgess, 1966
Bulk density (g cm⁻³)	1	0.8	* Ross et al., 2013 **Stevenson and Laubscher, 2018
Cation Exchange Capacity	32	28	*,** NSDR, 2020.
Anion Adsorption Capacity (%)	< 20	> 90	*,**NSD, 2020
Phosphorus retention (%)	36	91	*,** NSDR, 2020.
Particle size (%)	Sand: 87 Silt: 7 Clay: 6	Sand: 40 Silt: 35 Clay: 24	*Ross et al., 2013 ** NSD, 2020

* Citation for Pukepuke soil, ** Citation for Stratford soil

In 2009, the OC and N content and stock of the Stratford soil in the mesocosms and the Pukepuke soil from the rings (and not mesocosms) was determined by Gentile (unpublished data; see Extended Data 4.2 for the timeline of the mesocosm experiment). Back then, no significant differences ($p > 0.05$) between eCO₂ and soil type were found on soil OC and N stocks based on equivalent soil mass (Table 5.2).

Table 5. 2: Soil organic carbon (OC) and nitrogen (N) stocks in the Pukepuke (from rings) and Stratford (mesocosm) soils in the 0 – 50 and 50 – 150 mm soil depth, in 2009 (after 12 and 4 years of exposure to elevated CO₂, respectively) from the NZ-FACE legume-based grazed pasture facility (unpublished data).

Soil type	Depth (mm)	OC (t ha ⁻¹)		N (t ha ⁻¹)	
		Ambient	Elevated	Ambient	Elevated
Pukepuke (ring)	0 - 50	23.7 ± 2.3	24.9 ± 1.1	2.1 ± 0.2	2.3 ± 0.1
	50 - 150	33.3 ± 5.0	33.6 ± 3.2	3.2 ± 0.4	3.3 ± 0.3
	0 - 150	57.0 ± 6.8	58.5 ± 4.3	5.3 ± 0.6	5.5 ± 0.4
Stratford (mesocosm)	0 - 50	30.9 ± 0.7	30.6 ± 1.9	3.7 ± 0.2	3.7 ± 0.2
	50 - 150	48.8 ± 0.1	49.5 ± 1.4	5.7 ± 0.1	5.7 ± 0.1
	0 - 150	79.7 ± 0.6	80.2 ± 2.6	9.4 ± 0.2	9.4 ± 0.3

During the study period from 2005 to 2020, the soils in the mesocosm at the NZ-FACE facility in the Manawatu district were subjected to some extreme weather events. According to the New Zealand Drought Index (NZDI), most of the Manawatu district experienced exceptionally dry conditions in most years of the study (NIWA, New Zealand Drought Monitor, 2021). Specifically, in 2015 and 2018 the district witnessed drought events, while 2011 and 2020 were marked by severe drought events (Figure 5.1). These drought events were accompanied by higher temperatures compared to the district's mean annual temperature (see meteorological data throughout the NZ-FACE experiment 1997 – 2020 in Chapter 3). The rainfall recorded during the drought events was ~60% below the average mean annual precipitation (NIWA,

2011, 2015, 2018 and 2020). In the 15 years prior to the start of the mesocosm experiment (1990 – 2004), the average mean annual temperature (MAT) was 13.9°C and mean annual precipitation (MAP) was 937.4 mm. In contrast, the average MAP and MAT during the study period (2005 – 2020) was warmer (14.4°C), with no change in rainfall (950.5 mm).

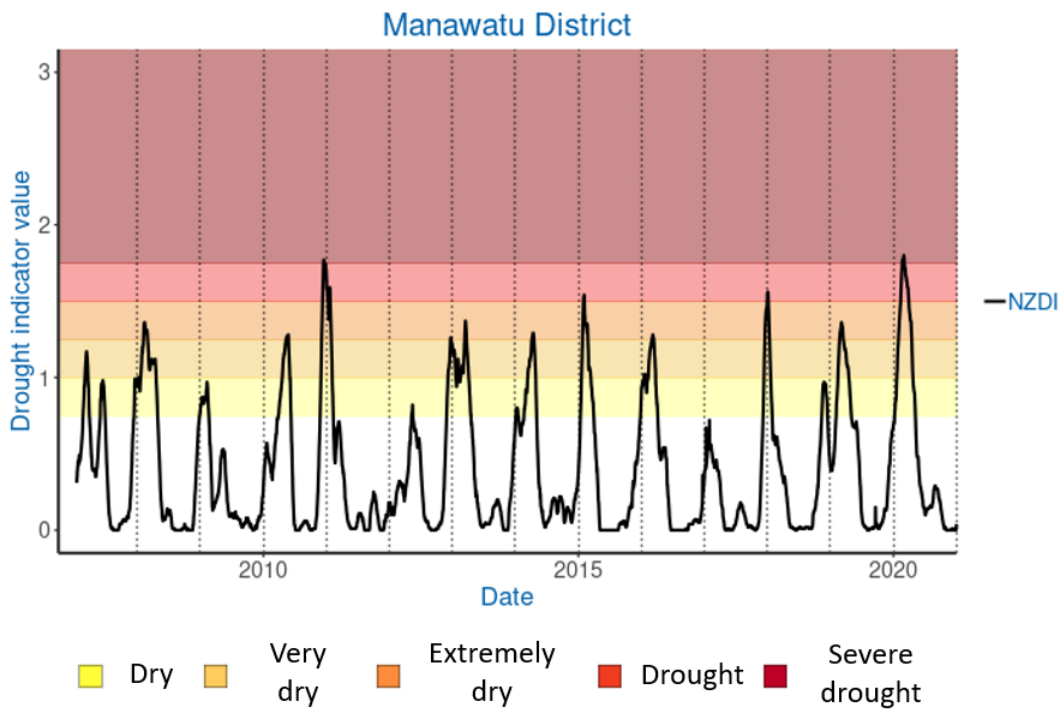


Figure 5. 1: New Zealand Drought Index (NZDI) chart between 2007 and 2020 in the Manawatu district (extracted from NIWA, New Zealand Drought Monitor, 2021).

5.2.2 Soil organic carbon and nitrogen analysis

In October 2020 during the southern hemisphere spring, after 15 years of eCO₂ exposure, soil was collected from all the mesocosms at the NZ-FACE facility (see Extended Data Figure 5.2 for timeline of the mesocosm experiment). Four soil cores (25 mm diameter x 150 mm depth) were collected from each mesocosm in each ring (ambient and eCO₂). The cores were divided

in-situ into two depths (0 – 50 and 50 – 150 mm). Two out of the four soil cores per mesocosm were individually oven-dried for 24 h at 105 °C prior to weighing for calculating bulk density. The remaining two soil cores from each ring were air-dried and sieved (< 2 mm) prior to OC and N analysis. The samples collected in 2009 and 2020 were analysed for total C and N by dry combustion in an Elementar analyser (Vario Max Cube; Analysensysteme GmbH, Germany). No acid pre-treatment to remove inorganic C was performed as the soil pH is close to neutral, thus insignificant amounts of inorganic C were expected to be found. Soil OC and N stocks down to a specific depth were determined on the equivalent soil mass (ESM) procedure proposed by Wendt and Hauser (2013) to overcome potential masking effects associated with changes in soil bulk density. In addition to comparing the effect of eCO₂ with that of aCO₂ at the end of the 15 years of the mesocosm experiment on soil OC and N contents, these soil properties were also compared for the aCO₂ treatment over time. Specifically, (i) changes in soil OC and N contents between 2009 and 2020 samples in the Stratford mesocosms; and (ii) changes in soil OC and N contents between 2009 samples in Pukepuke from rings (it was assumed that conditions in the Pukepuke mesocosm under aCO₂ conditions were identical as those in the ring) and 2020 samples in Pukepuke from mesocosms.

5.2.3 Characterization of soil organic matter molecular composition

Analytical Pyrolysis (Py) Gas Chromatography (GC) followed by a Mass Spectrometer (MS) and thermally assisted hydrolysis methylation (THM) GC-MS analysis, allows the determination of the molecular composition of soil OM, after thermal degradation of macromolecules and subsequent separation (through GC) and identification/quantification (through MS) of their fragments (Derenne and Quenea, 2015). Both techniques were used to investigate the differences in the soil molecular composition of two contrasting soils under ambient and eCO₂.

A mild acid pre-treatment was performed on finely ground samples to remove reactive mineral phases such as Fe (oxy)(hydro)oxides. Briefly, 0.2 g of the sample was weighed into centrifuge tubes, to which an aliquot of 10% HCl was added to dissolve carbonates, and then 2% aqueous HF solution was added to reach the 40 mL volume. After 24 hrs of shaking, the suspensions were centrifuged (2500 rpm for 10 min) and the supernatant was discarded. The obtained residue was then rinsed three times in distilled water to wash away salts and remaining acid (with centrifugation/decantation cycles in between). The final residue was dried at 50 °C and homogenized before pyrolysis-GC-MS and THM-GC-MS analysis.

Conventional Py-GC-MS was performed with a Pyroprobe (CDS Analytical) coupled to an 8860 GC and 5977 MS detector (Agilent Technologies). The samples (1 mg of ground and HF-treated material) were embedded in glass wool-containing fire-polished quartz tubes and pyrolyzed at 650 °C for 20 seconds (heating rate 10 °C ms⁻¹). The pyrolysis-GC interface, GC inlet, and GC-MS interface were set at 325 °C. The GC was equipped with a non-polar HP-5MS 5% phenyl, 95% dimethylpolysiloxane column (length 300 mm; internal diameter 0.25 mm; film thickness 0.25 µm). Helium was used as the carrier gas (constant gas flow, 1 ml min⁻¹). The GC oven was heated from 60 to 325 °C at 20 °C min⁻¹. The ion source of the MS operated in electron impact mode (70 eV) at 230 °C and the quadrupole detector was held at 150 °C, measuring products based on the mass to charge number of ions ratio (m/z) in the 50–500 range. The instrumentation and most parameters for Py-GC-MS, were also used for THM-GC-MS. Before inserting the sample-containing quartz tubes, an aliquot of 25% tetramethylammonium hydroxide (aqueous TMAH from Sigma-Aldrich) was added and the mixture was allowed to stand for one hour. Analytical parameters that differed from the ones for Py-GC-MS were the use of a five-minute solvent delay (to allow the reactant and solvent to elute before activation of the MS) and a GC oven temperature program from 70 to 325 at 20 °C min⁻¹ with a five-minute initial and three-minute final isothermal hold periods. Relative

proportions of the pyrolysis and THM products were calculated as the proportion (in %) of the total quantified peak area (TQPA), using the main fragment ions (m/z) of each product. A total of 134 and 72 chemical compounds were identified through pyrolysis GC/MS and THM GC/MS analysis, respectively (Extended Data Tables 4.2 and 4.3, respectively). These were statistically analysed by individual products followed by cluster analysis based on chemical similarities. We quantified the relative proportions of the pyrolysis and THM products to assess the origin of the soil OC (Extended Data Table 5.4 and 4.5 respectively) under ambient and eCO₂ conditions on both soils.

5.2.4 Statistical analysis

The differences between soil type, depths, CO₂ treatments and their interaction effects were explored. Linear mixed effect models (lme) for the nested block design followed by pairwise tests and permutations were applied to aboveground biomass, soil nutrient status (Extended Data 5.4.2 Changes in soil nutrient status, above-ground biomass and botanical composition) and soil OC and N data. The pyrolysis and THM results were evaluated using principal components analysis (PCA) by correlation to identify factors with major influence on product distributions in the whole dataset. The relative proportions of individual products (% TQPA), sums of types of products (% TQPA) and the principal components obtained by PCA were used to compare results from Py-GC-MS and THM-GC-MS analysis (individual compounds % as input) to soil OC content and C/N ratio. The qualitative analysis was followed by a lme analysis on the sum of the type of products and each individual product to identify the effects of CO₂ treatment, soil type and depth on the soil OM molecular composition. R Studio was used to run all the statistical analysis through “lme” and “predictmeans” packages (RStudio version 1.2.5033).

5.3 Results

5.3.1 Soil organic carbon and nitrogen stocks

5.3.1.1 Differences in soil organic carbon and nitrogen stocks under ambient CO₂ over time

Under aCO₂ conditions, independent of soil type and depth, there was a significant decrease of soil OC and N stocks ($p = 0.0001$ and < 0.0001 , respectively; Table 5.3) and content ($p < 0.0001$, for both soils; Extended Data Table 5.6) over time (years compared were 2009 and 2020). By 2020, the Stratford soil has lost 5.1 and 1.0 t ha⁻¹ of soil OC and N stocks, respectively, across the top 150 mm depth considered, which represents a decrease on average, of 6% and 11%, of the soil OC and the N stock in 2009, respectively. In contrast, the loss of OC and N stocks of the Pukepuke soil by 2020, was much larger compared to the Stratford soil, with a total loss of 16.1 and 1.5 t ha⁻¹, respectively, representing a -28 and -29% of the OC and N stocks in 2009, respectively.

Table 5. 3: Soil organic carbon (OC) and nitrogen (N) stocks on soil samples collected in 2009 and 2020 from the NZ-FACE facility under ambient CO₂. Values are given based on ESM calculation.

		Ambient CO ₂					
Soil type	Depth (mm)	OC (t ha ⁻¹)			N (t ha ⁻¹)		
		2009	2020	ΔOC (%)	2009	2020	ΔN (%)
Pukepuke*							
	0 – 50	23.7 ± 2.3 e	16.2 ± 1.0 f	-32	2.1 ± 0.2 e	1.5 ± 0.1 f	-31
	50 – 150	33.3 ± 5.0 b	24.7 ± 2.5 de	-26	3.2 ± 0.4 d	2.3 ± 0.2 e	-27
Profile	0 – 150	57.0 ± 6.8 B	40.9 ± 3.4 C	-28	5.3 ± 0.6 C	3.8 ± 0.3 D	-29
Stratford							
	0 – 50	30.9 ± 0.7 bc	27.8 ± 1.0 cd	-10	3.7 ± 0.2 c	3.1 ± 0.1 d	-16
	50 – 150	48.8 ± 0.1 a	46.8 ± 1.4 a	-4	5.7 ± 0.1 a	5.3 ± 0.1 b	-7
Profile	0 – 150	79.7 ± 0.6 A	74.6 ± 0.6 A	-6	9.4 ± 0.2 A	8.4 ± 0.1 B	-11

*Results of Pukepuke soil in 2009 are from soils inside the rings, 2020 results are from soil in mesocosm.

5.3.1.2 The interactive effect between elevated CO₂ and soil type on soil organic carbon and nitrogen stocks

After 15 years of mesocosm confinement, the influence of eCO₂ on soil OC and N contents and stocks differed markedly between the two soils. There was a strong and consistent interaction effect between CO₂ treatment and soil type on soil OC ($p = 0.0385$) and N contents ($p = 0.0457$) and associated stocks ($p = 0.0454$ and $p = 0.0472$, respectively). A positive effect of eCO₂ on soil OC and N compared with aCO₂ was observed only in the Pukepuke soil, where soil OC and N contents (Figure 5.2a and b) and stocks (Figure 5.2c and d) were larger after 15 years of exposure to eCO₂ than those under aCO₂. The larger OC stocks in the eCO₂ Pukepuke soil compared with aCO₂ conditions amounted to an extra 2.5 and 4.0 t ha⁻¹ in the 0 – 50 mm and 50 – 150 mm depths, respectively, and 0.2 and 0.3 t ha⁻¹ of N stocks in the 0 – 50 mm and 50 – 150 mm depths, respectively. Thus, after 15 years of eCO₂, soil OC stocks were 15 and 16% larger in the 0 – 50 and 50 – 150 mm, respectively, compared to those under aCO₂ conditions. Likewise, N stocks under eCO₂ were 14 and 12% larger in the 0 – 50 mm and 50 – 150 mm soil layers, respectively, than those under aCO₂ conditions. The larger OC and N stocks in the Pukepuke soil under eCO₂, compared with aCO₂ soils resulted in a slight widening of the soil C:N ratio, though this was not significant to $p < 0.05$ (Extended Data Table 5.7). In sharp contrast, soil OC and N content (Figure 5.2a and b) and stocks (Figure 5.2c and d) of the Stratford soil after 15 years of exposure to eCO₂ were not significantly different to the same soil under aCO₂ conditions.

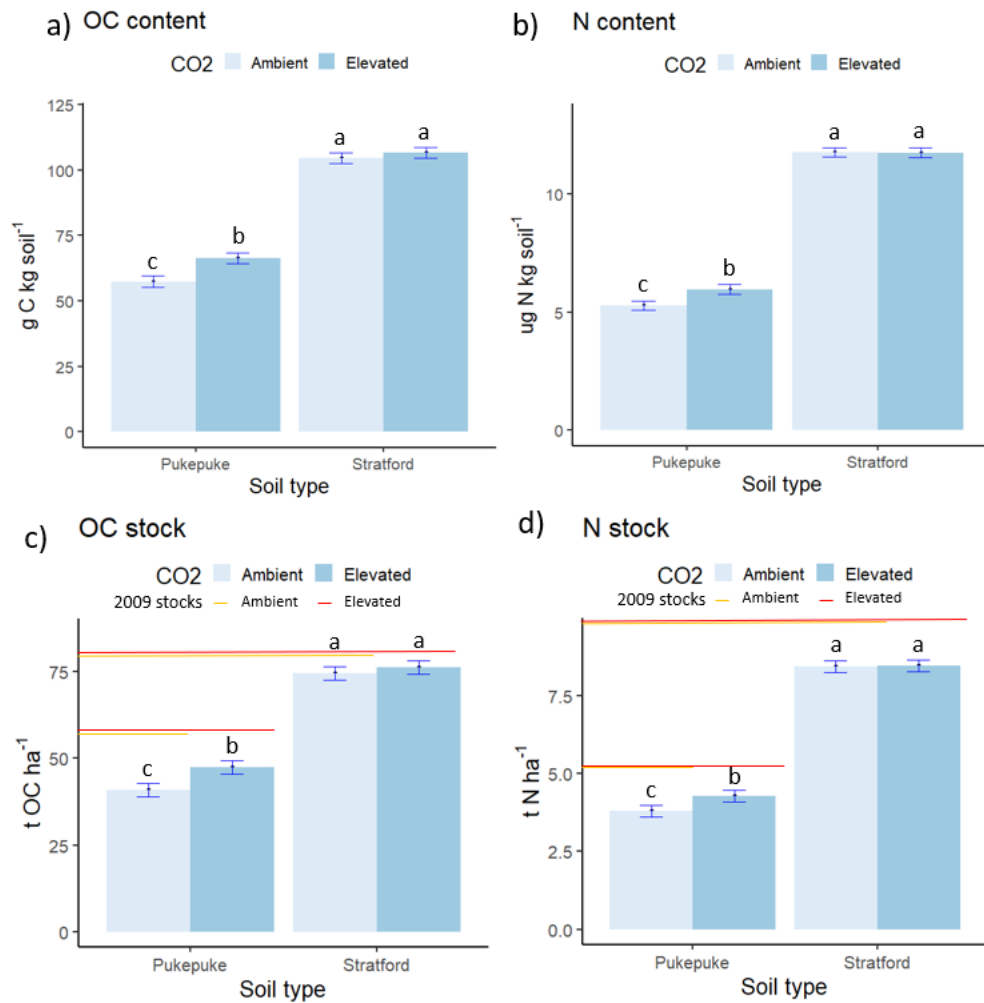


Figure 5. 2: Interactive effect of elevated CO₂ and soil type on a) soil organic carbon (OC) content, b) soil nitrogen (N) content, c) soil organic carbon (OC) stock and d) soil nitrogen (N) stock in the 0 – 150 mm depth in the two soils in the mesocosms sited at the NZ Free Air CO₂ Enrichment facility after 15 years of exposure to elevated CO₂. Error bars indicate SD (n = 3, letters indicate differences to p < 0.05). Note that values for Pukepuke 2009 samples are soils collected from the rings and not the mesocosm.

5.3.1.3 The interactive effect between elevated CO₂ and soil depth on soil organic carbon and nitrogen stocks

Independent of soil type, an interactive effect between CO₂ treatment and soil depth ($p = 0.0072$) was found in the soil bulk density, where the topsoil (0 – 50 mm) in eCO₂ soils was less dense than in aCO₂ soils (0.81 vs 0.87 g soil cm⁻³; Extended Data Figure 5.3a).

5.3.2 Soil organic matter molecular composition

To assess the effect of long-term exposure (15 years) to eCO₂ on the molecular composition of the soil OM in the two soils in the mesocosms, the soils were sampled to two depths (0 – 50 and 50 – 150 mm) in 2020 and analysed by Py-GC-MS and THM-GC-MS.

5.3.2.1 Inherent differences in soil organic matter molecular composition between soil types and depths

The PCA plot shows the distribution of different pyrolytic groups across two principal components, with PC1 explaining 30.8% of the variance and PC2 explaining 23.2% of the variance (Figure 5.3a). The plots show a clear separation between the samples from Pukepuke and Stratford soils and depths along PC1 (Figure 5.3a and b). Loadings analysis reveals that certain molecular components are driving the separation between the soil types and depths. Phenol and unspecific polysaccharide products have high loadings on PC1, indicating that they are strongly correlated with the variation between soil depth. In contrast, N-containing and lignin products have a high loading on PC2, indicating that it is more strongly correlated with the variation within soil type.

Across the two CO₂ treatments and soil depths, the molecular composition of the OM in the Pukepuke and Stratford soils showed a clear difference, with the former having more plant-derived fingerprints and the latter more microbial-derived fingerprints (Figure 5.3a). This was

reflected in the higher proportions of lignin products ($p = 0.0362$) in the Pukepuke soil, especially guaiacol lignin ($p = 0.0298$) and syringol lignin ($p = 0.0365$). This sandy soil also showed higher proportions of plant polysaccharides, though not significant at $p < 0.05$. The Stratford soil had higher proportions of N-containing products principally from chitin-related products (benzotrile ($p = 0.0444$) and 4-pyridone ($p = 0.0087$)) compared to Pukepuke soil. The Stratford soil also contained higher proportions of halogen-containing products ($p = 0.0004$), especially the proportions of iodine ($p = 0.0025$) compared to Pukepuke soil.

For both soils, across the two CO₂ treatments, the molecular composition of the OM changed strongly with soil layers (0 – 50 vs. 50 – 150 mm; Figure 5.3b). With increasing soil depth, the proportions of phenols ($p = 0.0108$), guaiacol lignin ($p < 0.0001$), p-hydroxyphenyl lignin ($p = 0.0005$), syringol lignin ($p < 0.0001$) and plant polysaccharides in the soil OM decreased, while the proportions of halogen-containing compounds increased with depth ($p = 0.0082$).

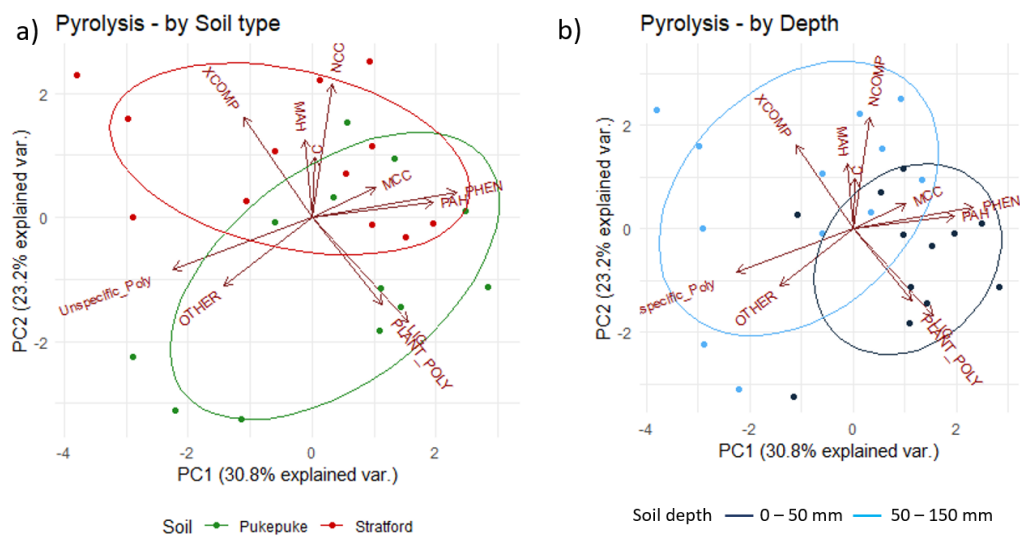


Figure 5. 3: Principal Component Analysis biplots, independent of CO₂ treatment, of the pyrolytic groups clustered by a) soil type and b) soil depth. in Pukepuke and Stratford soil from mesocosms at NZ-FACE facility Abbreviations of products: MCC = aliphatic, NCOMP = N-containing, PHEN = phenols, MAH/PAH = mono-/polycyclic-aromatic hydrocarbons, OTHER = unidentified, LIG = the sum of lignin G, H and S (guaiacol, and syringyl), Unspecific Poly =

unspecific polysaccharides, PLANT_POLY = plant polysaccharides and XCOMP = halogen-containing.

5.3.2.2 Interactive effects of elevated CO₂ and soil type on the organic matter molecular composition

The impact of eCO₂ on the pyrolytic groups, clustered by the chemical similarity of their components (see Extended Data Table 5.4), was mainly observed in the Pukepuke soil. Under eCO₂ conditions, the Pukepuke soil showed a larger proportion of total lignin (12.4%; $p = 0.0279$) compared to aCO₂ conditions (9.7%; Figure 5.4a). This increase in lignin content was primarily driven by the rise in the proportion of lignin guaiacol ($p = 0.0154$; Figure 5.4b). In contrast, no significant differences were found in any of the pyrolytic groups in the Stratford soil between CO₂ treatments, including carbohydrates, lignin S, lignin H, aliphatic, N-containing, monoaromatic hydrocarbons, polyaromatic hydrocarbons, phenol, or halogen-containing groups. Similarly, there were no significant differences between ambient and eCO₂ conditions in terms of lignin oxidation parameters, plant polysaccharides, unspecific polysaccharides, or their ratios in either soil.

Out of the 134 individual pyrolysis products identified in the two soils used in the mesocosm study, there were no direct effects of eCO₂, and only a few interactive effects between eCO₂ and soil types were observed. In the eCO₂-treated Pukepuke soil, enriched proportions of vanillin (a lignin G; $p = 0.0498$) and alkene C₂₇ (an aliphatic product; $p = 0.0362$) were found, while alkyl-amide C₁₈ (an aliphatic product; $p = 0.0346$) was depleted in the 50 – 150 mm depth compared to aCO₂ conditions. Additionally, eCO₂ in the Pukepuke soil led to larger proportions of 4-(2-propenyl) guaiacol (trans) ($p = 0.0347$) and enrichment of fatty acid C₁₈ ($p = 0.0419$; Extended Data Figure 5.4a to e, respectively). In the Stratford soil, eCO₂ resulted in

the depletion of certain aliphatic products such as alkane C₃₂ ($p = 0.0476$) and alkene C₁₅ (an aliphatic product; $p = 0.0025$) and alkene C₂₅ ($p = 0.0217$) in the 50 – 150 mm depth (Extended Data Figure 5.5a, b, and c, respectively).

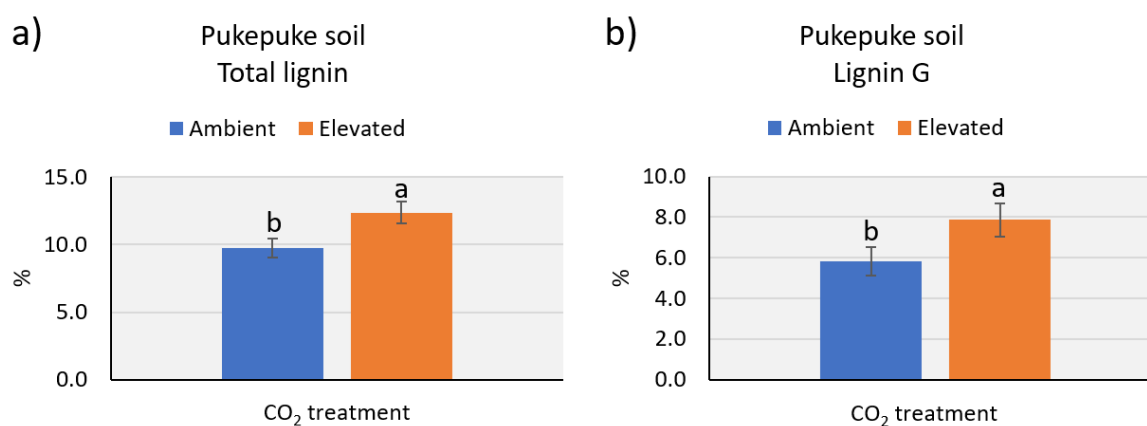


Figure 5. 4: Effect of elevated CO₂ on the pyrolytic products found in the Pukepuke soil samples from the NZ Free Air CO₂ Enrichment facility after 15 years of elevated CO₂ enrichment on a) total lignin and b) guaiacol lignin (Lignin G). Error bars indicate SD ($n = 3$, letters indicate differences to $p < 0.05$).

We found no direct effect of eCO₂ on THM-GC-MS products on either soil and only a small interaction effect between eCO₂ and soil type. This effect was limited to the Pukepuke soil with eCO₂ enriching monomethoxy benzene (1MB) group ($p = 0.0405$), and corroborated by the 4-methoxybenzoic acid (P6) a 1MB product (0.0394), also enriching azelaic acid a short methylated fatty diacids (C₉ DAME; $p = 0.0262$), iso-anteiso C₁₅ FAME, a short aliphatic chain ($p = 0.0187$) and N,N-dimethyl-Cxx-alkylamide, a long-chain chain aliphatic backbone product ($p = 0.0101$; Extended Data Figure 5.6a to d, respectively). The Pukepuke soil under eCO₂ also showed depletion of an unidentified carbohydrate ($p = 0.05$; Extended Data Figure 5.6e).

5.3.3.3 The interactive effect of elevated CO₂ and soil depth on the molecular composition of soil organic matter

Irrespective of soil type, a stronger interaction effect between CO₂ treatment and soil depth was observed in the pyrolytic groups. In the top 0 – 50 mm soil layer, across both soil types, eCO₂ led to an enrichment of several lignin products, including higher proportions of 4-methyl guaiacol ($p = 0.0197$), 4-ethyl guaiacol ($p = 0.0168$), and 4-methyl syringol ($p = 0.0221$; Extended Data Figure 5.7a, b, and c, respectively). Conversely, short-chain fatty acid methyl esters (C₁₆ and C₁₈; $p = 0.0362$ and 0.0221 , respectively) and fatty acid C₁₆ ($p = 0.0017$) were depleted under eCO₂ (Extended Data Figure 5.8a, b, and c, respectively).

Regardless of soil type, eCO₂ resulted in higher proportions of unspecific polysaccharides at the 50 – 150 mm depth ($p = 0.0336$), leading to a reduction in the plant/unspecific polysaccharides ratio ($p = 0.0301$) in this soil layer (Figure 5.5a and b, respectively). Both eCO₂ soil treatments at the 50 – 150 mm depth showed depletion in polycyclic aromatic hydrocarbons (PAH; $p = 0.0044$) and phenols ($p = 0.0313$; Extended Data Figure 5.9a and b, respectively), although their origin as plant-derived or microbial-derived carbon could not be determined, limiting their diagnostic use.

Soils in the 50 – 150 mm layer under eCO₂ exhibited depletion in various aliphatic (plant- and microbial-derived) products, such as fatty acid C₁₆ ($p = 0.0017$; Figure 5.5c), short- and long-chain alkanes including C₃₂ ($p = 0.0277$; Figure 5.5d), and C₁₃, C₁₅, C₁₈, C₂₀, C₂₂, C₂₄, C₃₁ (Extended Data Figure 5.10a to g, respectively), as well as short- and long-chain alkenes like C₁₅ ($p = 0.0004$; Figure 5.5e), C₂₅ ($p = 0.0006$; Figure 5.5f), C₁₃, C₁₄, C₁₆, C₁₇, C₁₈, C₂₁, C₂₂, C₂₄, and C₂₅ (Extended Data Figure 5.11a to i, respectively). Similarly, soils under eCO₂ at the 50 – 150 mm depth showed depletion in several N-containing products, including pyrrole ($p =$

0.0476; Figure 5.5g), benzonitrile ($p = 0.0325$; Figure 5.5h), benzene acetonitrile ($p = 0.0347$), and indole ($p = 0.0234$; Extended Data Figure 5.12a and b, respectively).

No significant interaction effect was found between eCO₂ and soil depth on any THM groups or individual products.

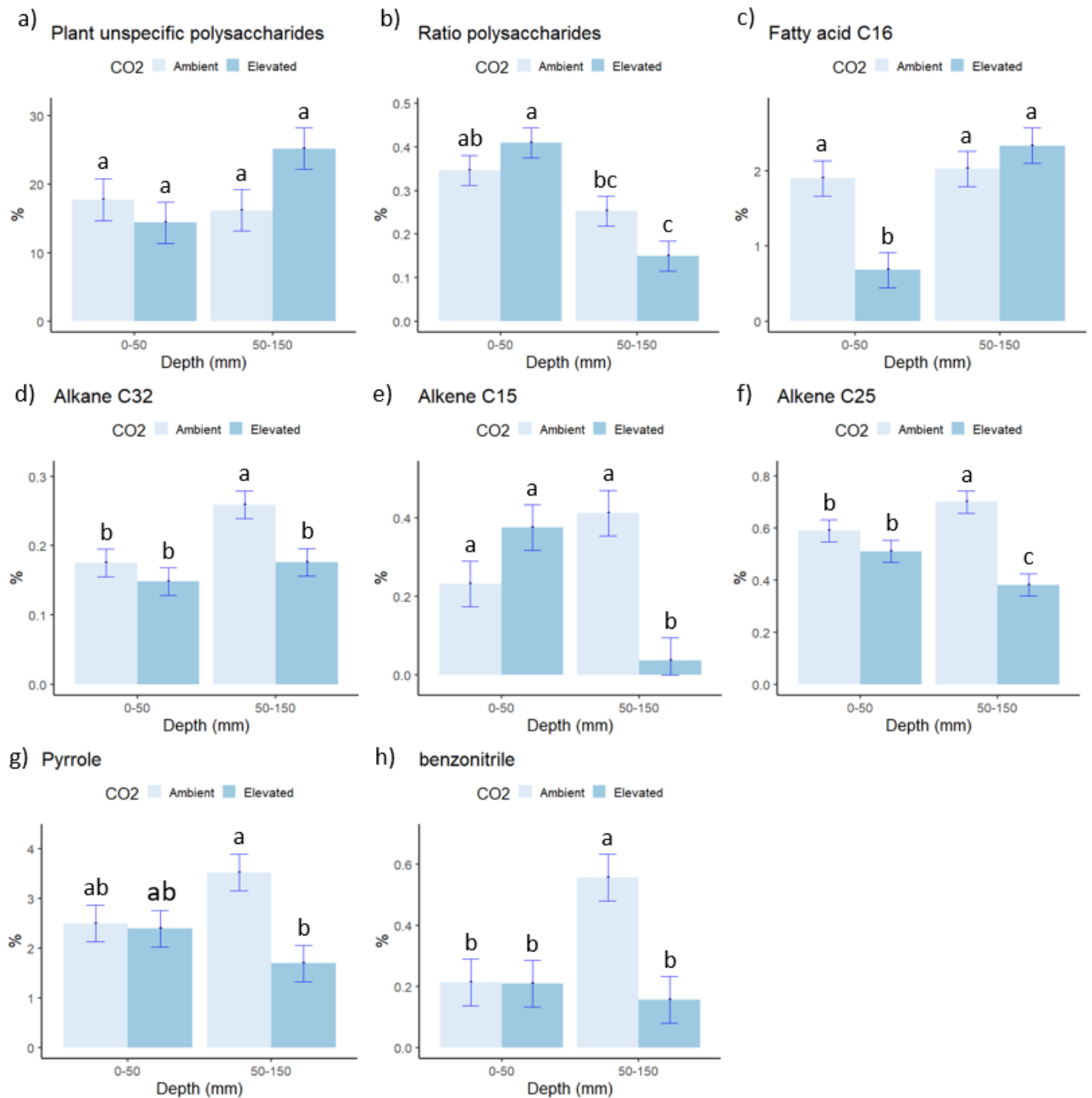


Figure 5. 5: Examples of interactive effects of elevated CO₂ and soil depth on the soil organic matter pyrolytic products (independent of soil type) from the mesocosm study sited at the NZ

Free Air CO₂ Enrichment facility legume-based grazed pasture after 15 years of exposure elevated CO₂. Error bars indicate SD (n = 3, letters indicate differences to p < 0.05).

5.4 Discussion

The present study is one of very few that has explored the effect of extended exposure (15 years) to eCO₂ on soil OC and N stocks, and its molecular composition in contrasting soils, under a permanent legume-based grazed pasture. To tease out the influence of soil attributes from other factors influencing grazed pastoral systems' response to eCO₂, were examined in a study at the same location, climate, fertiliser application and livestock management practices.

5.4.1 Understanding how inherent soil properties can explain the evolution of soil organic carbon over time under ambient concentrations of atmospheric CO₂

The well-developed structure of the Stratford soil is related to the mineralogy common to volcanic soils. The Stratford soil contains allophane and aluminium (Al) and iron (Fe) oxyhydroxides, providing the soil with a highly reactive surface (Parfitt, 1990). These short-range order constituents contribute to the unique chemical and physical properties of these soils, including a high cation exchange capacity, high anion retention, high water-holding capacity, good physical structure and a low bulk density. But most importantly, they favour the formation of short-range bonds between organic compounds and Al and Fe hydroxylated surfaces. These organic compounds are characterised by high chemical diversity molecules of highly processed OM, resulting in high protection from microbial decomposition (Matus et al., 2014). The organo-mineral complexes formed are also an integral part of the soil aggregate building

capacity, which adds to their potential to protect soil OC from the microbial community within the soil aggregates.

In sharp contrast, the Pukepuke soil is derived from sedimentary material, as it is developed on sand dunes and contains 87% of sand. Its coarse texture combined with a very small clay fraction of low reactivity (Cowie and Hall, 1965), limits the ability of this soil to protect OM from decomposers and thus, mineralization. The inherent differences are reflected in the soil OC and N contents and stocks where the Stratford soil contains larger stocks compared to the Pukepuke soil (Extended Data 4.4.1 Inherent differences in soil OC and N stocks in the two soils): Soil OC stocks in the top 150 mm of the two soil under aCO₂ conditions in 2009 were 79.7 and 57.0 t ha⁻¹ for the Stratford and the Pukepuke soils, respectively. Differences between the OC stocks of the two soils became larger in 2020 with values of 74.6 and 40.9 t ha⁻¹, respectively.

The observed sharp decline in soil OC and N over 15 years in the Pukepuke soil under aCO₂ conditions, in contrast to the small decline in the Stratford soil, can be explained by the distinct inherent soil properties, that contribute to the stabilisation and protection of OC incorporated into soil aggregates of the two soils. The Pukepuke soil with its very limited ability to build and sustain soil aggregates, would be more vulnerable to (i) the impact of soil disturbance, which would have occurred during the establishment of the mesocosms, (ii) the increased frequency of drought events and associated higher average temperatures (see Figure 5.1 and meteorological data provided by Gonzalez-Moreno in Chapter 3), which would have weakened the integrity of soil aggregates, and (iii) the reduced ability to preserve OM through mineral associations (MAOM fraction; Chapters 3 and 4) compared with the Stratford soil (Gentile, 2009, unpublished data; Li et al., 2020). Indeed, in 2009, despite both soils having larger OC stocks under aCO₂ conditions compared to values in 2020, the proportion of protected and

unprotected OC differed. The average particle size of the labile coarse particulate OM was 48.5% in the Pukepuke soil and 18.0% in the Stratford soil (Gentile, 2009; unpublished data).

Under steady-state conditions, a pasture's soil has the capacity to retain a significant amount of unprotected (labile) OC (Shen et al., 2018), which undergoes decomposition at a rate comparable to the input of new plant detritus. However, during periods of drought stress, the input of plant detritus can be compromised, leading to a depletion of the unprotected OC fraction in the soil. In contrast, the Stratford soil, with a larger fraction of protected OC through interactions with reactive surfaces (17.2% of MAOM; Gentile, 2009; unpublished data) and protection within micro-aggregates compared with the Pukepuke soil (of only 3.8% of MAOM; Chapter 3), is expected to be less susceptible to the decrease in plant detritus caused by drought and increased temperatures, at least in the short term (Chen et al., 2020; Dong et al., 2022).

5.4.2. Understanding how inherent soil properties can explain the different responses of the two soils to elevated atmospheric CO₂

After 15 years of exposure to eCO₂, the Pukepuke soil at 0 – 150 mm soil depth, had 6.5 and 0.5 t ha⁻¹ larger soil OC and N stocks, respectively, compared to the same soil under aCO₂ conditions. However, these larger stocks were not sufficient to compensate for the 28% loss in OC and 29% loss in N stocks in the Pukepuke soil that occurred over the 15 years under aCO₂ conditions. These findings indicate that the enrichment of the atmosphere with CO₂ played a beneficial role in replenishing some of the loss of OC over time. This can be attributed to the stimulation of plant growth under eCO₂, resulting in an increased input of detritus into the soil. This effect is particularly prominent in C₃ plants, which are the main component of the sward in the mesocosms (and at the NZ-FACE facility), where C₃ grasses are more efficient in fixing the higher concentration of atmospheric CO₂ compared to C₄ plants (Reich et al., 2018). Thus,

C₃ grasses are more sensitive to changes in atmospheric CO₂ concentrations with a stronger photosynthetic response to eCO₂ conditions, leading to a stronger boost in plant biomass compared to C₄ plants (Ainsworth and Long, 2005).

The enhanced plant growth led to a higher rate of OM accumulation in the Pukepuke soil under eCO₂ and contributed to partly restoring the OC and N stocks compared to aCO₂. In contrast, the Stratford soil did not exhibit a significant response to eCO₂ compared to the Pukepuke soil, as it lost very little OC over the course of the 15-year mesocosm study and hence has little capacity to store any additional OC. Potential reasons for this lack of response are discussed below.

Both mesocosms were subjected to the same fertiliser application (4.2.1 Experimental setup) and while nutrient availability was not assessed at the end of the experiment, data collected in 2006 and 2007 provided some insights (Extended Data 4.4.2 Changes in soil nutrient status, aboveground biomass, and botanical composition). These data revealed a 25% decline (yet not significant at $p < 0.05$) in resin extractable phosphate (PO₄) in the Stratford soil under eCO₂, during the early years of the experiment, and this decline was more pronounced than with the Pukepuke soil. It is worth noting that PO₄ is a vital nutrient for legume growth and N₂ fixation, and this decline in resin PO₄ may have constrained the potential increase in aboveground biomass production (Jin et al., 2015) in the Stratford soil despite the enriched CO₂ atmosphere (Gentile et al., 2012). Interestingly, the reduction in resin PO₄ levels aligns with the observed decrease in legume content of the sward (Extended Data 4.4.2 Changes in soil nutrient status, aboveground biomass, and botanical composition). This correlation is in accordance with findings by Edward et al. (2005) who found that legume grasses on soils with low PO₄ availability do not show a boost in aboveground biomass under eCO₂.

The andic properties of the Stratford soil impart, by definition, a high capacity for retaining PO_4 (Parfitt, 1990) due to the presence of large amounts of short-range order mineral constituents limits the availability of PO_4 in the soil solution. With both soils receiving the same amount of PO_4 each year, the Stratford soil, with a high PO_4 retention capacity (NSDR, 2020), compared with the Pukepuke soil which has a very low anion retention capacity likely resulted in a lower plant PO_4 availability over time. Hence 15 years of eCO_2 exposure could have led to a more limited increase in aboveground biomass in the Stratford than in the Pukepuke soil, consistent with the observations of Newton et al. (2014). Consequently, plants in the Stratford soil may have relied on priming the decomposition of native OM to compensate for their higher nutrient demand under eCO_2 conditions, as further discussed in the following section.

A potential secondary effect that could have had an impact on the OC content of the Stratford soil, regardless of the CO_2 treatment, is related to the fact that climatic conditions at its original site are very different from those at Bulls where the mesocosm study is located (Table 5.2). The mean annual rainfall at Bulls which averages 1000 mm was lower than the 1900 mm found at the site where the Stratford was sourced, which combined with a lower average temperature could have reduced the input of plant detritus to the soil compared with that occurring at the time the samples were taken in 2005.

5.4.3 Understanding how the inherent soil properties influence the quality of the organic matter under elevated atmospheric CO_2

The 16% greater soil OC stocks in Pukepuke soil (0 – 150 mm) under eCO_2 (6.5 t ha^{-1}) than under aCO_2 was paralleled by a larger proportion of plant-derived OM in the topsoil (0 – 50 mm) and microbial-derived OM in the subsoil (50 – 150 mm) compared with the same soil

under aCO₂. Considering these findings, together with the absence of a decline in PO₄ levels in the Pukepuke soil under eCO₂ conditions, we hypothesise that an atmosphere enriched in CO₂ caused an increased input of fresh OC in the soil and this accelerated OM mineralization. The above-described changes in the proportions of plant-derived and microbially processed OM under eCO₂, reflect the logically larger input of plant residues in the topsoil, and larger capacity to preserve them when microbially processed at depth. Molecular analysis of the Pukepuke soil OM revealed a modest increase in the proportion of lignin-derived products in the topsoil under eCO₂, suggesting an increased input of OC due to higher net herbage accumulation or selective preservation (Buurman et al., 2009), which mitigated the ongoing decrease in soil OC stocks observed under aCO₂. Other OM components of the Pukepuke soil, including carbohydrates, aliphatic compounds, and N-containing products, showed no significant change under eCO₂ conditions. In contrast, the soil OC stocks in the Stratford soil did not exhibit any changes under eCO₂, although the molecular composition showed a slight depletion of long-chain aliphatic products (alkanes and alkenes), possibly due to a lack of response in aboveground biomass (Buurman et al., 2007). However, it cannot be ruled out that any additional soil OC input through aboveground and/or belowground biomass was mineralized and lost through soil respiration (Kögel-Knabner, 2002; Kuzyakov et al., 2019).

Interestingly the interaction effect of eCO₂ and soil depth on the OM molecular composition of the two soils was stronger compared to the interaction effect between eCO₂ and soil type. In the topsoil there were higher proportions of 4-methyl guaiacol, 4-ethyl guaiacol, and 4-methyl syringol indicating higher proportions of intact plant-derived OC under eCO₂. The higher proportion of lignin products under eCO₂ than under aCO₂ was somewhat more evident in the Pukepuke soil compared to the Stratford soil under the same conditions (Extended Data Figure 5.15). The higher proportions of unspecific polysaccharides at 50 – 150 mm of the eCO₂ compared to the aCO₂ treatment, led to a reduction of the plant/unspecific polysaccharides

ratio, indicating that eCO₂ increased the relative contribution of microbial-derived OC to the soil at 50 – 150 mm. Again, this effect was to some degree also stronger in the eCO₂ Pukepuke soil compared to the Stratford soil under the same conditions. Furthermore, independent of soil types, eCO₂ also depleted the soil of aliphatic and N-containing products at 50 – 150 mm which is a clear indication of a relative increase of microbial-derived OC (Buurman and Roscoe, 2011). As these products (aliphatic and N-containing) tend to become enriched along the plant degradation pathways (accumulation of recalcitrant aliphatic OM and formation of microbial N-rich and aliphatic OM (Kögel-Knabner, 2002; Buurman and Roscoe, 2011), this also suggests that eCO₂ either suppressed the OM decay or accelerated the inputs from plant biomass (diluting the microbial signal), especially in the Stratford soil under eCO₂ as opposed to the Pukepuke soil under the same CO₂ conditions (Extended Data Figure 5.16a and b respectively). However, these results are less easily interpreted.

5.4.4 Exploring mesocosm effects on soil organic carbon dynamics

To overcome any potential influence of the previous history of the FACE experiment at the site on the Pukepuke soil, when placing the mesocosm, the Pukepuke soil was collected from outside the rings (thus, under aCO₂). For both soils, the Pukepuke and Stratford soils, the mesocosms were then placed in all six rings. Therefore, we provided the same experimental settings and starting point for the eCO₂ exposure to both soils. However, as indicated earlier, the climatic conditions at Stratford's original site had much higher precipitation than at the NZ-FACE facility (udic vs. xeric moisture regime; ~50% less rainfall), despite both sites being classified as warm temperate climate by Köppen and Geiger (Cfb; Climate-Data.org). Consequently, the different environmental conditions at the new site may have had impacted the cycling of the OM in the Stratford soil, potentially altering its quality and susceptibility to experimental treatments (i.e., CO₂ treatment).

A direct comparison between the findings from the mesocosm study and the Pukepuke soil in the rings is not possible due to the different durations of eCO₂ exposure. The Pukepuke in the mesocosm had been exposed to eCO₂ for only 15 years, while the Pukepuke in the rings had been exposed for 23 years. Moreover, during the process of transferring the soils into the mesocosms, it was inevitable that some level of disturbance occurred, leading to the disruption of soil structure and the breakage of soil aggregates (Extended Data 5.3.2.4 Soil organic carbon and nitrogen concentration of the Pukepuke soil from the mesocosm and ring). Consequently, this disturbance might have been the cause for a greater loss of soil OC and N stocks compared to the losses observed over time in the Pukepuke soil directly sampled from the rings. Additionally, under mesocosm conditions, there is a potential risk that the physical barrier in the soil – due to edge effects – can modify water movement, drying, oxygen diffusion and biology activity which in turn might drive changes in root growth and exploration, and thus microbial dynamics, which could have caused a different impact on the aboveground response between CO₂ treatments and, thus, on the OC and N inputs and dynamics in the soil.

Accepting no direct comparison can be made in the changes in the soil OC and N stocks in the mesocosm and rings, at first glance the lesser decline in OC and N content and stock in the Pukepuke soil in the mesocosms after 15 years of exposure to eCO₂, seems at odds with the findings on the Pukepuke soil in the rings after 23 years to eCO₂ (Chapter 3), where long-term exposure to eCO₂ did not result in larger soil OC and N stocks. Although no direct comparison can be made, a closer examination of soil OC and N contents and stocks revealed a significant decline between 2009 and 2020 (Table 5.3), with the decline appearing greater in the mesocosms than in the rings, particularly under ambient CO₂ conditions (Figure 5.3). This suggests a slower decline of soil OC and N stocks in the Pukepuke soil over the course of the mesocosm study.

Despite these limitations, the data collected from the mesocosm experiments still contributes new insights and enhances our understanding of the influence of soil mineralogy on soil OC stabilization under increasing atmospheric CO₂ concentrations in a legume-based grazed grassland soil.

5.5 Conclusion

This novel study gives new insights into the effect of long-term exposure (15 years) to eCO₂ on soil OC and N stocks and the soil OM molecular composition in soils with contrasting properties under on a legume-based grazed pasture. The findings revealed that soils with different physical and mineral properties have distinct responses not only to eCO₂ but to other stressors driving the soil OC stabilisation process (e.g., soil disturbance, climate conditions, management practices).

The Pukepuke soil, a coarse-textured soil, would appear to be less resilient (i.e., more vulnerable) to soil disturbance and extreme weather events under aCO₂ conditions, based on the significant decline in soil OC and N stocks observed over the study period. In contrast, the Stratford soil a well-developed soil, showed resilience to environmental stresses and remained relatively stable due to its ability to protect soil OC and N from microbial decomposition.

An increase in the atmospheric concentration of CO₂, compensated to a degree for the losses of soil OC and N stocks in the Pukepuke soil over the course of the study. This indicates that eCO₂ – by increasing the supply of OC through increased plant growth – mitigated the decline of soil OC and N stocks below its saturation limit (i.e., the maximum amount this soil could store and protect). The Stratford soil did not show significant changes in OC and N stocks between CO₂ treatments, though it is possible that the Stratford soil was also impacted by disturbance during the establishment of the mesocosms, the changes in climatic conditions

(especially rainfall) and along with a potential PO_4 deficiency might have masked or impaired the larger stocks expected under eCO_2 .

The differences in soil OC and N stocks were associated with variations in the molecular composition of soil OM influenced by eCO_2 , particularly evident at different soil depths. Under eCO_2 , higher proportions of intact plant-derived OC were observed in the topsoil (0 – 50 mm) of the Pukepuke soil. This suggests that in the upper soil layers under eCO_2 , there is either an increase in the input of plant-derived OC (boost in aboveground biomass) or an enhanced preservation of plant-derived OC. Conversely, in the 50 – 150 mm depth, depletion of long-chain aliphatic products was observed under eCO_2 , indicating faster mineralisation rates shifting the composition of soil OM in response to eCO_2 , with potential implications for OC stabilization pathways.

It is crucial to consider that the mesocosm conditions might have introduced new variables due to physical barriers and potential modifications of water movement and biological activity, which could affect root growth, microbial dynamics, and the aboveground response to eCO_2 . Extrapolating the findings to field conditions at the NZ-FACE facility and elsewhere requires cautious interpretation. Nevertheless, these findings highlight the contrasting responses of the Pukepuke and Stratford soils to eCO_2 and emphasize the importance of the soil's inherent properties and depth in mediating the effects of eCO_2 on soil OC and N dynamics. The study contributes to our understanding of how eCO_2 influences soil OC stocks and OM molecular composition, giving insight into the mechanisms underlying soil OC stabilization in different soil types and depths within grazed pastures in a changing climate.

Appendix II – Extended Data for Chapter 5

STATEMENT OF CONTRIBUTION DOCTORATE WITH PUBLICATIONS/MANUSCRIPTS

We, the student and the student's main supervisor, certify that all co-authors have consented to their work being included in the thesis and they have accepted the student's contribution as indicated below in the Statement of Originality.

Student name:

Name and title of
main supervisor:

In which chapter is the manuscript/published work?

What percentage of the manuscript/published work
was contributed by the student?

Describe the contribution that the student has made to the manuscript/published work:

Please select one of the following three options:

The manuscript/published work is published or in press

Please provide the full reference of the research output:

The manuscript is currently under review for publication

Please provide the name of the journal:

It is intended that the manuscript will be published, but it has not yet been submitted to a journal

Student's signature:



Main supervisor's signature:

This form should be placed at the beginning of each relevant thesis chapter.

Extended Data 5.1 Introduction

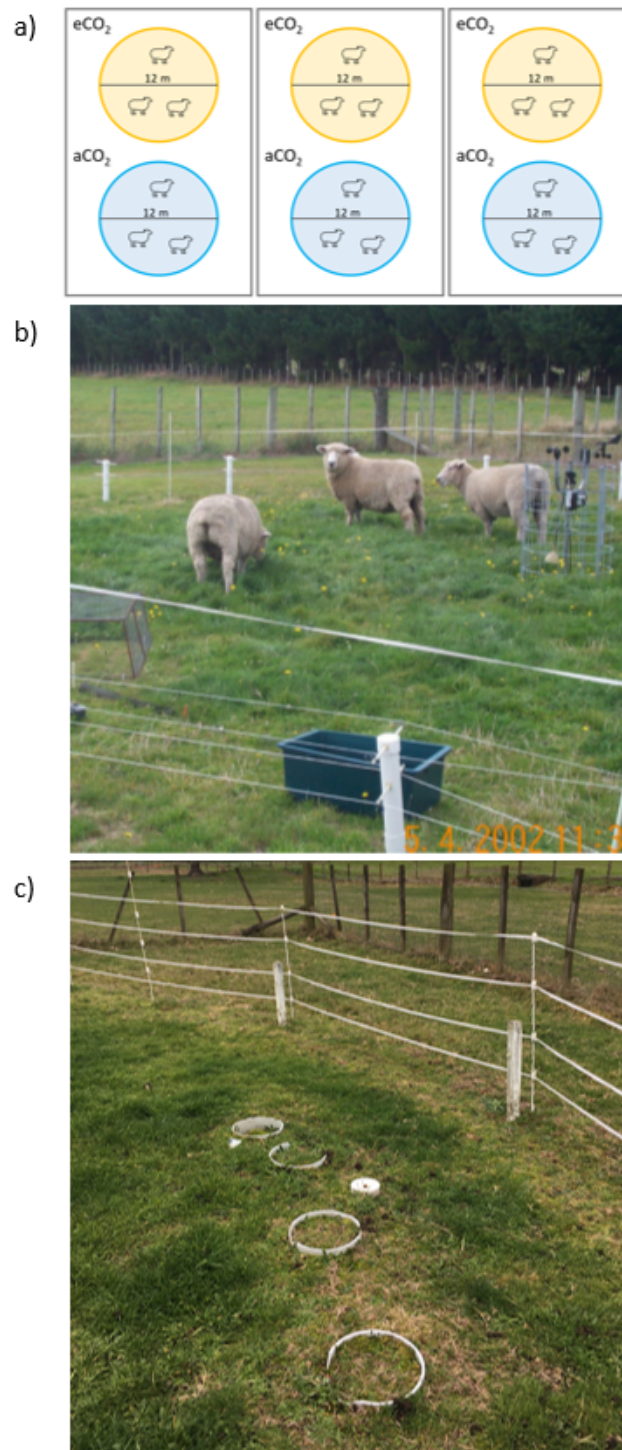
Extended Data Table 5.1: Experimental settings of grassland Free Air CO₂ Enrichment facilities worldwide.

Facility	Country	eCO ₂ (ppm)	Years of exposure	Additional treatment	MAP	MAT	Plant type	Soil type	Soil pH	References
BioCon	USA	560	5	N fertilization	660	6	16 grassland species equally divided over four functional groups (C ₄ grasses, C ₃ grasses, C ₃ legumes, C ₃ forbs)	Nutrient-poor sandy outwash plain		Dijkstra et al., 2004, 2005, 2006
Tasmania-FACE	Australia	550	6	Warming (+2°C)	560	11.6	Dominated by a perennial C ₄ grass, <i>Themeda triandra</i> Forssk and the C ₃ grasses <i>Austrodanthonia caespitosa</i> (Gaudich.) H. P. Linder, <i>Austrodanthonia carphoides</i> (Benth.) H. P. Linder and <i>Austrostipa mollis</i> (R. Br.) S. W. L. Jacobs & J. Everett.	Mixed mineralogy; black basaltic clay	neutral	Pendall et al., 2011; Hovenden et al., 2006
Guissen-FACE	Germany	+20%	6	-	580	9.4	Temperate grassland	Sandy clay loam	6.4	Guenet et al., 2012; Lenhart et al., 2016; Keidel et al., 2018

USDA-ARS (PHASE)	USA	600	6	Warming (+1.5°C)	384	10	Northern mixed-grass prairie with the warm-season C ₄ grass and the cool-season C ₃ grasses	Fine-loamy, mesic Aridic Argiustoll, mixed Ascalon and Altvan series	7	Dijkstra et al., 2011; Carrillo et al., 2011
Denmark-FACE	Denmark	510	8	-	610	8	<i>Deschampsia flexuosa</i> (L.), c. 70% cover) and an evergreen dwarf shrub (<i>Calluna vulgaris</i> (L.), c. 30% cover)	Coarse textured sandy Arenosol	5	Vestergard et al., 2016; Thaysen et al., 2017; Dietzen et al., 2019
JRGCE	USA	700	9	Warming (+1°C) and N fertilization			California annual grassland	Loam	6.5-7	Liang and Balser, 2012; Liang et al., 2015
Swiss-FACE	Switzerland	600	10	N fertilisation	1108	8.6	<i>Lolium perenne</i> L and <i>Trifolium repens</i> L	Sandy loam soil/clay loam	7.1	Six et al., 2001; van Groenigen et al., 2002; de Graaf et al., 2004; Xie et al., 2005; van Kessel et al., 2006; Theis et al., 2007
NZ-FACE	New Zealand	500	10	Grazing	870	12.9	Mix of more than 25 vascular species including C ₃ , C ₄ , forbes and legumes.	Pukepuke black sand	mildly acid	Ross et al., 2013

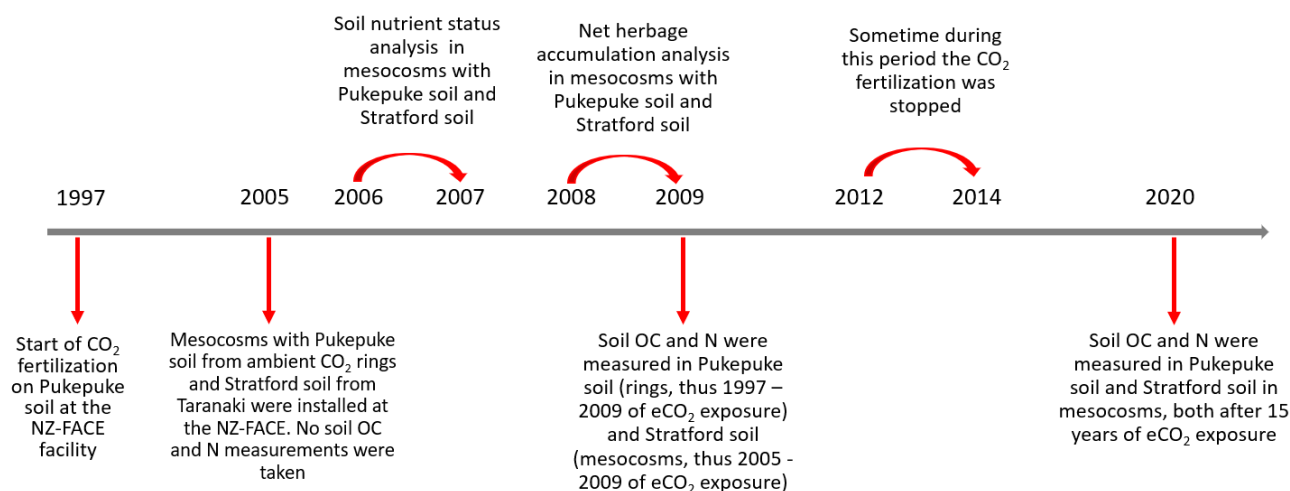
Extended Data 5.2 Methods

Extended Data 5.2.1 Experimental set up



Extended Data Figure 5.1: Pictures of the New Zealand Free Air CO₂ Enrichment facility related to a) experimental design, b) grazing dynamics and c) mesocosms with Pukepuke and Stratford soils.

Time line of mesocosm experiment at the NZ-FACE



Extended Data Figure 5.2: Timeline of mesocosm experiment at the NZ Free Air CO₂ Enrichment facility.

Extended Data 5.2.3 Soil organic matter molecular composition

Extended Data Table 5.2: List of pyrolysis-GC/MS products found in soil fractions after 22 years of exposure to elevated CO₂ at the NZ Free Air CO₂ Enrichment facility.

Retention Time	m/z	Product	group
1.474	94+96	Bromomethane	XCOMP
1.494	142+127	Iodomethane	XCOMP
1.504	60	Acetic acid	CARB
1.614	78	Benzene	MAH
1.735	79	Pyridine	NCOMP
1.735	67	Pyrrole	NCOMP
1.785	91+92	Toluene	MAH
1.815	59	Acetamide	NCOMP
1.815	84+54	(2H)-furan-3-one	CARB
1.906	95+96	3/2-furaldehyde	CARB
1.966	80+81	Methylpyrrole	NCOMP
2.026	93+66	Methylpyridine	NCOMP
2.298	110+109	5-methyl-2-furaldehyde	CARB
2.328	94+66	Phenol	PHEN
2.418	103	Benzonitrile	NCOMP
2.438	114+58	4-hydroxy-5,6-dihydro-(2H)-pyran-2-one	CARB

2.569	112	2-hydroxy-3-methyl-2-cyclopenten-1-one	CARB
2.609	113+128	Dianhydrorhamnose	CARB
2.739	107+108	4-methylphenol	PHEN
2.800	128	Methyl-4-hydroxy-5,6-dihydro-(2H)-pyran-2-one	CARB
2.830	109+124	Guaiacol	LIG G
2.930	98+68	Levoglucofenone	CARB
2.970	95	4-pyridone (T)	NCOMP
3.021	99	2,5-pyrrolidinedione (succinamide)	NCOMP
3.051	117+89	Benzene acetonitrile	NCOMP
3.061	107+122	Dimethylphenol	PHEN
3.141	107+122	4-ethylphenol	PHEN
3.292	57+69	5-hydroxymethyl-2-tetrahydrofuraldehyde-3-one	CARB
3.382	69+57	1,4:3,6-dianhydro-alpha-D-glucofuranose	CARB
3.312	128	Naphthalene	PAH
3.282	123+138	4-methylguaiacol	LIG G
3.392	120+91	4-vinylphenol	LIG H
3.412	133+134	Ethylbenzaldehyde (T)	OTHER
3.483	83+125	Unidentified compound	OTHER
3.643	79	Picolinamide (T)	NCOMP
3.663	137+152	4-ethylguaiacol	LIG G
3.774	134+119	Unidentified compound	OTHER
3.784	117+89	Indole	NCOMP
3.804	142+115	Methylnaphthalene	PAH
3.884	142+115	Methylnaphthalene	PAH
3.834	150+135	4-vinylguaiacol	LIG G
3.985	154+139	Syringol	LIG S
4.164	154	Biphenyl	PAH
4.206	130+131	Methyl-indole	NCOMP
4.256	151+152	Vanillin	LIG G
4.206	60+73	Levogalactosan	CARB
4.487	60+73	Levomannosan	CARB
4.768	60+73	Levoglucofan	CARB
4.396	168+153	4-methylsyringol	LIG S
4.416	164+149	4-(2-propenyl)guaiacol (trans)	LIG G
4.457	116	4-methylbenzoic acid	OTHER
4.517	100	Unidentified compound	OTHER
4.929	100	Unidentified compound	OTHER
4.607	94	Unidentified compound	OTHER
4.627	151+166	4-acetylguaiacol	LIG G
4.698	125+167	Trihydro-2-acetamido-2-deoxyglucose (Stankiewicz)	NCOMP
4.718	167+182	4-ethylsyringol	LIG S
4.788	137	4-(propan-2-one)guaiacol	LIG G
4.889	180	4-vinylsyringol	LIG S
5.059	166	Fluorene	PAH
5.099	121+138	Vanillic acid (T)	LIG G

5.310	182+181	Syringaldehyde	LIG S
5.421	194+179	4-(2-propenyl)guaiacol (trans)	LIG S
5.451	55+56	Prist-1-ene	MCC
5.561	186+93	Diketodipyrrole	NCOMP
5.571	181+196	4-acetylsyringol	LIG S
5.702	167+210	4-(propan-2-one) syringol	LIG S
5.863	178	Phenanthrene/anthracene (DP)	PAH
5.943	70+154	Diketopiperazine	NCOMP
6.048	70+154	Diketopiperazine	NCOMP
6.084	81+82	Phytadiene 2	MCC
6.144	74+87	Fame C ₁₆	MCC
6.375	70+194	Diketopiperazine (Cyclo(Pro-Pro))	NCOMP
6.797	74+87	Fame C ₁₈	MCC
6.877	55+69	Fatty acid C _{18:1}	MCC
6.998	97	Alkyl nitrile C ₁₈	MCC
7.470	83+280	Unidentified compound	OTHER
7.610	175+272	Unidentified compound	OTHER
9.579	151+416	Gamma-tocopherol	OTHER
9.880	165+430	Alpha-tocopherol	OTHER
7.018	59+72	Alkylamide C ₁₆	MCC
7.610	59+72	Alkylamide C ₁₈	MCC
8.665	59+72	Alkylamide C ₂₂	MCC
8.434	58+59	Methylketone C ₂₅	MCC
9.017	58+59	Methylketone C ₂₇	MCC
9.686	58+59	Methylketone C ₂₉	MCC
10.553	58+59	Methylketone C ₃₁	MCC
5.582	60+73	Fatty acid C ₁₄	MCC
5.823	60+73	Fatty acid i/a C ₁₅	MCC
5.933	60+73	Fatty acid C ₁₅	MCC
6.285	60+73	Fatty acid C ₁₆	MCC
6.917	60+73	Fatty acid C ₁₈	MCC
7.510	60+73	Fatty acid C ₂₀	MCC
8.072	60+73	Fatty acid C ₂₂	MCC
3.674	57+71	Alkane C ₁₃	MCC
4.115	57+71	Alkane C ₁₄	MCC
4.537	57+71	Alkane C ₁₅	MCC
4.939	57+71	Alkane C ₁₆	MCC
5.321	57+71	Alkane C ₁₇	MCC
5.692	57+71	Alkane C ₁₈	MCC
6.044	57+71	Alkane C ₁₉	MCC
6.375	57+71	Alkane C ₂₀	MCC
6.696	57+71	Alkane C ₂₁	MCC
7.008	57+71	Alkane C ₂₂	MCC
7.299	57+71	Alkane C ₂₃	MCC
7.580	57+71	Alkane C ₂₄	MCC
7.851	57+71	Alkane C ₂₅	MCC

8.113	57+71	Alkane C ₂₆	MCC
8.374	57+71	Alkane C ₂₇	MCC
8.635	57+71	Alkane C ₂₈	MCC
8.929	57+71	Alkane C ₂₉	MCC
9.227	57+71	Alkane C ₃₀	MCC
9.569	57+71	Alkane C ₃₁	MCC
9.940	57+71	Alkane C ₃₂	MCC
10.372	57+71	Alkane C ₃₃	MCC
3.643	55+69	Alkene C ₁₃	MCC
4.085	55+69	Alkene C ₁₄	MCC
4.507	55+69	Alkene C ₁₅	MCC
4.909	55+69	Alkene C ₁₆	MCC
5.300	55+69	Alkene C ₁₇	MCC
5.672	55+69	Alkene C ₁₈	MCC
6.024	55+69	Alkene C ₁₉	MCC
6.355	55+69	Alkene C ₂₀	MCC
6.676	55+69	Alkene C ₂₁	MCC
6.988	55+69	Alkene C ₂₂	MCC
7.289	55+69	Alkene C ₂₃	MCC
7.570	55+69	Alkene C ₂₄	MCC
7.851	55+69	Alkene C ₂₅	MCC
8.103	55+69	Alkene C ₂₆	MCC
8.384	55+69	Alkene C ₂₇	MCC
8.675	55+69	Alkene C ₂₈	MCC
8.959	55+69	Alkene C ₂₉	MCC
9.217	55+69	Alkene C ₃₀	MCC
9.589	55+69	Alkene C ₃₁	MCC

Extended Data Table 5.3: List of thermally assisted hydrolysis and methylation (THM-GC/MS) products found in soil fractions after 22 years of exposure to elevated I at the NZ Free AICO₂ Enrichment facility.

RT	m/z	THM product	group
6.955	74+87	C ₁₄ FAME	sFAME
7.146	74+87	iso/anteiso C ₁₅ FAME	sFAME
7.226	74+87	C ₁₅ FAME	sFAME
7.506	74+87	C ₁₆ FAME	sFAME
8.020	74+87	C ₁₈ FAME	sFAME
8.484	74+87	C ₂₀ FAME	IFAME
8.924	74+87	C ₂₂ FAME	IFAME
9.376	74+87	C ₂₄ FAME	IFAME
9.898	74+87	C ₂₆ FAME	IFAME
10.571	74+87	C ₂₈ FAME	IFAME

11.374	74+87	C ₃₀ FAME	IFAME
8.090	55+74	Omega-methoxy C ₁₆ FAME	oFAME
9.456	55+74	Omega-methoxy C ₂₂ FAME	oFAME
9.998	55+74	Omega-methoxy C ₂₄ FAME	oFAME
10.671	55+74	Omega-methoxy C ₂₆ FAME	oFAME
11.545	55+74	Omega-methoxy C ₂₈ FAME	oFAME
5.609	98	Unidentified proline product	NCOMP
6.724	98	Unidentified proline product	NCOMP
7.076	98	Unidentified proline product	NCOMP
8.331	98	C ₁₆ DAME (tr)	IDAME
9.245	98	C ₂₀ DAME (tr)	IDAME
9.747	98	C ₂₂ DAME	IDAME
10.350	98	C ₂₄ DAME	IDAME
11.123	98	C ₂₆ DAME	IDAME
5.268	129	C ₆ metasaccharinic acid ME	CARB
5.368	129	C ₆ metasaccharinic acid ME	CARB
6.021	129	C ₆ metasaccharinic acid ME	CARB
6.152	129	C ₆ metasaccharinic acid ME	CARB
6.242	129	C ₆ metasaccharinic acid ME	CARB
5.188	135+136	4-methoxybenzaldehyde (P4)	1MB
5.770	135+166	4-methoxybenzoic acid ME (P6)	1MB
5.760	144+145	Dimethyl-indole	NCOMP
5.720	153+168	1,2,3-trimethoxybenzene (S1)	3MB
5.810	101+127	Unidentified carbohydrate	CARB
5.861	88	Trimethyl-levoglucosan	CARB
5.820	171 (58, 114)	1,3,5-trimethyl-2,4,6-trione-1,3,5-triazine (TMAH)	OTHER
5.911	168+139	1,3,5-trimethoxybenzene	MB 135
6.011	121	4-methoxybenzeneacetic acid ME (P24)	1MB
6.021	55+69	Unidentified MCC	non-FAME MCC
6.102	118+161	Unidentified N compound	NCOMP
6.111	163	Benzene dicarboxylic acid ME	BCA
6.321	163	Benzene dicarboxylic acid ME	BCA
6.182	115+175	C ₅ metasaccharinic acid ME	CARB
6.212	166+165	3,4-dimethoxybenzaldehyde (G4)	2MB
6.403	55+59	Azelaic acid ME (C ₉ DAME)	sDAME
6.453	158+159	Trimethyl-indole	NCOMP
6.523	165+180	3,4-dimethoxyacetophenone (G5)	2MB
6.383	151+182	Vanillic acid ME	2MB
6.594	196+165	3,4-dimethoxybenzoic acid ME (G6)	2MB
6.704	151+210	3,4-dimethoxybenzeneacetic acid ME (G24)	2MB
6.754	194+179	2-(3,4-dimethoxyphenyl)-1-methoxyethylene (G7,G8) (DP)	2MB
6.835	69+111	Unidentified product	OTHER
6.895	161+192	Trans 1-propenoic acid-4-methoxybenzene ME (P18)	MB cinn

6.895	195+210	3,4,5-trimethoxyacetophenone (S5)	3MB
6.995	226+211	3,4,5-trimethoxybenzoic acid ME (S6)	3MB
7.076	148+186	Unidentified product	OTHER
7.166	209+224	1-(3,4,5-trimethoxyphenyl)-2-methoxyethylene (S7,S8)	3MB
7.216	181	1-(3,4-dimethoxyphenyl)-1,2,3-trimethoxypropane (G14,G15)	2MB
7.468	222+191	Trans-3-(3,4-dimethoxyphenyl)-3-propenoate (G18)	MB cinn
7.538	211	1-(3,4,5-trimethoxyphenyl)-1,2,3- trimethoxypropane (S14,S15)	3MB
7.980	241+256	Unidentified product	OTHER
8.401	71+95	10,16-dimethoxy C ₁₆ FAME	midsub FAME
8.562	169+201	Unidentified mid-chain substituted FAME	midsub FAME
8.622	187+201	8,16-dimethoxy C ₁₆ FAME	midsub FAME
8.813	87+155	Unidentified mid-chain substituted FAME	midsub FAME
9.035	71+81	9,10,18-trimethoxy C ₁₈ FAME	midsub FAME
9.245	71+81	Unidentified mid-chain substituted FAME	midsub FAME
9.637	83+97	Methoxy-alkane	non-FAME MCC
10.942	83+97	Methoxy-alkane	non-FAME MCC
9.697	73+86	N-methyl-C _{xx} -alkylamide	non-FAME MCC
9.772	87+100	N,N-dimethyl-C _{xx} -alkylamide	non-FAME MCC
10.440	179+444	Alpha-tocopherol (methylated)	OTHER

Extended Data Table 5.4: Main soil organic matter pyrolytic products (Py-GC-MS) clustered by chemical similarity, and their predominant source of origin found at the NZ FreIr CO₂ Enrichment.

Product	The potential source of origin
Methylene chain compounds (MCC)	Compounds with a long-chain chain aliphatic backbone (alkanes, alkenes, fatty acids, etc.). Derived from microbial and plant-derived molecules (cutin, suberin, epicuticular waxes, etc.).
Carbohydrate products	A chemically diverse group, including acetic acid, furans, furaldehydes, cyclopentenones, pyrans and anhydrosugars. Largely derived from structural polysaccharides in plants (e.g., cellulose, hemicellulose, starch) and microbial polysaccharides (chitin, peptidoglycan).
N-containing products	Compounds with at least one atom of N, including pyrroles, pyridines, acetamidogugars, cyanobenzenes, indoles and diketopiperazines. Derived mainly from macromolecules of protein (of plant and microbial origin), chitin (from fungi and arthropods) and peptidoglycan (bacterial OM). Acetamide, succinimide, acetamidogugars are used as markers of chitin.
Lignin	The products of lignin (4-vinylphenol, guaiacols, syringols) indicate vascular plant-derived OM. These products are useful as markers of plant-derived OM and their balance can provide indications of lignin source (e.g., herbaceous vs. woody).
Other phenols	Other phenols are products of microbial OM, lignin and other sources, and therefore of little diagnostic value.
Halogen-containing	Two compounds containing halogens, i.e., bromomethane and iodomethane, were included in the analysis due to quite large peaks in some samples. We associate this with the small distance from the FACE to the coastline.
Monocyclicaromatic hydrocarbons (MAH)	Compounds such as benzene, toluene and xylenes are not indicative of a specific source. Given that toluene prevails in most samples suggests most of the MAH signal corresponds to microbial OM.
Polycyclic aromatic hydrocarbons (PAH)	The PAHs can be pyrogenic, but at low levels (< 1 %, which is the case here), the presence of such OM cannot be ascertained because secondary reactions of uncharred OM and resinous moieties can also yield PAHs.
Others	Benzaldehydes, tocopherols and unidentified products.

Extended Data Table 5.5: Main soil organic matter thermally assisted hydrolysis and methylation (THM-GC-MS) products clustered by chemical similarity and the predominant source of origin found on soil samples at the NZ Free Air CO₂ Enrichment.

Products	The potential source of origin
Short-chain FAME (sFAME)	Aliphatic, short chain (< C ₂₀) length fatty acid methyl ester (sFAME) are probably mostly bacterial in origin, possible products of any OM precursor. They include a branched C ₁₅ FAME (iso/anteiso configuration) which is probably mostly bacterial, whereas the other short FAMES are possible products of any OM precursor.
Long-chain FAME (IFAME)	Aliphatic, long chain (≥ C ₂₀) fatty acid methyl esters (IFAME), mostly from plant-derived aliphatic macromolecules (cutin and suberin) and epicuticular waxes.
ω-methoxy-FAME	ω-methoxy-FAMES (oFAMES), usually ascribed to cutin and suberin.
Short-chain DAME (sDAME)	Mainly azelaic acid (dimethyl ester), from fragmented unsaturated C ₁₈ fatty acids (e.g., oleic acid).
Long-chain DAME (IDAME)	Long-chain (> C ₂₀) methylated fatty diacids are key products of suberin and are thus associated with bark and root-derived materials.
Other MCC	Other methylene chain compounds include <i>N</i> -methyl-alkylamides and <i>N,N</i> -dimethylalkylamides, two methoxyalkanes and an unidentified compound (alkene or unsaturated FAMES).
N-containing	Include proline derivatives, alkylindoles and a phthalimide. Mostly of microbial origin. As the TMAH reagent contains N and hydrolysis of microbial OM under THM conditions is poor, these compounds are to be interpreted with caution.
Carbohydrate products	The carbohydrate products, e.g., C ₅ and C ₆ methylated metasaccharinic acids and trimethyllevoglucosan. Underestimation of polysaccharides due to poor hydrolysis.
1MB	Monomethoxy benzenes are, in this case, mainly lignin-derived (compounds P4, P6 and P24 in lignin nomenclature).
2MB	1,2-dimethoxybenzenes are probably mostly derived from guaiacyl structures in lignin (plant-derived).
3MB	1,2,3-trimethoxybenzenes may originate from syringyl moieties in lignin and pyrogallol moieties in tannin (plant-derived).

MB135	1,3,5-trimethoxybenzenes. May originate from cutan and condensed tannin (plant-derived).
MBcinn	“Cinnamyl type” methoxybenzenes (THM products of <i>p</i> -coumaric, ferulic and caffeic acid) are often associated with lignin and lignin-like phenolics in herbaceous litter but suberin (aliphatic macromolecule) also contains a phenolic domain that can yield these THM products
BCA	Methylated benzene carboxylic acids are not diagnostic of any specific source. They are likely THM products of lignin or degraded lignin, but other sources may contribute.
Mid-chain methoxy-FAME	C ₁₆ and C ₁₈ FAMEs with methoxy substitution at the C ₉ and/or C ₁₀ , and terminal (C ₁₆ /C ₁₈) positions. Key products of cutin and suberin. The proportions of mid-chain methoxy-FAMEs and long DAMEs provide information on the balance between cutin from plant cuticles and suberin from barks and roots.
Other	Other compounds include α -tocopherol and two unidentified products.

Extended Data 5.3 Results

Extended Data 5.3.1 Soil organic carbon and nitrogen stocks

Extended Data 5.3.1.1 Differences in soil organic carbon and nitrogen stocks under ambient CO₂ over time

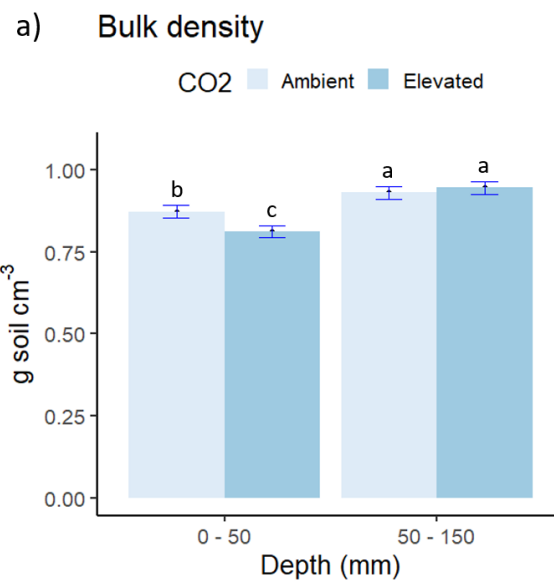
Extended Data Table 5.6: Differences in soil organic carbon (OC) and nitrogen (N) content under ambient CO₂ condition between 2009 and 2020 at the NZ Free Air CO₂ Enrichment facility.

Soil	Depth (mm)	Ambient CO ₂					
		OC content (%)			N content (%)		
		2009	2020	ΔC (%)	2009	2020	ΔN (%)
Pukepuke							
	0 – 50	44.9	33.1	-26	4.1	3.0	-28
	50 – 150	30.0	25.3	-16	2.9	2.4	-19
Profile	0 – 150	74.9	58.4	-22	7.1	5.4	-24
Stratford							
	0 – 50	61.9	56.6	-55	7.5	6.3	-15
	50 – 150	49.1	48.1	-5	5.7	5.5	-5
Profile	0 – 150	111.0	104.7	-33	13.2	11.8	-11

Extended Data Table 5.7: Soil attributes of Pukepuke and Stratford soils from the NZ Free Air CO₂ Enrichment facility (2020) at two soil depths under ambient and elevated CO₂. Soil organic carbon (OC) and nitrogen (N) stocks were calculated based on ESM method. Values are given with SD (n = 3).

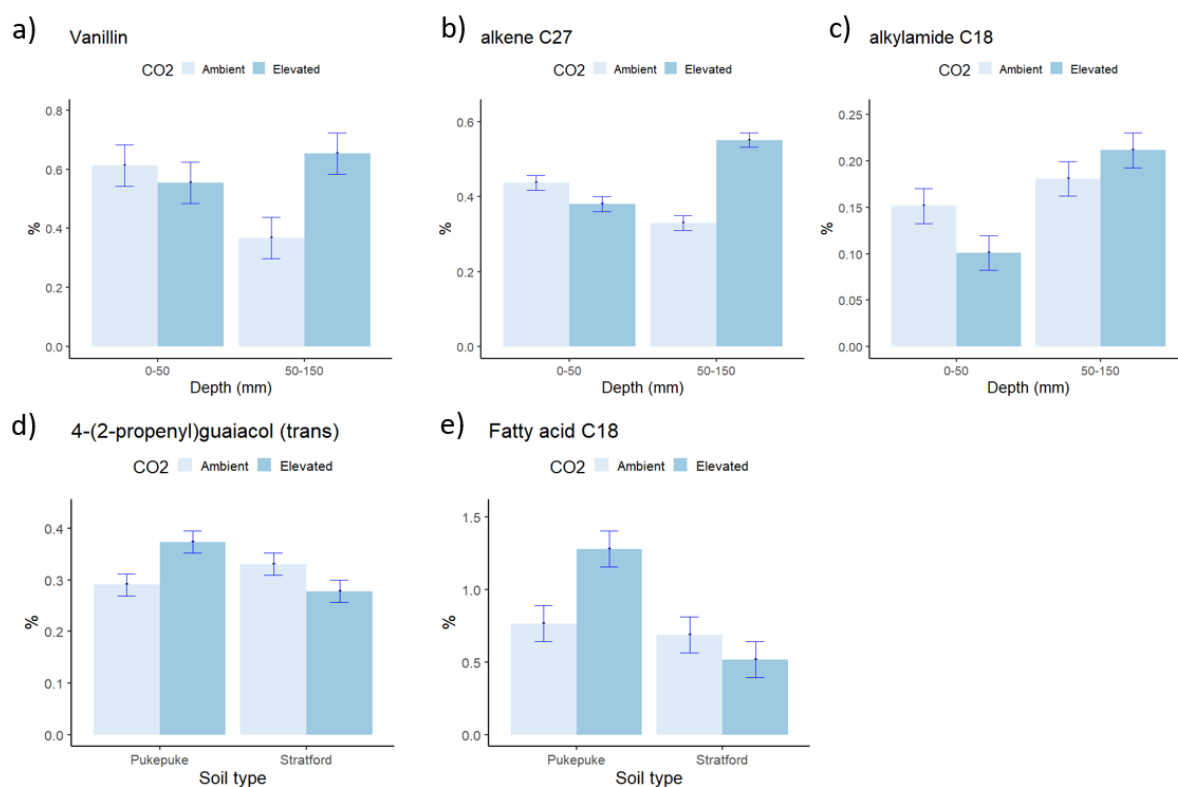
Depth (mm)	Soil	CO ₂	Bulk density (g cm ⁻³)	OC content (g kg soil ⁻¹)	N content (mg kg soil ⁻¹)	C:N	OC stock (t ha ⁻¹)	N stock (t ha ⁻¹)	
0 – 50	Pukepuke	Ambient	1.0 ± 0.0	33.1 ± 1.9	3.0 ± 0.2	11.1 ± 0.1	16.2 ± 1.0	1.5 ± 0.1	
		Elevated	0.9 ± 0.1	38.6 ± 1.3	3.4 ± 0.1	11.3 ± 0.1	18.7 ± 1.4	1.7 ± 0.2	
	Stratford	Ambient	0.7 ± 0.0	56.6 ± 2.4	6.3 ± 0.2	9.0 ± 0.1	27.8 ± 1.0	3.1 ± 0.1	
		Elevated	0.7 ± 0.1	57.1 ± 2.4	6.2 ± 0.3	9.2 ± 0.1	27.9 ± 1.0	3.1 ± 0.1	
	50 – 150	Pukepuke	Ambient	1.0 ± 0.1	25.3 ± 2.1	2.4 ± 0.2	10.6 ± 0.1	24.7 ± 2.5	2.3 ± 0.2
			Elevated	1.0 ± 0.1	29.0 ± 1.6	2.7 ± 0.1	10.9 ± 0.1	28.7 ± 3.8	2.6 ± 0.4
Stratford		Ambient	0.8 ± 0.0	48.1 ± 0.9	5.5 ± 0.1	8.8 ± 0.1	46.8 ± 1.4	5.3 ± 0.1	
		Elevated	0.8 ± 0.0	49.6 ± 1.8	5.5 ± 0.2	9.0 ± 0.1	48.3 ± 1.6	5.4 ± 0.1	
0 – 150		Pukepuke	Ambient	1.0 ± 0.0	58.4 ± 2.0	2.7 ± 0.2	10.9 ± 0.1	40.9 ± 3.4	3.8 ± 0.3
			Elevated	0.9 ± 0.1	67.6 ± 1.4	3.0 ± 0.1	11.1 ± 0.1	47.4 ± 5.2	4.3 ± 0.5
	Stratford	Ambient	0.8 ± 0.0	104.7 ± 0.8	5.9 ± 0.1	8.9 ± 0.0	74.6 ± 0.6	8.4 ± 0.1	
		Elevated	0.7 ± 0.0	106.7 ± 2.0	5.9 ± 0.2	9.1 ± 0.1	76.2 ± 2.6	8.4 ± 0.3	

Extended Data 5.3.1.2 The interactive effect between elevated CO₂ and soil depth on soil OC and N stocks

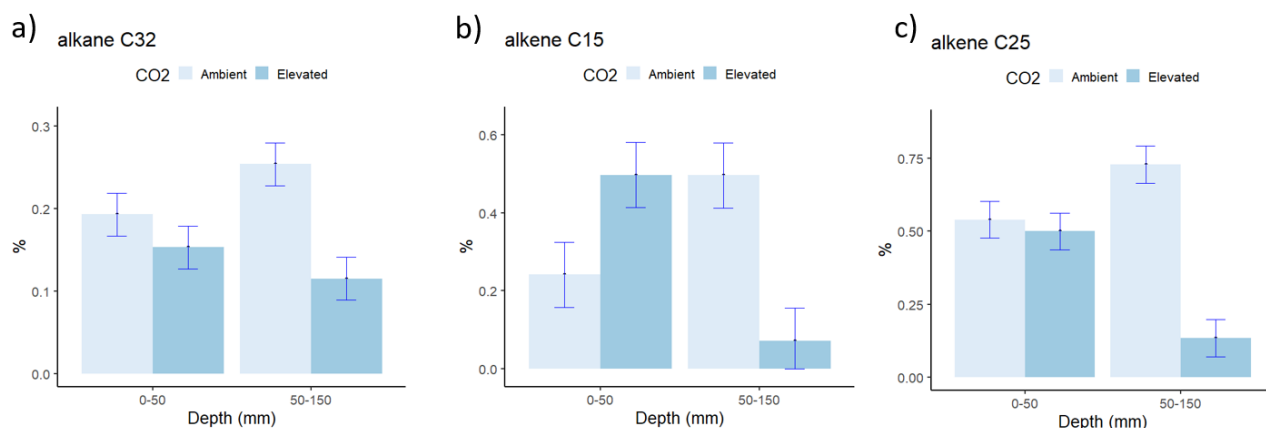


Extended Data Figure 5.3: Interactive effect between elevated CO₂ and soil depth independent on soil type after 15 years of elevated CO₂ exposure to soils in mesocosms at the NZ Free Air CO₂ Enrichment facility on bulk density.

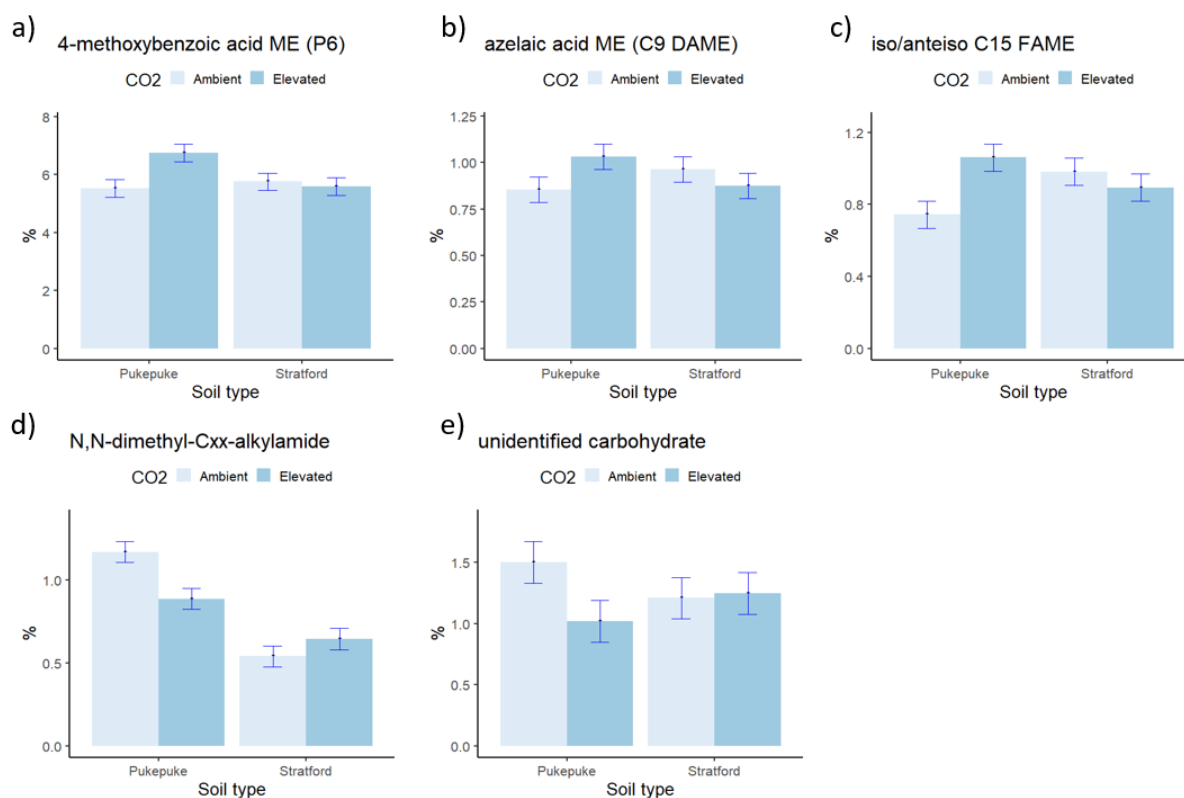
Extended Data 5.3.2.3 Interactive effect of elevated CO₂ and soil type on soil organic matter molecular composition



Extended Data Figure 5.4: Effect of elevated CO₂ on the pyrolytic products in the Pukepuke soil at the NZ Free Air CO₂ Enrichment on a) vanillin, b) alkene C₂₇, c) alkylamide C₁₈, d) 4-(2-propenyl)guaiacol (trans) and e) fatty acid C₁₈.

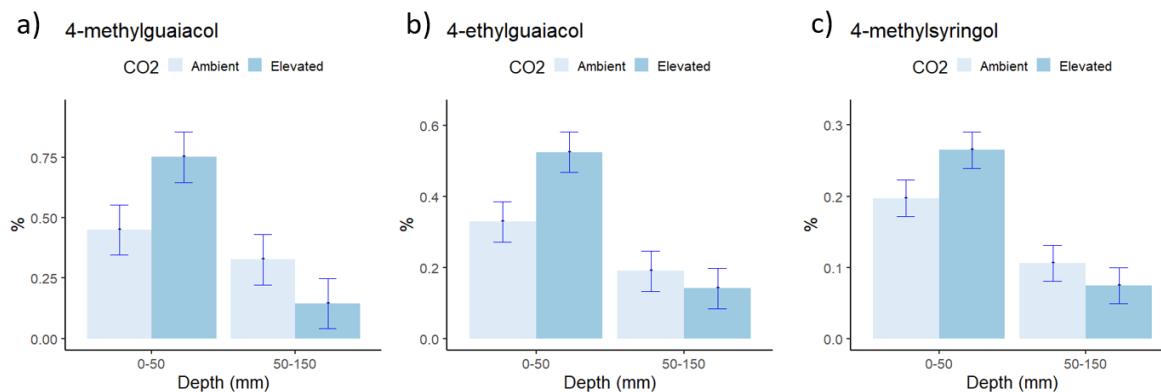


Extended Data Figure 5.5: Effect of elevated CO₂ on the pyrolytic products at the NZ Free Air CO₂ Enrichment in the Stratford soil of a) alkane C₃₂, b) alkene C₁₅ and c) alkene C₂₅.

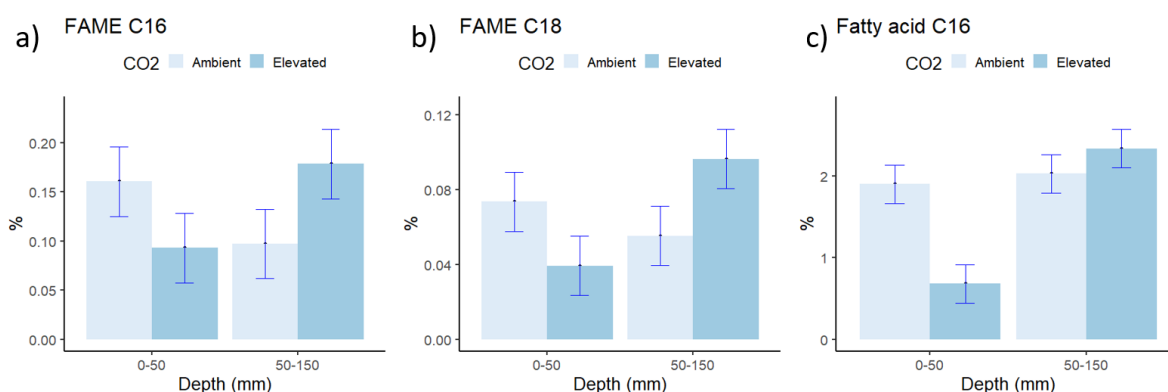


Extended Data Figure 5.6: Interactive effect of elevated CO₂ and soil type at the NZ Free Air CO₂ Enrichment on the thermally assisted hydrolysis and methylation (THM-GC-MS) products a) 4-methoxybenzoic acid ME (P6), b) azelaic acid ME (C₉ dimethyl ester (DAME)), c) iso/anteiso C₁₅ fatty acid methyl ester (FAME), d) N,N-dimethyl-Cxx-alkylamide, e) unidentified carbohydrate

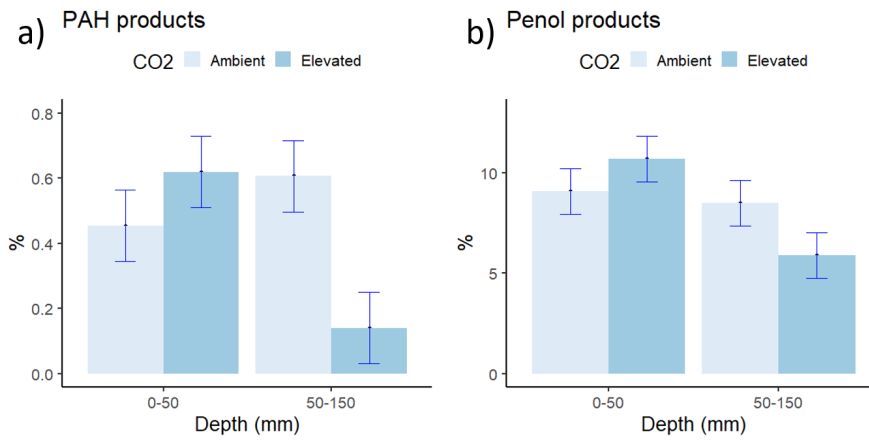
Extended Data 5.3.3.4 The interactive effect of elevated CO₂ and soil depth on the molecular composition of soil organic matter



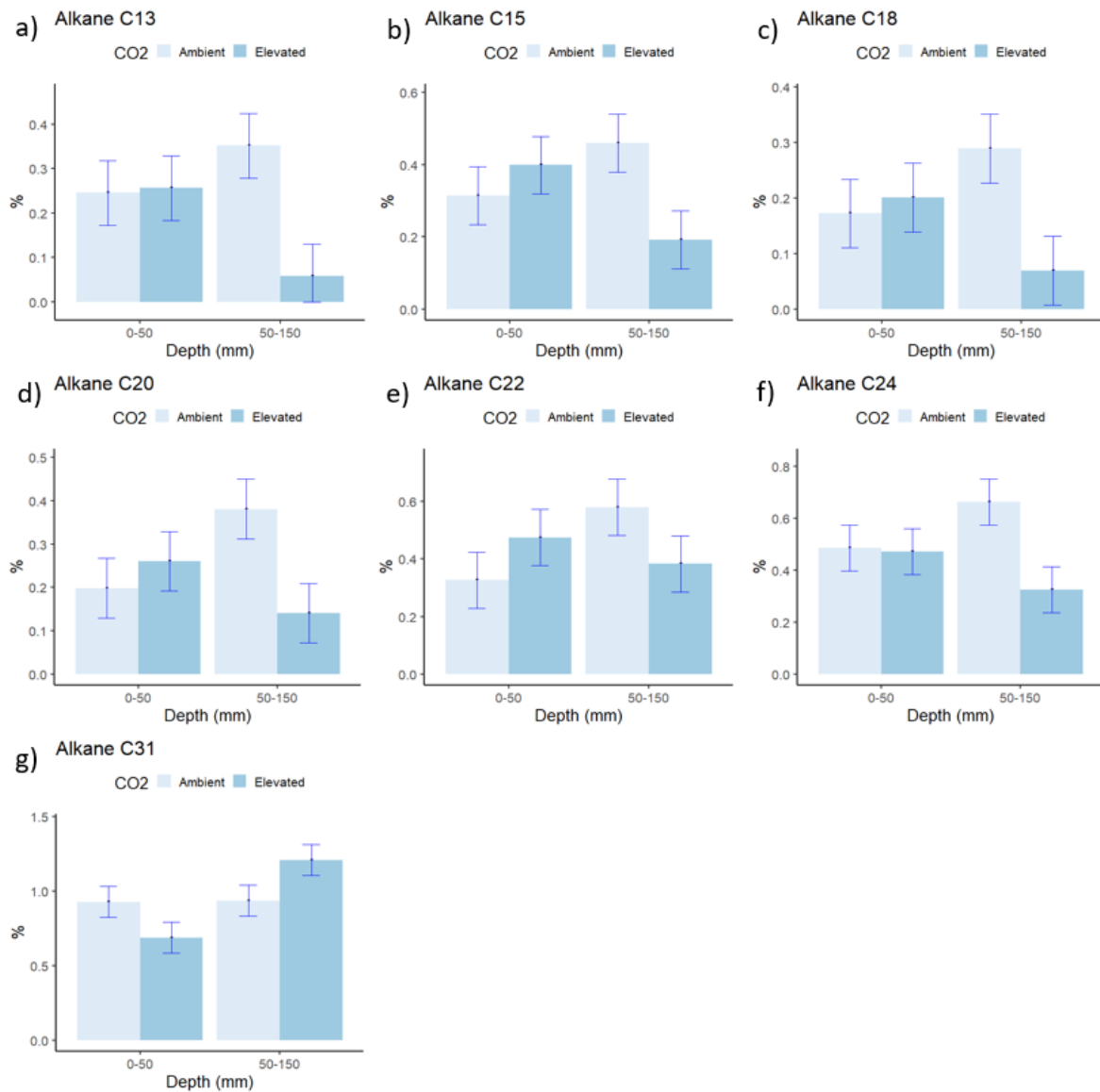
Extended Data Figure 5.7: Interactive effect between elevated CO₂ and soil depth found on soil samples at the NZ Free Air CO₂ Enrichment facility after 15 years of elevated CO₂ exposure on a) 4-methyl guaiacol, b) 4-ethyl guaiacol and c) 4-methyl syringol.



Extended Data Figure 5.8: Interactive effect between elevated CO₂ and soil depth found on soil samples at the NZ Free Air CO₂ Enrichment facility after 15 years of elevated CO₂ exposure on: a) short-chain fatty acid methyl esters (FAME C₁₆) b) short-chain fatty acid methyl esters (FAME C₁₈), and c) fatty acid C₁₆.

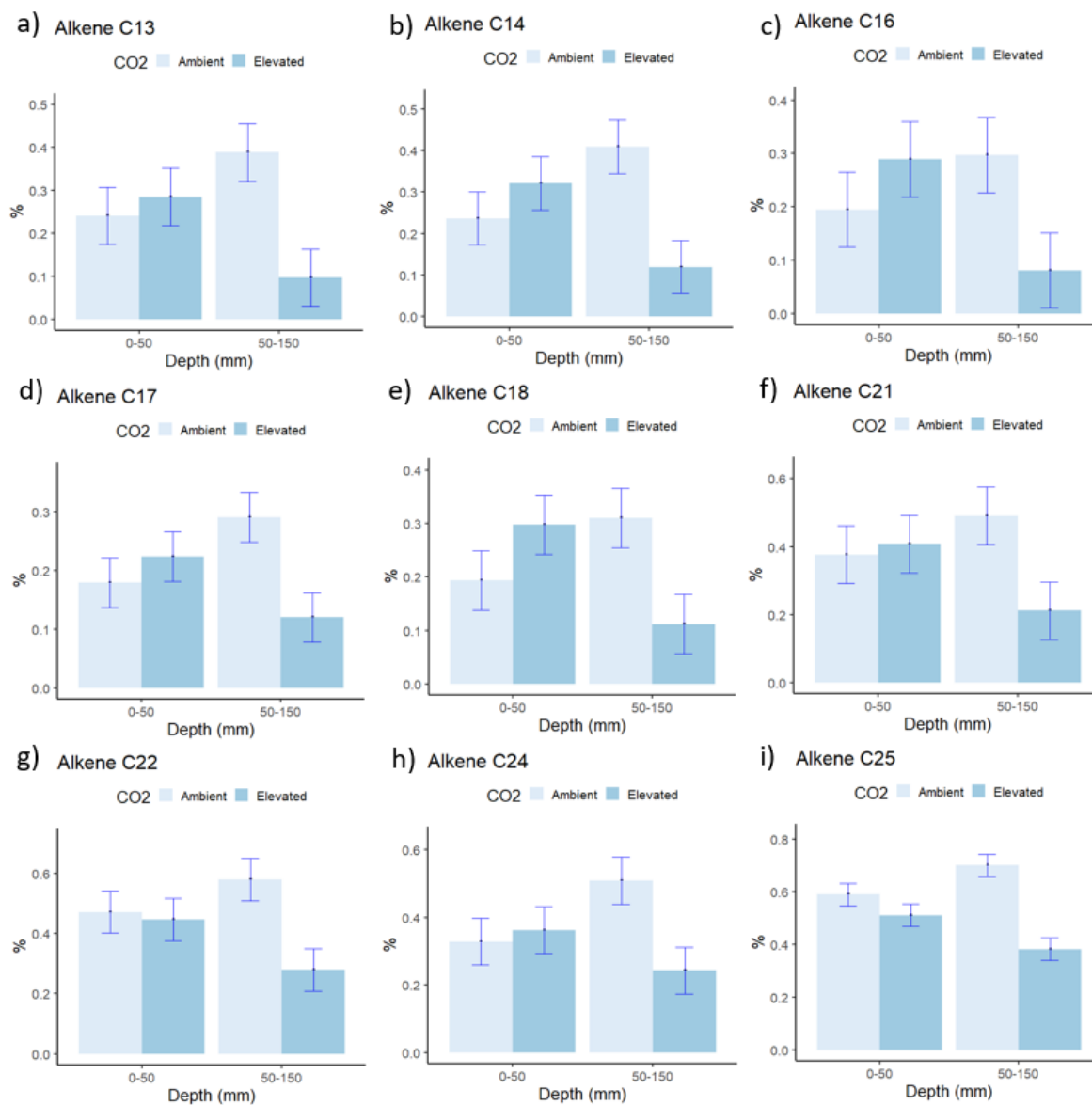


Extended Data Figure 5.9: Interactive effect between elevated CO₂ and soil depth found on soil samples at the NZ Free Air CO₂ Enrichment facility after 15 years of eCO₂ exposure on a) Polyaromatic hydrocarbons (PAH) and b) Phenol products.

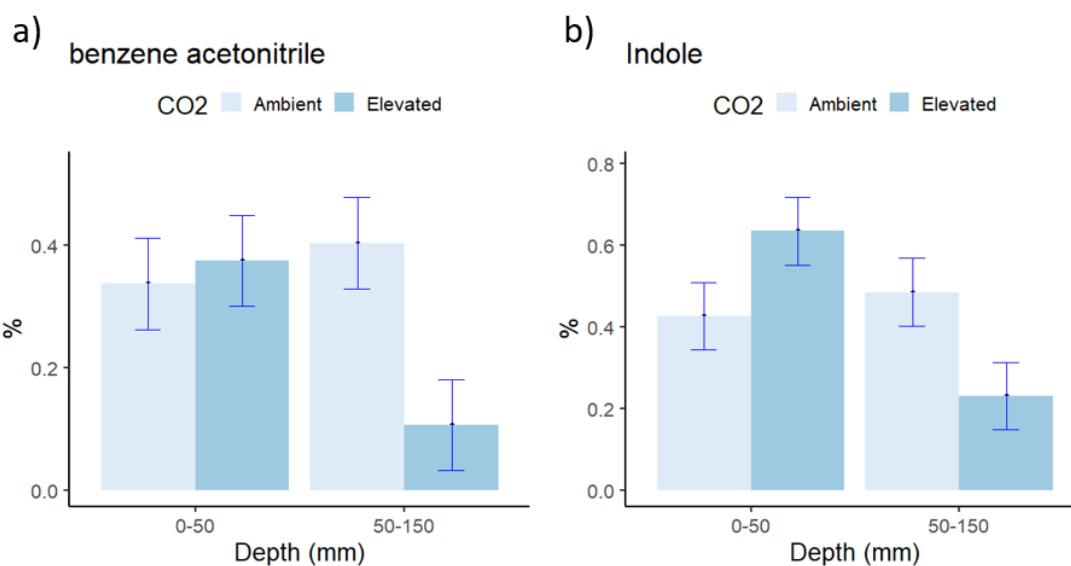


Extended Data Figure 5.10: Interactive effect between elevated CO₂ and soil depth found on soil samples at the NZ Free Air CO₂ Enrichment facility after 15 years of elevated CO₂

exposure on a) alkane C₁₃, b) alkane C₁₅, c) alkane C₁₆, d) alkane C₂₀, e) alkane C₂₂, f) alkane C₂₄ and g) alkane C₃₁.



Extended Data Figure 5.11: Interactive effect between elevated CO₂ and soil depth found on soil samples at the NZ Free Air CO₂ Enrichment facility after 15 years of elevated CO₂ exposure on a) alkene C₁₃, b) alkene C₁₄, c) alkene C₁₆, d) alkene C₁₇, e) alkene C₁₈, f) alkene C₂₁, g) alkene C₂₂, h) alkene C₂₄ and i) alkene C₂₅.



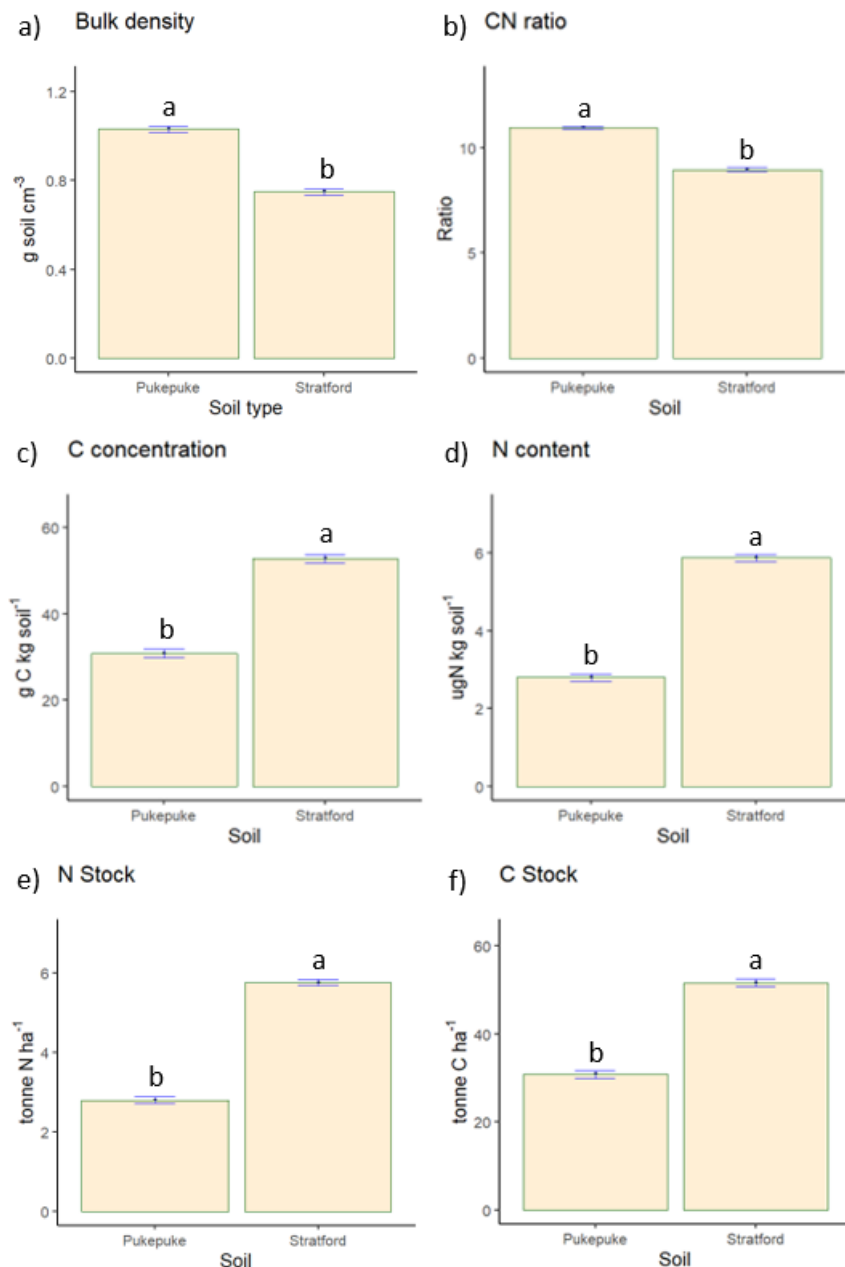
Extended Data Figure 5.12: Interactive effect between elevated CO₂ and soil depth found on soil samples at the NZ Free Air CO₂ Enrichment facility after 15 years of elevated CO₂ exposure on a) benzene acetonitrile and b) indole.

Extended Data 5.4 Discussion

Extended Data 5.4.1 Inherent differences in soil organic carbon and nitrogen stocks in the two soils

At the end of the study (2020) the Stratford soil had higher soil OC ($p < 0.0001$) and N concentration ($p < 0.0001$; Extended Data Figure 5.13c and d, respectively) and OC and N stocks (for both $p < 0.0001$) compared to the Pukepuke soil (Extended Data Figure 5.13e and f respectively). The soil bulk density was lower in the Stratford soil compared to the Pukepuke soil ($p < 0.0001$; Extended Data Figure 5.13b and a respectively). Compared with the top 0 – 50 mm soil layer, the 50 – 150 mm soil layer had a higher soil bulk density ($p < 0.0001$), as

expected. The soil OC and N concentration ($p < 0.0001$ for both) and the corresponding C:N ratios ($p = 0.0003$) decreased with depth (Extended Data Table 5.7).



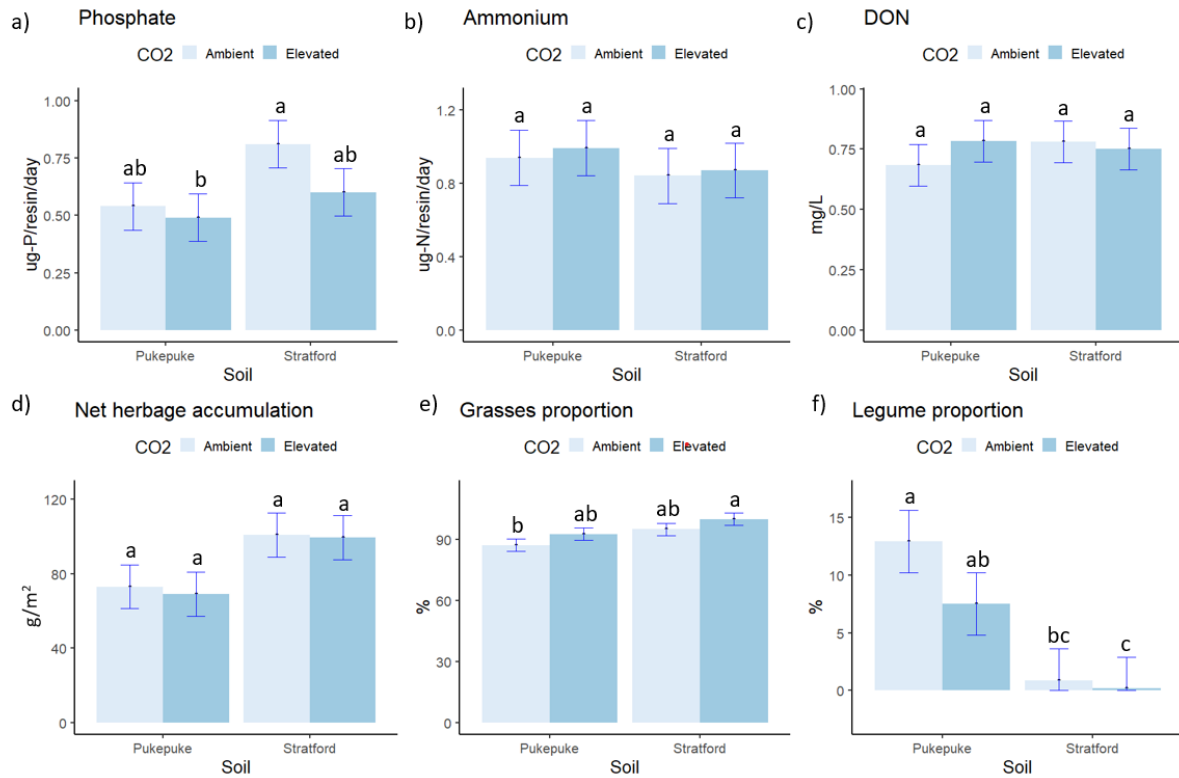
Extended Data Figure 5.13: Inherent differences between Pukepuke soil and Stratford soil from mesocosms at the NZ Free Air CO₂ Enrichment facility on soil: a) bulk density, b) C:N ratio value, c) Carbon concentration, d) Nitrogen concentration e) Nitrogen stock and f) Carbon stock.

Extended Data 5.4.2 Changes in soil nutrient status, aboveground biomass and botanical composition

One year after the start of the mesocosm study (2006 - 2007), no significant effect of eCO₂ was found on the PO₄ ($p = 0.4229$; Extended Data Figure 5.14a), NH₄ ($p = 0.8924$; Extended Data Figure 5.14b) and DON concentrations ($p = 0.03234$; Extended Data Figure 5.14c) in either the Pukepuke or Stratford soil. Nevertheless, some trends were noted including (despite lacking statistical significance), for example, the resin extractable PO₄ concentration in the Stratford soil was 25% lower under eCO₂ than aCO₂, while in the Pukepuke soil resin extractable PO₄ concentration was similar under both CO₂ treatments. Three years into the mesocosm study (2008), average net herbage accumulation (NHA, Extended Data Figure 5.14d), the proportion of grasses (Extended Data Figure 5.14e) or that of legumes (Extended Data Figure 5.14f) were not significantly affected by eCO₂. Despite the lack of statistical significance, the grass proportion under eCO₂ increased by 5% in both soils while legumes content decreased; in the Pukepuke soil from 12.9 to 7.5%, and in the Stratford soil from 0.9 to 0.2%.

During the early stages of the mesocosm experiment, the NHA did not increase under eCO₂, but there were some changes in botanical composition and in resin extractable P availability (Extended Data Figure 5.14). Interestingly the drop in legume content is consistent with the reduction measured in resin PO₄ (Extended Data Figure 5.14) measured in 2006 and 2007, a period when the pasture in rings at the NZ-FACE was not boosted under eCO₂ (Ross et al., 2013). The absence of any consistent and prolonged dry matter response by the legume-based grazed pasture to eCO₂ at the NZ-FACE probably reflects the fact that other factors, including water and N supply, other than CO₂ could have limited the potential plant response to eCO₂. Nevertheless, the differences reported on NHA in the mesocosms during 2008 might not be representatives of the overall effect of eCO₂ on NHA overtime as the pasture in rings at the NZ-FACE was not boosted under eCO₂ during this period (Ross et al., 2013). However, in

some other years as in 2005 the pasture growth has been boosted under eCO₂ with significant increases in NHA and changes in the botanical composition of the pasture (Ross et al., 2013; Newton et al., 2014).

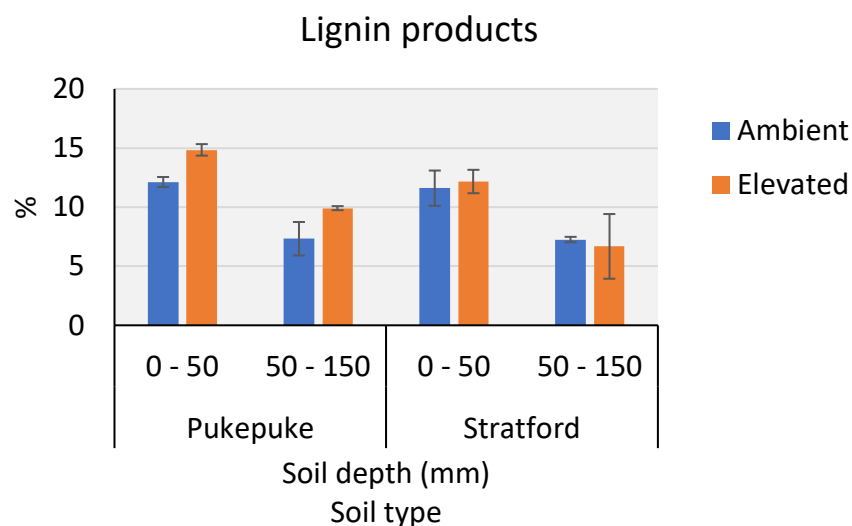


Extended Data Figure 5.14: Interactive effect of elevated CO₂ and soil type at the NZ Free Air CO₂ Enrichment legume-based grazed pasture facility on a) Resin phosphate and b) ammonium concentration in the soil solution and c) dissolved organic nitrogen (DON) during the first year of the study (2006-2007) and d) net herbage accumulation (NHA), e) grasses proportion, f) legume proportion in 2008. Error bars represent SD (n = 3).

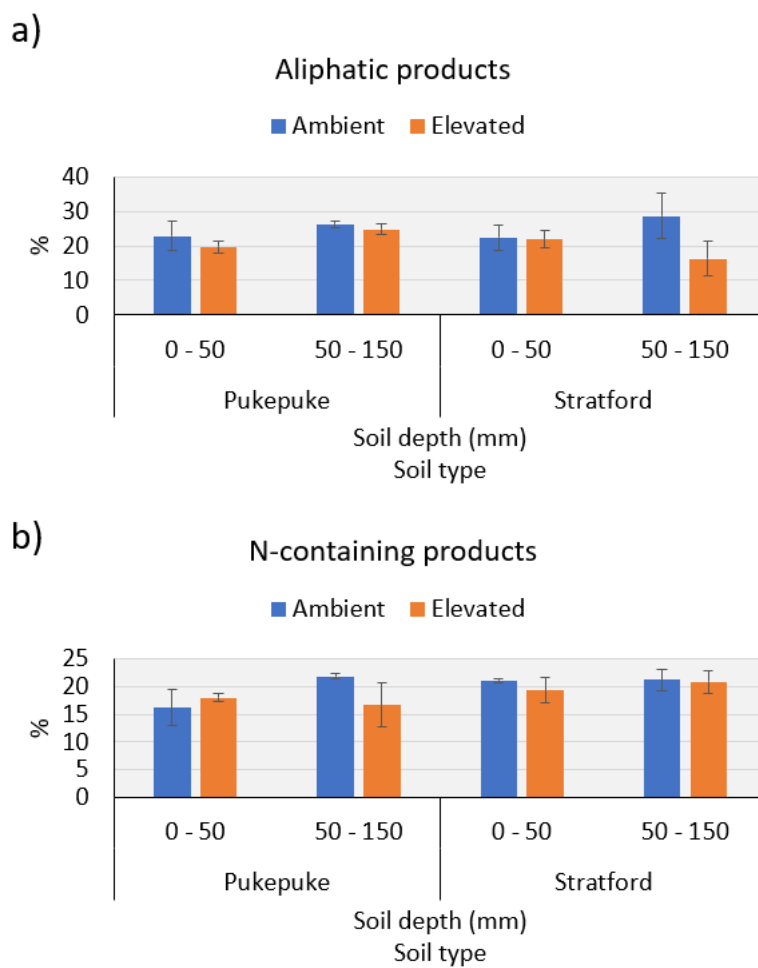
Extended Data 5.4.2.1 Nutrient status, aboveground biomass, and botanical composition analyses

Over the course of April 2006 to 2007, the concentrations of ammonium (NH₄), phosphate (PO₄) and dissolved OC (DOC) in the mesocosms of both soils were monitored (39 sampling

times), using the resin method (Newton et al., 2010), with the extracts measured by Autoanalyzer (Flow Injection Analysis on a Lachat QuikChem 8500 Analyser). Aboveground biomass was also measured from the mesocosms in May, September, October, and November 2008 – that is, in late autumn and during the whole spring in the southern hemisphere, using frames of 105 mm diameter. For this, the frames were placed on top of the soil and the grass was cut to 20 mm above the ground. A sub-sample was used to determine the amount of standing above-ground biomass that was oven dried (60 °C) until reaching a constant weight prior to weighing. Another sub-sample was used to determine the proportion of grasses and legumes of the pasture. Briefly, fresh herbage samples were separated based on the plant functional type (grasses and legumes), prior to oven drying (60 °C) to a constant weight; the weight of each plant type was determined. Even though the measures were short-term (< 2 years; unpublished data), these analyses (including the early plant-soil response to eCO₂ exposure) provide data that will assist with the overall assessment of the potential effects that eCO₂ has on soil OC and N concentrations and stocks.



Extended Data Figure 5.15: Interactive effect of elevated CO₂ and soil type at the NZ Free Air CO₂ Enrichment legume-based grazed pasture facility on soil organic matter pyrolytic lignin products.

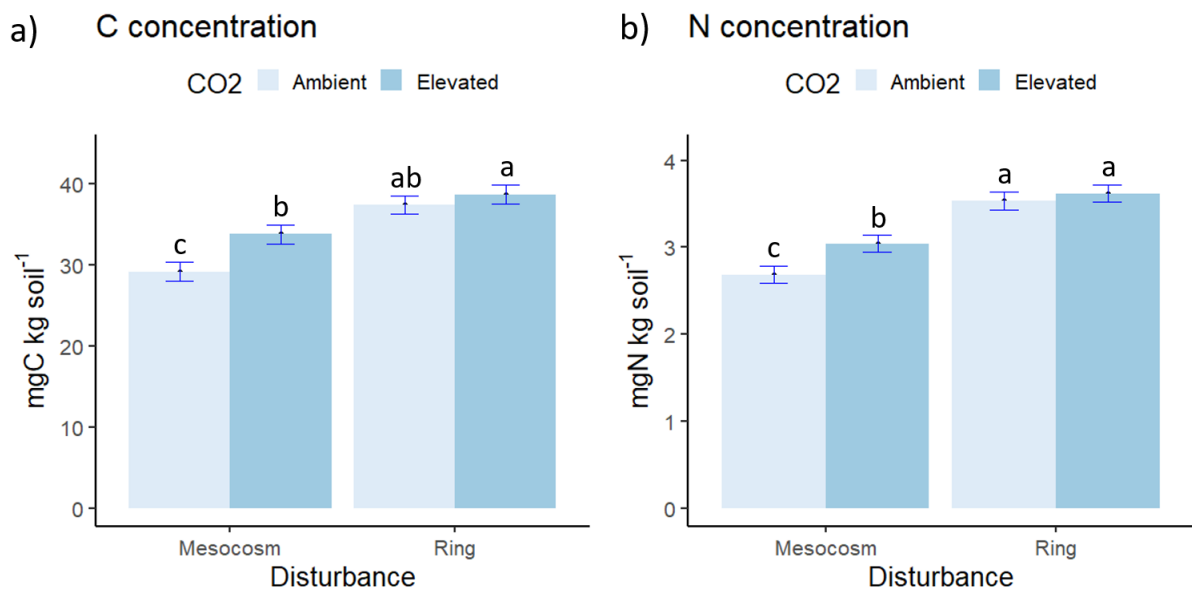


Extended Data Figure 5.16: Interactive effect of elevated CO₂, soil type and depth at the NZ Free Air CO₂ Enrichment legume-based grazed pasture facility on soil organic matter pyrolytic of a) aliphatic products and b) Nitrogen-containing products.

Extended Data 5.3.2.4 Soil organic carbon and nitrogen concentration of the Pukepuke soil from the mesocosm and ring

The experimental setting significantly interacted with eCO₂ affecting the soil OC and N concentration ($p = 0.0410$ and 0.0304 , respectively) as eCO₂ increased the soil OC and N concentration in Pukepuke soil from the mesocosms after 15 years of exposure to eCO₂ but not from the rings after 23 years exposure to eCO₂ (Extended Data Figure 5.17a and b, respectively).

The OC and N concentrations were both lower in the Pukepuke soil from the mesocosm than rings, suggesting a loss of organic matter over the course of the study, but this decline was less under eCO₂.



Extended Data Figure 5.17: Differences in a) the soil organic carbon (C) and b) nitrogen (N) concentration in Pukepuke soil from the mesocosm and rings from the NZ Free Air CO₂ Enrichment legume-based grazed pasture facility after 15 (mesocosm) and 23 years (ring) of exposure to eCO₂.

Chapter 6: Overall summary and recommendation for future research

6.1 Overall Summary

6.1.1 Changes in soil organic carbon partitioning and molecular composition of soil organic matter in a grazed pasture after 22 years of elevated CO₂

Reflecting on the impact of 22 years of elevated CO₂ (eCO₂) exposure at the NZ-FACE facility on a grazed legume-based pasture on:

1. Organic carbon (OC) inputs (net herbage accumulation),
2. the soil's capacity to support the boost in plant growth (soil properties that influence nutrient status), and,
3. the dynamics of old and new organic matter (OM). This encompasses soil OC and nitrogen (N) content, stocks, distribution, and molecular composition within soil fractions of the Pukepuke soil during two periods: I (2005 – 2009) and II (2015 – 2019)

From these analyses, the following insights have emerged:

- (i) Despite increases in pasture growth and the associated increase in fresh OC inputs during period II, by the end of this period (2019) and independent of CO₂ treatment, the soil OC and N stocks were 9.3 t ha⁻¹ (equivalent to -11.7%) lower at 0 – 250 mm depth compared with stocks from 10 years earlier (2009). This can be attributed to several contributing factors. First, an increase in soil moisture and temperature over time might have favoured a high fresh herbage detritus input to the soil, and thus an enhanced microbial growth (also favoured by the increase in soil moisture and temperature), which under the existing low phosphate and sulphate fertility conditions might have led to positive priming (due to the fresh high quantity of low-quality OC input; Lavalley et al., 2020). Second, this positive priming might have caused a residual concentration of alkalinity in the system (e.g., residual

concentration of calcium and magnesium), causing the increased soil pH. Third, this alkalinisation of the soil solution weakens inner-sphere bonds and hydrogen bonds between soil particles and organic molecules, and thus the strength through which this OC is protected (Kleber, 2010).

- (ii) The reduction of soil OC and N stocks over time was accompanied by changes in the soil OC partitioning where the faster mineralisation of the labile OM pool during period II led to a reduced N and OC contribution from coarse particulate OM to the bulk soil, despite the larger net herbage accumulation and a proportion of micro-aggregates fraction. The mineral-associated OM fraction did not show significant changes over time, therefore priming of old or new OC in the stable pool can be disregarded. Nonetheless, a saturation of the specific contact area of the mineral fraction cannot be ignored, given the fact that the soil has a long history of pastoral use, which combined with a low silt and clay content, limits the OC storage capacity of this soil.
- (iii) Most importantly, the results have shown that the soil OC and N stocks and partitioning into the soil fraction, have not changed after 22 years of exposure to eCO₂. We also conclude that the bulk soil and its fractions have the same susceptibility to losing soil OC and N under eCO₂ and ambient CO₂ soils when subjected to other drivers that have an impact on soil OC stabilization (such as increased average temperatures, increased soil moisture, enhanced net herbage accumulation, increased soil pH, the release of cations, and reduced phosphate and sulphate availability).
- (iv) Despite no changes in soil OC stocks there was a strong influence of eCO₂ on the molecular composition of the relatively labile pools (coarse particulate organic matter and micro-aggregates) found in the soil at the NZ-FACE (from which we

infer was undergoing priming of fresh inputs). It was shown that eCO₂ caused the enrichment of unspecific polysaccharides (probably microbial-derived) and the depletion of aliphatic compounds in cPOM. In micro-aggregates, eCO₂ appears to cause a depletion of short alkanes and increases the long-chain alkane and alkene, perhaps due to stronger input fluxes rather than an in-soil decomposition effect. The changes observed in the molecular composition of the labile OC pool suggest that even when there are larger OC fluxes into the soil) under eCO₂, the mineralization rate at 50 – 150 mm is stronger than the stabilisation processes of soil OC (especially in the coarse particulate organic matter).

6.1.2 The long-term interactive effect between elevated CO₂ and the grazing animal on soil carbon stocks and molecular composition of soil organic matter

We investigated the interaction between eCO₂ and the grazing animals on soil organic carbon (OC) and nitrogen (N) stocks. Additionally, we examined the soil OC and N partitioning and stability, by quantifying changes in the molecular composition of soil organic matter (OM). To assess the multiple effects of the grazing animal three defoliation treatments were included, first, areas accessible to the grazing animal including the effects of selective defoliation, trampling, and nutrient return in dung and urine. Second, areas limiting to the selective defoliation by the grazing animal, but protected from treading, dung and urine return to the pasture, and a third area where the animal is excluded, and the pastures are hand-cut.

Independently of the CO₂ treatment, the grazing animal by returning nutrients in urine and dung and trampling plant litter sustained the soil OC and N content and respective stocks in the top 0 – 50 mm depth, compared with soils where the animal could graze but were there was no

nutrient return through urine and dung and no trampling of plant litter. The OC and N stocks were 5.1 and 0.5 t ha⁻¹, respectively, higher (equivalent to 22 and 23% increase, respectively) where the grazing animals were an integral part of the agroecosystem. Smaller soil OC and N stocks were found where the pasture was hand-cut with reductions of 2.6 and 0.2 t ha⁻¹ (equivalent to 11 and 10%), respectively. These findings highlight the significance of nutrient return and trampling of plant litter by the grazing animals in sustaining existing soil OC and N stocks.

There was no positive or negative interactive effect between long-term exposure (22 years) to eCO₂ and the grazing animal on soil OC and N stocks in the Pukepuke soil. The grazing animal, in returning nutrients in urine and dung and in trampled plant litter did not contribute to an increase in soil OC and N contents under eCO₂ in any of the three soil depths (0 – 50, 50 – 150 and 150 – 250 mm). These results indicate that even though there was some enhancement in net herbage accumulation (NHA, Chapter 3) and selective grazing under eCO₂ (Newton et al., 2014), defoliation, nutrient return and trampling by the grazing animal did not limit or increase the soils' potential for OC sequestration under eCO₂. Furthermore, the return of faecal and urine depositions by the grazing animal did not show any interaction effect with eCO₂ (compared to soils where the pasture is defoliated by the sheep yet there is no treading and no dung or urine is deposited), indicating that the nutrient return through the depositions by the grazing animal was not able to alleviate the progressive N limitation previously detected at the site.

Nevertheless, the molecular composition of soil OM was subject to the interaction effect between CO₂ and the defoliation treatment indicating that the OC stabilization pathways do differ with a change in pasture management under eCO₂. Grazed pasture soils showed accumulation of plant-derived OC, whereas where the grazing animals were excluded eCO₂ promoted the accumulation of root-derived OC, especially in deeper soil layers.

Data and findings from the treatment that excluded the animal with pastures cut enable a comparison to be made with other FACE studies throughout the world where cutting is exclusively used to manage pastures. Our results are consistent with those reported from long-term experiments where eCO_2 has not increased soil OC content or stocks.

6.1.3 Influences of elevated CO_2 on soil organic carbon quantity and quality in two contrasting soils

Between 2005 and 2020 a mesocosm study was conducted at the NZ-FACE facility to examine the effect of long-term exposure of a grazed pasture to elevated CO_2 (eCO_2) on soil organic carbon (OC) and N stocks (to 150 mm depth) and molecular composition of the soil organic matter in two contrasting soils. The Pukepuke soil originally from the NZ-FACE facility (and under ambient CO_2 conditions) and the Stratford soil, from the Taranaki district in NZ (140 km northwest of the NZ-FACE facility) were chosen for the study due to their different inherent properties (e.g., texture and cation exchange capacity). From this long-term mesocosm study, two main findings emerged; (i) the Pukepuke soil (a sandy soil), under ambient CO_2 atmosphere (aCO_2), had a sharp decline in its OC and N stocks (16.1 and 1.5 $t\ ha^{-1}$, respectively) while those of the Stratford soil (an allophanic soil) were subjected to a smaller decline (5.1 and 1.0 $t\ ha^{-1}$, respectively). (ii) the Pukepuke soil responded more than the Stratford soil to exposure to eCO_2 , partly compensating for the losses in soil OC (and N) stocks (observed over time under aCO_2) by retaining and or sequestering 6.5 $t\ ha^{-1}$ in the 0 – 150 mm soil depth. In contrast, the Stratford soil showed no significant change in OC and N stocks between CO_2 treatments ($p < 0.05$) over the 15 years of the comparison.

Overall, these results reveal that the Pukepuke soil is less resilient (i.e., more vulnerable) than the Stratford soil to physical disruption (when setting up the mesocosms) and to weather

extremes (that occurred during the experimental period). This can be attributed to the poor protection of soil OC, higher content of labile organic matter of the Pukepuke soil and lower resilience to water stress than the Stratford soil.

However, over time, eCO₂ was able to partially mitigate the loss of soil OC and N stocks in the Pukepuke soil. This was attributed to the effect of eCO₂ on enhancing plant growth and related plant-detritus input to soils (especially lignin-derived OC), with this effect being more accentuated in the top 50 mm of soil. In sharp contrast, the soil OC and N stocks of the Stratford soil did not change under the increased concentration of atmospheric CO₂. We hypothesise that the lack of clear response in the Stratford soil could be attributed to its potential ongoing adaptation to the climatic conditions at the NZ-FACE facility, which was drier than those at the original Stratford site.

This mesocosm study also allowed us to compare the response of the Pukepuke soil in the ring vs. that in the mesocosm. Between 2009 and 2020, under a CO₂, the Pukepuke soil from the mesocosms lost 16.1 t ha⁻¹ (equivalent to 28%) in the 0 – 150 mm depth whereas the Pukepuke in the rings only lost 3.6 t ha⁻¹ (equivalent to 6.3%) down to that same depth. The response under eCO₂ was also different with an increase of 6.5 t ha⁻¹ down to 150 mm depth in the mesocosm compared with only a 0.5 t ha⁻¹ increase in the ring. This could be explained by the apparent changes in the long-term equilibrium undergone in the mesocosm soil due to soil disruption. Thus, caution is needed when interpreting these results and highlights the influence method, in addition to treatment can have on the result.

6.2 Highlights of the thesis

Soils at the NZ-FACE facility independent of CO₂ treatment have suffered a significant loss in soil OC and N stocks in recent years (between 2009 and 2020), despite having higher soil OC

inputs during that period; Chapter 3). Overall, long-term exposure to eCO₂ of a legume-based pastured grazed by livestock had little influence on the above-ground response, soil OC and N stocks, or in the partitioning and stability of OC in the soil fractions.

The grazing animal by returning nutrients through urine and faeces and trampling on plant material sustained soil OC and N stocks, compared to pastures that limited the effect of the grazing animal to defoliated, where soil OC and N stocks declined. This highlights the potential of grazing in sustaining the current soil OC and N stocks. No interaction effect was observed between eCO₂ and the grazing animal on the soil OC and N stocks (Chapter 4). In pasture grazed by the animal, eCO₂ increased the accumulation of lignin-derived OM and promoted the accumulation of shoot-derived OC in the soil. In hand-cut pasture soils, eCO₂ promoted the accumulation of root-derived OC, especially in deeper soil layers.

The lack of a significant direct effect of eCO₂ or interaction effect between eCO₂ and the three defoliation treatments was overwhelmed by the impact of the increasing temperature and drought episodes that resulted in a reduction in the soil OC and N stock over the past 10 years, masking or limiting the expression of any the interaction effect between eCO₂ and grazing. Either way, the lack of significant differences in soil OC and N in the Pukepuke soil under eCO₂ in the sites with and without grazing, which includes no interactive effect of eCO₂ and defoliation treatments (Chapter 4), suggests other variables (such as temperature and extreme weather conditions) have a stronger controlling influence on the soil OC and N mineralisation and stabilisation processes.

There were only small measurable changes in soil OC and N stocks as a response to eCO₂ in the mesocosm study, which showed different dynamics of soil OM stabilization and nutrient cycling in the soil (Chapter 5). The setting up of the mesocosm would have caused physical disruption of the soil, and this is hypothesised to have had a key impact on soil OC stocks of

the Pukepuke soil, where protected OM is limited due to its sandy texture. The impact of setting up of the mesocosm was much smaller with the Stratford soil, developed from volcanic ash, and this was attributed to the fact that most of the OM is physico-chemically protected. Nevertheless, under eCO₂ the Pukepuke soil was able to replenish part of the OC stock lost. This highlights the role of an increase in plant-derived OC input to the soil caused by eCO₂ in the recovery of soil OC stocks of this soil.

6.3 Further research

- It has been proposed that the effect of eCO₂ on boosting plant productivity depends on a variety of factors, including water availability, nutrient supply, soil type and mineralogy. Different soil types have different levels of resilience, to changes in nutrient availability and climatic conditions, which can affect how well plants are able to utilize the additional atmospheric CO₂. Pasture growth in the current study was reliant on rainfed water. Combined with the limited water-holding capacity of the Pukepuke soil, for significant periods of the year pasture growth would have been limited by moisture. Furthermore, since 1997, the annual mean air temperature at the FACE under climate change has increased on average by ~1°C with increasing drought episodes, further limiting available moisture for plant growth. Thus, extending the research to investigate the influence of soil type on pasture growth under eCO₂ in changing weather (increased water stress due to higher temperatures and lower rainfall events) and the subsequent effect on soil OC persistence in FACE facilities is needed. Would reducing moisture stress (through irrigation) increase the opportunity for plants to benefit from eCO₂?

- The soil organic matter molecular composition under eCO₂ had higher proportions of carbohydrates (plant- and/or microbial-derived OC) compared to ambient CO₂ soils. Plants growing under eCO₂ often have increased biomass and root exudation, which in turn can stimulate the activity of soil microorganisms and affect their abundance and activity. This can influence the rate of OM decomposition and the availability of nutrients to support the boost of plant growth under eCO₂. This can result in a shift in the types of microorganisms present in the soil and the activities they perform, as the nutrients required for their growth and metabolism may become limiting. More data is needed to clarify the mechanisms on different layers throughout the soil profile (e.g., through microbial mineralization vs. extracellular enzyme stabilization) of how eCO₂ affects the microbial community and activity on the soil OC stabilization pathways (e.g., through metabolomic or isotopic analysis).
- In the current study the nutrient inputs were limited to phosphate and sulphate in fertiliser and N through biological N₂ fixation by the legume component of the pasture. This N was made available to grasses through the decomposition of legume litter and through the return of N in dung and urine by the grazing animals. Given that a legume-based pasture system is responsive to N fertiliser throughout the year, it is unclear to what degree the pasture response under eCO₂ is limited by N availability. Furthermore, understanding why under eCO₂ soil PO₄ levels were consistently lower than under aCO₂ conditions require further investigation, given the critical role PO₄ plays in the nutrition and growth of the legume component of the sward. Any drivers affecting PO₄ requirements or availability would have major implications for the pastoral sector going forward on multiple fronts, yet it is still uncertain if the increased nutrient uptake under eCO₂ will severely deplete the soil of nutrients, leading by default to a sustained reduction of forage supply. Further research needs to explore: (i) Would applying N

fertilisation increase pasture growth after decades of eCO₂ exposure? and (ii) given that under eCO₂ there is no apparent difference with or without animal on soil OC and N content, which factors are contributing to the reduced PO₄ availability under eCO₂?

- The Pukepuke soils in the present study, both in the rings and mesocosm had a long history of pastoral use and therefore, their OC stocks were likely to have been at or near the maximum amount that could be stored. Introducing soils that had previously experienced depletion of OC stocks, such as through continuous arable cropping would help confirm whether, under eCO₂, replenishment of soil OM would occur at the same rates as reported in other long-term studies under ambient CO₂ conditions and return soil OC stocks back to those observed previously under long term pasture use. This information would be invaluable to the arable and vegetable sectors that constantly struggle to sustain sufficient amounts of organic matter to ensure the physical integrity of the soil allow for minimum tillage for seedbed preparation and good conditions for seed germination, emergence, and plant growth.

References

- Abdalla, M., Hastings, A., Chadwick, D. R., Jones, D. L., Evans, C. D., Jones, M. B., Smith, P. (2018). Critical review of the impacts of grazing intensity on soil organic carbon storage and other soil quality indicators in extensively managed grasslands. *Agric Ecosyst Environ*, 253, 62-81. doi:10.1016/j.agee.2017.10.023
- Ainsworth, E. A., & Long, S. P. (2005). What have we learned from 15 years of free-air CO₂ enrichment (FACE)? A meta-analytic review of the responses of photosynthesis, canopy properties and plant production to rising CO₂. *New Phytologist*, 165(2), 351-372. doi:10.1111/j.1469-8137.2004.01224.x
- Allard, V., Newton, P. C. D., Lieffering, M., Clark, H., Matthew, C., Soussana, J. F., & Gray, Y. S. (2003). Nitrogen cycling in grazed pastures at elevated CO₂: N returns by ruminants. *Global Change Biology*, 9(12), 1731-1742. doi:10.1111/j.1365-2486.2003.00711.x
- Allard, V., Newton, P. C. D., Lieffering, M., Soussana, J. F., Carran, R. A., & Matthew, C. (2005). Increased quantity and quality of coarse soil organic matter fraction at elevated CO₂ in a grazed grassland are a consequence of enhanced root growth rate and turnover. *Plant and Soil*, 276(1-2), 49-60. doi:10.1007/s11104-005-5675-9
- Allard, V., Newton, P. C. D., Lieffering, M., Soussana, J. F., Grieu, P., & Matthew, C. (2004). Elevated CO₂ effects on decomposition processes in a grazed grassland. *Global Change Biology*, 10(9), 1553-1564. doi:10.1111/j.1365-2486.2004.00818.x
- Baumann, K., Eckhardt, K., Schoning, I., Schrumpf, M., Leinweber, P., (2022). Clay fraction properties and grasslands management imprint on soil organic matter composition and stability at molecular level. *Soil Use Manage*. 2022; 00:1–19. DOI: 10.1111/sum.12815
- Baumhardt, R. L., & Schwartz, R. C. (2005). CRUSTS | Structural. In D. Hillel (Ed.), *Encyclopedia of Soils in the Environment* (pp. 347-356). Oxford: Elsevier.
- Burgess, A.C. 1966. *Soil Fertility Problems of Taranaki*. New Zealand Grassland Publication. DOI: <https://doi.org/10.33584/jnzg.1951.13.970>
- Baumhardt, R. L., & Schwartz, R. C. (2005). CRUSTS | Structural. In D. Hillel (Ed.), *Encyclopedia of Soils in the Environment* (pp. 347-356). Oxford: Elsevier.

Buurman, P., Roscoe, R., (2011). Different chemical composition of free light, occluded light and extractable SOM fractions in soils of Cerrado and tilled and untilled fields, Minas Gerais, Brazil: a pyrolysis-GC/MS study. *Eur. J. Soil Sci.* 62, 253–266.

Buurman, P., Peterse, F., Martin, G.A., (2007). Soil organic matter chemistry in allophanic soils: a pyrolysis-GC/MS study of a Costa Rican Andosol catena. *Eur. J. Soil Sci.* 58, 1330–1347.

Buurman, P., Nierop, K.G.J., Kaal, J., Senesi, N. (2009). Analytical pyrolysis and thermally assisted hydrolysis and methylation of EUROSIL humic acid samples: a key to their source. *Geoderma* 150, 10–22.

Cowie, J.D., Hall, A.D., (1965). Soils and agriculture of the Flock House Farm of Instruction, Bulls, Manawatu, N. Z. (N. Z. Soil Bureau Report No. 1/1965). Department of Scientific and Industrial Research, Wellington, New Zealand. <https://doi.org/10.7931/DL1-SBREP-65-1>

Cowie, J.D., (1968). Pedology of soils from wind-blown sand in the Manawatu District. *New Zealand Journal of Science* 11, 459–487.

Cowie, J.D., Smith, B.A.J., (1958). Soils and agriculture of Oroua Downs, Taikorea, and Glen Oroua Districts, Manawatu County (New Zealand Soil Bureau Bulletin No. 16). Department of Scientific and Industrial Research, Wellington, New Zealand. <https://doi.org/10.7931/dl1-sbb-016>

Carrillo, Y., Dijkstra, F., LeCain, D., Blumenthal, D., & Pendall, E. (2018). Elevated CO₂ and warming cause interactive effects on soil carbon and shifts in carbon use by bacteria. *Ecology Letters*, 21(11), 1639-1648. doi:10.1111/ele.13140

Chen, L., Liu, L., Qin, S., Yang, G., Fang, K., Zhu, B., Yang, Y. (2019). Regulation of priming effect by soil organic matter stability over a broad geographic scale. *Nature Communications*, 10(1). doi:10.1038/s41467-019-13119-z

Chen, Q., Niu, B., Hu, Y., Luo, T., & Zhang, G. (2020). Warming and increased precipitation indirectly affect the composition and turnover of labile-fraction soil organic matter by directly affecting vegetation and microorganisms. *Science of the Total Environment*, 714. doi:10.1016/j.scitotenv.2020.136787

- Cheng, X., Yang, Y., Li, M., Dou, X., & Zhang, Q. (2013). The impact of agricultural land use changes on soil organic carbon dynamics in the Danjiangkou Reservoir area of China. *Plant and Soil*, 366(1-2), 415-424. doi:10.1007/s11104-012-1446-6
- Chenu, C., Angers, D. A., Barré, P., Derrien, D., Arrouays, D., & Balesdent, J. (2019). Increasing organic stocks in agricultural soils: Knowledge gaps and potential innovations. *Soil and Tillage Research*, 188, 41-52. doi:10.1016/j.still.2018.04.011
- Conant, R. T., Ryan, M. G., Ågren, G. I., Birge, H. E., Davidson, E. A., Eliasson, P. E., Bradford, M. A. (2011). Temperature and soil organic matter decomposition rates - synthesis of current knowledge and a way forward. *Global Change Biology*, 17(11), 3392-3404. doi:10.1111/j.1365-2486.2011.02496.x
- Cornforth IS., and Sinclair AG., (1984). Fertiliser and lime recommendations for Pastures and Crops in New Zealand. Ministry of Agriculture and Fisheries, Wellington, New Zealand.
- Cotrufo, M. F., Soong, J. L., Horton, A. J., Campbell, E. E., Haddix, M. L., Wall, D. H., & Parton, W. J. (2015). Formation of soil organic matter via biochemical and physical pathways of litter mass loss. *Nature Geoscience*, 8(10), 776-779. doi:10.1038/ngeo2520
- Cowie JD, Hall AD (1965) Soils and agriculture of Flock House, Bulls, Manawatu, NZ. NZ Soil Bureau Report no. 1/1965.
- Cowie and Campbell, (1965). Soils of the Wanganui District. Proceedings N.Z. Grassland Association
- de Graaff, M. A., Six, J., Harris, D., Blum, H., & Van Kessel, C. (2004). Decomposition of soil and plant carbon from pasture systems after 9 years of exposure to elevated CO₂: Impact on C cycling and modeling. *Global Change Biology*, 10(11), 1922-1935. doi:10.1111/j.1365-2486.2004.00862.x
- Deng, Q., Cheng, X., Bowatte, S., Newton, P. C. D., & Zhang, Q. (2016). Rhizospheric carbon-nitrogen interactions in a mixed-species pasture after 13 years of elevated CO₂. *Agriculture, Ecosystems and Environment*, 235, 134-141. doi:10.1016/j.agee.2016.10.016
- Deng, Q., Hui, D., Luo, Y., Elser, J., Wang, Y.-P., Loladze, I., Dennis, S. (2015). Down-regulation of tissue N:P ratios in terrestrial plants by elevated CO₂. *Ecology*, 96(12), 3354–3362.

- Derenne, S., & Quéné, K. (2015). Analytical pyrolysis as a tool to probe soil organic matter. *Journal of Analytical and Applied Pyrolysis*, 111, 108-120. doi:10.1016/j.jaap.2014.12.001
- Dietzen, C. A., Larsen, K. S., Ambus, P. L., Michelsen, A., Arndal, M. F., Beier, C., Schmidt, I. K. (2019). Accumulation of soil carbon under elevated CO₂ unaffected by warming and drought. *Global Change Biology*, 25(9), 2970-2977. doi:10.1111/gcb.14699
- Dignac, M.-F., Houot, S., Francou, C., Derenne, S., (2005). Pyrolytic study of compost and waste organic matter. *Org. Geochem.* 36, 1054–1071.
- Dijkstra, F. A., Hobbie, S. E., Knops, J. M. H., & Reich, P. B. (2004). Nitrogen deposition and plant species interact to influence soil carbon stabilization. *Ecology Letters*, 7(12), 1192-1198. doi:10.1111/j.1461-0248.2004.00679.x
- Dijkstra, F. A., Hobbie, S. E., Reich, P. B., & Knops, J. M. H. (2005). Divergent effects of elevated CO₂, N fertilization, and plant diversity on soil C and N dynamics in a grassland field experiment. *Plant and Soil*, 272(1-2), 41-52. doi:10.1007/s11104-004-3848-6
- Dodd, MB., (2013). Elevated CO₂ impacts on grazed pasture: long-term lessons from the New Zealand FACE. *Proceedings of the 22nd International Grassland Congress, Climate change impacts on grassland production, composition, distribution and adaptation*, 2013.
- Dong, H., Lin, J., Lu, J., Li, L., Yu, Z., Kumar, A., Chen, B. (2022). Priming effects of surface soil organic carbon decreased with warming: a global meta-analysis. *Plant and Soil*. doi:10.1007/s11104-022-05851-1
- Dorji, T., Field, D. J., & Odeh, I. O. A. (2020). Soil aggregate stability and aggregate-associated organic carbon under different land use or land cover types. *Soil Use and Management*, 36(2), 308-319. doi:10.1111/sum.12549
- Dorodnikov, M., Kuzyakov, Y., Fangmeier, A., & Wiesenberg, G. L. B. (2011). C and N in soil organic matter density fractions under elevated atmospheric CO₂: Turnover vs. stabilization. *Soil Biology and Biochemistry*, 43(3), 579-589. doi:10.1016/j.soilbio.2010.11.026
- Edwards, E, McCaffery, S & Evans, J (2005). Phosphorus status determines biomass response to elevated CO₂ in a legume: C₄ grass community, *Global Change Biology*, vol. 11, pp. 1968-1981.

Edwards, G. R., Newton, P. C. D., Tilbrook, J. C., & Clark, H. (2001). Seedling performance of pasture species under elevated CO₂. *New Phytologist*, 150(2), 359-369. doi:10.1046/j.1469-8137.2001.00100.x

Edwards, G. R., Newton, P. C. D., Tilbrook, J. C., & Clark, H. (2001). Seedling performance of pasture species under elevated CO₂. *New Phytologist*, 150(2), 359-369. doi:10.1046/j.1469-8137.2001.00100.x

FAO, (2019). Measuring and modelling soil carbon stocks and stock changes in livestock production systems: Guidelines for assessment (Version 1). Livestock Environmental Assessment and Performance (LEAP) Partnership. Rome, FAO. 170 pp. Licence: CC BY-NC-SA 3.0 IGO

Fontaine, S., Mariotti, A., & Abbadie, L. (2003). The priming effect of organic matter: a question of microbial competition? *Soil Biology and Biochemistry*, 35(6), 837-843. doi:https://doi.org/10.1016/S0038-0717(03)00123-8

Gentile, R., Dodd, M., Lieffering, M., Brock, S. C., Theobald, P. W., & Newton, P. C. D. (2012). Effects of long-term exposure to enriched CO₂ on the nutrient-supplying capacity of a grassland soil. *Biology and Fertility of Soils*, 48(3), 357-362. doi:10.1007/s00374-011-0616-7

Hagedorn, F., Maurer, S., Egli, P., Blaser, P., Bucher, J. B., & Siegwolf, R. (2001). Carbon sequestration in forest soils: Effects of soil type, atmospheric CO₂ enrichment, and N deposition. *European Journal of Soil Science*, 52(4), 619-628. doi:10.1046/j.1365-2389.2001.00412.x

Hebeisen, T., Lüscher, A., Zanetti, S., Fischer, B. U., Hartwig, U. A., Frehner, M., Nösberger, J. (1997). Growth response of *Trifolium repens* L. and *Lolium perenne* L. as monocultures and bi-species mixture to free air CO₂ enrichment and management. *Global Change Biology*, 3(2), 149-160. doi:10.1046/j.1365-2486.1997.00073.x

Horwath, W., (2015). Carbon cycling: the dynamics and formation of organic matter. Chapter 12, *Soil Microbiology, Ecology and Biochemistry*, fourth edition, 339-382.

Hungate, B. A., van Groenigen, K. J., Six, J., Jastrow, J. D., Luo, Y., de Graaff, M. A., Osenberg, C. W. (2009). Assessing the effect of elevated carbon dioxide on soil carbon: A comparison of four meta-analyses. *Global Change Biology*, 15(8), 2020-2034. doi:10.1111/j.1365-2486.2009.01866.x

IPCC, (2014). Climate Change 2014: Synthesis Report. Contribution of Working Groups I, II and III to the Fifth Assessment Report of the Intergovernmental Panel on Climate Change [Core Writing Team, R.K. Pachauri and L.A. Meyer (eds.)]. IPCC, Geneva, Switzerland, 151 pp.

IPCC, (2018). The carbon cycle and atmospheric carbon dioxide, TAR-03 pp 185-237

IPCC, (2021). Summary for Policymakers. In: Climate Change 2021: The Physical Science Basis. Contribution of Working Group I to the Sixth Assessment Report of the Intergovernmental Panel on Climate Change [Masson-Delmotte, V., P. Zhai, A. Pirani, S. L. Connors, C. Péan, S. Berger, N. Caud, Y. Chen, L. Goldfarb, M. I. Gomis, M. Huang, K. Leitzell, E. Lonnoy, J.B.R.

Jastrow, J. D., Michael Miller, R., Matamala, R., Norby, R. J., Boutton, T. W., Rice, C. W., & Owensby, C. E. (2005). Elevated atmospheric carbon dioxide increases soil carbon. *Global Change Biology*, 11(12), 2057-2064. doi:10.1111/j.1365-2486.2005.01077.x

Jiang, M., Medlyn, B. E., Drake, J. E., Duursma, R. A., Anderson, I. C., Barton, C. V. M., Ellsworth, D. S. (2020). The fate of carbon in a mature forest under carbon dioxide enrichment. *Nature*, 580(7802), 227-231. doi:10.1038/s41586-020-2128-9

Jin, J., Tang, C., & Sale, P. (2015). The impact of elevated carbon dioxide on the phosphorus nutrition of plants: A review. *Annals of Botany*, 116(6), 987-999. doi:10.1093/aob/mcv088

Jones, A. G., Scullion, J., Ostle, N., Levy, P. E., & Gwynn-Jones, D. (2014). Completing the FACE of elevated CO₂ research. *Environment International*, 73, 252-258. doi:10.1016/j.envint.2014.07.021

Jones, M. B., & Donnelly, A. (2004). Carbon sequestration in temperate grassland ecosystems and the influence of management, climate and elevated CO₂. *New Phytologist*, 164(3), 423-439. doi:10.1111/j.1469-8137.2004.01201.x

Kleber, M., Sollins, P., Sutton, R. (2007) A conceptual model of organo-mineral interactions in soils: self-assembly of organic molecular fragments into zonal structures on mineral surfaces. *Biogeochemistry* (2007) 85:9–24 DOI 10.1007/s10533-007-9103-5

Keidel, L., Lenhart, K., Moser, G., & Müller, C. (2018). Depth-dependent response of soil aggregates and soil organic carbon content to long-term elevated CO₂ in a temperate grassland soil. *Soil Biology and Biochemistry*, 123, 145-154. doi:10.1016/j.soilbio.2018.05.005

- Keiluweit, M., Bougoure, J. J., Nico, P. S., Pett-Ridge, J., Weber, P. K., & Kleber, M. (2015). Mineral protection of soil carbon counteracted by root exudates. *Nature Climate Change*, 5(6), 588-595. doi:10.1038/nclimate2580
- Kleber, M. (2010). What is recalcitrant soil organic matter? *Environmental Chemistry*, 7(4), 320-332. doi:10.1071/EN10006
- Kleber M, Bourg IC, Coward EK, Hansel CM, Myneni SC, Nunan N (2021). Dynamic interactions at the mineral–organic matter interface. *Nature Rev Earth Environ* 2(6):402–421. <https://doi.org/10.1038/s43017-021-00162-y>
- Kien and Kogel-Knaber, (2003). Contribution of lignin and polyssacharides to the refractory carbon pool in C-depleted arable soils. *Soil Biology and Biochemistry* 35, 101 – 118
- Kögel-Knabner, I., (2000). Analytical approaches for characterizing soil organic matter. *Org. Geochem.* 31, 609–625.
- Kögel-Knabner, I., (2002). The macromolecular organic composition of plant and microbial residues as inputs to soil organic matter. *Soil Biol. Biochem.* 34, 139– 162.
- Kögel-Knabner, I., Ekschmitt, K., Flessa, H., Guggenberger, G., Matzner, E., Marschner, B., & Von Lützow, M. (2008). An integrative approach of organic matter stabilization in temperate soils: Linking chemistry, physics, and biology. *Journal of Plant Nutrition and Soil Science*, 171(1), 5-13. doi:10.1002/jpln.200700215
- Kuzyakov, Y., Horwath, W. R., Dorodnikov, M., & Blagodatskaya, E. (2019). Review and synthesis of the effects of elevated atmospheric CO₂ on soil processes: No changes in pools, but increased fluxes and accelerated cycles. *Soil Biology and Biochemistry*, 128, 66-78. doi:10.1016/j.soilbio.2018.10.005
- Lal, R. (2018). Digging deeper: A holistic perspective of factors affecting soil organic carbon sequestration in agroecosystems. *Global Change Biology*, 24(8), 3285-3301. doi:10.1111/gcb.14054
- Lal, R., Negassa, W., & Lorenz, K. (2015). Carbon sequestration in soil. *Current Opinion in Environmental Sustainability*, 15, 79-86. doi:10.1016/j.cosust.2015.09.002
- Langley, J. A., McKinley, D. C., Wolf, A. A., Hungate, B. A., Drake, B. G., & Megonigal, J. P. (2009). Priming depletes soil carbon and releases nitrogen in a scrub-oak ecosystem exposed

to elevated CO₂. *Soil Biology and Biochemistry*, 41(1), 54-60. doi:10.1016/j.soilbio.2008.09.016

Lavallee, J. M., Soong, J. L., & Cotrufo, M. F. (2020). Conceptualizing soil organic matter into particulate and mineral-associated forms to address global change in the 21st century. *Global Change Biology*, 26(1), 261-273. doi:10.1111/gcb.14859

Lehmann, J., Hansel, C. M., Kaiser, C., Kleber, M., Maher, K., Manzoni, S., Kögel-Knabner, I. (2020). Persistence of soil organic carbon caused by functional complexity. *Nature Geoscience*, 13(8), 529-534. doi:10.1038/s41561-020-0612-3

Lehmann, J., & Kleber, M. (2015). The contentious nature of soil organic matter. *Nature*, 528(7580), 60-68. doi:10.1038/nature16069

Lenhart, K., Kammann, C., Boeckx, P., Six, J., & Müller, C. (2016). Quantification of ecosystem C dynamics in a long-term FACE study on permanent grassland. *Rapid Communications in Mass Spectrometry*, 30(7), 963-972. doi:10.1002/rcm.7515

Li, Z., Zhang, Z., Li, M., Wu, H., & Jiang, M. (2020). Molecular Fingerprints of Soil Organic Carbon in Wetlands Covered by Native and Non-native Plants in the Yellow River Delta. *Wetlands*, 40(6), 2189-2198. doi:10.1007/s13157-020-01340-2

Liang, C., & Balser, T. C. (2012). Warming and nitrogen deposition lessen microbial residue contribution to soil carbon pool. *Nature Communications*, 3. doi:10.1038/ncomms2224

Liang, C., Gutknecht, J. L. M., & Balser, T. C. (2015). Microbial lipid and amino sugar responses to long-term simulated global environmental changes in a California annual grassland. *Frontiers in Microbiology*, 6(MAY). doi:10.3389/fmicb.2015.00385

Liang, C., Schimel, J. P., & Jastrow, J. D. (2017). The importance of anabolism in microbial control over soil carbon storage. *Nature Microbiology*, 2(8). doi:10.1038/nmicrobiol.2017.105

Luo, Y., Su, B., Currie, W. S., Dukes, J. S., Finzi, A., Hartwig, U., Field, C. B. (2004). Progressive nitrogen limitation of ecosystem responses to rising atmospheric carbon dioxide. *Bioscience*, 54(8), 731-739. doi:10.1641/0006-3568(2004)054[0731:PNLOER]2.0.CO;2

Madhu, M., & Hatfeld, J. L. (2013). Dynamics of plant root growth under increased atmospheric carbon dioxide. *Agronomy Journal*, 105(3), 657-669. doi:10.2134/agronj2013.0018

Matus, F., Rumpel, C., Neculman, R., Panichini, M., Mora, M.L. (2014) Soil carbon storage and stabilisation in andic soils: A review

McNally, S., Beare, M.H., Curtin, D., Meenken, E.D., Kelliher, F., Calvelo Pereira, R., Shen, Q., Baldock, J., 2017. Soil carbon sequestration potential of permanent pasture and continuous cropping soils in New Zealand. *Glob. Change Biol.* 23, 4544–4555.

McSherry, M. E., & Ritchie, M. E. (2013). Effects of grazing on grassland soil carbon: a global review. *Glob Chang Biol*, 19(5), 1347-1357. doi:10.1111/gcb.12144

Newton, P. C. D., Carran, R. A., & Lawrence, E. J. (2004). Reduced water repellency of a grassland soil under elevated atmospheric CO₂. *Global Change Biology*, 10(1), 1-4. doi:10.1111/j.1365-2486.2003.00715.x

Newton, P.C.D., Allard, V., Carran, R.A., and Lieffering, M. (2006). Impacts of Elevated CO₂ on a Grassland Grazed by Sheep: the New Zealand FACE Experiment. DOI: 10.1007/3-540-31237-4_9

Newton, P. C. D., Lieffering, M., Bowatte, W. M. S. D., Brock, S. C., Hunt, C. L., Theobald, P. W., & Ross, D. J. (2010). The rate of progression and stability of progressive nitrogen limitation at elevated atmospheric CO₂ in a grazed grassland over 11 years of Free Air CO₂ enrichment. *Plant and Soil*, 336(1), 433-441. doi:10.1007/s11104-010-0493-0

Newton, P. C. D., Lieffering, M., Parsons, A. J., Brock, S. C., Theobald, P. W., Hunt, C. L., Hovenden, M. J. (2014). Selective grazing modifies previously anticipated responses of plant community composition to elevated CO₂ in a temperate grassland. *Global Change Biology*, 20(1), 158-169. doi:10.1111/gcb.12301

Niwa, (2011). National Climate Centre, Annual Climate Summary 2011, available at: <https://niwa.co.nz/climate/summaries/annual>. Visited in January, 2023.

Niwa, (2015). National Climate Centre, Annual Climate Summary 2015, available at: <https://niwa.co.nz/climate/summaries/annual>. Visited in January, 2023.

Niwa, (2018). National Climate Centre, Annual Climate Summary 2018, available at: <https://niwa.co.nz/climate/summaries/annual>

Niwa, (2020). National Climate Centre, Annual Climate Summary 2020, available at: <https://niwa.co.nz/climate/summaries/annual>

Norby, R. J. (2011) Ecological and evolutionary lessons from free air carbon enhancement (FACE) experiments. In: Vol. 42. Annual Review of Ecology, Evolution, and Systematics.

NSD, (2020). Manaaki Whenua - Landcare Research 2020. National Soils Database (NSD). <https://doi.org/10.26060/95m4-cz25>

NSDR, (2020). Manaaki Whenua - Landcare Research 2020. National Soils Data Repository (NSDR). <https://doi.org/10.26060/gcxk-e905>

Okolo, C. C., Gebresamuel, G., Zenebe, A., Haile, M., & Eze, P. N. (2020). Accumulation of organic carbon in various soil aggregate sizes under different land use systems in a semi-arid environment. *Agriculture, Ecosystems and Environment*, 297. doi:10.1016/j.agee.2020.106924

Parfitt, R. L., Roberts, A. H. C., Thomson, N. A., Cook, F. J. (1985) Water use, irrigation, and pasture production on Stratford silt loam, *New Zealand Journal of Agricultural Research*, 28:3, 393-401, DOI: 10.1080/00288233.1985.10430444

Parfitt, R.L. (1990). Allophane in New Zealand—A review. *Australian Journal of Soil Research*, 1990 DOI: 10.1071/SR9900343

Parfitt, R.L. (2009). Allophane and imogolite: role in soil biogeochemical processes. *Clay Minerals*, (2009) 44, 135–155. DOI: 10.1180/claymin.2009.044.1.135

Pendall, E., Osanai, Y., Williams, A. L., & Hovenden, M. J. (2011). Soil carbon storage under simulated climate change is mediated by plant functional type. *Global Change Biology*, 17(1), 505-514. doi:10.1111/j.1365-2486.2010.02296.x

Pineiro, G., Paruelo, J. M., Oesterheld, M., & Jobbágy, E. G. (2010). Pathways of grazing effects on soil organic carbon and nitrogen. *Rangeland Ecology and Management*, 63(1), 109-119. doi:10.2111/08-255.1

Poirier, V., Roumet, C., & Munson, A. D. (2018). The root of the matter: Linking root traits and soil organic matter stabilization processes. *Soil Biology and Biochemistry*, 120, 246-259. doi:10.1016/j.soilbio.2018.02.016

Polley, H. W., Morgan, J. A., & Fay, P. A. (2011). Application of a conceptual framework to interpret variability in rangeland responses to atmospheric CO₂ enrichment. *Journal of Agricultural Science*, 149(1), 1-14. doi:10.1017/S0021859610000717

- Procter, A. C., Christopher Ellis, J., Fay, P. A., Wayne Polley, H., & Jackson, R. B. (2014). Fungal community responses to past and future atmospheric CO₂ differ by soil type. *Applied and Environmental Microbiology*, 80(23), 7364-7377. doi:10.1128/AEM.02083-14
- Procter, A. C., Gill, R. A., Fay, P. A., Polley, H. W., & Jackson, R. B. (2015). Soil carbon responses to past and future CO₂ in three Texas prairie soils. *Soil Biology and Biochemistry*, 83, 66-75. doi:10.1016/j.soilbio.2015.01.012
- Reich, P. B., Hobbie, S. E., Lee, T., Ellsworth, D. S., West, J. B., Tilman, D., Trost, J. (2006). Nitrogen limitation constrains sustainability of ecosystem response to CO₂. *Nature*, 440(7086), 922-925. doi:10.1038/nature04486
- Reich, P. B., Hobbie, S. E., Lee, T., Pastore, M., (2018). Unexpected reversal of C₃ versus C₄ grass response to elevated CO₂ during 20-year field experiment. *Plant Ecology*, Science 360, 317-320. <https://doi.org/10.1126/science.aas9313>
- Richardson, A., Lynch, J., Ryan, P., Delhaize, E., Smith, F., Smith, S., Harvey, P., Ryan, M., Veneklaas, E., Lambers, H., Oberson, A., Culvenor, R., Simpson, R. (2011). Plant and microbial strategies to improve the phosphorus efficiency of agriculture. *Plant Soil* (2011) 349:121–156 DOI 10.1007/s11104-011-0950-4
- Robinson, B. (2000). The Effect of 40 years of effluent irrigation on soil and pasture properties of the lactose new zealand land treatment site. Thesis, Institute of natural resources, Massey University.
- Ross, D. J., Newton, P. C. D., & Tate, K. R. (2004). Elevated CO₂ effects on herbage production and soil carbon and nitrogen pools and mineralization in a species-rich, grazed pasture on a seasonally dry sand. *Plant and Soil*, 260(1-2), 183-196. doi:10.1023/B:PLSO.0000030188.77365.46
- Ross, D. J., Newton, P. C. D., & Tate, K. R. (2004). Elevated CO₂ effects on herbage production and soil carbon and nitrogen pools and mineralization in a species-rich, grazed pasture on a seasonally dry sand. *Plant and Soil*, 260(1-2), 183-196. doi:10.1023/B:PLSO.0000030188.77365.46
- Ross, D. J., Newton, P. C. D., Tate, K. R., & Luo, D. (2013). Impact of a low level of CO₂ enrichment on soil carbon and nitrogen pools and mineralization rates over ten years in a

seasonally dry, grazed pasture. *Soil Biology and Biochemistry*, 58, 265-274. doi:10.1016/j.soilbio.2012.12.011

Schipper LA, Baisden WT, Parfitt RL, Ross C, Claydon JJ, Arnold G. 2007. Large losses of soil C and N from soil profiles under pasture in New Zealand during the past 20 years. *Global Change Biology*. 13:1138–1144. doi: 10.1111/j.1365-2486.2007.01366.x

Schipper LA, Dodd MB, Pronger J, Mudge PL, Upsdell M, Moss RA. 2013. Decadal changes in soil carbon and nitrogen under a range of irrigation and phosphorus fertilizer treatments. *Soil Science Society of America Journal*. 77:246–256. doi: 10.2136/sssaj2012.0126

Schipper LA, Mudge PL, Kirschbaum, MUF, Hedley, CB, Golubiewski, NE, Smaill, SJ. 2017. A review of soil carbon change in New Zealand's grazed grasslands. *New Zealand Journal of Agricultural Research*. Doi: 10.1080/00288233.2017.1284134

Schipper LA, Parfitt RL, Fraser S, Littler RA, Baisden WT, Ross C. 2014. Soil order and grazing management effects on changes in soil C and N in New Zealand pastures. *Agriculture Ecosystems & Environment*. 184:67–75. doi: 10.1016/j.agee.2013.11.012

Schipper LA, Parfitt RL, Ross C, Baisden WT, Claydon JJ, Fraser S. 2010. Gains and losses in C and N stocks of New Zealand pasture soils depend on land use. *Agriculture Ecosystems & Environment*. 139:611–617. doi: 10.1016/j.agee.2010.10.005

Shen, Q., Suarez-Abelenda, M., Camps-Arbestain, M., Calvelo Pereira, R., McNally, S. R., & Kelliher, F. M. (2018). An investigation of organic matter quality and quantity in acid soils as influenced by soil type and land use. *Geoderma*, 328, 44-55. doi:10.1016/j.geoderma.2018.05.006

Sillen, W. M. A., & Dieleman, W. I. J. (2012). Effects of elevated CO₂ and N fertilization on plant and soil carbon pools of managed grasslands: a meta-analysis. *Biogeosciences*, 9(6), 2247-2258. doi:10.5194/bg-9-2247-2012

Sitters, J., Wubs, E. R. J., Bakker, E. S., Crowther, T. W., Adler, P. B., Bagchi, S., Veen, G. F. (2020). Nutrient availability controls the impact of mammalian herbivores on soil carbon and nitrogen pools in grasslands. *Global Change Biology*, 26(4), 2060-2071. doi:10.1111/gcb.15023

- Six, J., Bossuyt, H., Degryze, S., & Denef, K. (2004). A history of research on the link between (micro)aggregates, soil biota, and soil organic matter dynamics. *Soil and Tillage Research*, 79(1), 7-31. doi:10.1016/j.still.2004.03.008
- Six, J., Carpentier, A., Van Kessel, C., Merckx, R., Harris, D., Horwath, W. R., & Lüscher, A. (2001). Impact of elevated CO₂ on soil organic matter dynamics as related to changes in aggregate turnover and residue quality. *Plant and Soil*, 234(1), 27-36. doi:10.1023/A:1010504611456
- Six, J., Conant, R. T., Paul, E. A., & Paustian, K. (2002). Stabilization mechanisms of soil organic matter: Implications for C-saturation of soils. *Plant and Soil*, 241(2), 155-176. doi:10.1023/A:1016125726789
- Six, J., Elliott, E. T., Paustian, K., & Doran, J. W. (1998). Aggregation and soil organic matter accumulation in cultivated and native grassland soils. *Soil Science Society of America Journal*, 62(5), 1367-1377. doi:10.2136/sssaj1998.03615995006200050032x
- Six, J., Paustian, K., Elliott, E. T., & Combrink, C. (2000). Soil structure and organic matter: I. Distribution of aggregate-size classes and aggregate-associated carbon. *Soil Science Society of America Journal*, 64(2), 681-689. Retrieved from <https://www.scopus.com/inward/record.uri?eid=2-s2.0-0034163132&partnerID=40&md5=9d237d22a767e659886f65accc2111a8>
- Sokol, N. W., & Bradford, M. A. (2019). Microbial formation of stable soil carbon is more efficient from belowground than aboveground input. *Nature Geoscience*, 12(1), 46-53. doi:10.1038/s41561-018-0258-6
- Stewart, C.E., Neff, J.C., Amatangelo, K.L., Vitousek, P.M., 2011. Vegetation effects on soil organic matter chemistry of aggregate fractions in a Hawaiian forest. *Ecosystems* 14, 382–397.
- Tandy, S., Hawkins, J. M. B., Dunham, S. J., Hernandez-Allica, J., Granger, S. J., Yuan, H., Blackwell, M. S. A. (2021). Investigation of the soil properties that affect Olsen P critical values in different soil types and impact on P fertiliser recommendations. *European Journal of Soil Science*, 72(4), 1802-1816. doi:10.1111/ejss.13082
- Terrer, C., Vicca, S., Stocker, B.D., Hungate, B.A., Phillips, R. P., Reich, P. B., Finzi, A.C., Prentice, I. C. (2018). Ecosystem responses to elevated CO₂ governed by plant-soil interactions

and the cost of nitrogen acquisition. *New Phytologist* (2018) 217: 507–522. doi:10.1111/nph.14872

Terrer, C., Phillips, R. P., Hungate, B. A., Rosende, J., Pett-Ridge, J., Craig, M. E., Jackson, R. B. (2021). A trade-off between plant and soil carbon storage under elevated CO₂. *Nature*, 591(7851), 599-603. doi:10.1038/s41586-021-03306-8

Thaysen, E. M., Reinsch, S., Larsen, K. S., & Ambus, P. (2017). Decrease in heathland soil labile organic carbon under future atmospheric and climatic conditions. *Biogeochemistry*, 133(1), 17-36. doi:10.1007/s10533-017-0303-3

Theis, D. E., Jaeggi, M., Aeschlimann, D., Blum, H., Frossard, E., & Siegwolf, R. T. W. (2007). Dynamics of soil organic matter turnover and soil respired CO₂ in a temperate grassland labelled with ¹³C. *European Journal of Soil Science*, 58(6), 1364-1372. doi:10.1111/j.1365-2389.2007.00941.x

Touhami, D., McDowell, R. W., Condrón, L. M., Lieffering, M., & Newton, P. C. D. (2020). Long-term atmospheric carbon dioxide enrichment decreases soil phosphorus availability in a grazed temperate pasture. *Geoderma*, 378. doi:10.1016/j.geoderma.2020.114621

Van Groenigen, K. J., Harris, D., Horwath, W. R., Hartwig, U. A., & Van Kessel, C. (2002). Linking sequestration of ¹³C and ¹⁵N in aggregates in a pasture soil following 8 years of elevated atmospheric CO₂. *Global Change Biology*, 8(11), 1094-1108. doi:10.1046/j.1365-2486.2002.00527.x

van Groenigen, K. J., Osenberg, C. W., Terrer, C., Carrillo, Y., Dijkstra, F. A., Heath, J., Hungate, B. A. (2017). Faster turnover of new soil carbon inputs under increased atmospheric CO₂. *Global Change Biology*, 23(10), 4420-4429. doi:10.1111/gcb.13752

van Kessel, C., Boots, B., de Graaff, M. A., Harris, D., Blum, H., & Six, J. (2006). Total soil C and N sequestration in a grassland following 10 years of free air CO₂ enrichment. *Global Change Biology*, 12(11), 2187-2199. doi:10.1111/j.1365-2486.2006.01172.x

Vestergård, M., Reinsch, S., Bengtson, P., Ambus, P., & Christensen, S. (2016). Enhanced priming of old, not new soil carbon at elevated atmospheric CO₂. *Soil Biology and Biochemistry*, 100, 140-148. doi:10.1016/j.soilbio.2016.06.010

von Lützow, M., Kögel-Knabner, I., Ekschmitt, K., Flessa, H., Guggenberger, G., Matzner, E., & Marschner, B. (2007). SOM fractionation methods: Relevance to functional pools and to

stabilization mechanisms. *Soil Biology and Biochemistry*, 39(9), 2183-2207. doi:10.1016/j.soilbio.2007.03.007

Von Lützow, M., Kögel-Knabner, I., Ludwig, B., Matzner, E., Flessa, H., Ekschmitt, K., Kalbitz, K. (2008). Stabilization mechanisms of organic matter in four temperate soils: Development and application of a conceptual model. *Journal of Plant Nutrition and Soil Science*, 171(1), 111-124. doi:10.1002/jpln.200700047

Walters RJK, and Evans EM., (1979). Evaluation of a sward sampling technique for estimating herbage intake by grazing sheep. *Grass and Forage Science*, 34, 37 – 44.

Wang, C., Sun, Y., Chen, H. Y. H., & Ruan, H. (2021). Effects of elevated CO₂ on the C:N stoichiometry of plants, soils, and microorganisms in terrestrial ecosystems. *Catena*, 201. doi:10.1016/j.catena.2021.105219

Wang, X., McConkey, B. G., VandenBygaart, A. J., Fan, J., Iwaasa, A., & Schellenberg, M. (2016). Grazing improves C and N cycling in the Northern Great Plains: a meta-analysis. *Sci Rep*, 6, 33190. doi:10.1038/srep33190

Wendt, J. W., & Hauser, S. (2013). An equivalent soil mass procedure for monitoring soil organic carbon in multiple soil layers. *European Journal of Soil Science*, 64(1), 58-65. doi:10.1111/ejss.12002

Whitehead, D., Schipper, L. A., Pronger, J., Moinet, G. Y. K., Mudge, P. L., Calvelo Pereira, R., Camps-Arbestain, M. (2018). Management practices to reduce losses or increase soil carbon stocks in temperate grazed grasslands: New Zealand as a case study. *Agriculture, Ecosystems and Environment*, 265, 432-443. doi:10.1016/j.agee.2018.06.022

Wiesmeier, M., Urbanski, L., Hobbey, E., Lang, B., von Lützow, M., Marin-Spiotta, E., Kögel-Knabner, I. (2019). Soil organic carbon storage as a key function of soils - A review of drivers and indicators at various scales. *Geoderma*, 333, 149-162. doi:10.1016/j.geoderma.2018.07.026

Xie, Z., Cadisch, G., Edwards, G., Baggs, E. M., & Blum, H. (2005). Carbon dynamics in a temperate grassland soil after 9 years exposure to elevated CO₂ (Swiss FACE). *Soil Biology and Biochemistry*, 37(7), 1387-1395. doi:10.1016/j.soilbio.2004.12.010

Xiong, L., Liu, X., Vinci, G., Spaccini, R., Drosos, M., Li, L., Pan, G. (2019). Molecular changes of soil organic matter induced by root exudates in a rice paddy under CO₂ enrichment

and warming of canopy air. *Soil Biology and Biochemistry*, 137. doi:10.1016/j.soilbio.2019.107544

Xiong, L., Liu, X., Vinci, G., Sun, B., Drosos, M., Li, L., Pan, G. (2021). Aggregate fractions shaped molecular composition change of soil organic matter in a rice paddy under elevated CO₂ and air warming. *Soil Biology and Biochemistry*, 159. doi:10.1016/j.soilbio.2021.108289

Xu, Q., Jin, J., Wang, X., Armstrong, R., & Tang, C. (2019). Susceptibility of soil organic carbon to priming after long-term CO₂ fumigation is mediated by soil texture. *Science of the Total Environment*, 657, 1112-1120. doi:10.1016/j.scitotenv.2018.11.437

Zegouagh, Y., Derenne, S., Dignac, M.F., Baruiso, E., Mariotti, A., Largeau, C., (2004). Demineralisation of a crop soil by mild hydrofluoric acid treatment Influence on organic matter composition and pyrolysis. *J. Anal. Appl. Pyrolysis* 71, 119–135.

Zhou, G., Zhou, L., & Zhou, X. (2019). Effects of Grazing Intensity on Belowground Carbon and Nitrogen Cycling. In.

Zhou, G., Zhou, X., He, Y., Shao, J., Hu, Z., Liu, R., Hosseinibai, S. (2017). Grazing intensity significantly affects belowground carbon and nitrogen cycling in grassland ecosystems: a meta-analysis. *Global Change Biology*, 23(3), 1167-1179. doi:10.1111/gcb.13431

Zhou, G. Y., & Wu, Y. Y. (2016). Meta-analysis of effects of grazing on carbon pools in grassland ecosystems in different climatic regions. *Acta Prataculturae Sinica*, 25(10), 1-10. doi:10.11686/cyxb2015579